

LIBRARY, NAVAL POSTGRADUATE SCHOOL
MONTEREY, CA 93940

NAVAL POSTGRADUATE SCHOOL

Monterey, California



THESIS

A NUMERICAL ANALYSIS OF PIPE FLOW STABILITY

by

David Bruce Wallace

December 1982

Thesis Advisor:

T. H. Gawain

Approved for public release; distribution unlimited

T207873

REPORT DOCUMENTATION PAGE		READ INSTRUCTIONS BEFORE COMPLETING FORM
1. REPORT NUMBER	2. GOVT ACCESSION NO.	3. RECIPIENT'S CATALOG NUMBER
4. TITLE (and Subtitle) A Numerical Analysis of Pipe Flow Stability		5. TYPE OF REPORT & PERIOD COVERED Master's Thesis December 1982
		6. PERFORMING ORG. REPORT NUMBER
7. AUTHOR(s) David Bruce Wallace		8. CONTRACT OR GRANT NUMBER(s)
9. PERFORMING ORGANIZATION NAME AND ADDRESS Naval Postgraduate School Monterey, California 93940		10. PROGRAM ELEMENT, PROJECT, TASK AREA & WORK UNIT NUMBERS
11. CONTROLLING OFFICE NAME AND ADDRESS Naval Postgraduate School Monterey, California 93940		12. REPORT DATE December 1982
		13. NUMBER OF PAGES 236
14. MONITORING AGENCY NAME & ADDRESS (if different from Controlling Office)		15. SECURITY CLASS. (of this report) Unclassified
		15a. DECLASSIFICATION/DOWNGRADING SCHEDULE
16. DISTRIBUTION STATEMENT (of this Report) Approved for public release; distribution unlimited		
17. DISTRIBUTION STATEMENT (of the abstract entered in Block 20, if different from Report)		
18. SUPPLEMENTARY NOTES		
19. KEY WORDS (Continue on reverse side if necessary and identify by block number) pipe flow stability critical Reynolds number vorticity transport equations hydrodynamic stability		
20. ABSTRACT (Continue on reverse side if necessary and identify by block number) Standard theoretical methods of analysis which work well for seemingly more complex problems fail to predict the experimentally observed instability of fully developed, incompressible pipe flow at any Reynolds number. Past research by Harrison and Arnold on the stability of pipe flow yielded erroneous results due to errors in the setup of the problem and formulation of the boundary conditions at the axis.		

19. KEY WORDS (Continued)

finite differencing techniques
velocity vector potential
least stable eigenvalue
eigenfunctions
eigensystem
axial perturbation velocity

20. ABSTRACT (Continued)

A revised theory with particular attention to the rather complex boundary conditions at the axis has recently been developed. Improved finite differencing techniques with consistent fourth order truncation error were also used to approximate the governing differential equations.

Numerical results for angular wave numbers zero and six show that the flow is stable at all Reynolds numbers. Results for angular wave number one contain instabilities at all Reynolds numbers for small values of the axial wave number. These results are tabulated, plotted, and discussed in detail in this paper.

Approved for public release; distribution unlimited

A Numerical Analysis of Pipe Flow Stability

by

David Bruce Wallace
Lieutenant, United States Navy
B.S., University of Kansas, 1975

Submitted in partial fulfillment of the requirements
for the degree of

MASTER OF SCIENCE IN AERONAUTICAL ENGINEERING

from the

NAVAL POSTGRADUATE SCHOOL
December 1982

ABSTRACT

Standard theoretical methods of analysis which work well for seemingly more complex problems fail to predict the experimentally observed instability of fully developed, incompressible pipe flow at any Reynolds number. Past research by Harrison and Arnold on the stability of pipe flow yielded erroneous results due to errors in the setup of the problem and formulation of the boundary conditions at the axis.

A revised theory with particular attention to the rather complex boundary conditions at the axis has recently been developed. Improved finite differencing techniques with consistent fourth order truncation error were also used to approximate the governing differential equations.

Numerical results for angular wave numbers zero and six show that the flow is stable at all Reynolds numbers. Results for angular wave number one contain instabilities at all Reynolds numbers for small values of the axial wave number. These results are tabulated, plotted, and discussed in detail in this paper.

TABLE OF CONTENTS

I.	INTRODUCTION -----	14
II.	THE VORTICITY TRANSPORT EQUATION -----	19
	A. BASIC THEORY -----	19
	B. THE VORTICITY TRANSPORT EQUATION -----	23
	C. THE VORTICITY TRANSPORT MATRIX EQUATION -----	30
	D. EQUATION FOR $n = 0$ -----	32
	E. EQUATIONS FOR $n = 1$ -----	33
	F. EQUATIONS FOR $n = 6$ -----	35
III.	BOUNDARY CONDITIONS -----	36
IV.	PERTURBATION VELOCITY -----	49
V.	NUMERICAL METHODS -----	52
	A. GENERAL METHODS USED -----	52
	B. FINITE DIFFERENCE EQUATIONS -----	57
	C. SPECIFIC METHODS FOR $n = 0, 1$, AND 6 -----	67
	D. COMPUTER PROGRAM USEAGE -----	83
VI.	RESULTS -----	86
	A. RESULTS FOR $n = 0$ -----	86
	B. RESULTS FOR $n = 1$ -----	99
	C. RESULTS FOR $n = 6$ -----	118
	D. NUMERICAL ACCURACY -----	134
VII.	RECOMMENDATIONS AND CONCLUSIONS -----	139

APPENDIX A:	COEFFICIENTS OF THE VORTICITY TRANSPORT EQUATIONS -----	142
APPENDIX B:	COEFFICIENTS OF THE TRANSFORMED VORTICITY TRANSPORT EQUATIONS FOR $n = 0, 1, \text{ AND } 6$ -----	144
APPENDIX C:	COEFFICIENTS OF THE BOUNDARY EQUATIONS AT THE AXIS -----	151
APPENDIX D:	SPECIAL CONDITIONS AT THE AXIS -----	154
COMPUTER PROGRAMS	-----	156
A.	MAIN INVESTIGATIVE PROGRAM FOR $n = 0$ -----	156
B.	MAIN INVESTIGATIVE PROGRAM FOR $n = 1$ -----	172
C.	MAIN INVESTIGATIVE PROGRAM FOR $n = 6$ -----	199
D.	PROGRAM TO COMPUTE THE NONCENTRAL FINITE DIFFERENCE COEFFICIENTS -----	220
LIST OF REFERENCES	-----	234
INITIAL DISTRIBUTION LIST	-----	236

LIST OF FIGURES

2-1	Velocity Profile of Fluid Flow in a Pipe -----	22
5-1	Radial Mesh, Standard Method -----	53
5-2	Radial Mesh, Half Station Method -----	54
5-3	[A] Matrix for $n = 0$ -----	69
5-4	[B] Matrix for $n = 0$ -----	70
5-5	[A] Matrix for $n \geq 6$ -----	74
5-6	[B] Matrix for $n \geq 6$ -----	75
5-7	[A] Matrix for $n = 1$ -----	80
5-8	[B] Matrix for $n = 1$ -----	81
6-1	Normalized Perturbation Velocity vs. Radius -----	90
6-2	Normalized Perturbation Velocity vs. Radius -----	91
6-3	Normalized Perturbation Velocity vs. Radius -----	92
6-4	Normalized Perturbation Velocity vs. Radius -----	93
6-5	Normalized Perturbation Velocity vs. Radius -----	94
6-6	Normalized Perturbation Velocity vs. Radius -----	95
6-7	Normalized Perturbation Velocity vs. Radius -----	96
6-8	Normalized Perturbation Velocity vs. Radius -----	97
6-9	Normalized Perturbation Velocity vs. Radius -----	98
6-10	GAMMA* vs. ALPHA, Reynolds Number Contours, $n = 1$ -----	104
6-11	GAMMA* vs. ALPHA, Reynolds Number Contours, $n = 1$ -----	105
6-12	GAMMA* vs. Reynolds Number, Alpha Contours, $n = 1$ -----	106
6-13	Normalized Perturbation Velocity vs. Radius -----	107
6-14	Normalized Perturbation Velocity vs. Radius -----	108

6-15	Normalized Perturbation Velocity vs. Radius -----	109
6-16	Normalized Perturbation Velocity vs. Radius -----	110
6-17	Normalized Perturbation Velocity vs. Radius -----	111
6-18	Normalized Perturbation Velocity vs. Radius -----	112
6-19	Normalized Perturbation Velocity vs. Radius -----	113
6-20	Normalized Perturbation Velocity vs. Radius -----	114
6-21	Normalized Perturbation Velocity vs. Radius -----	115
6-22	Normalized Perturbation Velocity vs. Radius -----	116
6-23	Normalized Perturbation Velocity vs. Radius -----	117
6-24	GAMMA* vs. ALPHA, Reynolds Number Contours, $n = 6$ -----	121
6-25	GAMMA* vs. ALPHA, Reynolds Number Contours, $n = 6$ -----	122
6-26	GAMMA* vs. Reynolds Number, Alpha Contours, $n = 6$ -----	123
6-27	Normalized Perturbation Velocity vs. Radius -----	124
6-28	Normalized Perturbation Velocity vs. Radius -----	125
6-29	Normalized Perturbation Velocity vs. Radius -----	126
6-30	Normalized Perturbation Velocity vs. Radius -----	127
6-31	Normalized Perturbation Velocity vs. Radius -----	128
6-32	Normalized Perturbation Velocity vs. Radius -----	129
6-33	Normalized Perturbation Velocity vs. Radius -----	130
6-34	Normalized Perturbation Velocity vs. Radius -----	131
6-35	Normalized Perturbation Velocity vs. Radius -----	132
6-36	Normalized Perturbation Velocity vs. Radius -----	133
6-37	Normalized Perturbation Velocity vs. Radius -----	136
6-38	Normalized Perturbation Velocity vs. Radius -----	137
6-39	Normalized Perturbation Velocity vs. Radius -----	138

LIST OF TABLES

2-1	Properties of the Vorticity Transport Equations -----	29
5-1	Properties of the [A] and [B] Matrices for $n \geq 6$ -----	73
6-1	Stability Data for Angular Wave Number $n = 0$ -----	88
6-2	Stability Data for Angular Wave Number $n = 1$ -----	100
6-3	Stability Data for Angular Wave Number $n = 1$ -----	101
6-4	Stability Data for Angular Wave Number $n = 6$ -----	119
6-5	Stability Data for Angular Wave Number $n = 6$ -----	120

TABLE OF SYMBOLS

D	Differential operator $\partial/\partial r$
D^2, D^3, D^4	Higher order partial derivatives with respect to r .
e	Base of natural logarithms.
$\vec{e}_x, \vec{e}_r, \vec{e}_\theta$	Unit vectors along the x , r , and θ axes in cylindrical coordinates.
F, G, H	Components of the velocity vector potential function defined in equation (2-28).
h	The increment of the radius in the finite difference equations, $h = 1/N$.
i	$+\sqrt{-1}$, the imaginary unit.
i	Used as an index to distinguish the transformed coefficient matrices $[M'_i]$ of equation (2-43) and in the discrete finite difference equations.
j	Used as an index to distinguish the transformed coefficient matrices $[N'_j]$ of equation (2-43).
N	The number of interior points along the pipe radius used in the finite difference mesh.
n	Angular wave number of the perturbation in the θ direction, where $n = 0, 1, 2, 3, \dots$
O	Symbol denoting the phrase "of order".
P	Pressure appearing in equations (2-4, 5, 11, and 12).

P	Component of the velocity vector potential derived from the component G after a change of variable.
Q	Component of the velocity vector potential derived from the component H after a change of variable.
R	Normalized pipe radius, $R = 1$.
\bar{R}	The dimensional pipe radius used to define Re in equation (2-6).
Re	Reynolds number based on pipe radius and mean volumetric velocity, as defined in equation (2-6).
t	Time.
U	The axial component of the mean dimensionless velocity of the flow as defined in equation (2-13).
\bar{U}	The mean dimensional volumetric velocity of the flow used to define Re in equation (2-6).
u, v, w	Components of the complex perturbation velocity.
\vec{V}	Velocity vector of the mean flow.
\vec{V}'	Velocity vector of the total or resultant flow.
\vec{v}	Complex perturbation velocity vector.
\vec{W}	The velocity vector potential function defined in equation (2-28).
x, r, θ	Cylindrical coordinates.
X	Symbol for $iax + in\theta + yt$, defined in equation (2-29).

$\{X^*\}$	Eigenvector corresponding to the least stable eigenvalue.
α	The real axial wave number of the perturbation in the x direction, where $\alpha \geq 0$.
γ	The complex frequency of the perturbation defined in equation (2-30).
γ^*	The maximum algebraic value of the real part of the complex frequency which is also the least stable eigenvalue, also referred to as GAMMA*.
$\vec{\Gamma}$	Shorthand notation of the vorticity transport equations as defined in equation (2-32).
$\Gamma_x, \Gamma_r, \Gamma_\theta$	Components of $\vec{\Gamma}$ in cylindrical coordinates.
ε	The residual error of the least stable eigenvalue solution of the governing equations.
ν	Kinematic viscosity.
μ	Viscosity.
ρ	Density.
$\vec{\Omega}$	Mean vorticity vector.
$\vec{\Omega}'$	Total or resultant vorticity vector.
$\vec{\omega}$	Perturbation vorticity vector.
∇	Linear vector operator (nabla).
\times	Vector cross-product operator.
$\nabla \times$	Vector curl operator.

- $\nabla \cdot$ Vector dot product operator.
- $[]$ Brackets enclosing a matrix.
- $\{\}$ Brackets enclosing a column vector.

I. INTRODUCTION

Osborne Reynolds [Ref. 1] conducted his classical experiments on the transition from laminar to turbulent flow of fluids in circular pipes nearly 100 years ago. Based on his experiments the critical Reynolds number for pipe flow was found to be 2300. An analytical solution for the problem of predicting instabilities of fully developed, three dimensional, incompressible flow of constant viscosity fluids in pipes has been pursued actively since then. Several approaches have been taken in solving the inherently nonlinear Navier-Stokes equations, which along with the continuity equation, govern the behavior of fluid flow in pipes of circular cross-section.

Salwen and Grosch [Ref. 2] studied pipe flow with purely sinusoidal streamwise (axial) perturbations. Infinitesimal velocity and pressure perturbations, which were explicit functions of time and not complex or exponential in form, were introduced into the flow field. Numerical calculations were carried out at various angular wave numbers and it was concluded that the flow was stable for all axial wave numbers and Reynolds numbers. Perturbations with exponential growth in space but a purely sinusoidal variation in time were explored by Garg and Rouleau [Ref. 3] and found to be stable. Gill [Ref. 4] studied combinations of exponential growth in space and in time using power series analysis and concluded that these flows were all stable.

Because of the general agreement that pipe flow is stable to infinitesimal disturbances, two other approaches to the problem of predicting instabilities at the experimentally observed critical Reynolds number have been pursued. First, investigations by Davy and Drazin [Ref. 5] confirmed that pipe Poiseuille flow was stable at all Reynolds numbers for infinitesimal disturbances that were both temporally and axially complex and exponential in nature. However, despite the fact that the governing equations must necessarily remain nonlinear with the introduction of disturbances of finite amplitude, they concluded that the flow is unstable with respect to finite disturbances. Similar theoretical examinations of plane Poiseuille flow between two parallel plates led McIntire and Lin [Ref. 6] to this same conclusion. Second, it was postulated by Huang and Chen [Ref. 7] and Leite [Ref. 8] that the origin of flow instabilities occur in the entrance region of the pipe, where the flow has not yet become fully developed. Both theoretical and experimental studies have been done to support these hypotheses. Garg [Ref. 9] also found that flow instabilities existed near the entry region for developing pipe flow. He concluded that results using the Hornbeck velocity profile more nearly approximated experimentally determined values of the critical Reynolds number. While these investigations have shown instabilities to exist in pipe flow, a completely generalized solution to the linearized problem of fully developed pipe flow has never been accomplished.

Recently, a more general theory consisting of perturbations which have a fully complex exponential form with respect to time and the axial

coordinate, a purely imaginary exponential form in the angular coordinate and are three dimensional in nature have been explored. Development of this theory by Harrison [Ref. 10] and further numerical investigations by Arnold [Ref. 11] failed to produce conclusive results that instabilities exist in fully developed pipe flow. Errors in the setup of the problem and inadequate formulation of the boundary conditions at the pipe axis contributed to these erroneous results. Arnold, however, was on the right track in his research by incorporating newly formulated boundary conditions at the axis developed by Gawain [Ref. 12].

Arnold's work, for the most part, remains valid except that he overlooked a small but significant detail that resulted in unclear definitions of stability and instability. He used a complex axial wave number α , of the form $\alpha = \alpha_R + i\alpha_I$, whereas the correct version should simply be a purely imaginary quantity of the form $i\alpha$. Thus, Arnold introduced an extra degree of freedom, namely the fictitious and incorrect quantity α_R . This accounts for the erroneous instabilities which he obtained in his numerical investigation of pipe flow.

Further work by Gawain [Ref. 13] refined the boundary conditions at the axis and incorporated the previously defined imaginary axial wave number, in exponential form, which represents only sinusoidal oscillations with respect to the axial coordinate. Using these advancements in the linearized theory, Gawain showed an asymptotic trend toward neutral stability of the flow with increasing Reynolds numbers for angular wave number, $n = 0$. This paper duplicates and confirms the results for $n = 0$, that the flow is stable at all Reynolds numbers and axial wave numbers. It is further shown that fully developed pipe flow for $n = 6$

is also stable and shows the same trends as for $n = 0$. Instabilities are shown to exist in the numerical analysis of the vorticity transport equations for $n = 1$. The paradox that now appears is that for angular wave numbers $n = 0$ and 6 the flow is apparently stable at all Reynolds numbers while for $n = 1$ the flow is apparently unstable at all Reynolds numbers. Neither of these theoretical results is consistent with the known experimental fact that there exists a critical Reynolds number below which pipe flow is stable and above which it is unstable. However, the new result for $n = 1$, while it can hardly be called correct, is at least encouraging in that it shows for the first time that instabilities can in fact exist in the solution of the linearized vorticity transport equations for fully developed pipe flow.

In addition to implementing the improved axis boundary conditions and the advancement in the linearized theory, improved finite differencing techniques were used to approximate the vorticity transport equations along a uniform radial mesh. Highly accurate numerical solutions for the previously mentioned angular wave numbers, $n = 0, 1$, and 6 , were obtained using double precision, complex numbers. Additionally, finite difference equations with consistent fourth order truncation error were used throughout. Details of the development of the vorticity transport equations and the central and non-central finite difference equations are discussed in later chapters. Systematic and extensive calculations remain to be accomplished for angular wave numbers, $n = 2, 3, 4, 5$, and $n > 6$. The results of these numerical analyses should prove to be fruitful in establishing a theory which

adequately explains the experimentally observed fact of the onset of flow instabilities at the critical Reynolds number.

II. THE VORTICITY TRANSPORT EQUATION

A. BASIC THEORY

The governing equations for laminar flow of fluids in a circular pipe are derived from Newton's second law of motion,

$$\vec{F} = m \vec{a} \quad (2-1)$$

and the conservation of mass principle through an infinitesimal control volume. Equation (2-1) results in the familiar Navier-Stokes equation, which is a vector equation in three cylindrical coordinates and in time. The equation for conservation of mass results in the continuity equation for incompressible flow and is given by,

$$\nabla \cdot \vec{V} = 0 \quad (2-2)$$

For the case at hand, the following assumptions are made,

1. The fluid is incompressible, $\rho = \text{constant}$
2. The fluid has constant viscosity, $\mu = \text{constant}$
3. The flow is fully developed, $U = f(r)$ only
4. The flow is three dimensional in nature
5. The mean flow is steady, $\partial \vec{V} / \partial t = 0$
6. The perturbation flow is unsteady, $\partial \vec{V} / \partial t \neq 0$
7. The effects of body forces are negligible

The resulting Navier-Stokes equation can be stated as the sum of the forces per unit mass is equal to the acceleration or,

$$\Sigma \frac{\text{Force}}{\text{mass}} = \text{acceleration} \quad (2-3)$$

The forces acting on the fluid are pressure forces and viscous forces. Body forces and hydrostatic forces balance out and are not a factor here.

Equation (2-3) in its dimensional form can be expressed as,

$$-\nabla^* \frac{p^*}{\rho^*} + \left(\frac{\mu^*}{\rho^*}\right) \nabla^{2*} \vec{V}^* = \frac{d\vec{V}^*}{dt^*} \quad (2-4)$$

where the starred quantities are fully dimensional.

It should be noted here that the equations presented through equation (2-18) represent the mean flow. Equation (2-4) can also be expressed in a nondimensional form as,

$$-\nabla P + \frac{1}{Re} \nabla^2 \vec{V} = \frac{d\vec{V}}{dt} \quad (2-5)$$

where Re is the Reynolds number and is defined as,

$$Re = \frac{\bar{R} \bar{U}}{\nu} \quad (2-6)$$

This definition of Reynolds number is based on the pipe radius \bar{R} as the characteristic length, the mean volumetric velocity \bar{U} as the characteristic velocity, and the kinematic viscosity ν which is constant. The three quantities on the right side of equation (2-6) are dimensional, but Re is a dimensionless quantity. On this basis, the critical Reynolds number for transition from laminar to turbulent flow becomes 1150 (vice the value of 2300 which is obtained if the Reynolds number is

defined in terms of pipe diameter). All subsequent equations presented in this paper are in nondimensional form.

Returning to the derivation of the mean flow, the acceleration term or substantial derivative, $d\vec{V}/dt$ can be expanded to the form,

$$\frac{d\vec{V}}{dt} = (\vec{V} \cdot \nabla) \vec{V} + \frac{\partial \vec{V}}{\partial t} \quad (2-7)$$

but $(\vec{V} \cdot \nabla)\vec{V}$ can be further expanded by a well known vector identity to,

$$(\vec{V} \cdot \nabla)\vec{V} = \nabla \left(\frac{U^2}{2} \right) - \vec{V} \times (\nabla \times \vec{V}) \quad (2-8)$$

Additionally, $\nabla^2 \vec{V}$ from equation (2-5) can be expanded to,

$$\nabla^2 \vec{V} = \nabla (\nabla \cdot \vec{V}) - \nabla \times (\nabla \times \vec{V}) \quad (2-9)$$

but $\nabla \cdot \vec{V} = 0$, since continuity must be satisfied and equation (2-9) becomes,

$$\nabla^2 \vec{V} = - \nabla \times (\nabla \times \vec{V}) \quad (2-10)$$

With appropriate substitutions, the final form of the Navier-Stokes equation becomes,

$$- \nabla P - \frac{1}{Re} \nabla \times (\nabla \times \vec{V}) = \nabla \left(\frac{U^2}{2} \right) - \vec{V} \times (\nabla \times \vec{V}) + \frac{\partial \vec{V}}{\partial t} \quad (2-11)$$

A more convenient form of equation (2-11) is,

$$- \nabla \left(P + \left(\frac{U^2}{2} \right) \right) = \frac{1}{Re} \nabla \times (\nabla \times \vec{V}) - \vec{V} \times (\nabla \times \vec{V}) + \frac{\partial \vec{V}}{\partial t} \quad (2-12)$$

As previously discussed, all the quantities in the equations have been nondimensionalized. Dimensionless cylindrical coordinates x , r , and θ are used with \vec{e}_x , \vec{e}_r and \vec{e}_θ denoting the unit vectors in the three coordinate directions, respectively. It is well known that the velocity profile for fully developed, three dimensional, incompressible flow in circular pipes can be expressed analytically by,

$$U = 2 (1 - r^2) \quad (2-13)$$

This function has the shape of a paraboloid of revolution as shown in Figure 2-1.

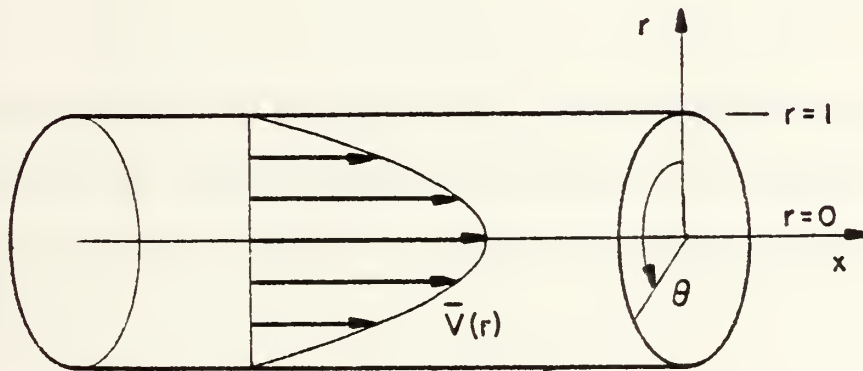


Figure 2-1. Velocity Profile of Fluid Flow in a Pipe

The nondimensional mean velocity vector $\vec{V}(r)$ of the flow is given by,

$$\vec{V}(r) = U \vec{e}_x = 2 (1 - r^2) \vec{e}_x \quad (2-14)$$

A second vector quantity $\vec{\Omega}$, the mean vorticity, is defined as the curl of the mean velocity vector and is given by,

$$\vec{\Omega} = \nabla \times \vec{V} = 4 r \vec{e}_\theta \quad (2-15)$$

which will be used later.

B. THE VORTICITY TRANSPORT EQUATION

The vorticity transport equation is now obtained by taking the curl of the Navier-Stokes equation (2-12), resulting in,

$$-\nabla \times \nabla \left(P + \left(\frac{U^2}{2} \right) \right) = \frac{1}{Re} \nabla \times (\nabla \times (\nabla \times \vec{V})) - \nabla \times (\vec{V} \times (\nabla \times \vec{V})) + \frac{\partial (\nabla \times \vec{V})}{\partial t} \quad (2-16)$$

The primary reason for taking the curl of the Navier-Stokes equation is to eliminate the unknown scalar on the left side of equation (2-16). Since the curl of the gradient of a scalar is equal to zero, equation (2-6) reduces to,

$$\frac{1}{Re} \nabla \times (\nabla \times (\nabla \times \vec{V})) - \nabla \times (\vec{V} \times (\nabla \times \vec{V})) + \frac{\partial (\nabla \times \vec{V})}{\partial t} = 0 \quad (2-17)$$

Equation (2-17) can be simplified by substituting the mean vorticity vector relation equation (2-15) into equation (2-17) resulting in,

$$\frac{1}{Re} \nabla \times (\nabla \times \vec{\Omega}) - \nabla \times (\vec{V} \times \vec{\Omega}) + \frac{\partial \vec{\Omega}}{\partial t} = 0 \quad (2-18)$$

In order to analyze this flow field and in particular to determine the transition from laminar to turbulent flow, a disturbance of small amplitude is introduced into the flow. It is assumed that the resulting flow is made up of the steady state, laminar flow and a small perturbation flow superimposed on the laminar flow. The total velocity and vorticity respectively become,

$$\vec{V}' = \vec{V} + \vec{v} \quad (2-19)$$

and

$$\vec{\Omega}' = \vec{\Omega} + \vec{\omega} \quad (2-20)$$

where \vec{v} and $\vec{\omega}$ are the velocity perturbations and vorticity perturbations, respectively. It is of course a necessary requirement that the continuity equation for the total flow be satisfied here as well,

$$\nabla \cdot \vec{V}' = \nabla \cdot \vec{V} + \nabla \cdot \vec{v} = 0 \quad (2-21)$$

In view of this relation and of equation (2-2), the perturbation flow independently satisfies the continuity condition and

$$\nabla \cdot \vec{v} = 0 \quad (2-22)$$

The introduction of the perturbation quantities into the vorticity transport equation is accomplished by substituting \vec{V}' for \vec{V} and $\vec{\Omega}'$ for $\vec{\Omega}$ into equation (2-18). This results in,

$$\frac{1}{Re} \nabla \times (\nabla \times (\vec{\Omega} + \vec{\omega})) - \nabla \times [(\vec{V} + \vec{v}) \times (\vec{\Omega} + \vec{\omega})] + \frac{\partial(\vec{\Omega} + \vec{\omega})}{\partial t} = 0 \quad (2-23)$$

which is the equation for the total or resultant flow field. Upon expanding equation (2-23), applying the mean steady flow assumption, $\partial \vec{V}/\partial t = 0$, and subtracting equation (2-18) from it, equation (2-23) becomes,

$$\frac{1}{Re} \nabla \times (\nabla \times \vec{\omega}) - \nabla \times [(\vec{V} \times \vec{\omega}) - (\vec{\Omega} \times \vec{V}) + (\vec{V} \times \vec{\omega})] + \frac{\partial \vec{\omega}}{\partial t} = 0 \quad (2-24)$$

Now equation (2-23) is linear in the perturbation quantities except for the second order term, $(\vec{V} \times \vec{\omega})$. Since the perturbations are assumed to be small, this term can be neglected.

The perturbation vorticity is defined as,

$$\vec{\omega} = \nabla \times \vec{V} \quad (2-25)$$

which is analogous to equation (2-15) for the mean flow. Making this substitution in equation (2-24) yields the linearized vorticity transport equation,

$$\frac{1}{Re} \nabla \times (\nabla \times (\nabla \times \vec{V})) - \nabla \times (\vec{V} \times (\nabla \times \vec{V})) + \nabla \times (\nabla \times (\vec{V} \times \vec{V})) + \nabla \times \frac{\partial \vec{V}}{\partial t} = 0 \quad (2-26)$$

As previously mentioned, the continuity equation (2-22) for the perturbation velocity must be satisfied. A convenient way to insure this is to express \vec{V} in terms of a velocity vector potential function \vec{W} as follows,

$$\vec{V} = \nabla \times \vec{W} \quad (2-27)$$

It can be verified that if \vec{V} is defined in this way, equation (2-22) is satisfied identically for any arbitrary vector function \vec{W} .

Instead of proceeding directly with the real vector functions \vec{V} and \vec{W} , it is advantageous to work with the Fourier transforms of \vec{V} and \vec{W} , which are in general complex functions. This is the form which is used here. It can be shown, because of the linearity of the basic equation, that if a solution can be found for the Fourier transforms, then the corresponding real vector functions will satisfy the basic equation as well. A detailed explanation of these functions was presented more elegantly by Gawain [Ref. 13]. The vector potential function \vec{W} , now representing the Fourier transform, can be expressed as,

$$\vec{W} = [F(r) \vec{e}_x + G(r) \vec{e}_r + H(r) \vec{e}_\theta] e^X \quad (2-28)$$

where X is a convenient abbreviation for the complex quantity,

$$X = i\alpha x + in\theta + \gamma t \quad (2-29)$$

The axial wave number α is a real quantity greater than or equal to zero which in the exponential form represents purely sinusoidal axial variations of \vec{V} . The angular wave number n is a positive integer and represents sinusoidal angular variations of \vec{V} which are periodic with respect to coordinate θ . The complex frequency γ contained in the exponent is of the form,

$$e^{\gamma t} = e^{(\gamma_R + i\gamma_I)t} = e^{\gamma_R t} (\cos \gamma_I t + i \sin \gamma_I t) \quad (2-30)$$

The quantity γ_R clearly represents the exponential time rate of growth or decay of the perturbation amplitude. The basic criteria for hydrodynamic stability can be defined in terms of γ_R . Positive values of γ_R represent growth and signify flow instability while negative values of γ_R represent decay and signify flow stability.

The vorticity transport equation can now be expressed in terms of the velocity vector, \vec{V} and the complex vector potential, \vec{W} . By making the substitution for \vec{v} , equation (2-26) now becomes,

$$\begin{aligned} \frac{1}{Re} \nabla \times (\nabla \times (\nabla \times (\nabla \times \vec{W}))) - \nabla \times (\vec{V} \times (\nabla \times (\nabla \times \vec{W}))) \\ + \nabla \times (\nabla \times (\vec{V} \times (\nabla \times \vec{W}))) + \nabla \times (\nabla \times \frac{\partial \vec{W}}{\partial t}) = 0 \end{aligned} \quad (2-31)$$

In convenient shorthand notation, equation (2-31) becomes,

$$\text{Equation (2-31)} = \vec{\Gamma}(r)e^x = [\Gamma_x(r) \vec{e}_r + \Gamma_r(r) \vec{e}_\theta + \Gamma_\theta(r) \vec{e}] e^x = 0 \quad (2-32)$$

and can be expressed in matrix notation as,

$$\vec{\Gamma} = \begin{Bmatrix} \Gamma_x \\ \Gamma_r \\ \Gamma_\theta \end{Bmatrix} = \begin{Bmatrix} 0 \\ 0 \\ 0 \end{Bmatrix} \quad (2-33)$$

Therefore, the three components of the vorticity transport equation are equivalent to three simultaneous scalar equations, namely,

$$\begin{aligned}\Gamma_x &= 0 \\ \Gamma_r &= 0 \\ \Gamma_\theta &= 0\end{aligned}\tag{2-34}$$

Of these three equations, only two are actually independent since, as can be seen from equation (2-31), $\vec{\Gamma} \cdot \vec{e}^x$ is itself the curl of another vector. Therefore $\vec{\Gamma} \cdot \vec{e}^x$ must necessarily be nondivergent. It can be shown that the components of $\vec{\Gamma}$ satisfy the identity, $\nabla \cdot (\vec{\Gamma} \cdot \vec{e}^x) \equiv 0$, or,

$$i\alpha\Gamma_x + \frac{1}{r} D(r\Gamma_r) + \left(\frac{in}{r}\right) \Gamma_\theta \equiv 0\tag{2-35}$$

where D is the symbol for the differential operator d/dr . Two linearly independent equations can now be formulated from equations (2-34) given the constraint of equation (2-35). This can be reduced to some appropriate linear combination of two of the equations which is set equal to zero and to the third equation which is also set equal to zero. This results in a system of two coupled, fourth order differential equations in three unknowns. Recall that the vector potential function \vec{W} is expressed in terms of $F(r)$, $G(r)$, and $H(r)$. It can be shown that one of these variables is redundant and may be eliminated without any loss of generality in the solution of the equations. For the present case, the solution assumes its most convenient form if,

$$F(r) = 0\tag{2-36}$$

This convention has therefore been adopted and now $G(r)$ and $H(r)$ become the two coupled eigenfunctions of the governing fourth order differential equations. Returning to the problem of selecting the proper linear combination of equations comprising $\vec{\Gamma}$, it is important to choose this combination in an optimum fashion by analyzing the algebraic structure of these equations. Table 2-1 is taken from reference [13], corrected, and duplicated here for that purpose. Notice that equations (1) and (3) in the table are third order in G . If the particular linear combination of these equations is chosen as appears in equation (4), the result reduces to an equation of second order in G . This does not affect the order of the result since the function H remains fourth order.

Table 2-1. Properties of the Vorticity Transport Equations

EQUATION	TERM OF HIGHEST ORDER IN G	TERM OF HIGHEST ORDER IN H	HIGHEST NEGATIVE POWER OF r
(1) $\Gamma_x(r) = 0$	$\frac{i\alpha}{Re} D^3G$	$-\frac{n\alpha}{rRe} D^2H$	r^{-3}
(2) $\Gamma_r(r) = 0$	$\frac{1}{Re} (\alpha^2 + \frac{n^2}{r^2}) D^2G$	$\frac{in}{rRe} D^3H$	r^{-4}
(3) $\Gamma_\theta(r) = 0$	$\frac{in}{rRe} D^3G$	$-\frac{1}{Re} D^4H$	r^{-4}
(4) $-\frac{n}{\alpha r} \Gamma_x(r) + \Gamma_\theta(r) = 0$	$-\frac{4in}{r^2Re} D^2G$	$-\frac{1}{Re} D^4H$	r^{-4}

The formulation of the problem is simplified greatly by choosing two independent vorticity transport equations in the form,

$$\Gamma_r = 0 \quad (2-37)$$

and

$$-\frac{n}{\alpha r} \Gamma_x + \Gamma_\theta = 0 \quad (2-38)$$

C. THE VORTICITY TRANSPORT MATRIX EQUATION

While the fourth order linear vector operations and the associated algebra becomes very lengthy and rather tedious, the investigator attempting to expand the final form of the linearized vorticity transport equation (2-31) should pay sufficient attention to these details. Recall that the curl operation on a vector in cylindrical coordinates takes the form,

$$\nabla \times \vec{W} = \begin{vmatrix} \frac{1}{r} \vec{e}_x & \frac{1}{r} \vec{e}_r & \vec{e}_\theta \\ \frac{\partial}{\partial x} & \frac{\partial}{\partial r} & \frac{\partial}{\partial \theta} \\ 0 & Ge^x & rHe^x \end{vmatrix} \quad (2-39)$$

After all the nabla (∇) operations are complete, the final equation will be in the form of a vector equation as defined in equation (2-32). The first vorticity transport equation consists of the coefficient represented by Γ_r and is set equal to zero. The second equation consists of

the previously defined linear combination of the coefficients represented by Γ_x and Γ_θ and is also set equal to zero. The two resulting simultaneous ordinary differential equations are then expanded and the coefficients of the derivatives regrouped so that equations (2-37) and (2-38) can be conveniently expressed in matrix format as follows,

$$\begin{aligned}
 & [M_4] \begin{Bmatrix} D^4G \\ D^4H \end{Bmatrix} + [M_3] \begin{Bmatrix} D^3G \\ D^3H \end{Bmatrix} + [M_2] \begin{Bmatrix} D^2G \\ D^2H \end{Bmatrix} + [M_1] \begin{Bmatrix} DG \\ DH \end{Bmatrix} \\
 & + [M_0] \begin{Bmatrix} G \\ H \end{Bmatrix} = \gamma \left([N_2] \begin{Bmatrix} D^2G \\ D^2H \end{Bmatrix} + [N_1] \begin{Bmatrix} DG \\ DH \end{Bmatrix} + [N_0] \begin{Bmatrix} G \\ H \end{Bmatrix} \right) \quad (2-40)
 \end{aligned}$$

As it turns out, the equations are a pair of coupled homogeneous differential equations that can be solved as an eigenvalue problem. This technique is discussed in the chapter on Numerical Methods.

The matrices which appear in equation (2-40) are 2 X 2 matrices and are summarized in detail in Appendix A. Equation (2-40) and the respective matrix elements contained in Appendix A are the generalized vorticity transport equations for all angular wave numbers n , at all axial wave numbers α , and all Reynolds numbers. As will be explained in detail in the chapter on Boundary Conditions, the generalized equations are transformed by appropriate changes of variable depending on the angular wave number. The changes of variables from the eigenfunctions $G(r)$ and $H(r)$ to the new eigenfunctions $P(r)$ and $Q(r)$, respectively, are determined by the original boundary conditions that must be satisfied, particularly at the pipe axis.

D. EQUATIONS FOR $n = 0$

For the case $n = 0$, equation (2-40) is greatly simplified in that the two equations uncouple and allow an independent investigation of either eigenfunction, $G(r)$ or $H(r)$. Miscellaneous trial calculations made earlier suggest that the solutions for $G(r)$ are probably stable for all values of α and Re . Therefore, only the solutions for $H(r)$ were investigated. It should also be noted that the examination of the axial perturbation velocity is of particular interest in this analysis and, in the case for $n = 0$, is not a function of $G(r)$. The change of variable required to satisfy the boundary conditions is,

$$H(r) = r Q(r) \quad (2-41)$$

Taking the derivatives of $H(r)$ yields,

$$\begin{aligned} DH &= r DQ + Q \\ D^2H &= r D^2Q + 2 DQ \\ D^3H &= r D^3Q + 3 D^2Q \\ D^4H &= r D^4Q + 4 D^3Q \end{aligned} \quad (2-42)$$

With the substitution of equations (2-41) and (2-42) into equation (2-40), the following expression is obtained,

$$M_4' D^4Q + M_3' D^3Q + M_2' D^2Q + M_1' DQ + M_0' Q = \gamma (N_2' D^2Q + N_1' DQ + N_0' Q) \quad (2-43)$$

The primed coefficients are actually the elements from row 2 and column 2 of the newly transformed coefficient matrices and are not enclosed in matrix brackets. However, in general, the new coefficient matrices $[M'_i]$ and $[N'_j]$, (where the indices $i = 0, 1, 2, 3, 4$ and $j = 0, 1, 2$), are formed after the change of variable is made and the terms are collected. The primed coefficients used to solve the transformed vorticity transport equation in terms of $Q(r)$ for $n = 0$ are defined in Appendix B, Part A.

E. EQUATIONS for $n = 1$

For the case $n = 1$, eigenfunctions $G(r)$ and $H(r)$ do not become uncoupled and must be solved for in a system of simultaneous equations in a form similar to equation (2-40). An additional parameter $H(0)$ is introduced into the equations by the change of variables. This particular change of variables is required because of the complicated nature of the boundary conditions at the axis and is thoroughly explained in the chapter on Boundary Conditions. For $n = 1$, the change of variables required to satisfy the boundary conditions are,

$$\begin{aligned} G(r) &= -i H(0) + r^2 P(r) \\ H(r) &= H(0) + r^2 Q(r) \end{aligned} \tag{2-44}$$

Taking the derivatives of $G(r)$ yields,

$$\begin{aligned} DG &= r^2 DP + 2r P \\ D^2G &= r^2 D^2P + 4r DP + 2 P \end{aligned} \tag{2-45}$$

and taking the derivatives of $H(r)$ yields,

$$\begin{aligned}
 DH &= r^2 DQ + 2r Q \\
 D^2H &= r^2 D^2Q + 4r DQ + 2 Q \\
 D^3H &= r^2 D^3Q + 6r D^2Q + 6 DQ \\
 D^4H &= r^2 D^4Q + 8r D^3Q + 12 D^2Q
 \end{aligned}
 \tag{2-46}$$

Remember that in general $D(H(0)) \neq DH(0)$, where $DH(0)$ is the value of the first derivative of $H(r)$ evaluated at the point $r = 0$. Since $D(H(0)) = 0$ here, it vanishes from the expressions for the derivatives of $G(r)$ and $H(r)$. In order to accommodate $H(0)$ in the system of equations where it appears explicitly, two additional 2×1 column matrices are required, namely $[M'_5]$ and $[N'_3]$. After the changes of variable have been made, equation (2-40) now becomes,

$$\begin{aligned}
 [M'_4] \begin{Bmatrix} D^4P \\ D^4Q \end{Bmatrix} + [M'_3] \begin{Bmatrix} D^3P \\ D^3Q \end{Bmatrix} + [M'_2] \begin{Bmatrix} D^2P \\ D^2Q \end{Bmatrix} + [M'_1] \begin{Bmatrix} DP \\ DQ \end{Bmatrix} + [M'_0] \begin{Bmatrix} P \\ Q \end{Bmatrix} \\
 + [M'_5] \{H(0)\} = \gamma \left([N'_2] \begin{Bmatrix} D^2P \\ D^2Q \end{Bmatrix} + [N'_1] \begin{Bmatrix} DP \\ DQ \end{Bmatrix} + [N'_0] \begin{Bmatrix} P \\ Q \end{Bmatrix} + [N'_3] \{H(0)\} \right)
 \end{aligned}
 \tag{2-47}$$

The coefficient matrices of equation (2-47) used to solve the transformed vorticity transport equations in terms of $P(r)$ and $Q(r)$ for $n = 1$ are defined in Appendix B, Part B.

F. EQUATIONS FOR $n = 6$

For the case $n = 6$, eigenfunctions $G(r)$ and $H(r)$ remain coupled. The change of variables does not introduce any additional parameters and the system of simultaneous equations is solved in the form of equation (2-40) once again. The change of variables required to satisfy the boundary conditions for $n = 6$ and additionally for all angular wave numbers $n > 6$ are,

$$\begin{aligned} G(r) &= r^4 P(r) \\ H(r) &= r^3 Q(r) \end{aligned} \quad (2-48)$$

Taking the derivatives of $G(r)$ yields,

$$\begin{aligned} DG &= r^4 DP + 4r^3 P \\ D^2G &= r^4 D^2P + 8r^3 DP + 12r^2 P \end{aligned} \quad (2-49)$$

and taking the derivatives of $H(r)$ yields,

$$\begin{aligned} DH &= r^3 DQ + 3r^2 Q \\ D^2H &= r^3 D^2Q + 6r^2 DQ + 6r Q \\ D^3H &= r^3 D^3Q + 9r^2 D^2Q + 18r DQ + 6 Q \\ D^4H &= r^3 D^4Q + 12r^2 D^3Q + 36r D^2Q + 24 DQ \end{aligned} \quad (2-50)$$

Substituting equations (2-48), (2-49), and (2-50) into equation (2-40) results in the transformed coefficient matrices for the system of equations. The coefficient matrices of the functions $P(r)$ and $Q(r)$ and their respective derivatives for $n = 6$ are defined in Appendix B, Part C.

III. BOUNDARY CONDITIONS

The incorrect formulation of the boundary conditions for the linearized vorticity transport equations at the pipe axis has probably been the primary reason that previous investigators have failed to predict the onset of flow instabilities in circular pipes at any Reynolds number. Gawain [Ref. 13] suggested that if these boundary conditions are formulated in a rigorous and systematic fashion and applied to the vorticity transport equations, a correct numerical solution may be computed which agrees with experimental results. It can be seen from equations (2-40) and from the coefficient matrices of Appendix A that the two vorticity transport equations are coupled, except for the case $n = 0$. The resulting pair of differential equations are second order in $G(r)$ and fourth order in $H(r)$. In order to obtain a determinate solution of the equations, a total of six boundary conditions are required. More specifically, at least two of the boundary conditions must involve $G(r)$ or its derivatives and at least four of the boundary conditions must involve $H(r)$ or its derivatives. It might be expected that when the equations are coupled, the boundary conditions may also be coupled. That is to say that the boundary conditions may consist of various linear combinations of the functions and their derivatives, which turns out to be the case and is shown later.

The boundary conditions at the pipe wall are determined in a fairly straight forward manner. They are derived from the fact that the components of the perturbation velocity must vanish at the wall. From the definition of the perturbation velocity, defined previously as,

$$\vec{v} = \nabla \times \vec{W} \quad (2-27)$$

it can be shown that the following three boundary conditions result.

$$\begin{aligned} G(1) &= 0 \\ H(1) &= 0 \\ DH(1) &= 0 \end{aligned} \quad (3-1)$$

Since six boundary conditions are required and three have been determined at the pipe wall, there remain three boundary conditions to be determined at the pipe axis. Of these three conditions, at least one must involve $G(r)$ or its derivatives and at least two must involve $H(r)$ or its derivatives.

The proper derivation of the three boundary conditions at the axis turns out to be a non-trivial problem. As can be seen in Table 2-1, the highest negative power of r that appears in the equations is r^{-4} . Closer inspection of the vorticity transport equations of equation (2-40) and the coefficient matrices in Appendix A reveals that the equations contain terms in r^{-4} , r^{-3} , r^{-2} , r^{-1} , and r^0 . At first glance, it may appear that these equations are not satisfied in the limit as r approaches zero. It should be noted that it would be incorrect to multiply the equations through by any positive power of r since that would alter the degree of the singularity of the equations at the axis.

This problem can be resolved and subsequently the boundary conditions at the axis can be deduced rigorously by expanding the functions $G(r)$ and $H(r)$ as power series in r . The highest negative power of r is r^{-4} and appears in the coefficient matrix $[M_0]$ for the pair of functions $G(r)$ and $H(r)$. The series expansion for $G(r)$, and similarly for $H(r)$, is carried to the fourth derivative as follows,

$$G(r) = G(0) + DG(0)r + D^2G(0) \frac{r^2}{2!} + D^3G(0) \frac{r^3}{3!} + D^4G(0) \frac{r^4}{4!} + \dots \quad (3-2)$$

It can be seen that when the series expansion expressions for $G(r)$ and $H(r)$ are substituted into equation (2-40), the higher order terms of equation (3-2) that contain powers of r greater than four will vanish in the limit as r approaches zero. For the first derivatives of $G(r)$ and $H(r)$, the highest negative power of r that appears in the coefficient matrix $[M_1]$ is r^{-3} . Therefore, the series expansion for the first derivative of $G(r)$, and similarly for $H(r)$, up to the fourth derivative term is,

$$DG(r) = 0 + DG(0) + D^2G(0)r + D^3G(0) \frac{r^2}{2!} + D^4G(0) \frac{r^3}{3!} + \dots \quad (3-3)$$

The remaining derivatives of the functions are expanded in a similar manner through the fourth derivative term. The resulting power series approximations for $G(r)$ and $H(r)$ and their derivatives are then substituted into equation (2-40). The coefficients are then regrouped in ascending powers of r .

As mentioned previously, the equations must be satisfied in the limit as r approaches zero. Therefore, the coefficients of the functions that contain r^{-4} , r^{-3} , r^{-2} , r^{-1} , and r^0 must all be zero. The remaining coefficients will contain positive powers of r and will vanish in the limit as r approaches zero. By considering only the terms containing negative powers of r and setting those coefficients equal to zero, five pair of equations in ten unknowns remain so that the boundary conditions can be determined. The unknowns are the functions of $G(r)$ and $H(r)$ and their first four derivatives evaluated at the pipe axis, $r = 0$. It is convenient to summarize these equations in matrix format below,

$$\frac{(n^2-1)}{Re} [C_1] \begin{Bmatrix} G(0) \\ H(0) \end{Bmatrix} = \begin{Bmatrix} 0 \\ 0 \end{Bmatrix} \quad (3-4)$$

$$\frac{n^2}{Re} [C_2] \begin{Bmatrix} DG(0) \\ DH(0) \end{Bmatrix} = \begin{Bmatrix} 0 \\ 0 \end{Bmatrix} \quad (3-5)$$

$$\frac{(n^2-1)}{Re} [C_3] \begin{Bmatrix} D^2G(0) \\ D^2H(0) \end{Bmatrix} = \begin{Bmatrix} 0 \\ 0 \end{Bmatrix} + (i\alpha[C_4] - \gamma [D_4]) \begin{Bmatrix} G(0) \\ H(0) \end{Bmatrix} = \begin{Bmatrix} 0 \\ 0 \end{Bmatrix} \quad (3-6)$$

$$\frac{n(n^2-4)}{Re} [C_5] \begin{Bmatrix} D^3G(0) \\ D^3H(0) \end{Bmatrix} + n \left(2i\alpha \left(1 - \frac{i\alpha}{Re} \right) + \gamma \right) [C_6] \begin{Bmatrix} DG(0) \\ DH(0) \end{Bmatrix} = \begin{Bmatrix} 0 \\ 0 \end{Bmatrix} \quad (3-7)$$

$$\frac{(n^2-9)}{Re} [C_7] \begin{Bmatrix} D^4 G(0) \\ D^4 H(0) \end{Bmatrix} + (i\alpha [C_8] - \gamma [D_8]) \begin{Bmatrix} D^2 G(0) \\ D^2 H(0) \end{Bmatrix} \\ + (i\alpha [C_9] - \gamma \alpha^2 [D_9]) \begin{Bmatrix} G(0) \\ H(0) \end{Bmatrix} = \begin{Bmatrix} 0 \\ 0 \end{Bmatrix} \quad (3-8)$$

The 2 X 2 matrices which appear in equations (3-4) through (3-8) are defined in detail in Appendix C. Special conditions at the axis arise when the determinants of these matrices are evaluated at specific angular wave numbers. They are summarized in Appendix D.

For each specific value of angular wave number n , it is possible to derive a set of boundary conditions at the axis. Special conditions at the axis occur for angular wave numbers that cause the coefficients in equations (3-4) through (3-8) to equal zero or the determinants in Appendix D to be zero. That is to say, if a coefficient vanishes or the pair of equations are linearly dependent, the functions may be arbitrarily specified and are in general not equal to zero. But if the coefficient, appearing in equations (3-4) through (3-8) is non-zero and the determinant exists, the pair of functions must be identically zero. This situation occurs for all five pairs of variables when the angular wave number $n \geq 6$.

By taking these special conditions into account for the case $n = 0$, it can be deduced from equations (3-6) and (3-8) that,

$$\begin{Bmatrix} G(0) \\ H(0) \end{Bmatrix} = \begin{Bmatrix} D^2 G(0) \\ D^2 H(0) \end{Bmatrix} = \begin{Bmatrix} 0 \\ 0 \end{Bmatrix} \quad (3-9)$$

Carrying out this procedure for $n = 1, 2, 3, 4, 5$, and 6 yields a simplified set of boundary conditions at the axis. The following sets of equations (3-10) through (3-16) are essentially the same as those of Gawain [Ref. 13] but were independently checked and appear here with a few minor corrections.

$n = 0$

$$G(0) = 0 \qquad H(0) = 0 \qquad (a)$$

$$D^2G(0) = 0 \qquad D^2H(0) = 0 \qquad (b)$$

(3-10)

$n = 1$

$$G(0) + i H(0) = 0 \qquad (a)$$

$$DG(0) = 0 \qquad DH(0) = 0$$

$$D^3G(0) = 0 \qquad D^3H(0) = 0 \qquad (b)$$

(3-11)

$$- \frac{8}{\text{Re}} [C_7] \begin{Bmatrix} D^4G(0) \\ D^4H(0) \end{Bmatrix} + (i\alpha [C_8] - \gamma [D_8]) \begin{Bmatrix} D^2G(0) \\ D^2H(0) \end{Bmatrix} \qquad (b)$$

$$+ (i\alpha [C_9] - \gamma \alpha^2 [D_9]) \begin{Bmatrix} G(0) \\ H(0) \end{Bmatrix} = \begin{Bmatrix} 0 \\ 0 \end{Bmatrix}$$

$n = 2$

$$G(0) = 0 \qquad H(0) = 0 \qquad (a)$$

$$DG(0) + i DH(0) = 0$$

$$D^2G(0) = 0 \qquad D^2H(0) = 0 \qquad (b)$$

$$D^4G(0) = 0 \qquad D^4H(0) = 0$$

(3-12)

$n = 3$

$$G(0) = 0$$

$$H(0) = 0$$

(a)

$$DG(0) = 0$$

$$DH(0) = 0$$

(3-13)

$$D^2G(0) + i D^2H(0) = 0$$

(b)

$$D^3G(0) = 0$$

$$D^3H(0) = 0$$

$n = 4$

$$G(0) = 0$$

$$H(0) = 0$$

$$DG(0) = 0$$

$$DH(0) = 0$$

(a)

$$D^2G(0) = 0$$

$$D^2H(0) = 0$$

(3-14)

$$D^3G(0) + i D^3H(0) = 0$$

(b)

$$D^4G(0) = 0$$

$$D^4H(0) = 0$$

$n = 5$

$$G(0) = 0$$

$$H(0) = 0$$

$$DG(0) = 0$$

$$DH(0) = 0$$

(a)

$$D^2G(0) = 0$$

$$D^2H(0) = 0$$

(3-15)

$$D^3G(0) = 0$$

$$D^3H(0) = 0$$

(b)

$$D^4G(0) + i D^4H(0) = 0$$

$n \geq 6$

$$G(0) = 0$$

$$DG(0) = 0$$

$$D^2G(0) = 0$$

$$D^3G(0) = 0$$

$$H(0) = 0$$

$$DH(0) = 0$$

$$D^2H(0) = 0$$

(a)

(3-16)

$$D^4G(0) = 0$$

$$D^3H(0) = 0$$

(b)

$$D^4H(0) = 0$$

Recall that exactly three boundary conditions are required at the axis to finalize the solution of the vorticity transport equations. Equations (3-10) through (3-16) contain from four to ten boundary constraints including linear combinations of several boundary conditions, as suggested earlier. By introducing appropriate changes of variables, the pair of functions in $G(r)$ and $H(r)$ and their respective derivatives can be transformed to a new pair of functions in terms of $P(r)$ and $Q(r)$ and their derivatives. The transformed system of equations take the form of equation (2-40) for all values of n , except for $n = 1$ where equation (2-47) is applicable. The change of variables is dependent on each specific value of n up through six and is chosen in such a way that the boundary conditions in subset (a) of equation (3-10) through (3-16) are satisfied identically. The boundary conditions in subset (b) must be satisfied explicitly in the finite difference equations near the axis. Development of the finite difference equations is discussed in the chapter on Numerical Methods.

The following sets of equations are taken from Gawain [Ref. 13] and are included here so that a complete treatment of the subject on boundary conditions is contained in this paper.

$n = 0$

Change of Variables

$$G(r) = rP(r) \quad (a)$$

$$H(r) = rQ(r)$$

Boundary Conditions at Axis (3-17)

$$\begin{aligned} DP(0) &= 0 & DQ(0) &= 0 \\ D^3Q(0) &= 0 \end{aligned} \quad (b)$$

Boundary Conditions at Wall

$$\begin{aligned} P(1) &= 0 & Q(1) &= 0 \\ DQ(1) &= 0 \end{aligned} \quad (c)$$

The solutions for $P(r)$ and $Q(r)$ become uncoupled for $n = 0$

$n = 1$

Change of Variables

$$G(r) = -i H(0) + r^2 P(r) \quad (a)$$

$$H(r) = H(0) + r^2 Q(r)$$

Boundary Conditions at Axis (3-18)

$$DP(0) = 0 \quad DQ(0) = 0$$

$$- \frac{96}{Re} [C_7] \begin{Bmatrix} D^2P(0) \\ D^2Q(0) \end{Bmatrix} + 2i\alpha[C_8] \begin{Bmatrix} P(0) \\ Q(0) \end{Bmatrix} + i\alpha[C_9] \begin{Bmatrix} -i \\ 1 \end{Bmatrix} H(0)$$

$$= + \gamma \left(2[D_8] \begin{Bmatrix} P(0) \\ Q(0) \end{Bmatrix} + \alpha^2 [D_9] \begin{Bmatrix} -i \\ 1 \end{Bmatrix} H(0) \right) \quad (b)$$

Boundary Conditions at Wall

$$\begin{aligned} -i H(0) + P(1) &= 0 & H(0) + Q(1) &= 0 \\ -2H(0) + DQ(1) &= 0 \end{aligned} \quad (c)$$

$$n = 2$$

Change of Variables

$$G(r) = -i r DH(0) + r^2 P(r) \quad (a)$$

$$H(r) = r DH(0) + r^2 Q(r)$$

Boundary Conditions at Axis (3-19)

$$P(0) = 0 \quad Q(0) = 0 \quad (b)$$

$$D^2P(0) = 0 \quad D^2Q(0) = 0$$

Boundary Conditions at Wall

$$-i DH(0) + P(1) = 0 \quad DH(0) + Q(1) = 0 \quad (c)$$

$$-DH(0) + DQ(1) = 0$$

$$n = 3$$

Change of Variables

$$G(r) = r^2 P(r) \quad (a)$$

$$H(r) = r^2 Q(r)$$

Boundary Conditions at Axis (3-20)

$$P(0) + i Q(0) = 0 \quad (b)$$

$$DP(0) = 0 \quad DQ(0) = 0$$

Boundary Conditions at Wall

$$P(1) = 0 \quad Q(1) = 0 \quad (c)$$

$$DQ(1) = 0$$

$$n = 4$$

Change of Variables

$$G(r) = r^3 P(r) \quad (a)$$

$$H(r) = r^3 Q(r)$$

Boundary Conditions at Axis (3-21)

$$P(0) + i Q(0) = 0 \quad (b)$$

$$DP(0) = 0 \quad DQ(0) = 0$$

Boundary Conditions at Wall

$$P(1) = 0 \quad Q(1) = 0 \quad (c)$$

$$DQ(1) = 0$$

$$n = 5$$

Change of Variables

$$G(r) = r^3 P(r) \quad (a)$$

$$H(r) = r^3 Q(r)$$

Boundary Conditions at Axis (3-22)

$$P(0) = 0 \quad Q(0) = 0 \quad (b)$$

$$DP(0) + i DQ(0) = 0$$

Boundary Conditions at Wall

$$P(1) = 0 \quad Q(1) = 0 \quad (c)$$

$$DQ(1) = 0$$

$$n \geq 6$$

Change of Variables

$$G(r) = r^4 P(r) \tag{a}$$

$$H(r) = r^3 Q(r)$$

Boundary Conditions at Axis (3-23)

$$P(0) = 0 \qquad Q(0) = 0 \tag{b}$$

$$DQ(0) = 0$$

Boundary Conditions at Wall

$$P(1) = 0 \qquad Q(1) = 0 \tag{c}$$

$$DQ(1) = 0$$

It should be noted that the change of variable relations in subset (a) of equations (3-17) through (3-23) does not change the order of the derivatives appearing in the transformed vorticity transport equations. Upon close examination of subsets (b) and (c) of these equations, it is apparent that the correct number of boundary conditions required for the solution of the transformed equations has resulted from the change of variables. The vorticity transport equations are now expressed in terms of $P(r)$ and $Q(r)$ and their derivatives and have exactly three boundary conditions at the pipe wall for all values of n and three boundary conditions at the axis for all values of n , except for $n = 1$ and 2 . The fact that there are four boundary conditions at the axis for angular wave numbers $n = 1$ and 2 warrants further comment here.

Notice in equations (3-18a) and (3-19a) for the cases $n = 1$ and 2 that an additional parameter is introduced by the change of variable equations. The additional parameter for $n = 1$ is $H(0)$ and for $n = 2$ is $DH(0)$. The introduction of the parameter for each case requires the specification of four boundary conditions at the axis instead of the usual three. This conclusion was reached by Gawain [Ref. 13] and is analyzed in detail in his paper. There is one other peculiarity about the boundary conditions at the axis for $n = 1$ that should be mentioned. The axis boundary conditions in equation (3-18b) contain a pair of equations that involve the complex perturbation frequency γ , which represents an eigenvalue of the solution for the equations. The presence of γ in the axis boundary condition for $n = 1$ is an important factor in formulating a solution for the vorticity transport equations and is included in the eigensystem of the finite difference equations. The details of the implementation are discussed later.

The solution of the problem for predicting the onset of flow instabilities in circular pipes is now at hand. The original vorticity transport equations (2-40) are transformed to the functions $P(r)$ and $Q(r)$ and their respective derivatives by the appropriate change of variables depending on the specific angular wave number being investigated. After imposing the rigorously deduced boundary conditions, a solution can be determined in the perturbation quantities.

IV. PERTURBATION VELOCITY

The solution of the transformed vorticity transport equations developed in the previous chapter can now be expressed in terms of the perturbation quantities $P(r)$ and $Q(r)$. The original functions $G(r)$ and $H(r)$ are actually components of the vector potential function \vec{W} defined in equation (2-28),

$$\vec{W} = [F(r) \vec{e}_x + G(r) \vec{e}_r + H(r) \vec{e}_\theta] e^x \quad (2-28)$$

The axial component $F(r)$ was previously set to zero since one function could be arbitrarily specified. From equation (2-27) the perturbation velocity vector was expressed as,

$$\vec{v} = \nabla \times \vec{W} \quad (2-27)$$

Therefore the functions $G(r)$ and $H(r)$ represent the behavior of the perturbation velocity in the flow field. Referring back to the definition of the curl operation in equation (2-39), the relation for $\nabla \times \vec{W}$ has already been set up. The resulting expression for the perturbation velocity is given by,

$$\vec{v} = u \vec{e}_x + v \vec{e}_r + w \vec{e}_\theta \quad (4-1)$$

The components of the perturbation velocity are,

$$u = DH(r) + \frac{H(r)}{r} - \frac{in}{r} G(r) \quad (4-2)$$

$$v = -i\alpha H(r) \quad (4-3)$$

$$w = i\alpha G(r) \quad (4-4)$$

Digressing for a moment, it can be readily seen that since the perturbation velocity necessarily vanishes at the pipe wall, $r = 1$, the boundary conditions at the wall in equation (3-1) can be deduced.

Recall that the functions $P(r)$ and $Q(r)$ appear as the result of the change of variables for each specific angular wave number contained in subset (a) of equations (3-17) through (3-23). Analysis of the axial component of the perturbation velocity u becomes useful in interpreting the behavior of the functions $P(r)$ and $Q(r)$ along the radius of the pipe. Equations for the axial perturbation velocity in terms of $P(r)$ and $Q(r)$ are derived from equations (4-2) through (4-4) with the change of variable applied for each angular wave number being investigated and appear as follows,

$$n = 0 : \quad u = 2 Q + r DQ \quad (4-5)$$

$$n = 1 : \quad u = 3 r Q + r^2 DQ - i r P \quad (4-6)$$

$$n = 6 : \quad u = 4 r^2 Q + r^3 DQ - i 6 r^3 P \quad (4-7)$$

The axial perturbation velocity is computed in part VII of the main investigative program for each angular wave number. To prepare the perturbation velocity u for plotting versus pipe radius, it is first

normalized. Since this velocity is in general a complex quantity, the perturbation velocity with the largest magnitude is determined by,

$$|u_c|_{\text{MAX}} = (u_R^2 + u_I^2)^{\frac{1}{2}} \quad (4-8)$$

The normalizing velocity constant will then become u_c and the maximum normalized velocity will become,

$$\frac{u}{u_c} = 1 + i(0) \quad (4-9)$$

The remaining normalized velocities are found by dividing through by u_c . The normalized perturbation velocity is then plotted versus the normalized pipe radius for various axial wave numbers and Reynolds numbers at the three angular wave numbers investigated. The plots and results are discussed in detail in the chapter on Results.

V. NUMERICAL METHODS

A. GENERAL METHODS USED

In general, the vorticity transport equations are a pair of coupled homogeneous differential equations which are second order in the perturbation quantity $G(r)$ and fourth order in the perturbation quantity $H(r)$. A change of variables is introduced so that the number of boundary conditions at the axis is reduced to three for each angular wave number investigated, except for $n = 1$. Recall for this case that there are four boundary conditions imposed at the axis because of the introduction of the additional parameter $H(0)$. By applying the change of variables to the original pair of equations, the vorticity transport equations are transformed into an equivalent pair of coupled homogeneous differential equations that are second order in $P(r)$ and fourth order in $Q(r)$. The solution of the vorticity transport equations will now be in terms of the perturbation quantities $P(r)$ and $Q(r)$ which are also referred to as eigenfunctions, and γ which is an eigenvalue. The axial perturbation velocity is expressed in terms of $P(r)$ and $Q(r)$ as derived previously and is examined to determine the behavior of the perturbation quantities. The resulting eigenvalue γ is of primary interest since the magnitude and sign of the real part of γ determines the relative stability or instability of the pipe flow problem.

A numerical solution of the transformed vorticity transport equations is now sought. The convenient matrix format of the equations is given below.

$$\begin{aligned}
 & [M_4'] \begin{Bmatrix} D^4P \\ D^4Q \end{Bmatrix} + [M_3'] \begin{Bmatrix} D^3P \\ D^3Q \end{Bmatrix} + [M_2'] \begin{Bmatrix} D^2P \\ D^2Q \end{Bmatrix} + [M_1'] \begin{Bmatrix} DP \\ DQ \end{Bmatrix} + [M_0'] \begin{Bmatrix} P \\ Q \end{Bmatrix} = \\
 & \gamma [N_2'] \begin{Bmatrix} D^2P \\ D^2Q \end{Bmatrix} + [N_1'] \begin{Bmatrix} DP \\ DQ \end{Bmatrix} + [N_0'] \begin{Bmatrix} P \\ Q \end{Bmatrix}
 \end{aligned} \tag{5-1}$$

The details of the transformed coefficient matrices for $n = 0, 1$, and 6 are given in Appendix B. It is convenient to approximate the derivatives of $P(r)$ and $Q(r)$ by a finite number of discrete unknowns along a radial mesh consisting of N interior points. It is not possible to compute the continuous values of the functions and their derivatives along the pipe radius using a digital computer. Therefore, discrete finite difference techniques are used. For the problem at hand, the normalized nondimensional radius of the pipe, which becomes the independent variable, is divided into a computational mesh. The standard method of representing this mesh is with uniformly spaced stations over the interval $0 < r < 1$, Figure 5-1.

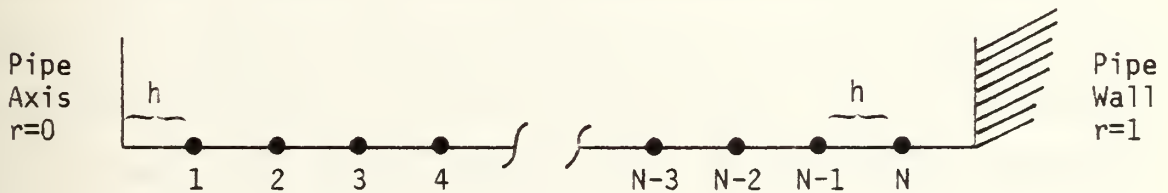


Figure 5-1. Radial Mesh, Standard Method

The vorticity transport equation coefficients are then evaluated at each station of the radial mesh resulting in N uniformly spaced discrete values with $N + 1$ equal intervals and $N + 2$ total points, including $r = 0$ and $r = 1$. The spacing between the stations is denoted by $h = 1/(N + 1)$.

A refinement of the method for generating a computational mesh is referred to as the half station method and is used in this numerical analysis. All the radial stations of Figure 5-1 are moved to mid-interval or one half station ($h/2$) toward the axis with an additional station appearing at one half station from the pipe wall, as shown in Figure 5-2.

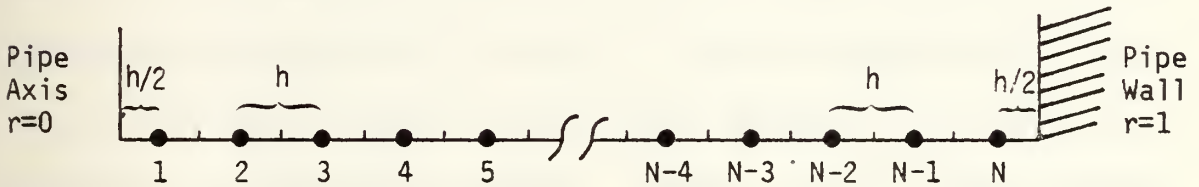


Figure 5-2. Radial Mesh, Half Station Method

Therefore for N interior stations, the method results in N intervals and $N + 2$ total points including the boundaries. The first station, r_1 , is a distance $h/2$ from the axis and the N th station, r_N , is a distance $h/2$ from the wall. The general expression for the i th station, corresponding to the i th increment of the radius, is given by,

$$r_i = h \left(i - \frac{1}{2} \right) ; i = 1, 2, 3, \dots, N \quad (5-2)$$

where $h = 1/N$.

An advantage of the half station method over the standard method is that there is better resolution at the stations near the boundaries where instabilities are thought to originate and where boundary layer effects are a factor. Therefore, the behavior of the perturbation quantities can be examined more closely. Additionally, better approximations for the derivatives of the functions $P(r)$ and $Q(r)$ can be realized with a smaller incremental distance to the points immediately adjacent to the boundaries. Even better resolution at the boundaries can be achieved by using a nonuniform computational mesh. Arnold [Ref. 11] introduced a change of independent variable by means of hyperbolic functions which included a mesh offset parameter so that he could control the concentration of mesh points at either the axis or wall. The method would certainly be useful in reducing computational time by reducing the total number of mesh points required for a satisfactory solution of the governing equations. However, the full implications of the nonuniform mesh with respect to α and γ dependence on the mesh offset parameter have not been fully explored. While this method is not used here, it may well prove to be useful in follow-on numerical investigations of the pipe flow problem.

The solution for the vorticity transport equations in terms of the perturbation quantities $P(r)$ and $Q(r)$ are now represented by a finite number of discrete unknowns. The governing differential equations are rewritten in finite difference form for N stations along the mesh resulting in a finite number of unknowns namely, $P_1, P_2, P_3, \dots, P_N$ and $Q_1, Q_2, Q_3, \dots, Q_N$. In general, this produces $2N$ simultaneous equations in $2N$

unknowns. The details of the derivation of the finite difference equations are explained shortly. Substituting the finite difference equations into the vorticity transport equation matrix format of equation (5-1) will result in N pairs of coupled simultaneous equations. These equations are regrouped and subsequently solved in the following eigenvalue problem format,

$$[A] \{X\} = \gamma [B] \{X\} \quad (5-3)$$

The column vector $\{X\}$ represents the rearranged unknowns as

$$\{X\} = \begin{Bmatrix} P_1 \\ P_2 \\ \vdots \\ P_i \\ \vdots \\ P_N \\ Q_1 \\ Q_2 \\ \vdots \\ Q_i \\ \vdots \\ Q_N \end{Bmatrix} \quad (5-4)$$

The symbol γ denotes the characteristic value or eigenvalue of the solution. Details of the composition of the $[A]$ and $[B]$ matrices are discussed for each specific angular wave number investigated.

B. FINITE DIFFERENCE EQUATIONS

The use of finite differencing techniques is the basis for solving the governing vorticity transport equations in the eigensystem equation (5-3). It is required that the governing equations must be satisfied at each of the interior stations $i = 1, 2, 3, \dots, N$, therefore producing $2N$ equations in $2N$ unknowns.

Except for stations adjacent to the boundaries, the derivatives of the perturbation quantities in the governing equations at the interior stations are usually approximated by standard central finite difference equations. These equations were taken from Table 7.27 of Ketter and Prawel [Ref. 14] and are summarized below,

$$DF_i = \frac{1}{12h} \left\{ F_{i-2} - 8F_{i-1} + 8F_{i+1} - F_{i+2} \right\} + \frac{1}{30} h^4 D^5 F_i \quad (5-5)$$

$$D^2 F_i = \frac{1}{12h^2} \left\{ -F_{i-2} + 16F_{i-1} - 30F_i + 16F_{i+1} - F_{i+2} \right\} + \frac{1}{90} h^4 D^6 F_i \quad (5-6)$$

$$D^3 F_i = \frac{1}{8h^3} \left\{ F_{i-3} - 8F_{i-2} + 13F_{i-1} - 13F_{i+1} + 8F_{i+2} - F_{i+3} \right\} + \frac{7}{120} h^4 D^7 F_i \quad (5-7)$$

$$D^4 F_i = \frac{1}{6h^4} \left\{ -F_{i-3} + 12F_{i-2} - 39F_{i-1} + 56F_i - 39F_{i+1} + 12F_{i+2} - F_{i+3} \right\} + \frac{7}{240} h^4 D^8 F_i \quad (5-8)$$

where F is an arbitrary function.

As can be seen from the equations above, the derivative of a function at a particular station can be approximated by a linear combination of the discrete unknown functions about a central point. The term outside the brackets in each equation represents the truncation error of the corresponding finite difference approximation. Notice that the truncation error of equations (5-5) through (5-8) are all of order h^4 ($O(h^4)$). It was hypothesized and shown by Gawain and Ball [Ref. 15] that finite difference approximations of consistent order truncation error reduced the overall error of the numerical solution in a typical problem by a factor of five for truncation error $O(h^2)$. For the present numerical analysis, a computational mesh of $N = 50$ was used for all cases. Now with the interval $h = 1/N = 0.02$, examination of the consistent fourth order truncation error term will yield an error of the order of 5×10^{-9} for all four derivatives approximated, since the magnitude of the normalized functions and derivatives are of order one. For an interval size of $h = 0.02$, a consistent truncation error $O(h^4)$ should significantly reduce the overall error of the solution.

Special problems arise in the derivation of the finite difference equations at stations near the boundaries. Several approaches can be taken to approximate the derivatives at these stations, which include backward, forward and central finite differencing techniques. Unfortunately, the central method previously discussed will involve imaginary stations outside the boundaries for stations close to the axis and wall, i.e., stations $i = -1, -2, -3$, and $N+1, N+2, N+3$ are involved in the fourth derivative approximation at station $i = 1$ and $i = N$, respectively. Unlike the boundary conditions for many problems well suited for this

type of numerical analysis, the vorticity transport equation boundary conditions for the pipe flow problem are very complicated by comparison. The boundary conditions for each angular wave number are different; some involve additional parameters while others contain the eigenvalue γ . In other words, the conditions at the imaginary stations for conventional problems can normally be expressed in terms of conditions at the real stations in the computational mesh. It is therefore impractical to use the central method for the pipe flow problem because of the complicated nature of the boundary conditions.

The method of forward differencing is used near the pipe axis and backward differencing is used near the wall. These two differencing methods will be referred to, collectively, as noncentral finite differencing techniques. It will be shown later that the two methods are essentially equivalent. A rigorous derivation of the noncentral finite difference equations is based on the Taylor series (power series) expansion of the function at a point. Since the governing equations contain the fourth order derivative of $Q(r)$, the derivation for this case is examined in detail here.

The Taylor series approximation of $Q_i(r)$ at station $i = 1$ appears as equation (5-9).

$$\begin{aligned}
 Q_1 = Q(0) + DQ(0) \frac{h}{2} + D^2Q(0) \frac{\left(\frac{h}{2}\right)^2}{2!} + D^3Q(0) \frac{\left(\frac{h}{2}\right)^3}{3!} + D^4Q(0) \frac{\left(\frac{h}{2}\right)^4}{4!} \\
 + D^5Q(0) \frac{\left(\frac{h}{2}\right)^5}{5!} + D^6Q(0) \frac{\left(\frac{h}{2}\right)^6}{6!} + D^7Q(0) \frac{\left(\frac{h}{2}\right)^7}{7!} + \dots
 \end{aligned} \tag{5-9}$$

The approximation for Q_i at stations $i = 1, 2, 3, 4, 5, 6$ are expressed in convenient matrix format below,

$$\begin{Bmatrix} Q_1 \\ Q_2 \\ Q_3 \\ Q_4 \\ Q_5 \\ Q_6 \end{Bmatrix} = \begin{bmatrix} 1 & \frac{1}{2} & \frac{(\frac{1}{2})^2}{2!} & \frac{(\frac{1}{2})^3}{3!} & \frac{(\frac{1}{2})^4}{4!} & \frac{(\frac{1}{2})^5}{5!} & \frac{(\frac{1}{2})^6}{6!} & \frac{(\frac{1}{2})^7}{7!} \\ 1 & \frac{3}{2} & \frac{(\frac{3}{2})^2}{2!} & \frac{(\frac{3}{2})^3}{3!} & \frac{(\frac{3}{2})^4}{4!} & \frac{(\frac{3}{2})^5}{5!} & \cdot & \cdot \\ 1 & \frac{5}{2} & \frac{(\frac{5}{2})^2}{2!} & \cdot & \cdot & \cdot & \cdot & \cdot \\ 1 & \frac{7}{2} & \frac{(\frac{7}{2})^2}{2!} & \cdot & \cdot & \cdot & \cdot & \cdot \\ 1 & \frac{9}{2} & \frac{(\frac{9}{2})^2}{2!} & \cdot & \cdot & \cdot & \cdot & \cdot \\ 1 & \frac{11}{2} & \frac{(\frac{11}{2})^2}{2!} & \cdot & \cdot & \cdot & \cdot & \cdot \end{bmatrix}$$

6x8

$$\begin{Bmatrix} Q(0) \\ hDQ(0) \\ h^2D^2Q(0) \\ h^3D^3Q(0) \\ h^4D^4Q(0) \\ h^5D^5Q(0) \\ h^6D^6Q(0) \\ h^7D^7Q(0) \end{Bmatrix} + \{E_1\} h^8D^8Q(0) \quad (5-10)$$

where the dots represent matrix elements that can be easily deduced.

Since the fourth order derivative of $Q(r)$ is present in the vorticity transport equations, there will be two boundary conditions specified at the axis and two at the wall. It can be shown that two columns of the matrix in equation (5-10) can be eliminated since two of the functions in the column vector are either zero or can be expressed in terms of additional parameters. The matrix, which will be denoted as $[AA]$, now becomes a square 6×6 matrix. Notice that the column vector $\{E_1\}$ represents the last nonvanishing term in the Taylor series. The approximation for the first derivative of $Q_i(r)$ at station $i = 1$ is given by,

$$\begin{aligned} DQ_1 = & DQ(0) + D^2Q(0) \frac{h}{2} + D^3Q(0) \frac{\left(\frac{h}{2}\right)^2}{2!} + D^4Q(0) \frac{\left(\frac{h}{2}\right)^3}{3!} + D^5Q(0) \frac{\left(\frac{h}{2}\right)^4}{4!} \\ & + D^6Q(0) \frac{\left(\frac{h}{2}\right)^5}{5!} + D^7Q(0) \frac{\left(\frac{h}{2}\right)^6}{6!} + \dots \end{aligned} \quad (5-11)$$

The Taylor series expansion for the second, third, and fourth derivative can be found by successive differentiation of equation (5-11). The first four derivatives of Q_i at station $i = 1$ can be expressed in matrix format as,

$$\begin{Bmatrix} hDQ_1 \\ h^2D^2Q_1 \\ h^3D^3Q_1 \\ h^4D^4Q_1 \end{Bmatrix} = \begin{bmatrix} 0 & 1 & (\frac{1}{2}) & \frac{(\frac{1}{2})^2}{2!} & \frac{(\frac{1}{2})^3}{3!} & \frac{(\frac{1}{2})^4}{4!} & \frac{(\frac{1}{2})^5}{5!} & \frac{(\frac{1}{2})^6}{6!} \\ 0 & 0 & 1 & (\frac{1}{2}) & \frac{(\frac{1}{2})^2}{2!} & \frac{(\frac{1}{2})^3}{3!} & \frac{(\frac{1}{2})^4}{4!} & \frac{(\frac{1}{2})^5}{5!} \\ 0 & 0 & 0 & 1 & (\frac{1}{2}) & \frac{(\frac{1}{2})^2}{2!} & \frac{(\frac{1}{2})^3}{3!} & \frac{(\frac{1}{2})^4}{4!} \\ 0 & 0 & 0 & 0 & 1 & (\frac{1}{2}) & \frac{(\frac{1}{2})^2}{2!} & \frac{(\frac{1}{2})^3}{3!} \end{bmatrix}$$

4x8

$$\begin{Bmatrix} Q(0) \\ hDQ(0) \\ h^2D^2Q(0) \\ h^3D^3Q(0) \\ h^4D^4Q(0) \\ h^5D^5Q(0) \\ h^6D^6Q(0) \\ h^7D^7Q(0) \end{Bmatrix} + \{E_2\} h^8D^8Q(0) \quad (5-12)$$

It can be shown here as well that two columns of the matrix in equation (5-12) can be eliminated so that the matrix denoted [CC] is now a 4 X 6 matrix. The column vector {E₂} also represents the last non-vanishing term in the Taylor series. It can be seen that the approximations for the derivatives of Q_i at stations i = 2 and i = 3 can be determined by replacing (1/2) in the [CC] matrix with (3/2) and (5/2), respectively.

To show how the noncentral finite difference approximations near the axis are formulated, the case for angular wave number $n \geq 6$ is examined. The boundary conditions at the axis for the function Q are,

$$Q(0) = 0 \quad \text{and} \quad DQ(0) = 0 \quad (5-13)$$

Applying these conditions to equations (5-10) and (5-12) will eliminate the first two columns of the $[AA]$ and $[CC]$ matrices since the first two terms of the column vectors vanish. The truncation error terms $\{E_1\}$ and $\{E_2\}$ are very small quantities and are neglected at this point. In shorthand notation, equation (5-10) now becomes,

$$\begin{Bmatrix} Q_1 \\ Q_2 \\ Q_3 \\ Q_4 \\ Q_5 \\ Q_6 \end{Bmatrix} = [AA]_{6 \times 6} \begin{Bmatrix} h^2 D^2 Q(0) \\ h^3 D^3 Q(0) \\ h^4 D^4 Q(0) \\ h^5 D^5 Q(0) \\ h^6 D^6 Q(0) \\ h^7 D^7 Q(0) \end{Bmatrix} \quad (5-14)$$

and equation (5-12) becomes,

$$\begin{Bmatrix} h D Q_1 \\ h^2 D^2 Q_1 \\ h^3 D^3 Q_1 \\ h^4 D^4 Q_1 \end{Bmatrix} = [CC]_{4 \times 6} \begin{Bmatrix} h^2 D^2 Q(0) \\ h^3 D^3 Q(0) \\ h^4 D^4 Q(0) \\ h^5 D^5 Q(0) \\ h^6 D^6 Q(0) \\ h^7 D^7 Q(0) \end{Bmatrix} \quad (5-15)$$

Equation (5-14) is multiplied through $[AA]^{-1}$ and becomes,

$$\begin{Bmatrix} h^2 D^2 Q(0) \\ h^3 D^3 Q(0) \\ h^4 D^4 Q(0) \\ h^5 D^5 Q(0) \\ h^6 D^6 Q(0) \\ h^7 D^7 Q(0) \end{Bmatrix} = [AA]_{6 \times 6}^{-1} \begin{Bmatrix} Q_1 \\ Q_2 \\ Q_3 \\ Q_4 \\ Q_5 \\ Q_6 \end{Bmatrix} \quad (5-16)$$

and is then substituted into equation (5-15) giving,

$$\begin{Bmatrix} h D Q_1 \\ h^2 D^2 Q_1 \\ h^3 D^3 Q_1 \\ h^4 D^4 Q_1 \end{Bmatrix} = [CC]_{4 \times 6} [AA]_{6 \times 6}^{-1} \begin{Bmatrix} Q_1 \\ Q_2 \\ Q_3 \\ Q_4 \\ Q_5 \\ Q_6 \end{Bmatrix} \quad (5-17)$$

Now, the fourth derivative of Q_i at station $i = 1$ is approximated in terms of the discrete functions of Q at the interior mesh points with truncation error Oh^4 . The values on the bottom row of the resulting 4×6 matrix after multiplication in equation (5-17) are the coefficients of the column vector Q_1 through Q_6 for $D^4 Q_1$. In order to have consistent truncation error Oh^4 , the last row and last column of the $[AA]$ and $[CC]$ matrices are deleted for the third derivative of Q . Matrix $[AA]$ becomes a 5×5 and is now inverted and matrix $[CC]$ becomes a 3×5 . The values on the bottom row of the resulting 3×5 matrix are

the coefficients of Q_1 through Q_5 which approximates D^3Q_1 . The rows and columns of matrices [AA] and [CC] are successively reduced to determine the coefficients for D^2Q_1 in terms of Q_1 through Q_4 , and DQ_1 in terms of Q_1 through Q_3 so that consistent truncation error Oh^4 is preserved throughout. The noncentral finite difference equation for D^4Q_1 will now appear as,

$$D^4Q_1 = \frac{1}{h^4} (A_1Q_1 + A_2Q_2 + A_3Q_3 + A_4Q_4 + A_5Q_5 + A_6Q_6) + Oh^4 \quad (5-18)$$

where A_1 through A_6 are the coefficients taken from the bottom row of the resulting matrix in equation (5-17)

In a similar manner, by imposing the required boundary conditions, this process can be carried out to determine the noncentral finite difference equations for the first two derivatives of $P(r)$ at several points near the boundaries as required.

It is important to note here that the noncentral finite difference approximations near the wall can be formulated by using the same techniques as those used near the axis. Once again taking the case for angular wave number $n \geq 6$, the boundary conditions at the pipe wall for the function Q are,

$$Q(1) = 0 \quad \text{and} \quad DQ(1) = 0 \quad (5-19)$$

Rather than set up complete new [AA] and [CC] matrices at different values of r in the Taylor series expansion near the wall, assume that the boundary conditions in equation (5-19) are imposed at the axis,

$r = 0$. Notice that the boundary conditions in equation (5-19) are now identical to the boundary conditions in equation (5-13). The method for computing the coefficients of the noncentral finite difference approximations at the wall can be carried out as discussed previously and, in this case, have already been computed. It can be shown that the A_i coefficients of equation (5-18) are applicable to D^4Q_N at the wall but will appear in reverse order. The noncentral finite difference equation for D^4Q_N is given by,

$$D^4Q_N = \frac{1}{h^4} (A_6Q_{N-5} + A_5Q_{N-4} + A_4Q_{N-3} + A_3Q_{N-2} + A_2Q_{N-1} + A_1Q_N) + Oh^4 \quad (5-20)$$

The method for determining the coefficients for the remaining derivatives of Q and P near the wall proceed as though the boundary conditions were imposed at the axis; the coefficients are computed, their order reversed and coefficients of the odd order derivatives undergo a sign change. Order reversal and sign changes are accomplished in part II of the main investigative program when the precomputed noncentral finite difference coefficients are read in as data.

As can be seen from the central finite difference approximations of equations (5-5) through (5-8), the third and fourth derivatives of a function require three points either side of the central point being approximated. The first and second derivatives require only two points either side of the central point. Therefore the central finite difference approximations are applicable only to interior stations $i = 4$ through $N-3$ for D^4Q_i and D^3Q_i , and stations $i = 3$ through $N-2$ for D^2Q_i ,

DQ_i , D^2P_i , and DP_i . This leaves either two or three points immediately adjacent to the boundaries to be approximated by the noncentral finite difference equations just developed.

Since the central finite difference approximations are applicable to the above mentioned interior mesh points and are valid for all the derivatives of $P(r)$ and $Q(r)$ as well, the coefficients are computed only once in part I of the main investigative program in double precision format. The coefficients of the noncentral finite difference approximations, which are dependent on the boundary conditions for each angular wave number, are computed in an independent computer program. The resulting noncentral coefficients for the derivatives of $P(r)$ and $Q(r)$ at mesh points near the boundaries are also computed in double precision format and are read into part II of the main investigative program as data.

C. SPECIFIC METHODS FOR $n = 0, 1$, AND 6

The vorticity transport equations have now been expanded into a set of discrete simultaneous equations with respect to a half station computational mesh of N points (stations). The derivatives of the governing equations were approximated by central and noncentral finite difference coefficients, with consistent fourth order truncation error, in terms of the discrete unknown functions of the system. The convenient matrix format of the eigensystem in equation (5-3) can now be solved on a digital computer using a specialized Fortran subroutine, which will be discussed later. It is important to understand the composition of the $[A]$ and $[B]$ matrices and the column vector of unknowns

{X}. The problem setup is examined in detail for each angular wave number investigated. In the following discussions, the vorticity transport equations are referred to in the transformed state after the change of variables to $P(r)$ and $Q(r)$ have been made. The boundary conditions in equations (3-17), (3-18), and (3-23), and the coefficients in Appendix B also apply.

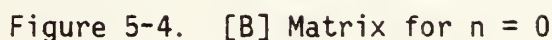
For the case $n = 0$, the pipe flow problem becomes greatly simplified in that the equations become uncoupled and only the solution for $Q(r)$ is investigated for reasons explained earlier. The governing equation in terms of $Q(r)$ is represented by equation (2-38). At the outset, it was determined that a mesh size of $N = 50$ was sufficient to produce a satisfactory numerical solution of the problem. It was necessary to determine when the solution was relatively independent of mesh size. Preliminary trial computations were performed for various mesh sizes, $N = 25$ to 100. From $N = 45$ to 100, the solution of the equation for $n = 0$ did not vary appreciably. Additionally, the solution was relatively independent of Reynolds numbers below 15,000 for mesh sizes of about 50. In order to reduce computation time and the eigensystem matrix size, a mesh of $N = 50$ was used in this analysis.

In general for angular wave number $n = 0$, the $[A]$ and $[B]$ matrices are 50×50 and appear as banded diagonal matrices. For a consistent order truncation error $O(h^4)$ used here, the derivative of highest order requires the greatest band width. From the governing equation in Q , it can be seen that the highest order derivative in $[A]$ is D^4Q and in $[B]$ is D^2Q . At stations near the boundaries, the noncentral finite difference coefficients require a band width of six in matrix $[A]$ and four in

matrix [B]. At interior stations, the central finite difference coefficients require a band width of seven for [A] and five for [B]. Therefore the [A] and [B] matrices of equation (5-3) contain nonzero elements as shown in Figures 5-3 and 5-4. The X elements contain non-central finite difference coefficients and the 0 elements contain central difference coefficients. The X and 0 symbols denote the station at which the approximation is made. The composition of the column vector {X} can also be seen in Figures 5-3 and 5-4.

$$\begin{bmatrix}
 \text{XXXXXX} \\
 \text{XXXXXX} \\
 \text{XXXXXX} \\
 0000000 \\
 0000000 & \dots\dots\dots \\
 & 0000000 & \dots\dots\dots \\
 & & 0000000 \\
 & & 0000000 \\
 & & \text{XXXXXX} \\
 & & \text{XXXXXX} \\
 & & \text{XXXXXX}
 \end{bmatrix}
 \begin{Bmatrix}
 Q_1 \\
 Q_2 \\
 Q_3 \\
 \vdots \\
 Q_i \\
 \vdots \\
 Q_{N-2} \\
 Q_{N-1} \\
 Q_N
 \end{Bmatrix}$$

Figure 5-3. [A] Matrix for $n = 0$


$$\gamma(N_2'_{ij} D^2 Q_{ij} + N_1'_{ij} DQ_{ij} + N_0'_{ij} Q_{ij}) \quad (5-21)$$

70

For example, the matrix elements for the first row of [A] can be found as follows, where the a_i coefficients are analogous to the coefficients A_i of equation (5-18) and are equal to $a_i = A_i/h^4$. Similarly $b_i = B_i/h^3$, $c_i = C_i/h^2$, and $d_i = D_i/h$, where b_i , c_i , and d_i are the noncentral finite difference coefficients of the remaining three derivatives.

$$A_{1,1} \{Q_1\} = (M'_{4,1} a_1 + M'_{3,1} b_1 + M'_{2,1} c_1 + M'_{1,1} d_1 + M'_{0,1}) \{Q_1\} \quad (5-22)$$

$$A_{1,2} \{Q_2\} = (M'_{4,1} a_2 + M'_{3,1} b_2 + M'_{2,1} c_2 + M'_{1,1} d_2) \{Q_2\} \quad (5-23)$$

$$A_{1,3} \{Q_3\} = (M'_{4,1} a_3 + M'_{3,1} b_3 + M'_{2,1} c_3 + M'_{1,1} d_3) \{Q_3\} \quad (5-24)$$

$$A_{1,4} \{Q_4\} = (M'_{4,1} a_4 + M'_{3,1} b_4 + M'_{2,1} c_4) \{Q_4\} \quad (5-25)$$

$$A_{1,5} \{Q_5\} = (M'_{4,1} a_5 + M'_{3,1} b_5) \{Q_5\} \quad (5-26)$$

$$A_{1,6} \{Q_6\} = (M'_{4,1} a_6) \{Q_6\} \quad (5-27)$$

where $A_{1,1}$ is the matrix element in the first row and the first column of [A], and so forth. This procedure is carried out for N equations along the computational mesh until all the nonzero matrix elements of [A] and [B] are computed.

Derivation of the noncentral finite difference coefficients for other angular wave numbers is fairly straightforward when accomplished by the methods outlined in the previous section. The boundary conditions for Q at the axis for $n = 0$ are,

$$DQ(0) = 0 \quad \text{and} \quad D^3Q(0) = 0 \quad (5-28)$$

After imposing these conditions, the second and fourth columns of the matrices in equations (5-10) and (5-12) can be eliminated since the corresponding terms in the column vectors vanish. The coefficients are then computed as described before in an independent computer program and then read into the main investigative program as data. Notice that the boundary conditions for the function Q at the wall are the same for $n = 0$ and $n \geq 6$. Therefore, the noncentral finite difference coefficients need to be computed only once.

The case for angular wave number $n \geq 6$ will be examined next since it more nearly represents the general case. Since the vorticity transport equations remain coupled for $n \geq 6$ and no additional parameters are introduced, a system of $2N$ equations in $2N$ unknowns will result. For a mesh size of 50, the $[A]$ and $[B]$ matrices become 100×100 and are solved in the form of equation (5-3). The first N equations of the system are represented by the discrete form of equation (2-37), which after transformation by the appropriate change of variables corresponds to the top equation of (5-1). The second N set of equations are represented by the discrete form of equation (2-38), which after transformation by the appropriate change of variables corresponds to the bottom equation of (5-1). As a matter of convenience for programming, the $[A]$ and $[B]$ matrices are partitioned into four 50×50 quadrants, which are individually banded diagonal matrices. The properties of the $[A]$ and $[B]$ matrices for $n \geq 6$ are summarized in Table 5-1.

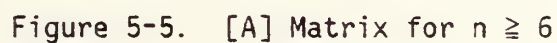
Table 5-1. Properties of the [A] and [B] Matrices for $n \geq 6$

MATRIX	QUADRANT	HIGHEST ORDER DERIVATIVE PRESENT	NONCENTRAL COEFFICIENTS REQUIRED	*	CENTRAL COEFFICIENTS REQUIRED
A	I	D^2P	5	2	5
A	II	D^3Q	5	3	7
A	III	D^2P	5	2	5
A	IV	D^4Q	6	3	7
B	I	P	-	-	1
B	II	DQ	3	2	5
B	III	P	-	-	1
B	IV	D^2Q	4	2	5
* Number of stations near the boundaries where the noncentral finite difference approximations apply.					

It can be deduced from the data given in Table 5-1 that the [A] and [B] matrices will contain nonzero elements as shown in Figures 5-5 and 5-6. The column vector $\{X\}$ of unknowns is also given.

The method for determining the noncentral finite difference coefficients for $n \geq 6$ was discussed in a previous example.

The case for $n = 1$ is unique in that an additional parameter $H(0)$ is introduced by the change of variables and a pair of coupled boundary conditions at the axis in equation (3-18b) contain the eigenvalue γ . These peculiarities are significant factors in correctly setting up the problem. Recall that in the coupled governing equations (2-47) the additional parameter $H(0)$ appears explicitly and two additional column



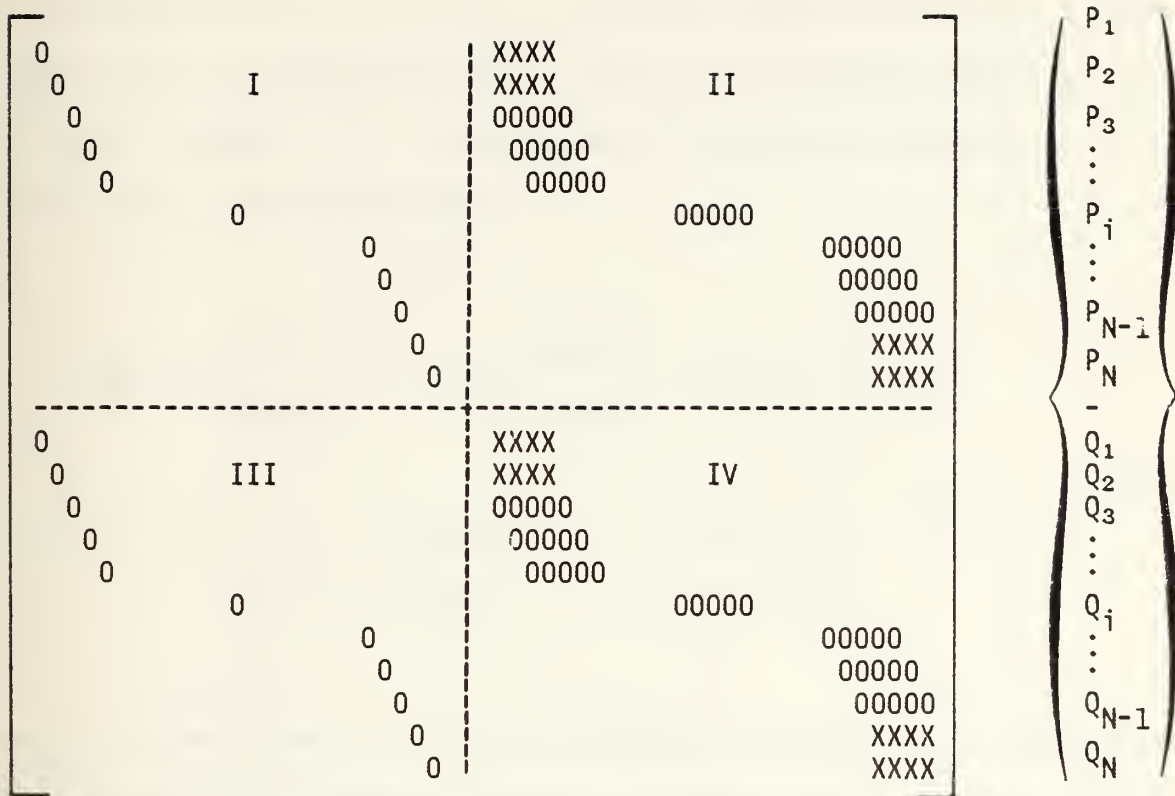


Figure 5-6. [B] Matrix for $n \geq 6$

matrices are required in the system of equations. This was due to the change of variables introduced by equations (2-44). The appearance of the eigenvalue γ in the pair of boundary equations at the axis comes about from the rigorous method in which the boundary conditions were derived in Chapter III. The coupled axis boundary conditions in equation (3-18b) are repeated here,

$$\begin{aligned}
 & -\frac{96}{\text{Re}} [C_7] \begin{Bmatrix} D^2P(0) \\ D^2Q(0) \end{Bmatrix} + 2i\alpha[C_8] \begin{Bmatrix} P(0) \\ Q(0) \end{Bmatrix} + i\alpha[C_9] \begin{Bmatrix} -i \\ 1 \end{Bmatrix} H(0) \\
 & = \gamma \left(2 [D_8] \begin{Bmatrix} P(0) \\ Q(0) \end{Bmatrix} + \alpha^2 [D_9] \begin{Bmatrix} -i \\ 1 \end{Bmatrix} H(0) \right)
 \end{aligned}
 \tag{5-29}$$

where the coefficient matrices are contained in Appendix C. Notice that the parameter $H(0)$ appears explicitly in these two equations as well. Additionally, the parameters $D^2P(0)$, $D^2Q(0)$, $P(0)$, and $Q(0)$ are also introduced. Obviously, this poses some problems since there are only two additional equations and five unknown parameters. $H(0)$ can be used since it appears in the 2N discrete equations of the system. $Q(0)$ is chosen as the second variable as a matter of convenience. The remaining three functions can be approximated in terms of discrete functions of P_i in the case for $D^2P(0)$ and $P(0)$, and Q_i and $Q(0)$ in the case of $D^2Q(0)$. By referring to the matrix form of the Taylor series expansion of a function at a point in equation (5-10), it can be seen how the approximations of these functions are made. For the present situation where

$DP(0) = 0$, eliminate the second column of the matrix and equation (5-10) will become,

$$\begin{Bmatrix} P_1 \\ P_2 \\ P_3 \\ P_4 \\ P_5 \end{Bmatrix} = [AA]_{5 \times 5} \begin{Bmatrix} P(0) \\ h^2 D^2 P(0) \\ h^3 D^3 P(0) \\ h^4 D^4 P(0) \\ h^5 D^5 P(0) \end{Bmatrix} + 0h^6 \quad (5-30)$$

Recall that the matrix in equation (5-30) is denoted $[AA]$ as before. After multiplying each side of the equation by $[AA]^{-1}$, the result becomes,

$$\begin{Bmatrix} P(0) \\ h^2 D^2 P(0) \\ h^3 D^3 P(0) \\ h^4 D^4 P(0) \\ h^5 D^5 P(0) \end{Bmatrix} = [AA]_{5 \times 5}^{-1} \begin{Bmatrix} P_1 \\ P_2 \\ P_3 \\ P_4 \\ P_5 \end{Bmatrix} - 0h^6 \quad (5-31)$$

Now $P(0)$ is approximated by the coefficients in the first row of $[AA]^{-1}$ and $D^2 P(0)$ is approximated by the coefficients in the second row of $[AA]^{-1}$ divided by h^2 , both expressed in terms of P_1 through P_5 . Notice that the approximation for $D^2 P(0)$ has truncation error $0h^4$ and $P(0)$ has truncation error $0h^6$, which is acceptable in this analysis.

The approximation for $D^2 Q(0)$ is similar except that $Q(0)$ will appear explicitly in the approximations with $DQ(0) = 0$. Equation (5-10) now becomes,

$$\begin{Bmatrix} Q_1 \\ Q_2 \\ Q_3 \\ Q_4 \\ Q_5 \\ Q_6 \end{Bmatrix} = \begin{bmatrix} 1 \\ 1 \\ 1 \\ 1 \\ 1 \\ 1 \end{bmatrix} \{Q(0)\} + \underset{6 \times 6}{[AA]} \begin{Bmatrix} h^2 D^2 Q(0) \\ h^3 D^3 Q(0) \\ h^4 D^4 Q(0) \\ h^5 D^5 Q(0) \\ h^6 D^6 Q(0) \\ h^7 D^7 Q(0) \end{Bmatrix} + O h^8 \quad (5-32)$$

After rearranging, equation (5-32) is multiplied through by $[AA]^{-1}$ and becomes,

$$\begin{Bmatrix} h^2 D^2 Q(0) \\ h^3 D^3 Q(0) \\ h^4 D^4 Q(0) \\ h^5 D^5 Q(0) \\ h^6 D^6 Q(0) \\ h^7 D^7 Q(0) \end{Bmatrix} = \underset{6 \times 6}{[AA]}^{-1} \begin{Bmatrix} Q_1 - Q(0) \\ Q_2 - Q(0) \\ Q_3 - Q(0) \\ Q_4 - Q(0) \\ Q_5 - Q(0) \\ Q_6 - Q(0) \end{Bmatrix} - O h^8 \quad (5-33)$$

The coefficients for $D^2 Q(0)$ are taken from the first row of $[AA]^{-1}$ and divided by h^2 . $D^2 Q(0)$ is now expressed in terms of $Q(0)$ and Q_1 through Q_6 and will have a truncation error $O h^6$.

The two additional boundary condition equations involving y can now be solved in the eigensystem of equations with $H(0)$ and $Q(0)$ appearing explicitly as the two required unknowns. It is convenient to express the $[C_9]$ and $[D_9]$ matrices of equation (5-29) in slightly different form,

$$[C_9] \begin{Bmatrix} -i \\ 1 \end{Bmatrix} H(0) \quad \text{as} \quad [C_9^*] \{H(0)\}$$

and

(5-34)

$$[D_9] \begin{Bmatrix} -i \\ 1 \end{Bmatrix} H(0) \quad \text{as} \quad [D_9^*] \{H(0)\}$$

where $[C_9^*]$ and $[D_9^*]$ become 2×1 column matrices,

$$[C_9^*] = \begin{bmatrix} \left(\frac{\alpha^3}{Re} - 4i + 2i\alpha^2 \right) \\ \left(-2\alpha^2 + \frac{i\alpha^3}{Re} \right) \end{bmatrix} \quad \text{and} \quad [D_9^*] = \begin{bmatrix} -i \\ 1 \end{bmatrix}$$
(5-35)

Substituting equations (5-35) into equation (5-29) yields,

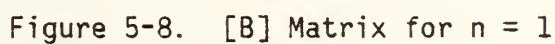
$$- \frac{96}{Re} [C_7] \begin{Bmatrix} D^2P(0) \\ D^2Q(0) \end{Bmatrix} + 2i\alpha [C_8] \begin{Bmatrix} P(0) \\ Q(0) \end{Bmatrix} + i\alpha [C_9^*] \{H(0)\}$$
(5-36)

$$= \gamma \left(2 [D_8] \begin{Bmatrix} P(0) \\ Q(0) \end{Bmatrix} + \alpha^2 [D_9^*] \{H(0)\} \right)$$

The solution of the eigensystem of $2N + 2$ equations in $2N + 2$ unknowns is now accomplished in the form of equation (5-3). The appearance of the $[A]$ and $[B]$ matrices are identical to those for $n \geq 6$ in Figures 5-5 and 5-6 except for the addition of two columns to accommodate the parameters $H(0)$ and $Q(0)$, and two rows to accommodate the pair of boundary equations in (5-36). Nonzero elements are present in the $[A]$ and $[B]$ matrices for $n = 1$ as shown in Figures 5-7 and 5-8.

XXXXX XXXXX 00000 00000 00000	I	XXXXX XXXXX XXXXX 0000000 0000000	II	X X X X X X X X X X X X X X X X X X
00000 00000 00000 00000 XXXXXX XXXXXX		00000000 00000000 XXXXXX XXXXXX XXXXXX		
XXXXX XXXXX 00000 00000 00000	III	XXXXXXX XXXXXXX XXXXXXX 0000000 0000000	IV	X X X X X X X X X X X X X X X X X X
00000 00000 00000 00000 XXXXXX XXXXXX		00000000 00000000 XXXXXX XXXXXX XXXXXX		
XXXXX XXXXX		XXXXXXX XXXXXXX		X X X X

Figure 5-7. [A] Matrix for $n = 1$



Derivation of the noncentral finite difference coefficients for the derivatives of P and Q at the wall are straightforward as shown for the other angular wave numbers. The columns of the [AA] and [CC] matrices are eliminated based on the fact that parameters P(1), Q(1), and DQ(1) are all expressed in terms of H(0), as seen in equations (3-18c). By imposing the boundary conditions for Q at the wall,

$$Q(1) = - H(0) \quad \text{and} \quad DQ(1) = 2 H(0) \quad (5-37)$$

equation (5-17) becomes,

$$\begin{pmatrix} hDQ_1 \\ h^2D^2Q_1 \\ h^3D^3Q_1 \\ h^4D^4Q_1 \end{pmatrix} = \begin{bmatrix} 2h \\ 0 \\ 0 \\ 0 \end{bmatrix} \{H(0)\} + \underset{4 \times 6}{[CC]} \underset{6 \times 6}{[AA]}^{-1} \begin{pmatrix} Q_1 + (1-h) H(0) \\ Q_2 + (1-3h) H(0) \\ Q_3 + (1-5h) H(0) \\ Q_4 + (1-7h) H(0) \\ Q_5 + (1-9h) H(0) \\ Q_6 + (1-11h) H(0) \end{pmatrix} \quad (5-38)$$

The coefficients in the resultant 4 X 6 matrix of equation (5-38) are in fact the same coefficients computed for $n \geq 6$ at the wall, and recall that they appear in reverse order when used at the wall. The details of the complete derivation of the noncentral finite difference coefficients near the boundaries is lengthy and not included here.

D. COMPUTER PROGRAM USEAGE

The solutions for the discrete transformed vorticity transport equations for the three angular wave numbers investigated are accomplished in the main investigative computer programs. Three separate programs were written rather than developing one program for the general case. The rationale for this is as follows: the changes of variables for each angular wave number $n \leq 6$ are different, the boundary conditions are different, the equations uncouple for $n = 0$, additional parameters are introduced for some, and $n = 1$ has a coupled boundary equation that contains γ that must be dealt with separately in the setup of the problem. It would be practical to write a general program for angular wave numbers $n \geq 6$, however.

For each specific angular wave number analyzed, the main computer program is divided into eight parts. Their functions are summarized below:

- | | |
|----------|----------------------------------------------------------------------------------------------------------------------------------------------------------------------------------|
| Part I | The central finite difference coefficient for the derivatives of P and Q are computed. |
| Part II | The noncentral finite difference coefficients for the derivatives of P and Q at the axis and wall are read in as data. Problem variables, Re and α , are read in as data. |
| Part III | Coefficients of the vorticity transport matrix equations are computed along the radial mesh. |
| Part IV | The [A] and [B] matrix elements are computed. |
| Part V | The eigenvalues and respective eigenvectors are computed in the subroutine EIGZC and the least stable eigenvalue is determined. |
| Part VI | Verification that the least stable eigenvalue and corresponding eigenvector satisfy the governing equations. |

Part VII The normalized axial perturbation velocity is computed from the least stable eigenvalue and its eigenvector.

Part VIII The normalized axial perturbation velocity is plotted versus normalized pipe radius utilizing the Versatec plotter.

The numerical analysis of the pipe flow stability problem is centered around the subroutine EIGZC once the problem is properly set up. The eigensystem of equation (5-3) is solved by this subroutine which returns a set of N , $2N + 2$, or $2N$ eigenvalues for $n = 0$, 1 , or 6 , respectively, and a corresponding set of normalized eigenvectors. Each eigenvalue and its eigenvector represent a solution of the governing equations. The primary objective of the main program and of this investigation is to determine the least stable eigenvalue which indicates flow characteristics. Recall that if γ_R is positive, the flow is unstable. For each value of α and Re chosen, the maximum algebraic value of γ_R is found, denoted as γ^* , to determine if instabilities exist in the flow field. The corresponding eigenvector of γ^* , denoted as $\{X^*\}$, is used to compute the incremental axial perturbation velocity along the radius. Plots of the normalized perturbation velocity versus normalized pipe radius have no significance in determining stability or instability of the flow but are indicators of the general nature and behavior of the flow field perturbations. Another independent program was written to plot Reynolds number stability contours using data taken from program results for $n = 1$ and 6 . The subroutines used to make plots on Versatec plotter are PLOTG, standard Versatec plotting functions and TITLE1 to print titles and legends on the plots.

The numerical accuracy of the solution was determined by substituting γ^* and its eigenvector into the governing equations. For this purpose, the residual error vector $\{\epsilon\}$ was computed by equation (5-39) and the magnitude of the error was examined.

$$\{\epsilon\} = [A] \{X^*\} - \gamma^* [B] \{X^*\} \quad (5-39)$$

The Fortran subroutine EIGZC is contained in the International Mathematical and Statistical Library (IMSL) available in most large computer system libraries utilizing Fortran compilers. Specifically, the numerical analysis of the vorticity transport equations in the form of equation (5-3) was computed on the IBM 370/3033 (assigned processor) system with the Fortran H Extended compiler at the U.S. Naval Postgraduate School. All calculations were performed in full double precision format to improve the accuracy of the solution by minimizing truncation and round off errors inherently introduced by digital computations. The main investigative programs and other auxiliary programs were all written in Fortran programming language to be compatible with all versions of Fortran compilers. The computer program listings with applicable data sets are included after the appendices in this paper.

VI. RESULTS

A. RESULTS FOR $n = 0$

Results of the pipe flow stability problem are obtained from the solution of the linearized vorticity transport equations by the methods previously described. A generalized solution of the governing differential equations for fully developed, three-dimensional pipe flow has been accomplished for three angular wave numbers, $n = 0, 1$, and 6 . The characteristics of the flow field perturbations for each angular wave number investigated are established by the parameters Re and α . The purpose of this numerical investigation was to determine flow stability at various Reynolds numbers and axial wave numbers for each angular wave number. Recall that the perturbation velocity vector \vec{v} is defined in equation (2-27) as the curl of the velocity vector potential \vec{W} . This function is expressed in terms of $G(r)$ and $H(r)$ and a complex exponential form e^X in equations (2-28) and (2-29). After appropriate changes of variables were introduced, solutions were determined from the eigen-system of equations which consists of a set of eigenvalues and their corresponding normalized eigenvectors for fixed values of Re and α . The resulting perturbation quantities now appear in terms of the eigenfunctions $P(r)$ and $Q(r)$ and are represented in discrete form in the eigenvector $\{X\}$ as P_i and Q_i , where $i = 1, 2, 3, \dots, N$. As can be seen from equation (2-30), the real part of the complex eigenvalue γ_R will determine the growth or decay rate in time of the perturbation. Positive

values of γ_R indicate that the flow is unstable. The eigenvalue whose real part has the largest algebraic value, denoted as γ^* , is the least stable and is reported in these results to show stability trends.

Gawain [Ref. 13] reported the numerical results for angular wave number $n = 0$ for the solution of the governing equation in his paper. Those numerical results which incorporated a purely imaginary axial wave number and the advancements in the derivation of the boundary conditions at the pipe axis were duplicated in this investigation. They are essentially the same results except for variations in the fourth decimal place of the value of γ^* . This is due to the improved accuracy of the solution as a result of the numerical methods used here. The primary emphasis of this investigation is centered on determining the onset of flow instabilities at a theoretical critical Reynolds number near 1150. However, solutions were obtained at other Reynolds numbers to show stability trends and are presented in tabular and plotted form.

Stability data for angular wave number $n = 0$ for various combinations of Re and α are given in Table 6-1. The least stable eigenvalue solution of the governing equation is based on a computational mesh of $N = 50$. Table entries which contain dashes indicate that the solution of the governing equations was not sufficiently accurate to be included as valid data. Two facts become very clear in examining Table 6-1. First of all, the flow is stable at all Re and α for $n = 0$. Secondly, there is an asymptotic trend towards neutral stability for increasing Reynolds numbers. This second result agrees with experimental observations in that increasing Reynolds number has a destabilizing effect on the flow. It can also be seen that increasing the axial wave number has

Table 6-1. Stability Data for Angular Wave Number $n = 0$

Growth or Decay Trends of Least Stable Eigenvalue, γ^*

Re	$\alpha=0.0$	$\alpha=0.05$	$\alpha=1.0$	$\alpha=2.0$	$\alpha=4.0$	$\alpha=8.0$	$\alpha=16.0$	$\alpha=32.0$
300	-0.0879	-0.1544	-0.2360	-0.3399	-0.5152	-0.8665	-1.7770	-4.7194
575	-0.0459	-0.1196	-0.1685	-0.2429	-0.3614	-0.5831	-1.1122	-2.7236
1150	-0.0229	-0.0836	-0.1188	-0.1703	-0.2498	-0.3891	-0.6937	-1.5548
2300	-0.0115	-0.0591	-0.0838	-0.1197	-0.1737	-0.2633	-0.4429	-0.9099
4600	-0.0057	-0.0418	-0.0592	-0.0842	-0.1212	-0.1796	-0.2871	-
9200	-0.0029	-0.0295	-0.0418	-0.0593	-0.0846	-0.1225	-	-
18400	-0.0014	-0.0209	-0.0295	-0.0416	-0.0586	-	-	-

Note: Values are based on 50 mesh points.

a stabilizing effect on the flow. Normalized axial perturbation velocity plots versus pipe radius were made at various Re and α to examine the behavior of the perturbation quantities corresponding to the least stable eigenvalue solution. Figures 6-1 through 6-9, on the following pages, are representative of the behavior of the axial perturbation velocity. The activity is concentrated near the pipe axis for $n = 0$ and dies out quickly as r approaches 1.0. Additionally, the perturbation velocity plots were made in order to determine if mesh fineness was sufficient to obtain an accurate solution of the equations. Trial calculations were made for uniform mesh sizes up to 100 where the numerical results did not vary appreciably from those reported here.

NORMALIZED PERTURBATION VELOCITY VS RADIUS

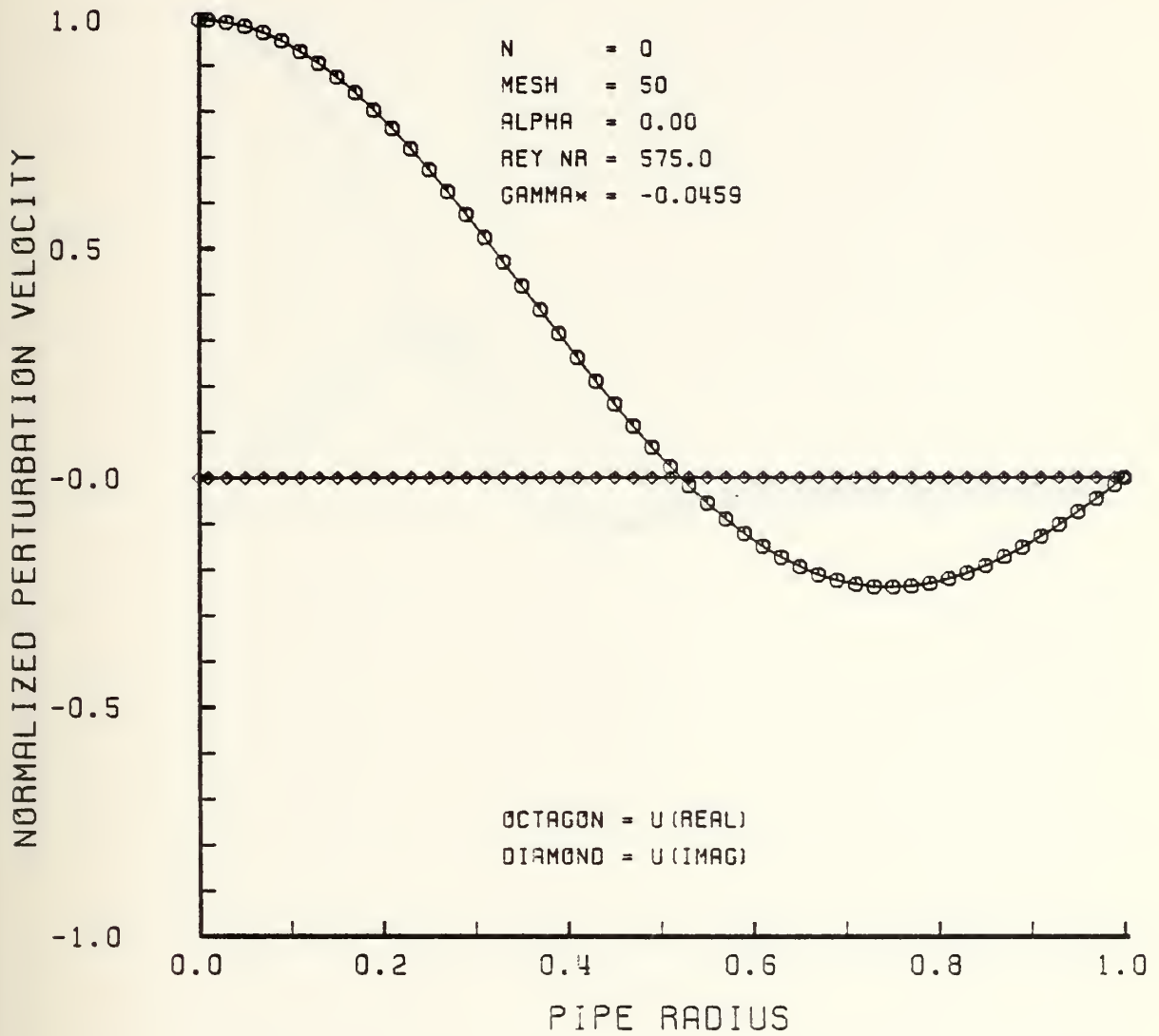


Figure 6-1

NORMALIZED PERTURBATION VELOCITY VS RADIUS

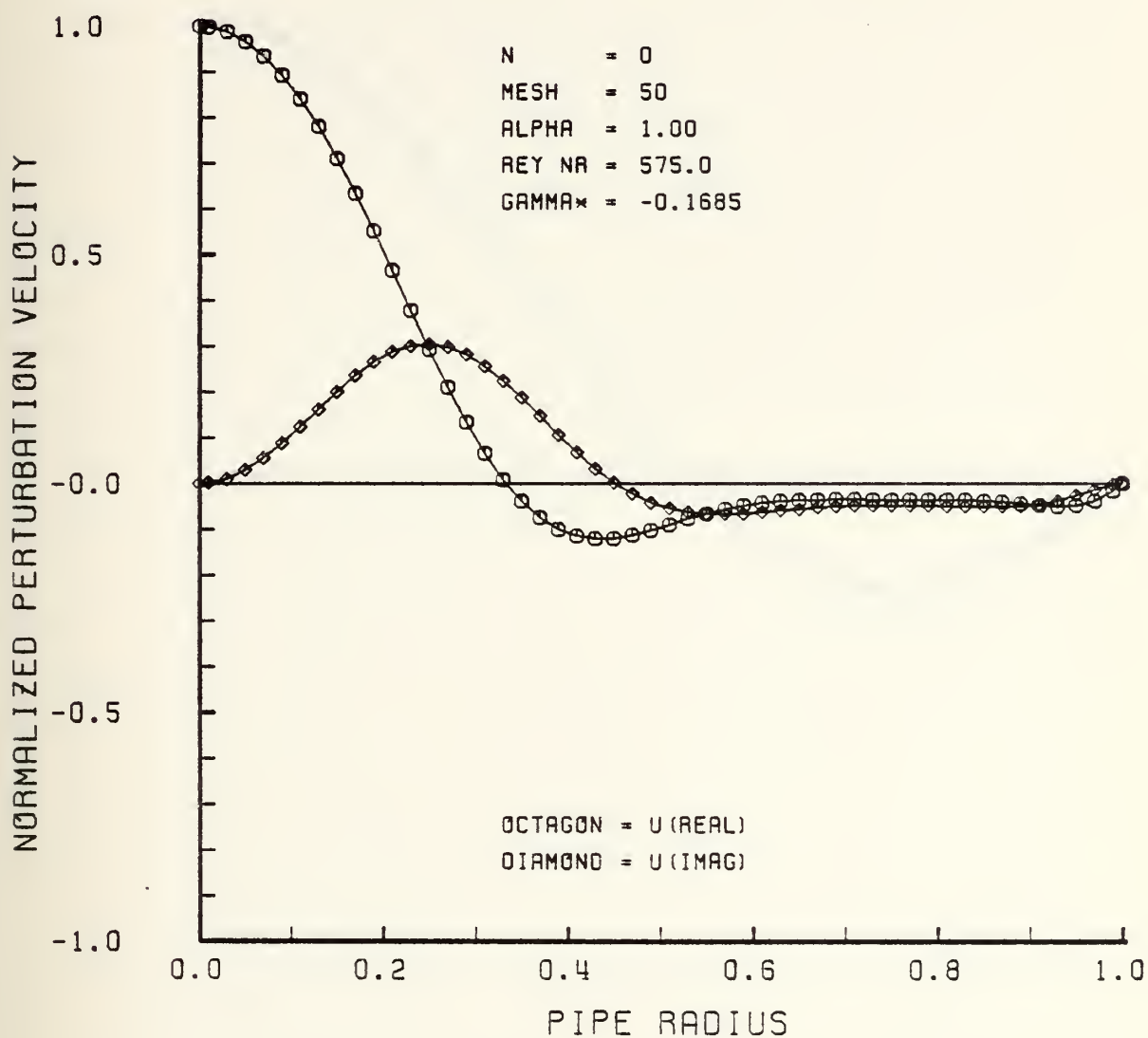


Figure 6-2

NORMALIZED PERTURBATION VELOCITY VS RADIUS

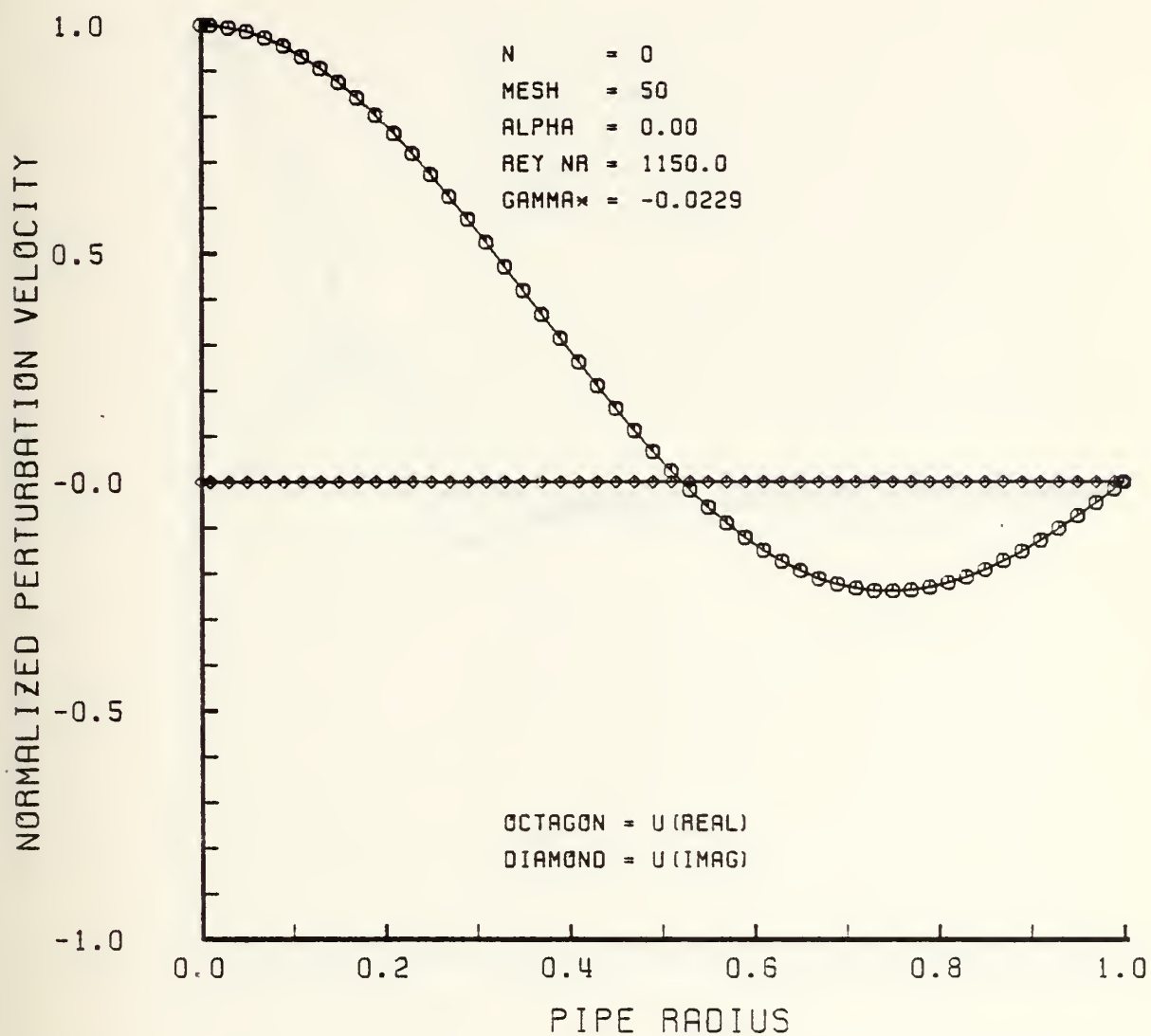


Figure 6-3

NORMALIZED PERTURBATION VELOCITY VS RADIUS

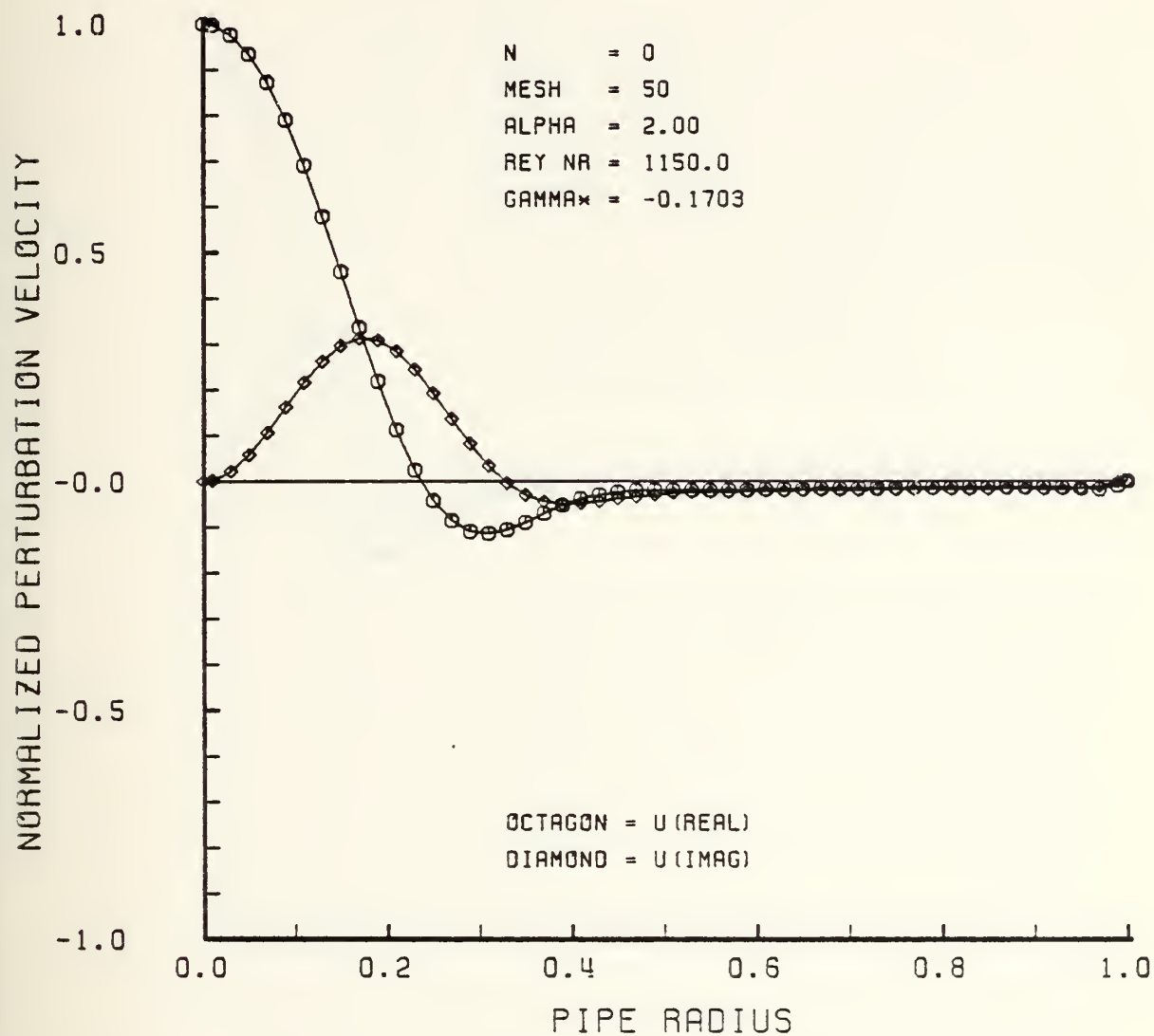


Figure 6-4

NORMALIZED PERTURBATION VELOCITY VS RADIUS

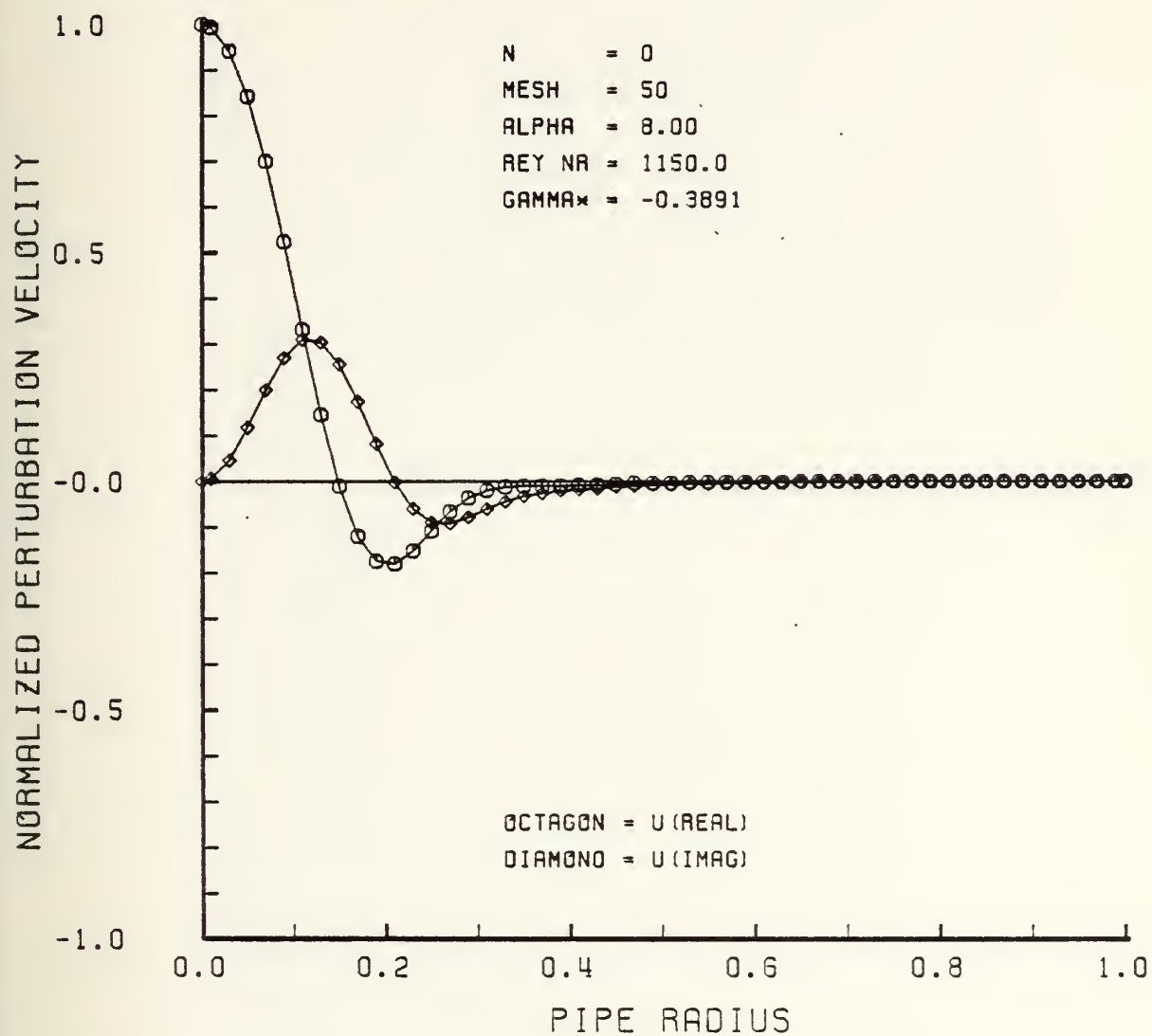


Figure 6-5

NORMALIZED PERTURBATION VELOCITY VS RADIUS

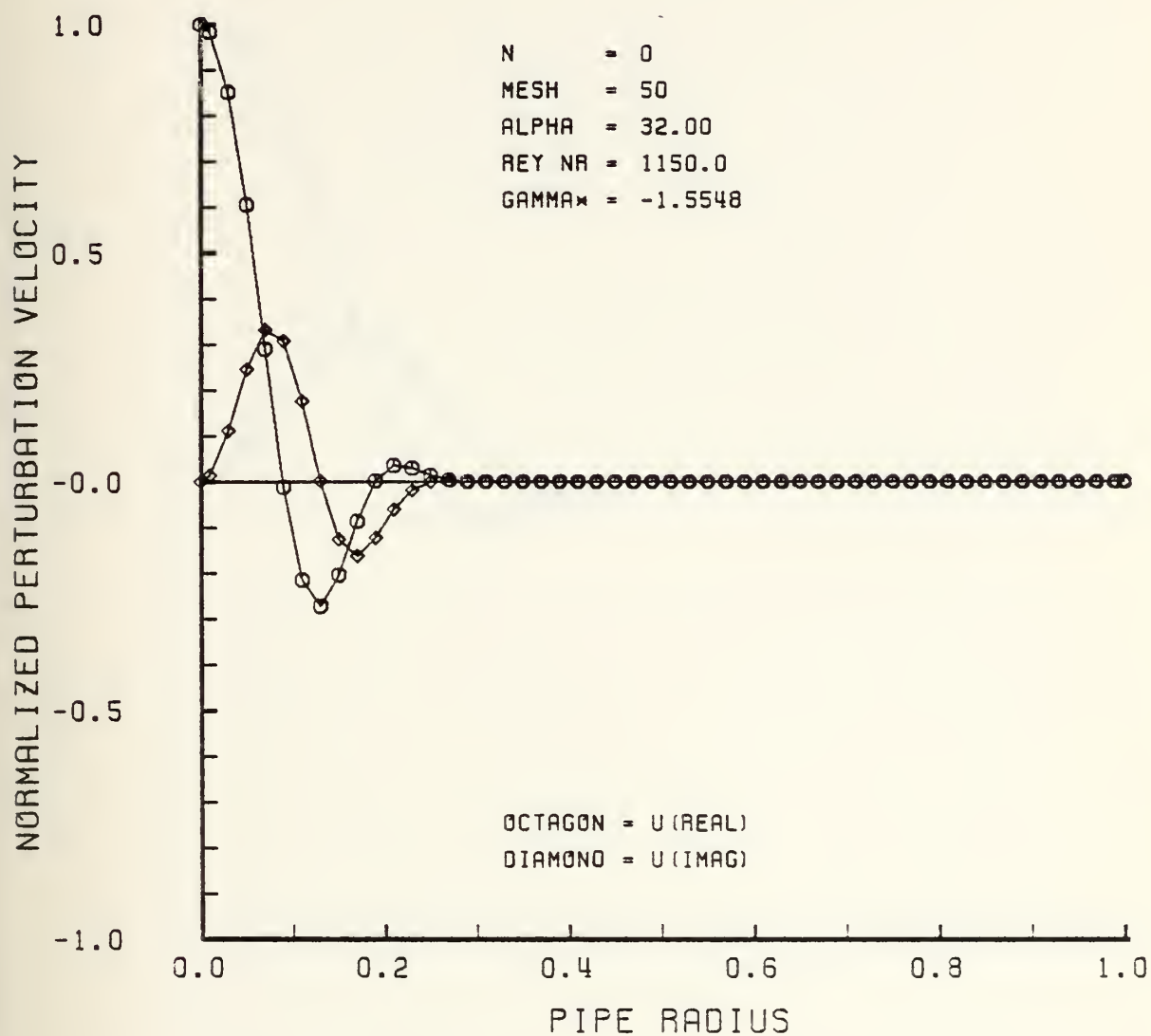


Figure 6-6

NORMALIZED PERTURBATION VELOCITY VS RADIUS

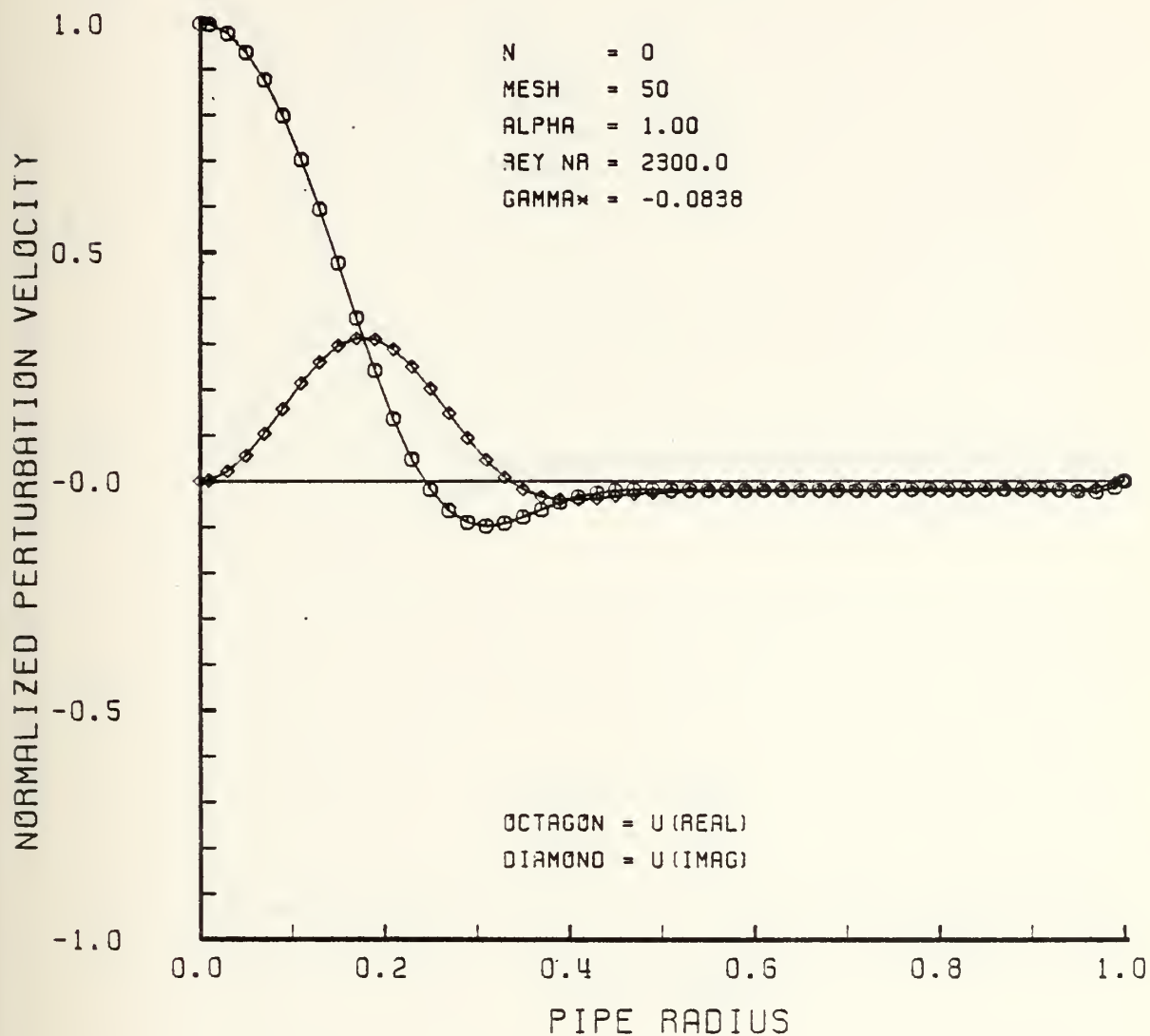


Figure 6-7

NORMALIZED PERTURBATION VELOCITY VS RADIUS

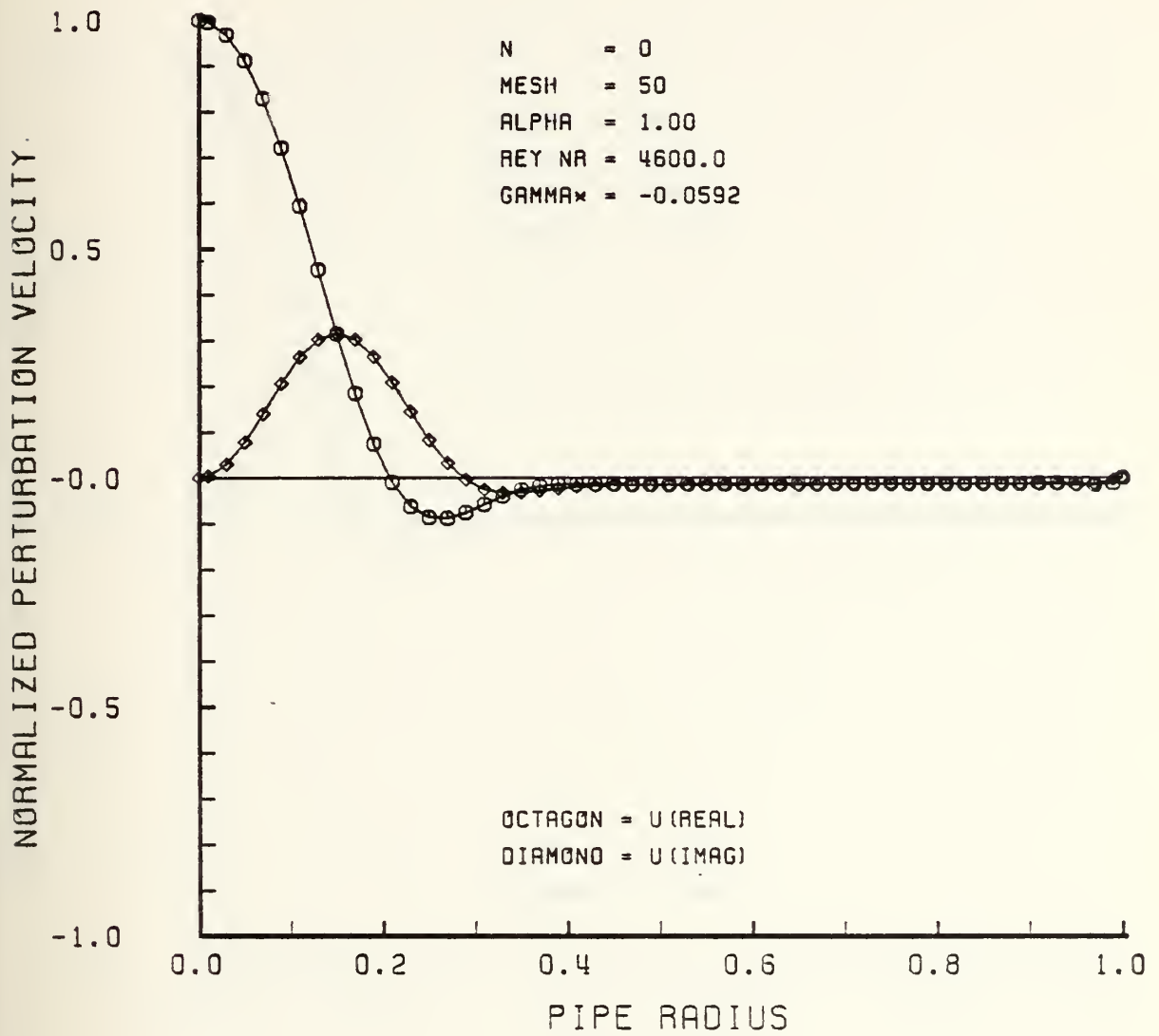


Figure 6-8

NORMALIZED PERTURBATION VELOCITY VS RADIUS

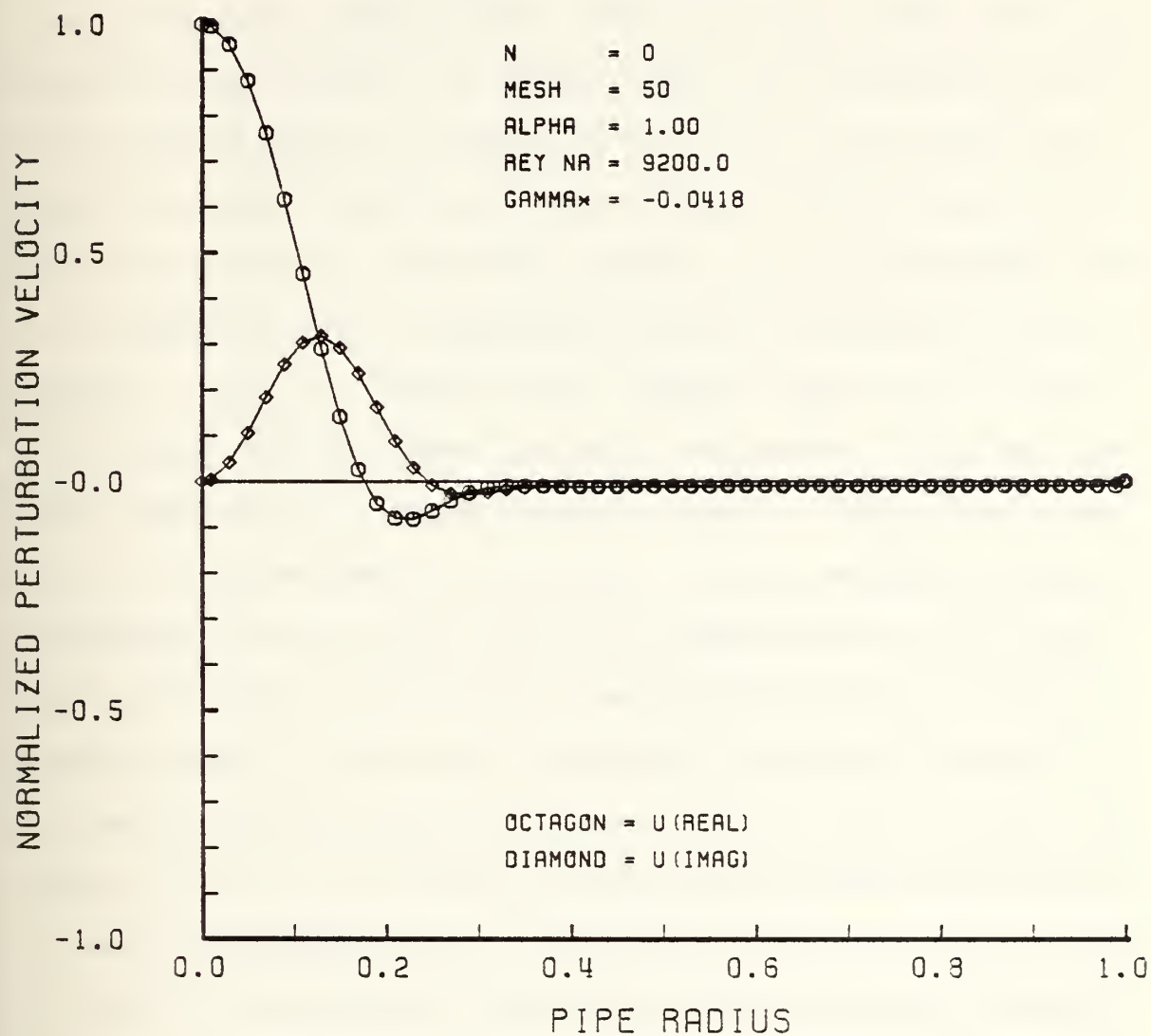


Figure 6-9

B. RESULTS FOR $n = 1$

The numerical results for angular wave number $n = 1$ indicate that flow instabilities indeed exist. There are four factors that may possibly account for the flow instabilities; (1) the complicated nature of the coupled governing equations for $n = 1$, (2) the rigorous way in which the boundary conditions at the axis were derived and enforced, (3) the introduction of additional parameters into the eigensystem, and (4) the appearance of the eigenvalue in a pair of the boundary condition equations. Table 6-2 summarizes the stability data for $n = 1$ over a wide range of Reynolds numbers and axial wave numbers. Once again the dashed table entries indicate inaccurate results. Notice that a mesh size of $n = 48$ was used for this case. This was necessary because of programming constraints that required the eigensystem to be less than or equal to 100×100 . It can be seen that flow instabilities exist at all Reynolds numbers. This occurs coincidentally with small values of α . More detailed stability data is presented in Table 6-3 for axial wave numbers $0 \leq \alpha \leq 1$. It is clear here that the flow becomes more unstable for very small values of $\alpha < 1$. The stability data presented in Tables 6-2 and 6-3 is more easily interpreted as Reynolds number contours in the plots of GAMMA^* vs. α . Figure 6-10 shows Reynolds number contours over a large range of α . It can be clearly seen that the flow is unstable at all Reynolds numbers for small values of axial wave numbers. Figure 6-11 shows a more detailed plot of the Reynolds number contours over a small range of α . Here it can be seen that the flow becomes more unstable for decreasing values of Reynolds numbers! It can

Table 6-2. Stability Data for Angular Wave Number $n = 1$

Growth or Decay Trends of Least Stable Eigenvalue, γ^*

Re	$\alpha=0.0$	$\alpha=0.05$	$\alpha=1.0$	$\alpha=2.0$	$\alpha=4.0$	$\alpha=8.0$	$\alpha=16.0$	$\alpha=32.0$
300	0.0606	0.0626	-0.0215	-0.2883	-0.3734	-0.7623	-1.3222	-
575	0.0316	0.0270	-0.0601	-0.1983	-0.2530	-0.4638	-1.1246	-0.7546
1150	0.0158	0.0026	-0.0876	-0.1362	-0.1723	-0.2805	-0.7067	-
2300	0.0079	-0.0131	-0.0675	-0.0947	-0.1205	-0.1745	-0.4004	-
4600	0.0039	-0.0237	-0.0476	-0.0664	-0.0860	-0.1117	-0.2327	-
9200	0.0020	-0.0239	-0.0336	-0.0467	-0.0617	-0.0736	-	-
18400	0.0010	-0.0169	-0.0238	-0.0328	-0.0436	-0.0497	-	-

Note: Values are based on 48 mesh points.

Table 6-3. Stability Data for Angular Wave Number $n = 1$

Growth or Decay Trends of Least Stable Eigenvalue, γ^*

Re	$\alpha=0.0$	$\alpha=0.05$	$\alpha=0.10$	$\alpha=0.15$	$\alpha=0.20$	$\alpha=0.50$	$\alpha=0.75$	$\alpha=1.0$
300	0.0606	0.0657	0.0718	0.0743	0.0743	0.0626	0.0322	-0.0215
575	0.0316	0.0374	0.0394	0.0395	0.0398	0.0270	-0.0057	-0.0601
1150	0.0158	0.0198	0.0204	0.0208	0.0202	0.0026	-0.0324	-0.0876
2300	0.0079	0.0103	0.0105	0.0096	0.0081	-0.0131	-0.0507	-0.0675
4600	0.0039	0.0053	0.0044	0.0028	0.0006	-0.0237	-0.0413	-0.0476
9200	0.0020	0.0022	0.0006	-0.0016	-0.0042	-0.0239	-0.0292	-0.0336
18400	0.0010	0.0003	-0.0018	-0.0044	-0.0074	-0.0169	-0.0206	-0.0238

Note: Values are based on 48 mesh points.

also be seen here that the flow becomes even more unstable for small values of α only slightly larger than zero. The reason for these results cannot be readily explained but it is obvious that they are in direct conflict with observed experimental results. When $\alpha > 1$, however, the contours show an asymptotic trend toward neutral stability for increasing Reynolds numbers; in other words, increasing Reynolds number has a destabilizing effect on the flow which agrees with experimental results. A slightly different method of presenting the data can be seen in Figure 6-12, as alpha contours in the plot of GAMMA* vs. Reynolds number. This plot further emphasizes the results discussed above; the flow is unstable at all Reynolds numbers for small alpha, increasing Reynolds number has a destabilizing effect on the flow and increasing axial wave number has a stabilizing effect.

Normalized perturbation velocity plots were also produced for this case and show some interesting trends. The behavior of the axial perturbation velocity for selected values of Re and α appear in Figures 6-13 through 6-23 on the following pages. Upon close examination of the perturbation velocity plots, it becomes apparent that the computational mesh is not sufficiently fine to adequately approximate the velocity function as α is increased. This problem will be discussed shortly.

It is interesting to note that the perturbation activity shifts from the pipe wall to the axis for increasing values of the axial wave number while Reynolds number remains constant. At small values of α , the activity originates at the wall. At larger values of α , the activity shifts to the axis, for the most part. At even larger values of α , the activity moves away from the axis to the region between the axis and

wall. However, some degree of activity remains at the wall for the last two cases. The change in the perturbation activity as described above can be seen in Figures 6-14 through 6-16 for $Re = 575$ and in Figures 6-19 through 6-21 for $Re = 2300$. The shift of perturbation activity to the axis with increasing axial wave number deserves comment here. Schlichting [Ref. 16] observed that the transition to turbulence is "characterized by the appearance of self-sustaining turbulent flashes which emanate from fluid layers near the wall along the tube." Therefore, it appears that unstable flows are associated with perturbation activity near the wall. As the activity shifts away from the wall with increasing axial wave number, the flow becomes stable. Additionally, after the activity moves to the axis, some degree of activity remains at the wall. While the solution appears to remain stable, it is recommended that this peculiarity be examined further. The use of a finer mesh to resolve this activity at the wall would be useful here.

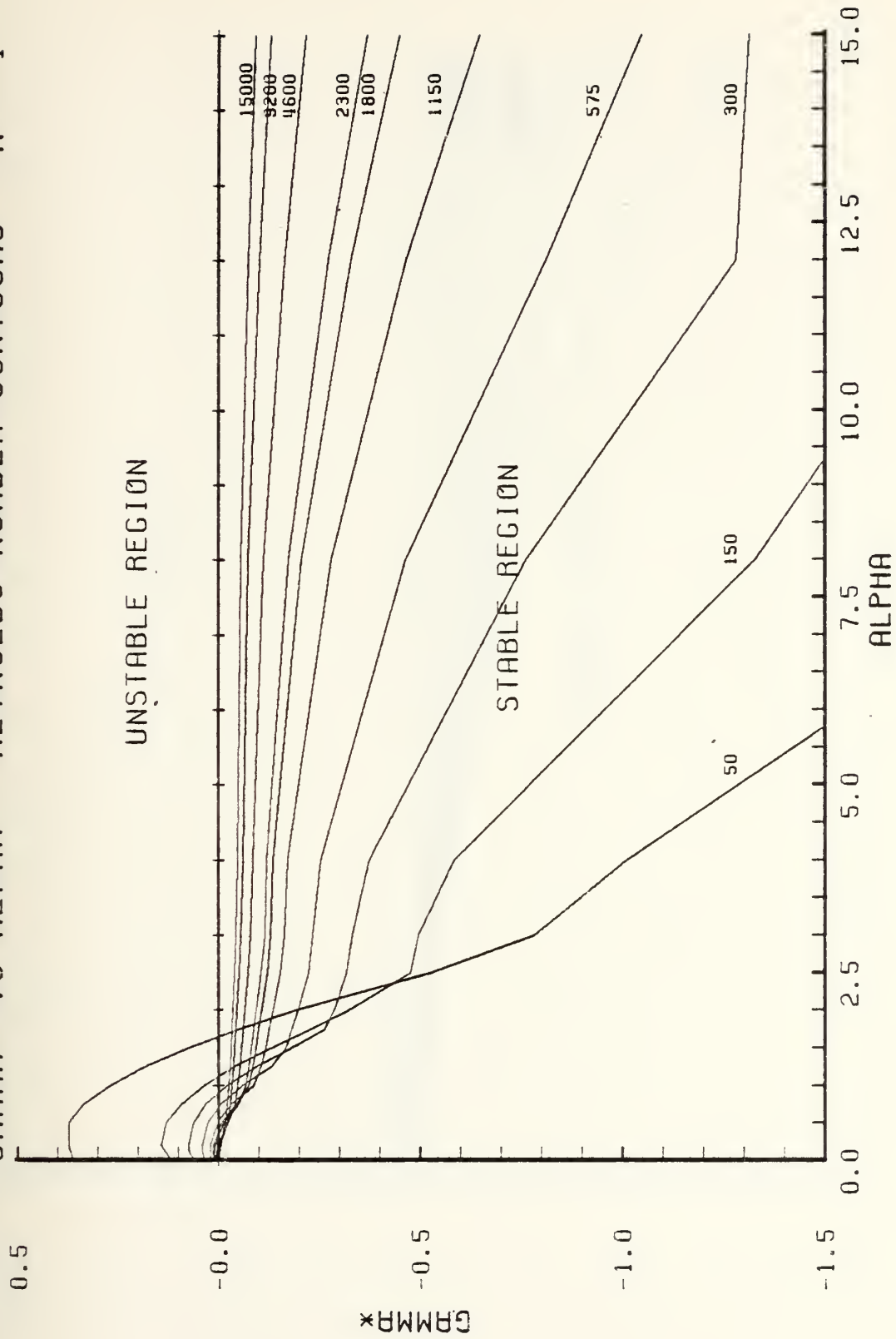


Figure 6-10

GAMMA* VS ALPHA REYNOLDS NUMBER CONTOURS N = 1

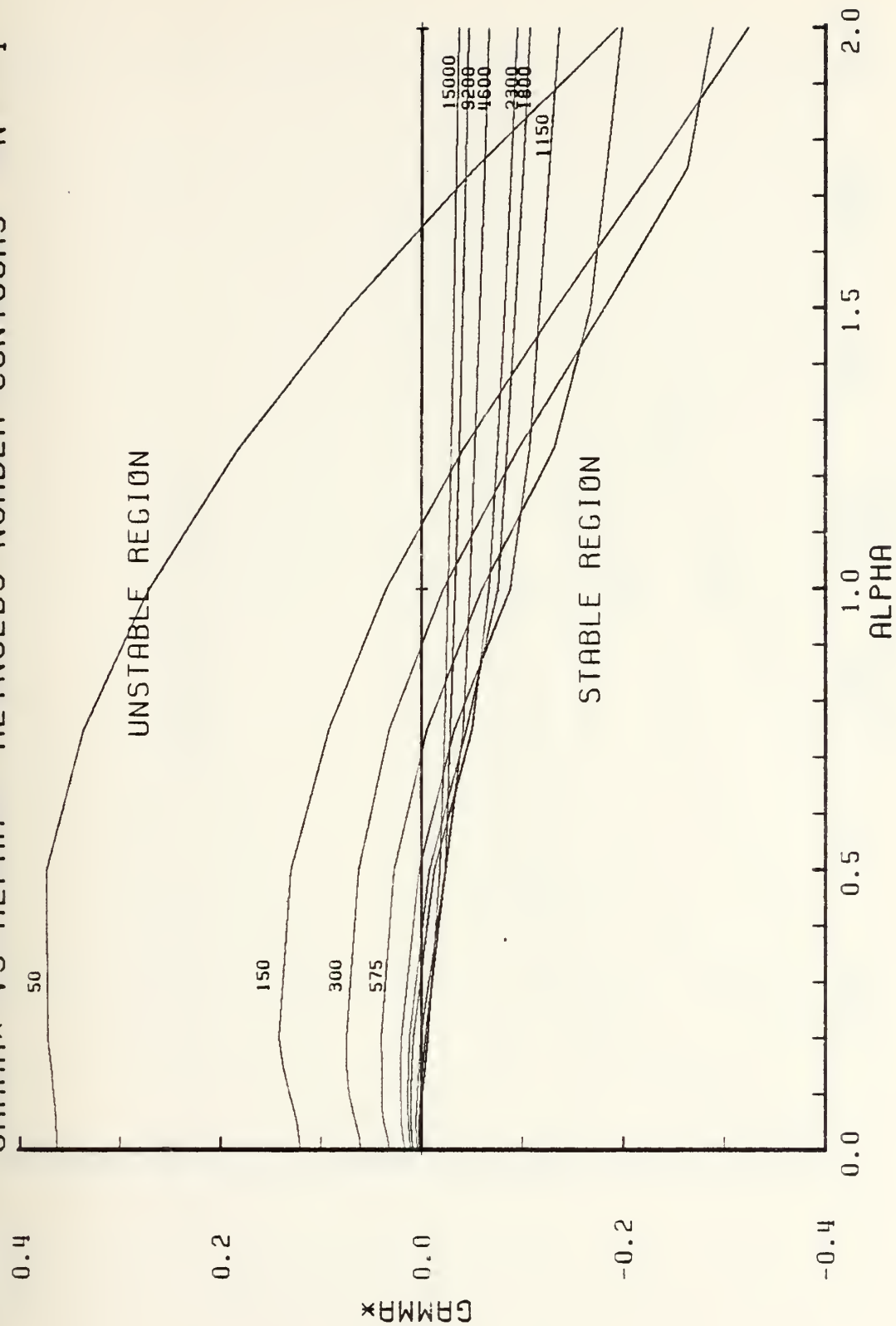


Figure 6-11

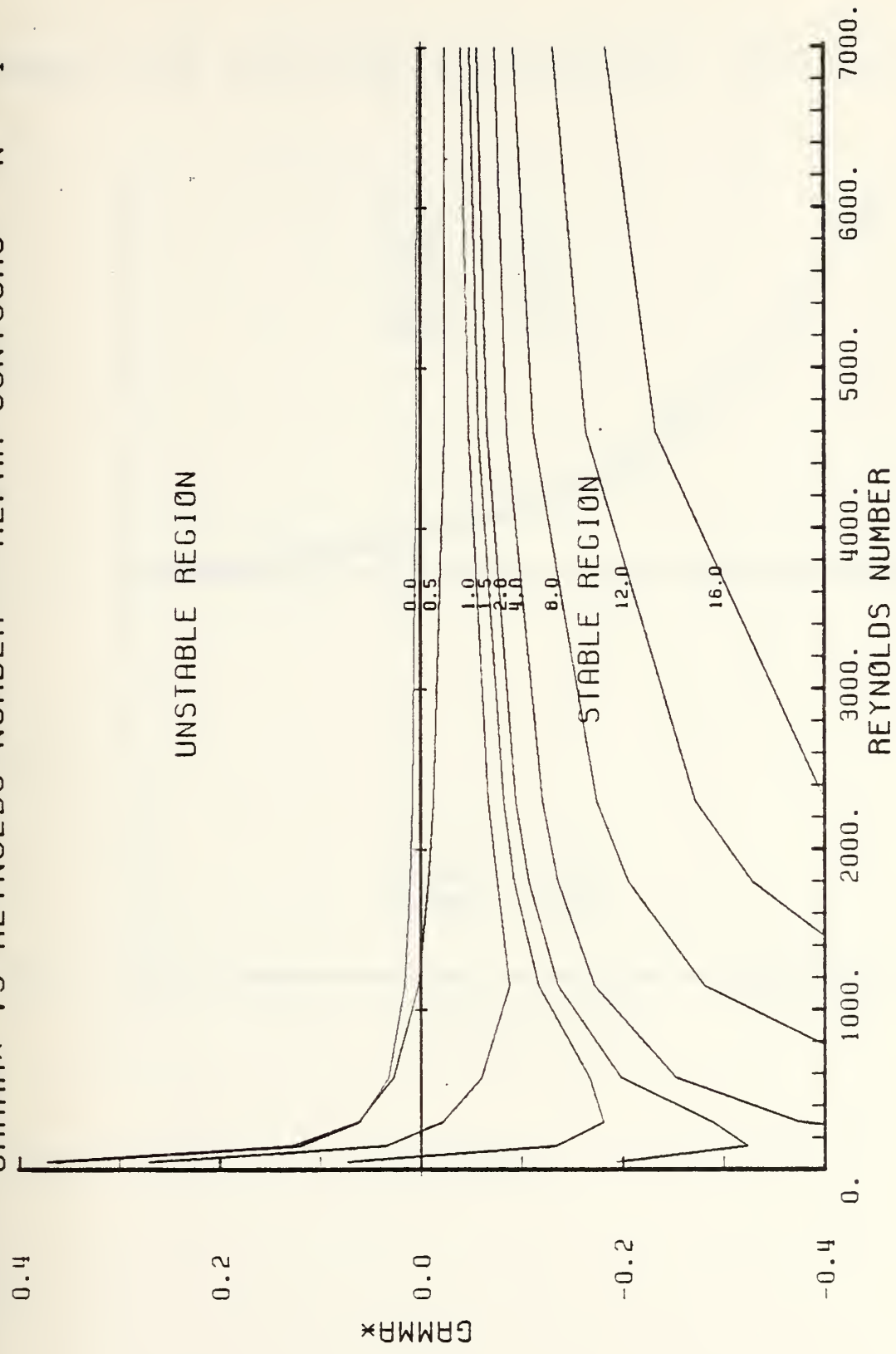


Figure 6-12

NORMALIZED PERTURBATION VELOCITY VS RADIUS

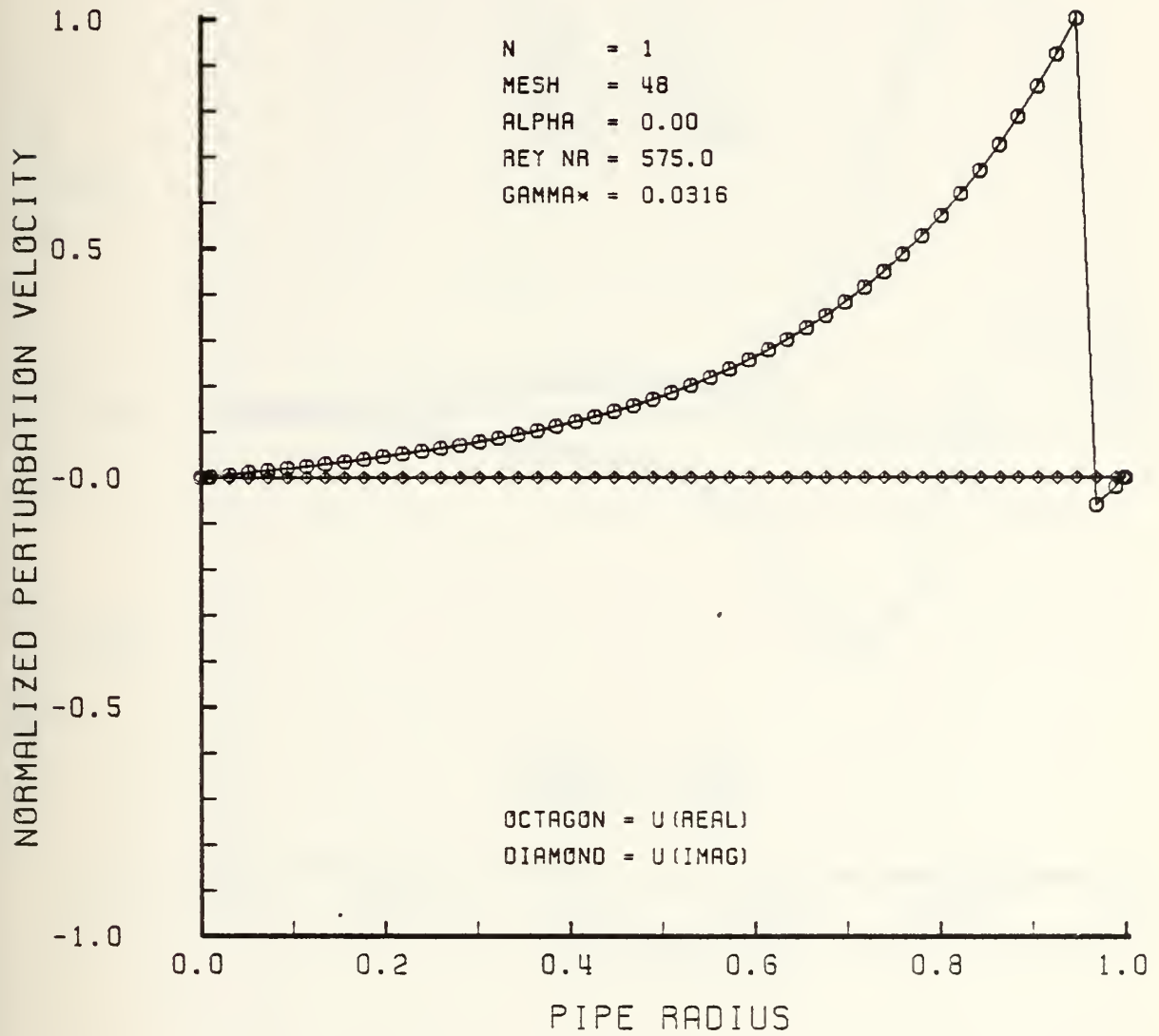


Figure 6-13

NORMALIZED PERTURBATION VELOCITY VS RADIUS

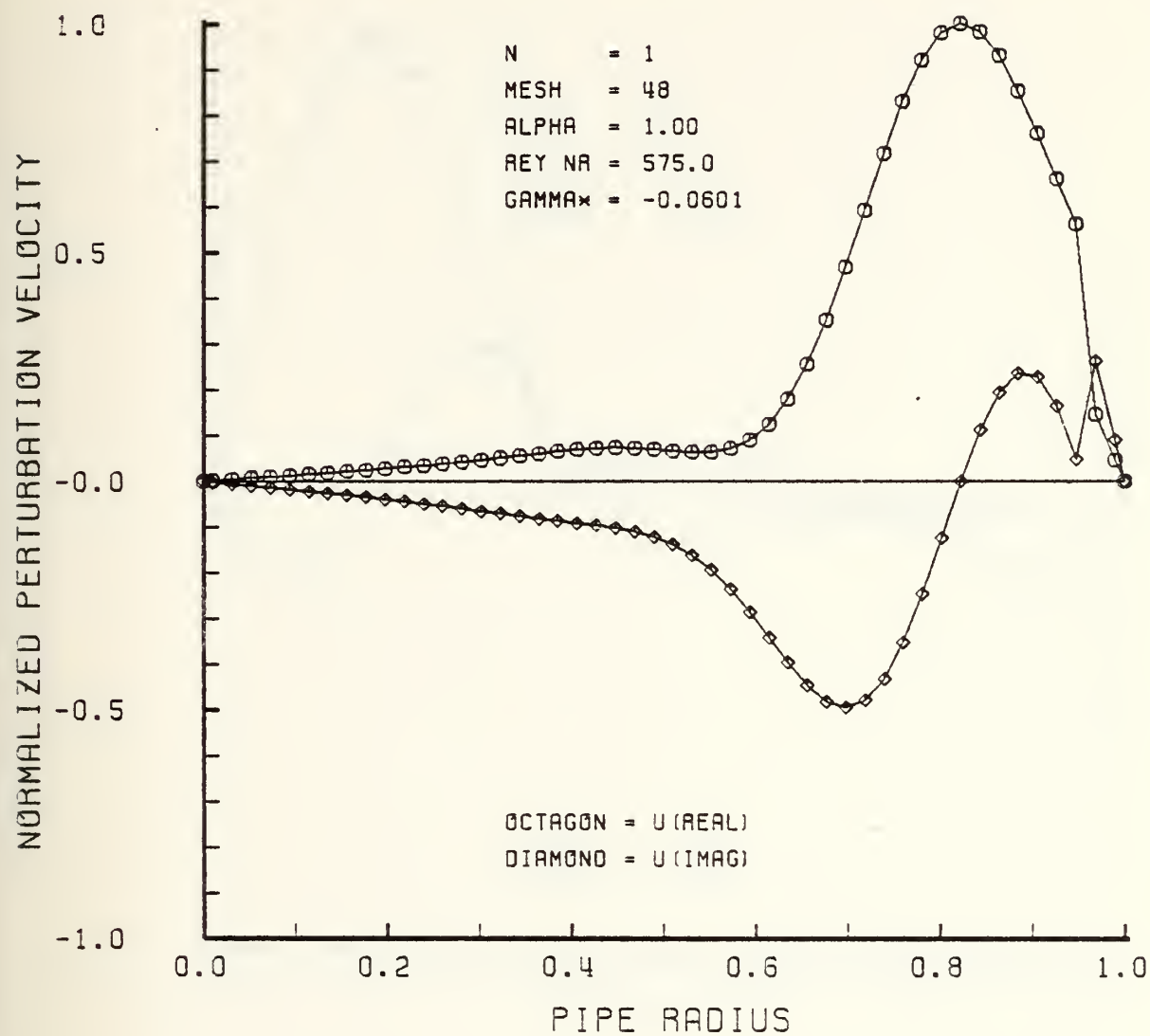


Figure 6-14

NORMALIZED PERTURBATION VELOCITY VS RADIUS

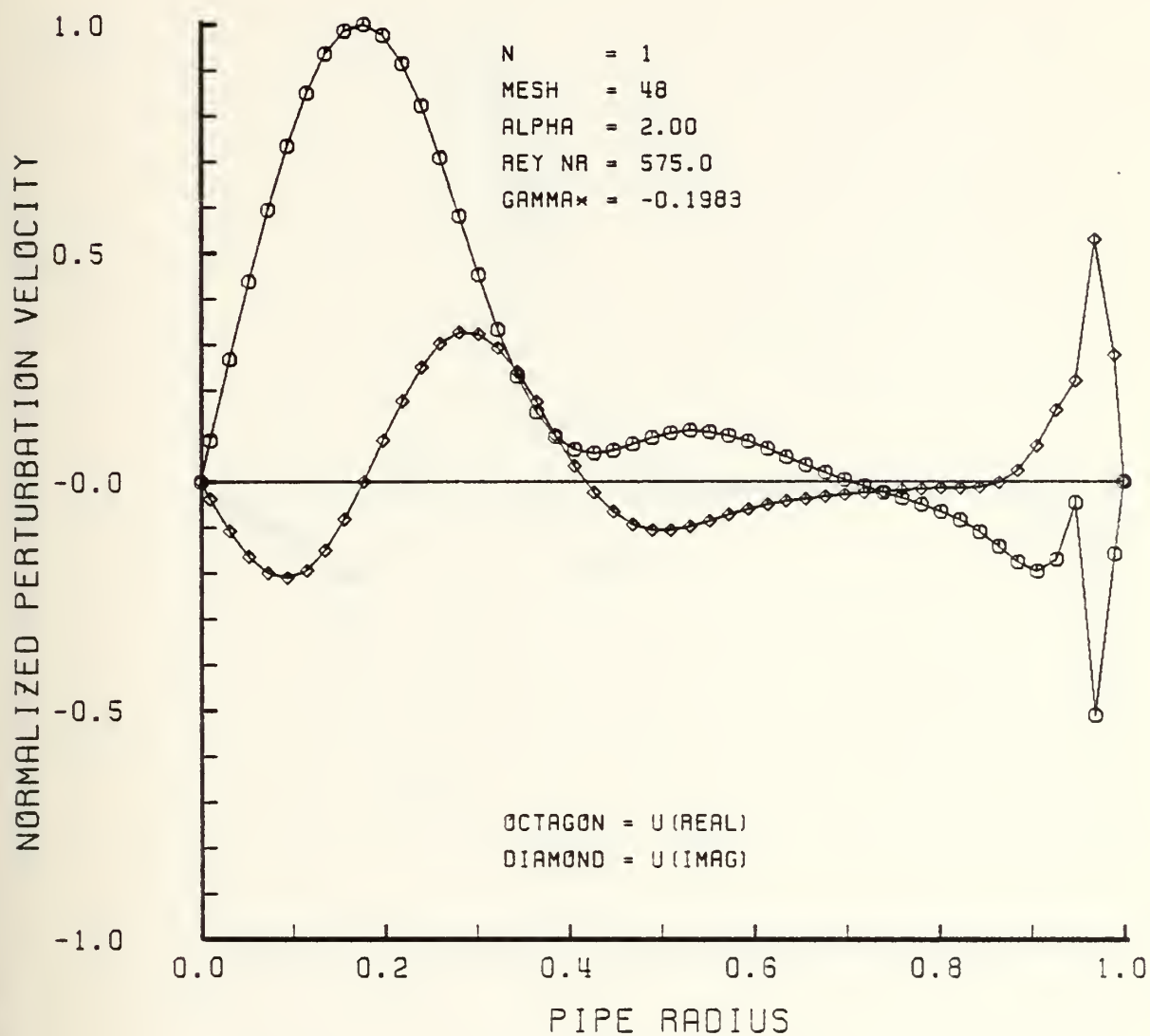


Figure 6-15

NORMALIZED PERTURBATION VELOCITY VS RADIUS

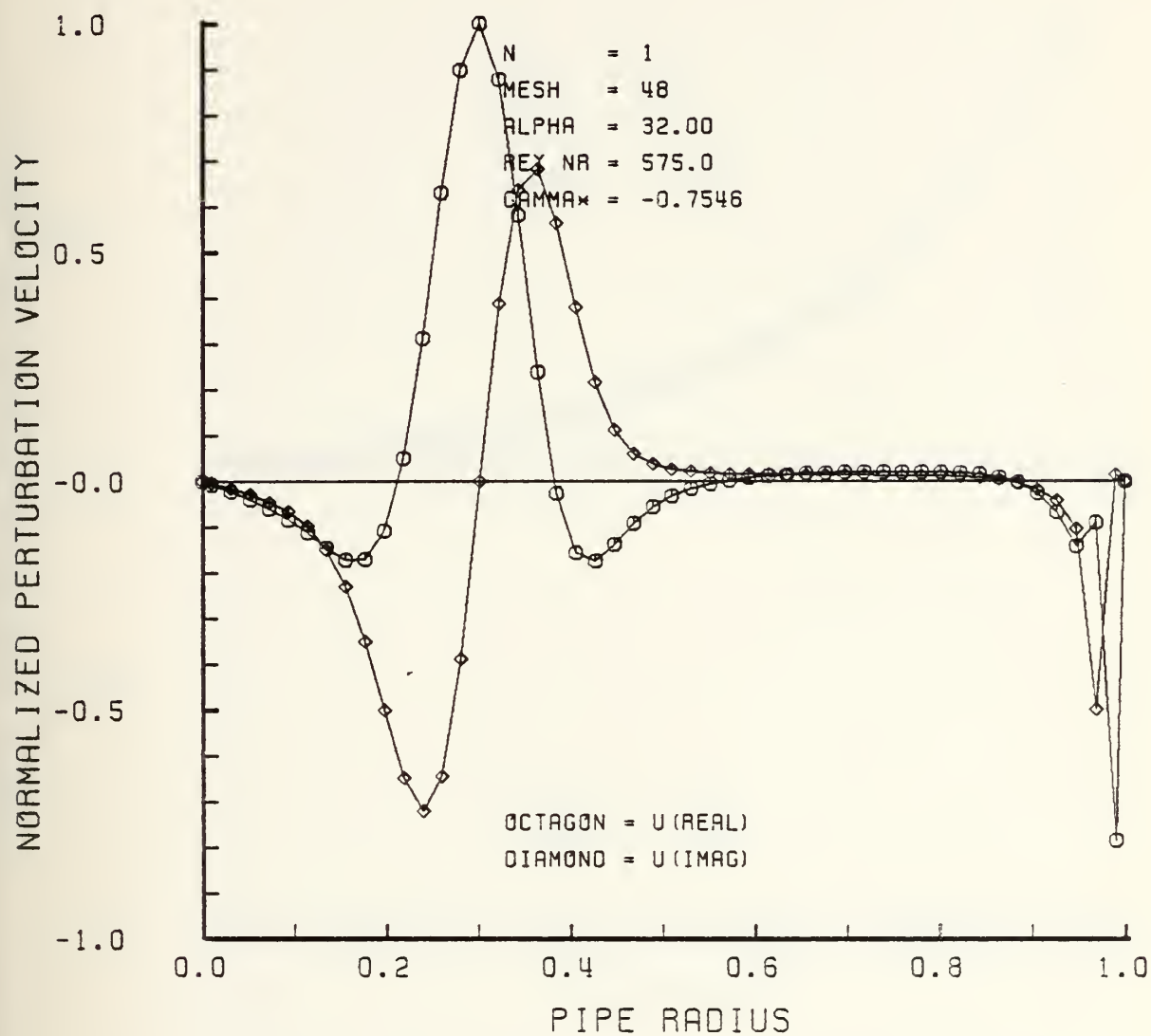


Figure 6-16

NORMALIZED PERTURBATION VELOCITY VS RADIUS

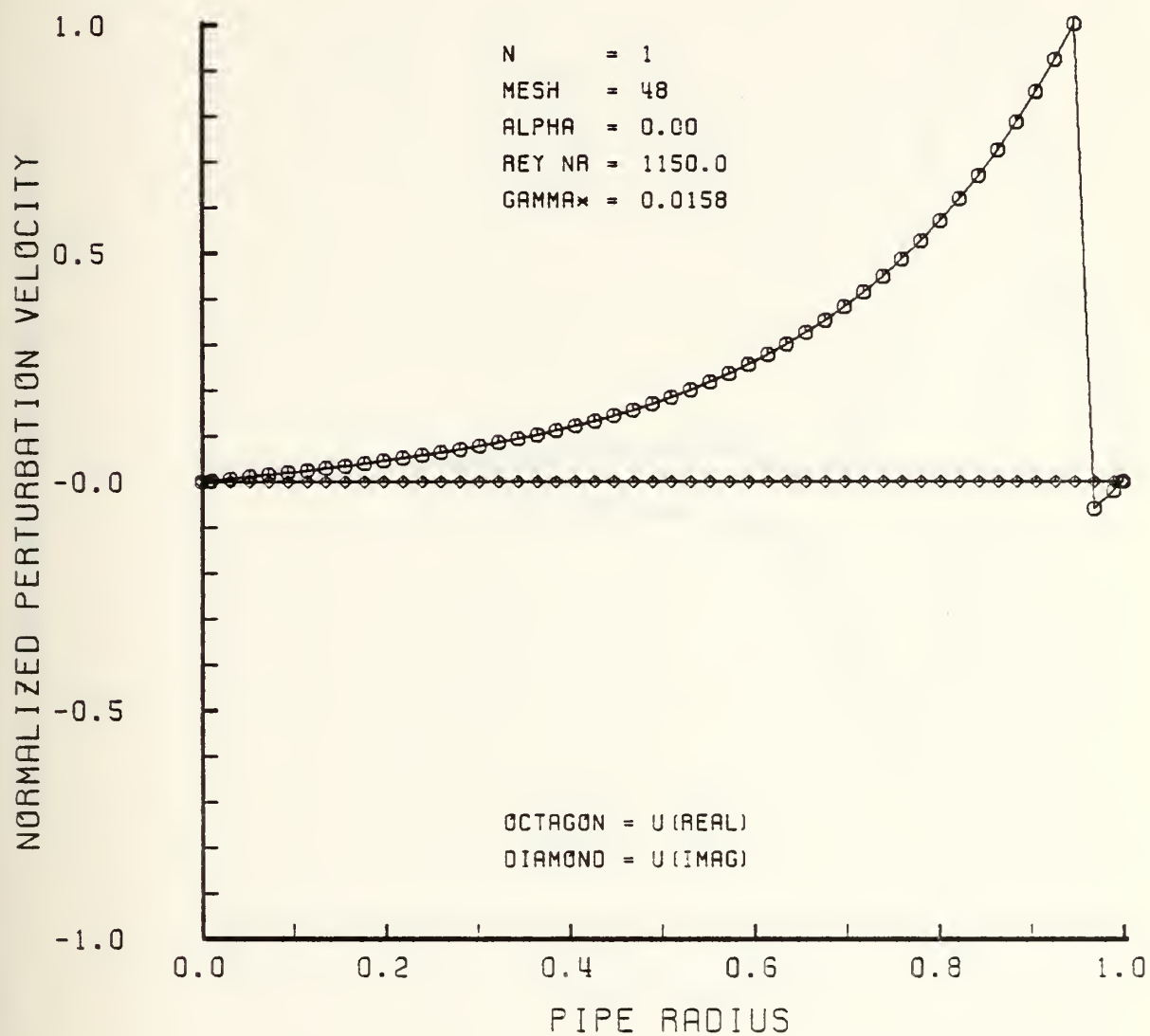


Figure 6-17

NORMALIZED PERTURBATION VELOCITY VS RADIUS

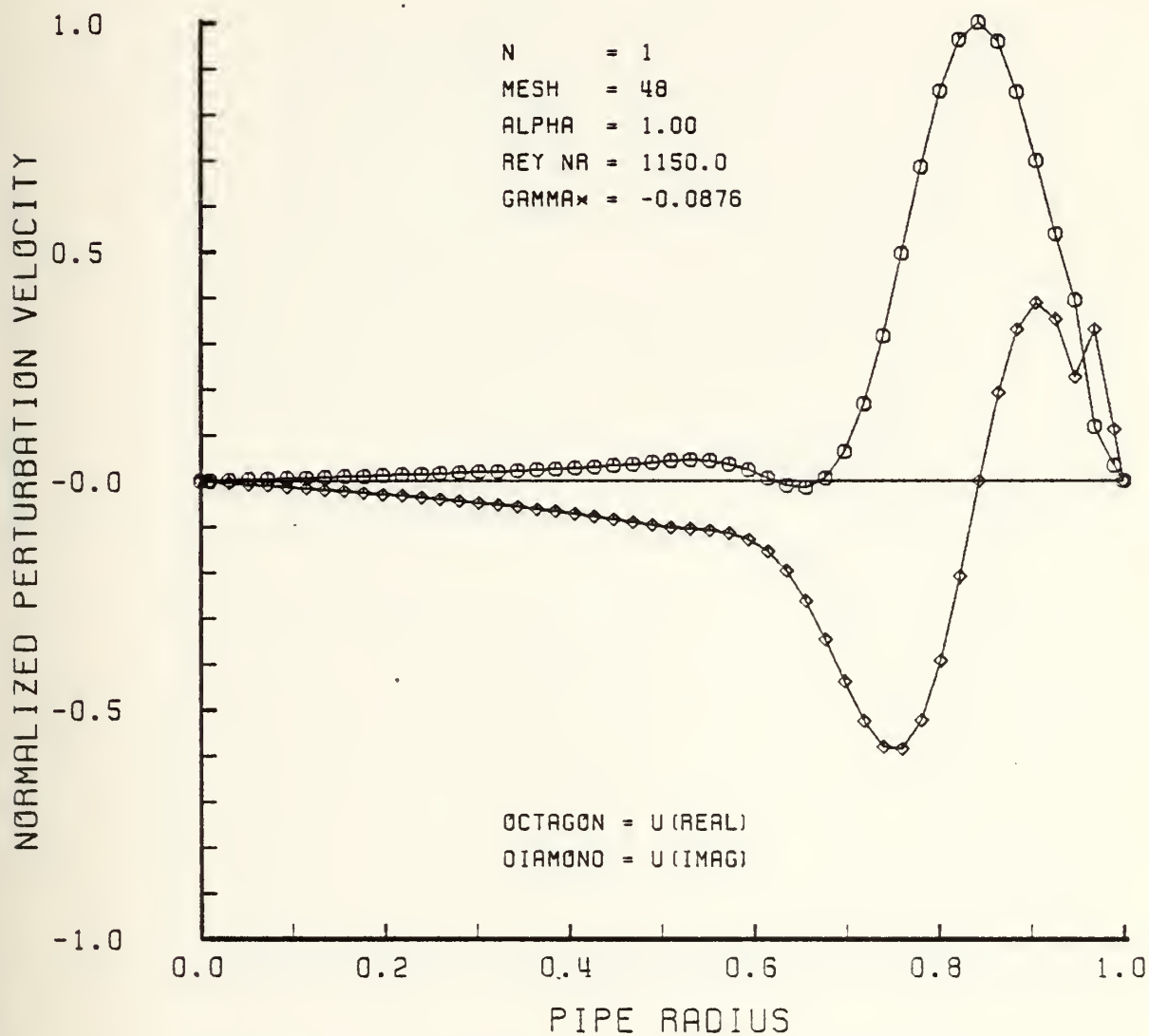


Figure 6-18

NORMALIZED PERTURBATION VELOCITY VS RADIUS

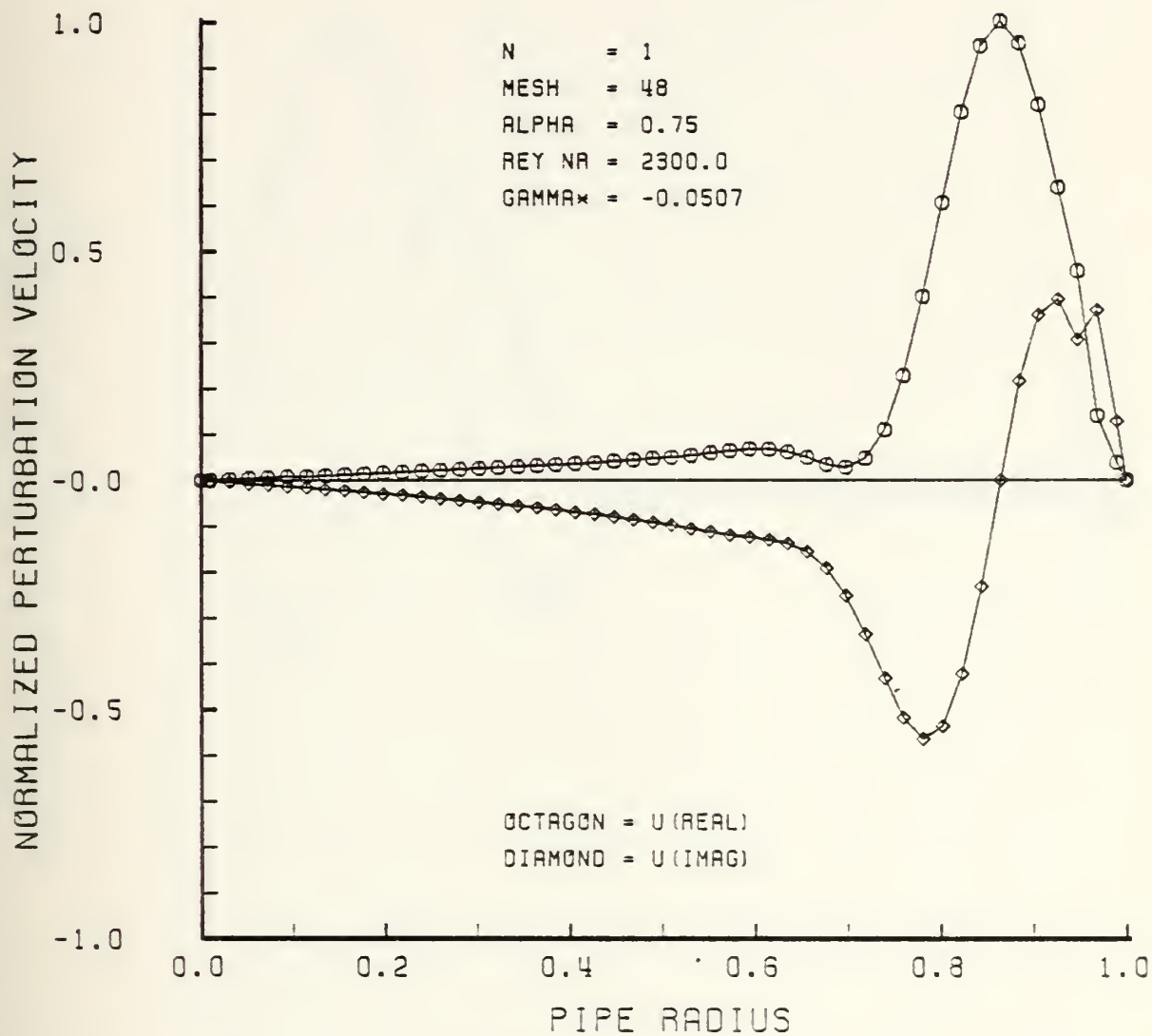


Figure 6-19

NORMALIZED PERTURBATION VELOCITY VS RADIUS

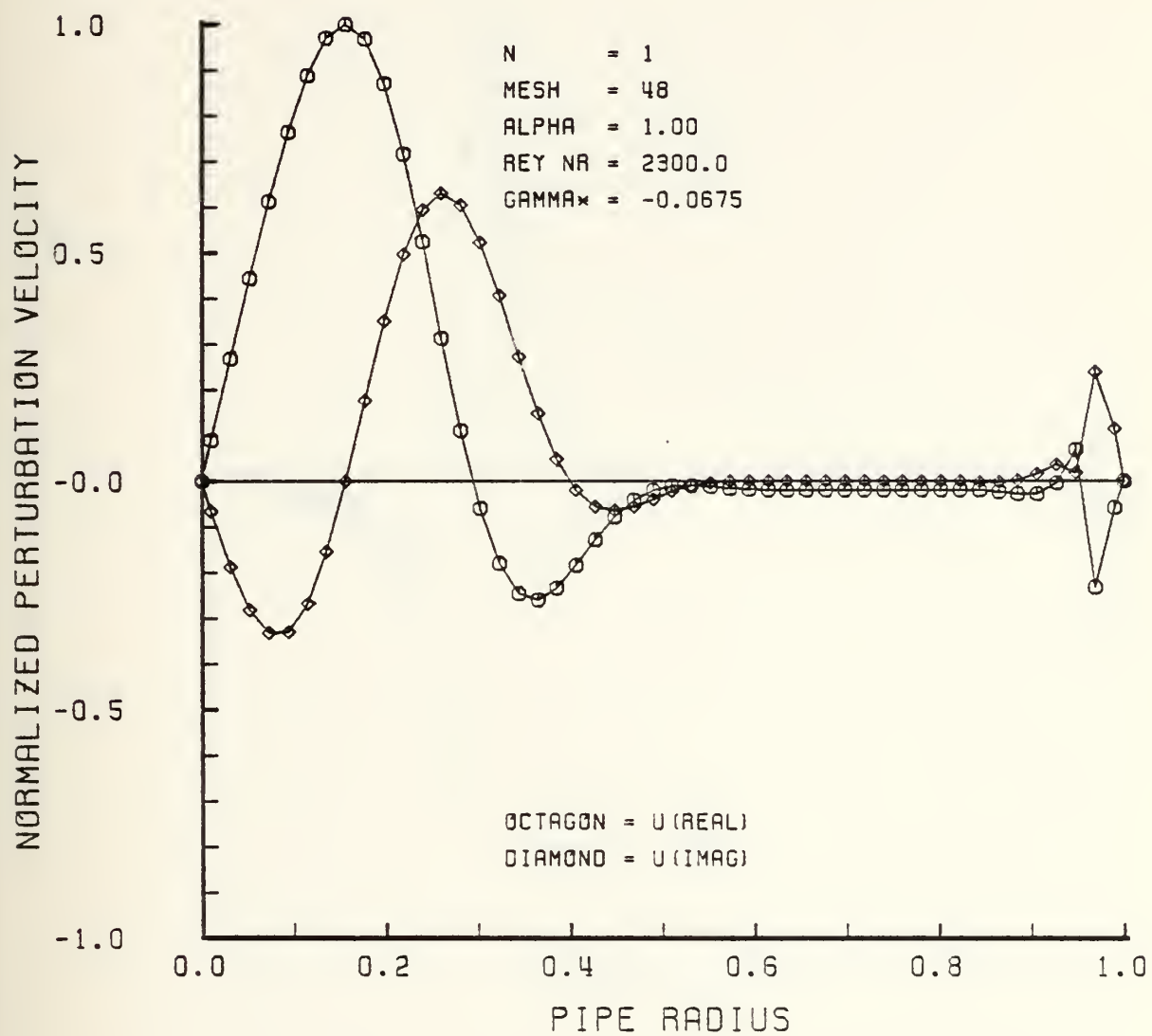


Figure 6-20

NORMALIZED PERTURBATION VELOCITY VS RADIUS

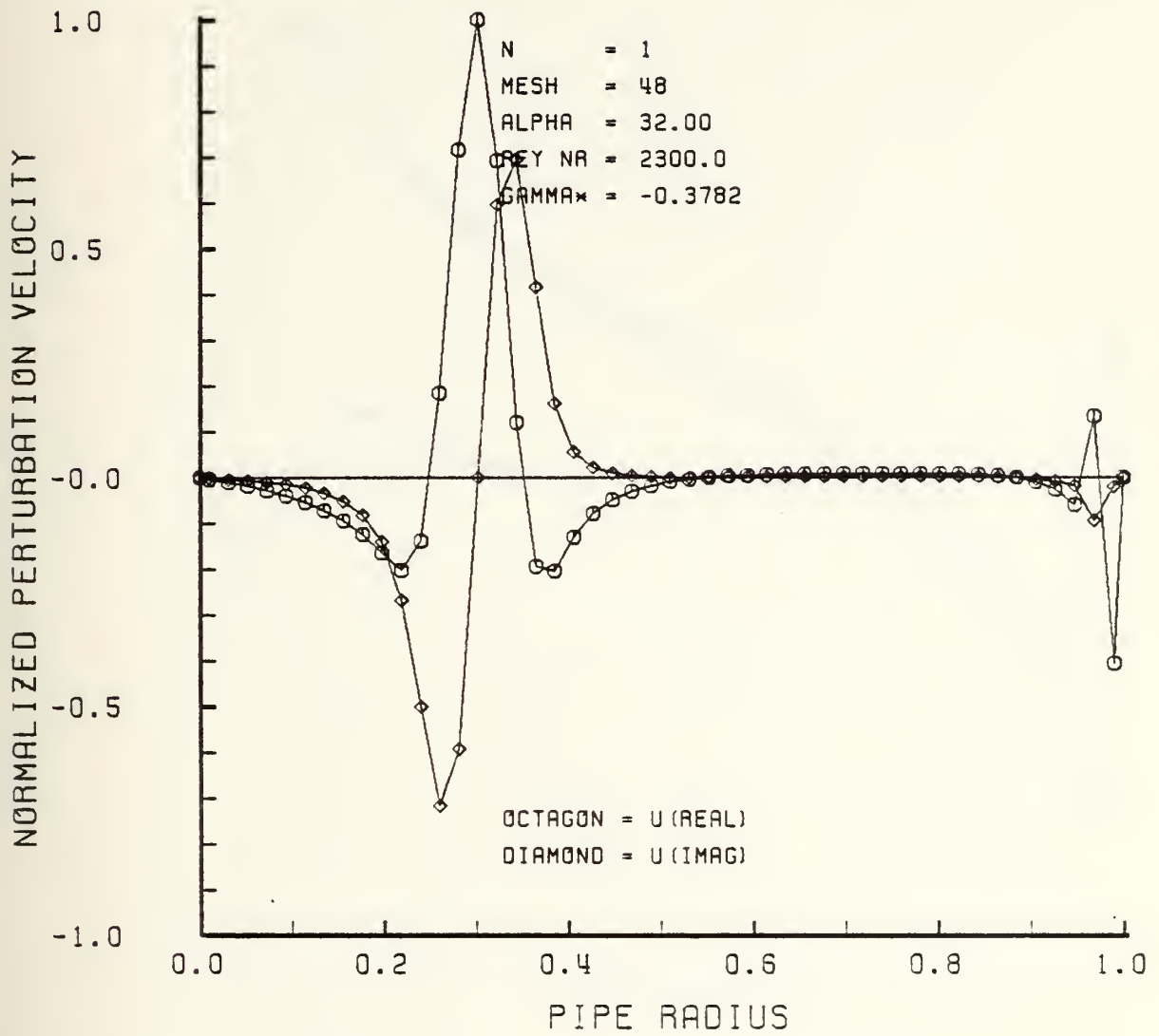


Figure 6-21

NORMALIZED PERTURBATION VELOCITY VS RADIUS

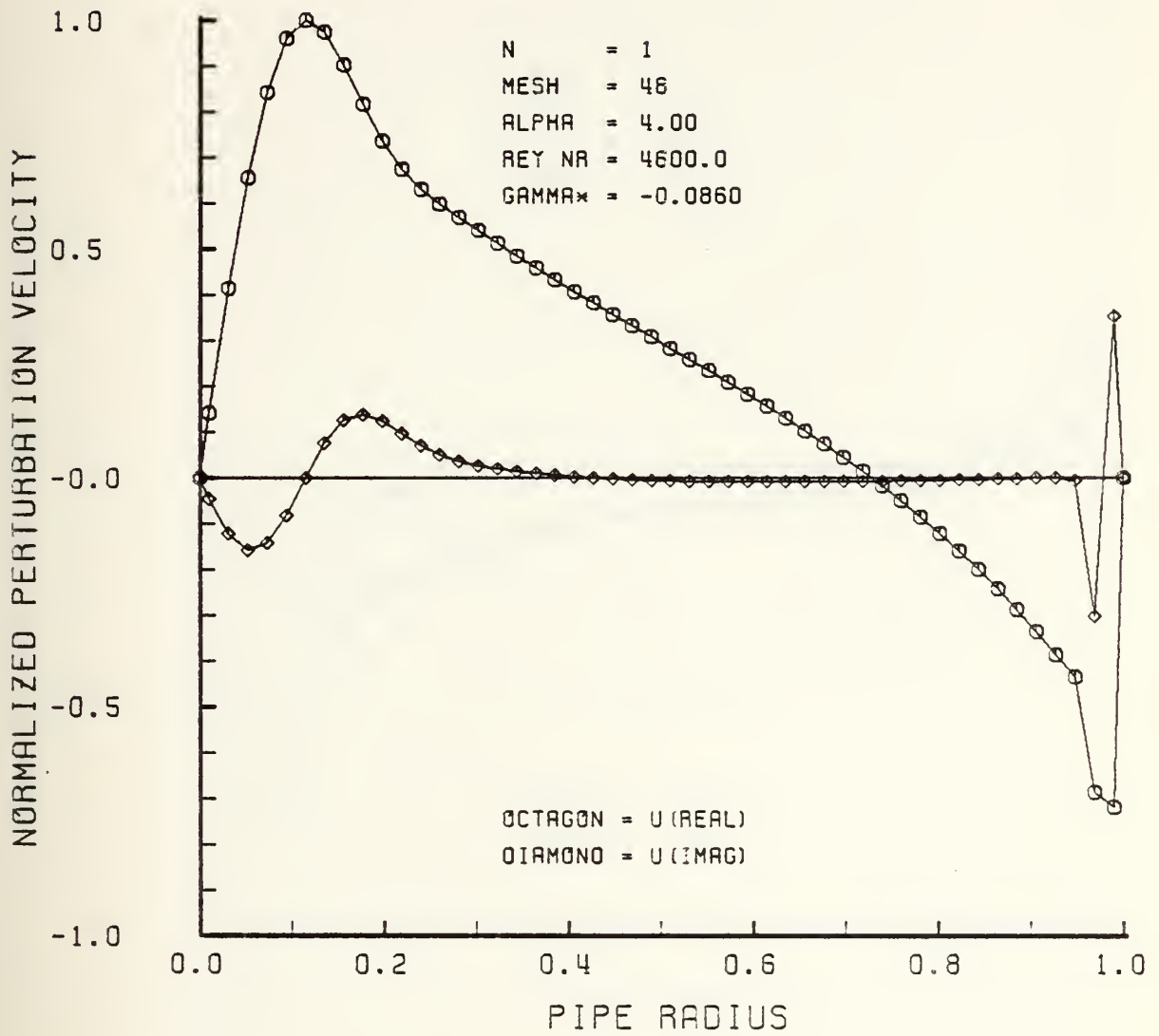


Figure 6-22

NORMALIZED PERTURBATION VELOCITY VS RADIUS

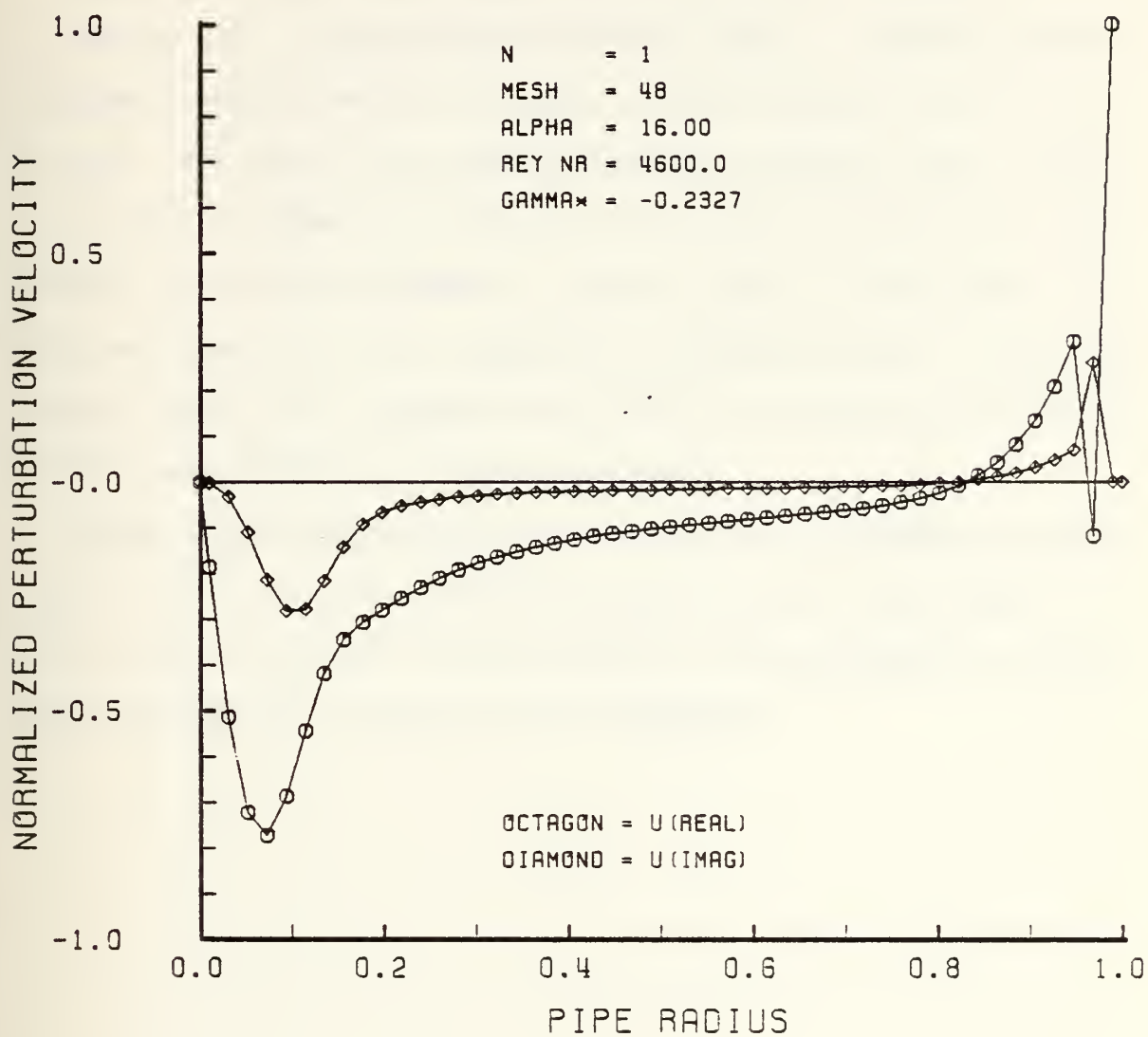


Figure 6-23

C. RESULTS FOR $n = 6$

Results for angular wave number $n = 6$ are similar to those for $n = 0$ in that the flow is stable at all Reynolds numbers. Stability data is presented in Tables 6-4 and 6-5 where it can be determined that this is the case. The data is once again presented as Reynolds number contours in the plots of GAMMA^* vs. α in Figures 6-24 and 6-25 and as α contours in the plot of GAMMA^* vs. Reynolds number in Figure 6-26. The trends are clear; the flow is stable at all Reynolds numbers, increasing Reynolds number has a destabilizing effect on the flow and increasing the axial wave number has a stabilizing effect.

Figures 6-27 through 6-36 are representative perturbation velocity plots for $n = 6$ at several Reynolds numbers and axial wave numbers. It can be seen in Figures 6-31 and 6-32 that the perturbation activity shifts from the wall to the axis for increasing α .

Table 6-4. Stability Data for Angular Wave Number $n = 6$

Growth or Decay Trends of Least Stable Eigenvalue, γ^*

Re	$\alpha=0.0$	$\alpha=0.05$	$\alpha=1.0$	$\alpha=2.0$	$\alpha=4.0$	$\alpha=8.0$	$\alpha=16.0$	$\alpha=32.0$
300	-0.3291	-0.3512	-0.4829	-0.7295	-1.1654	-1.9718	-2.8067	-4.6185
575	-0.1717	-0.2450	-0.3644	-0.5651	-0.9064	-1.4798	-2.0927	-
1150	-0.0858	-0.1814	-0.2789	-0.4386	-0.7049	-1.0532	-	-
2300	-0.0429	-0.1390	-0.2173	-0.3447	-0.5136	-	-	-
4600	-0.0215	-0.1084	-0.1712	-0.2549	-0.3631	-	-	-
9200	-0.0107	-0.0855	-0.1272	-0.1802	-0.2565	-	-	-
18400	-0.0054	-0.0636	-0.0899	-0.1273	-0.1811	-	-	-

Note: Values are based on 50 mesh points.

Table 6-5. Stability Data for Angular Wave Number $n = 6$

Growth or Decay Trends of Least Stable Eigenvalue, γ^*

Re	$\alpha=0.0$	$\alpha=0.05$	$\alpha=0.10$	$\alpha=0.15$	$\alpha=0.20$	$\alpha=0.50$	$\alpha=0.75$	$\alpha=1.0$
300	-0.3291	-0.3267	-0.3228	-0.3201	-0.3192	-0.3512	-0.4156	-0.4829
575	-0.1717	-0.1686	-0.1665	-0.1679	-0.1727	-0.2450	-0.3071	-0.3644
1150	-0.0858	-0.0833	-0.0864	-0.0960	-0.1092	-0.1814	-0.2325	-0.2789
2300	-0.0429	-0.0432	-0.0546	-0.0675	-0.0794	-0.1390	-0.1801	-0.2173
4600	-0.0215	-0.0273	-0.0397	-0.0505	-0.0603	-0.1084	-0.1414	-0.1712
9200	-0.0107	-0.0198	-0.0302	-0.0390	-0.0469	-0.0855	-0.1102	-0.1272
18400	-0.0054	-0.0151	-0.0234	-0.0305	-0.0368	-0.0636	-0.0779	-0.0899

Note: Values are based on 50 mesh points.

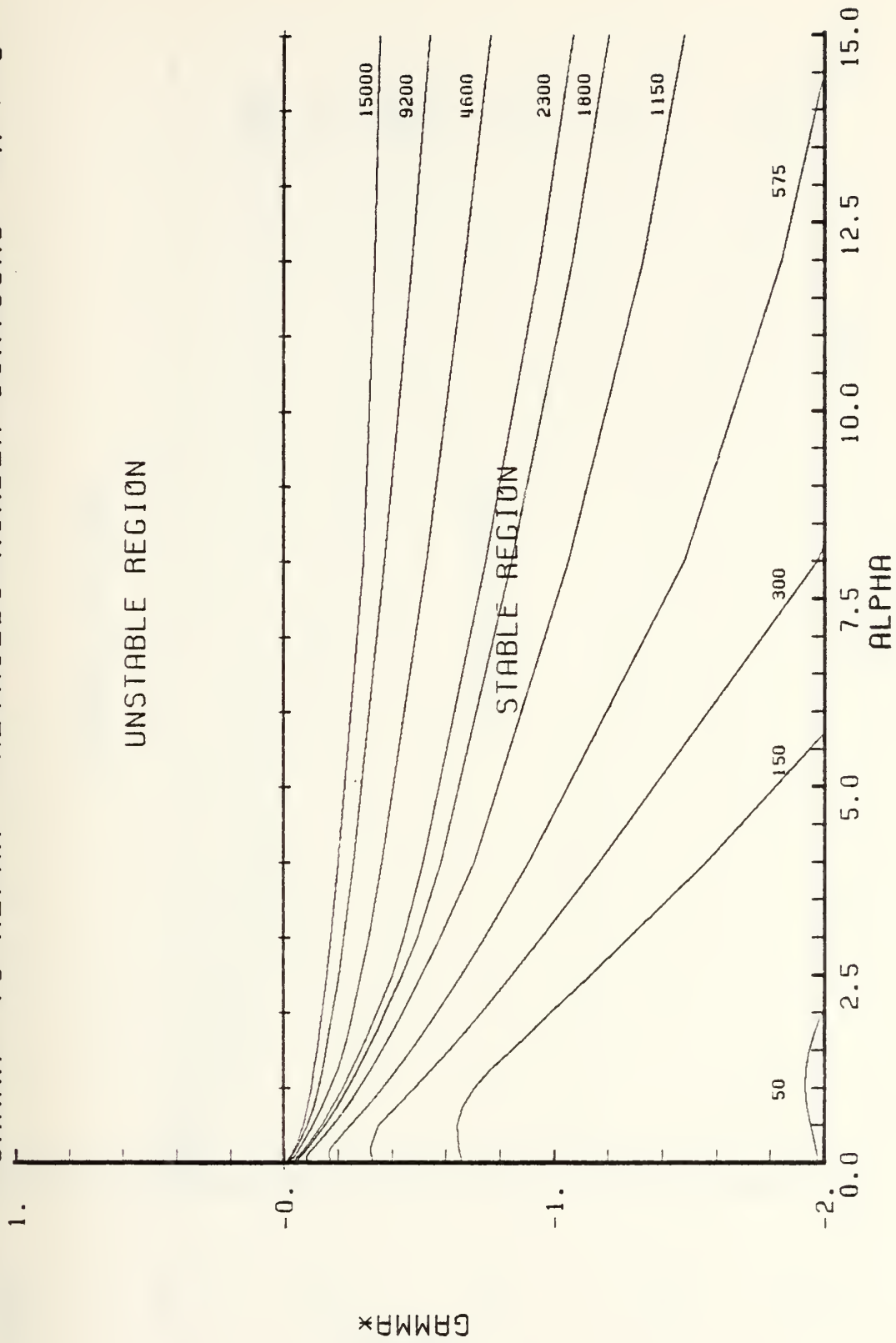


Figure 6-24

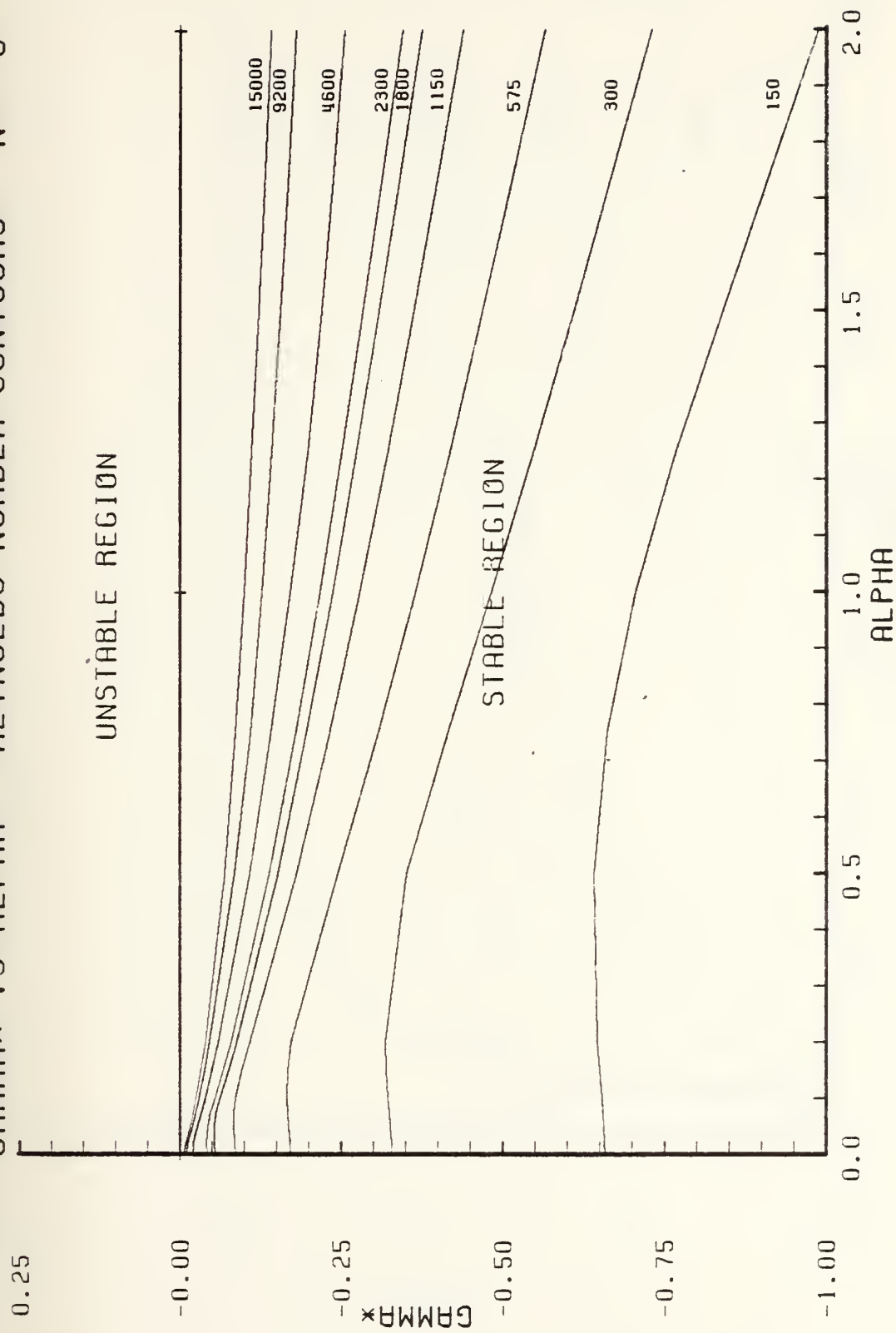


Figure 6-25

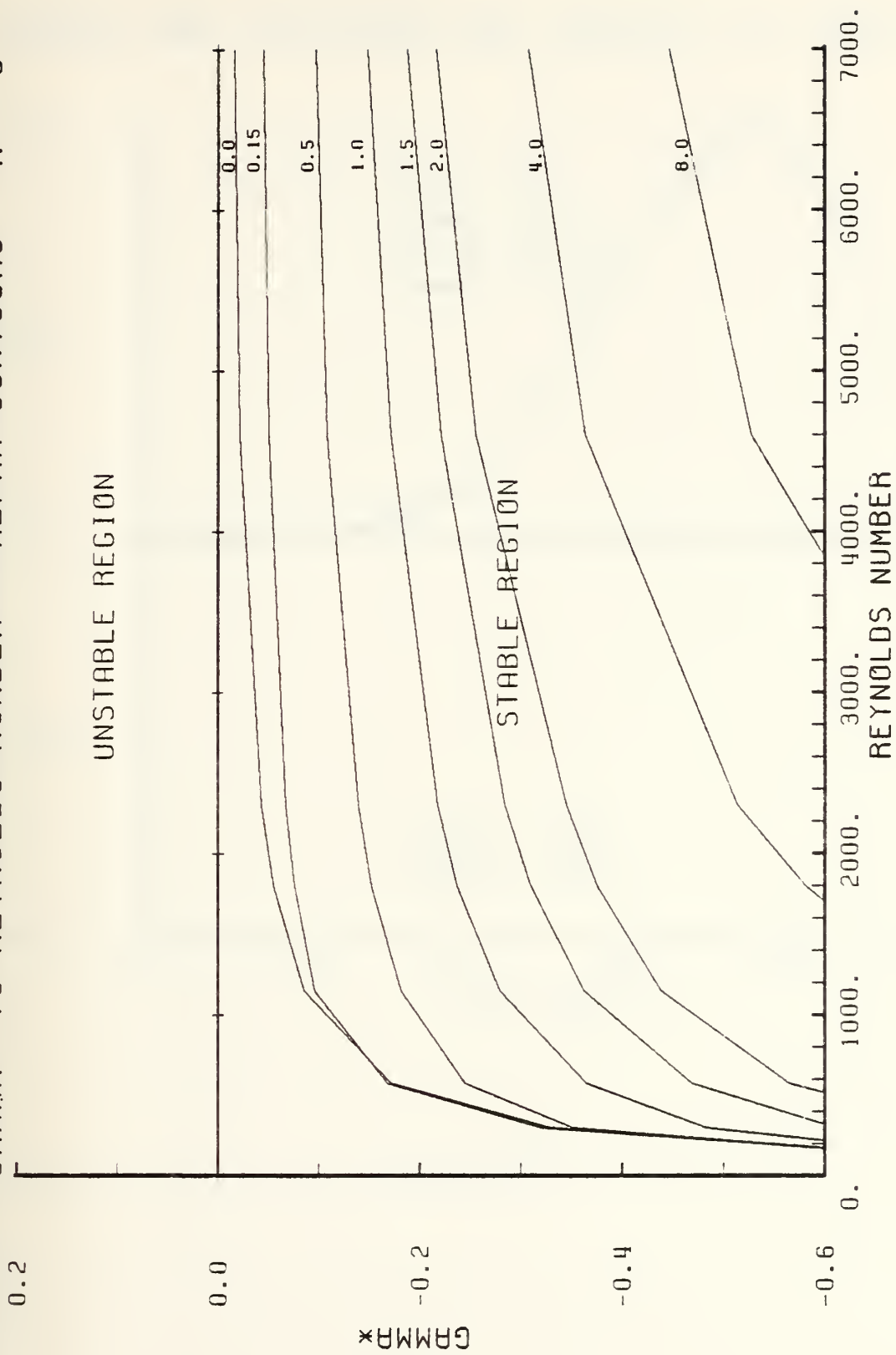


Figure 6-26

NORMALIZED PERTURBATION VELOCITY VS RADIUS

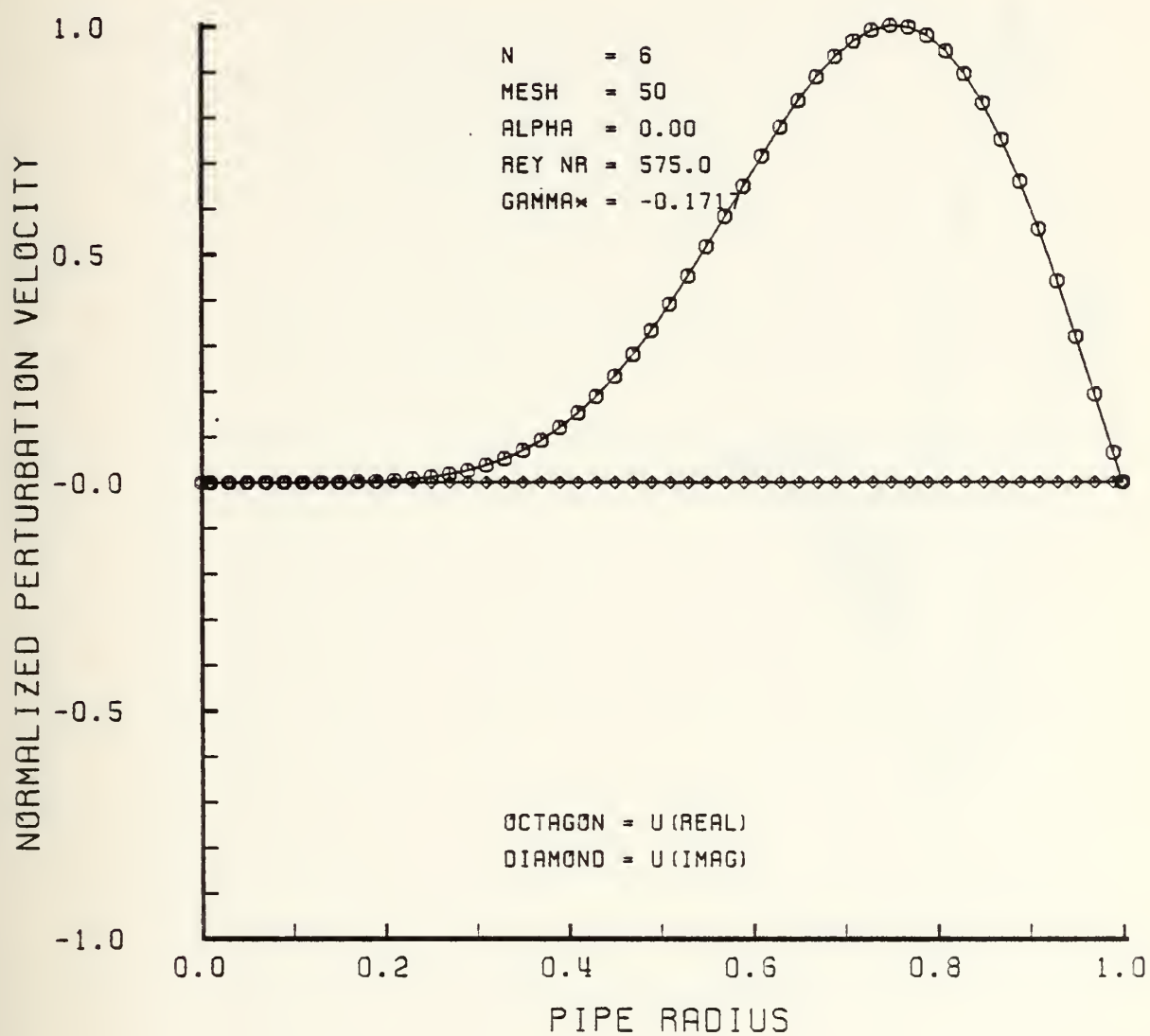


Figure 6-27

NORMALIZED PERTURBATION VELOCITY VS RADIUS

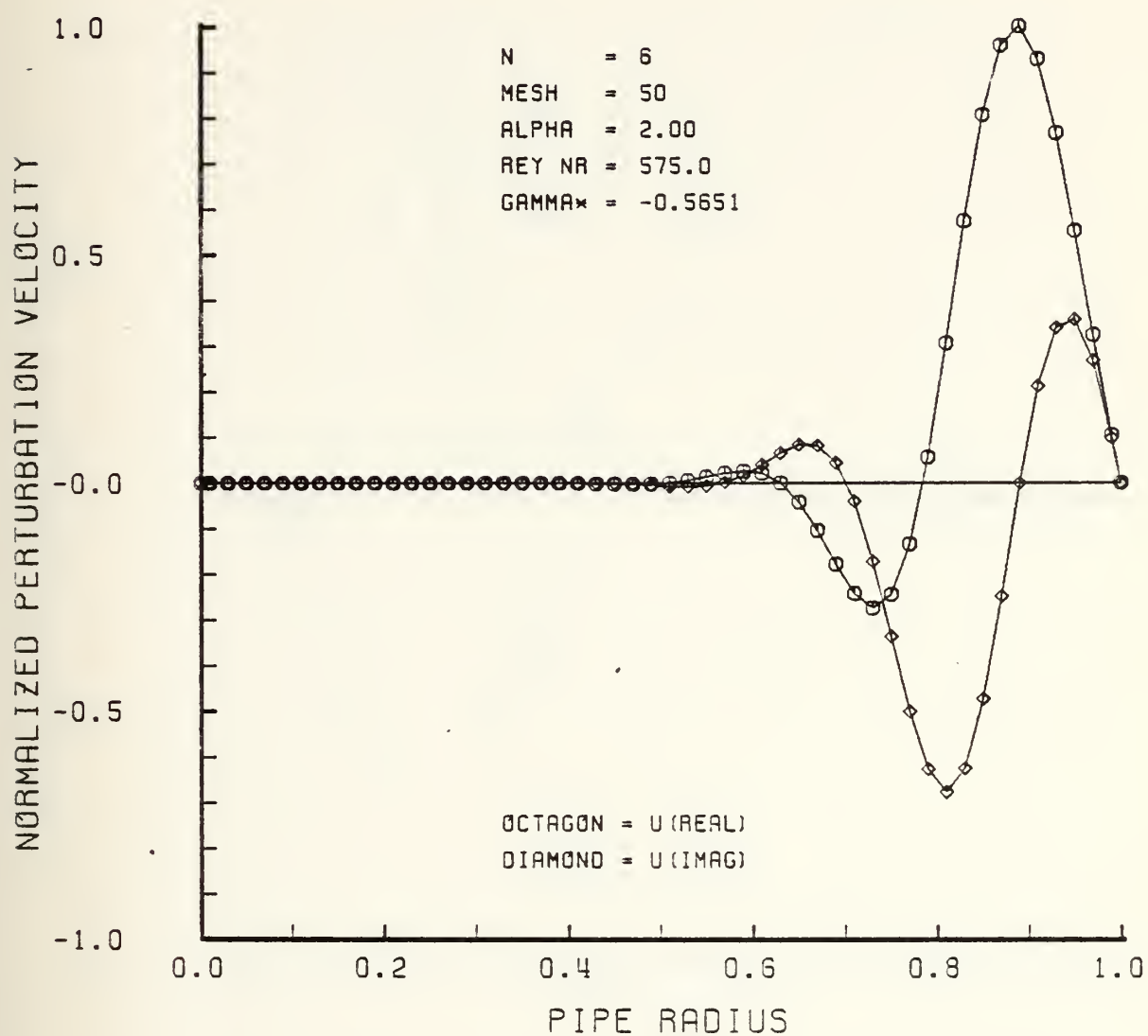


Figure 6-28

NORMALIZED PERTURBATION VELOCITY VS RADIUS

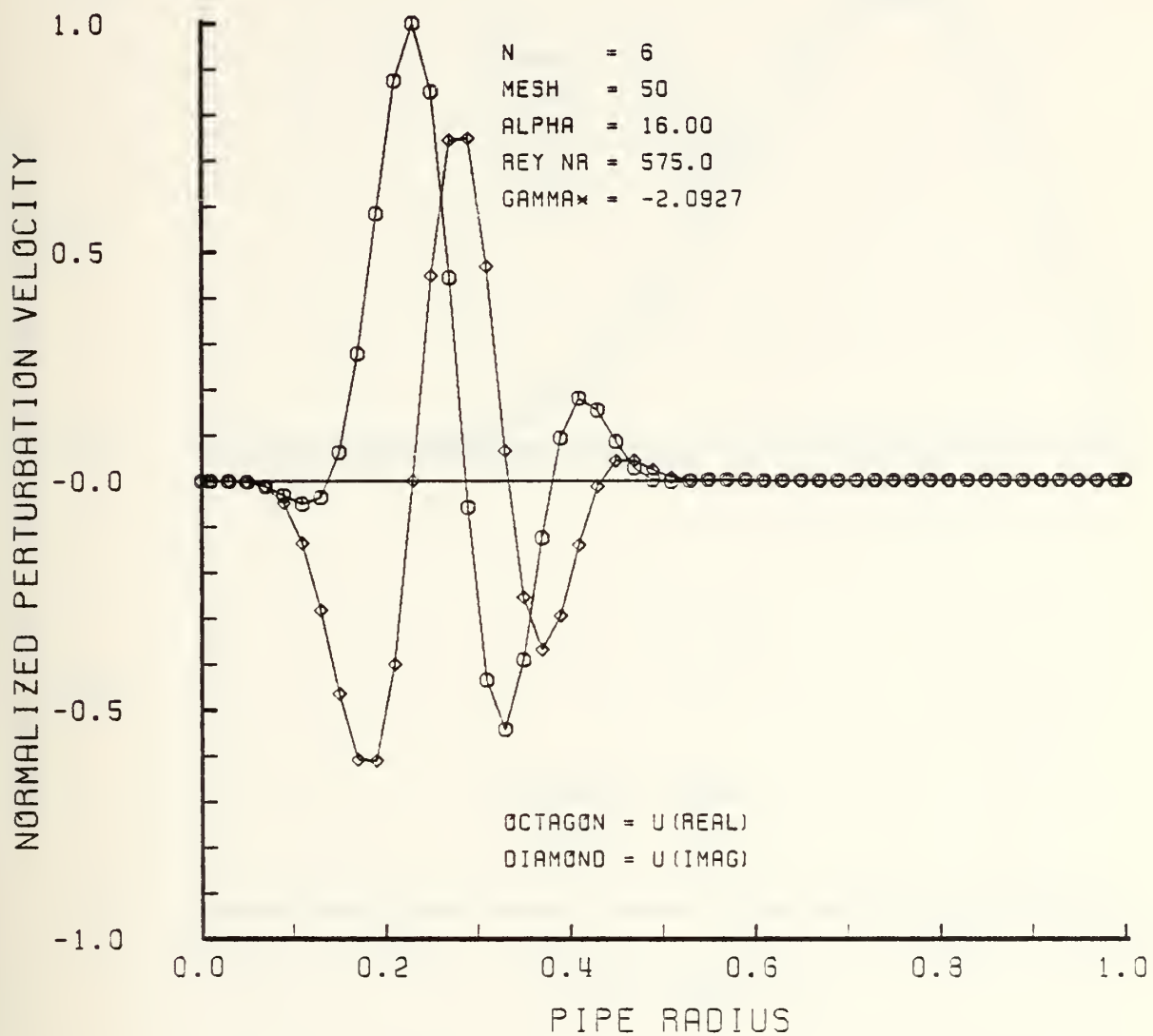


Figure 6-29

NORMALIZED PERTURBATION VELOCITY VS RADIUS

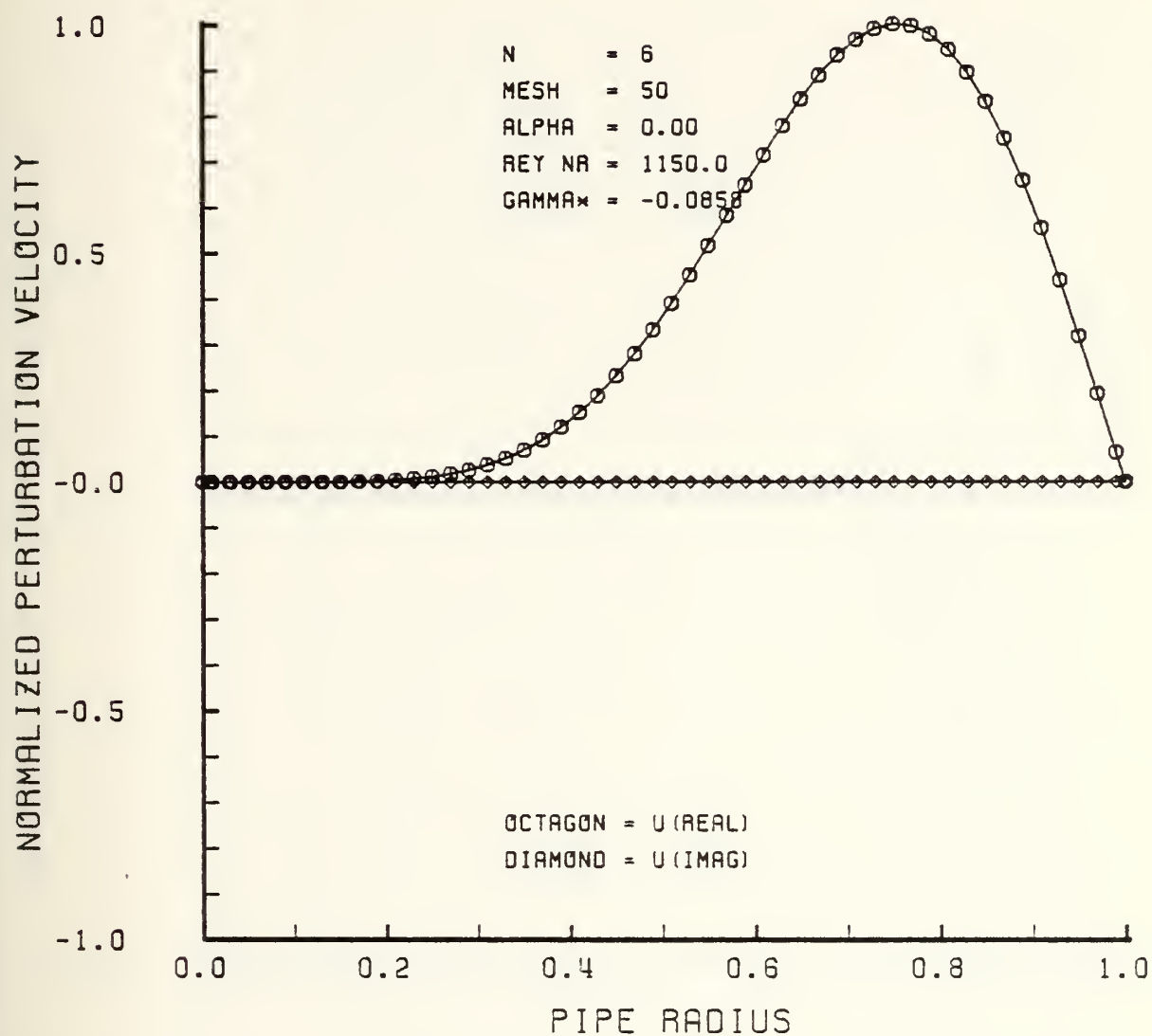


Figure 6-30

NORMALIZED PERTURBATION VELOCITY VS RADIUS

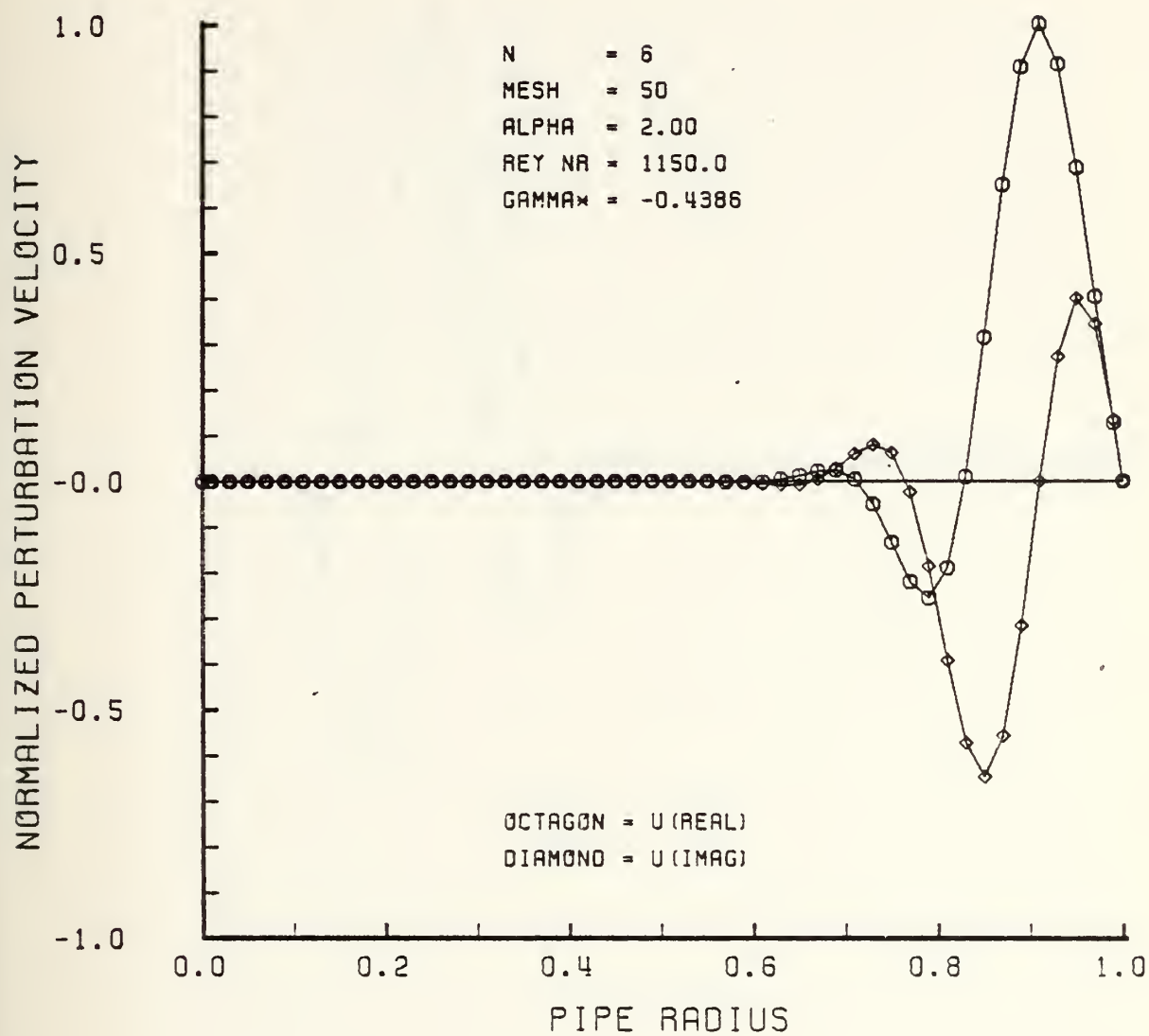


Figure 6-31

NORMALIZED PERTURBATION VELOCITY VS RADIUS

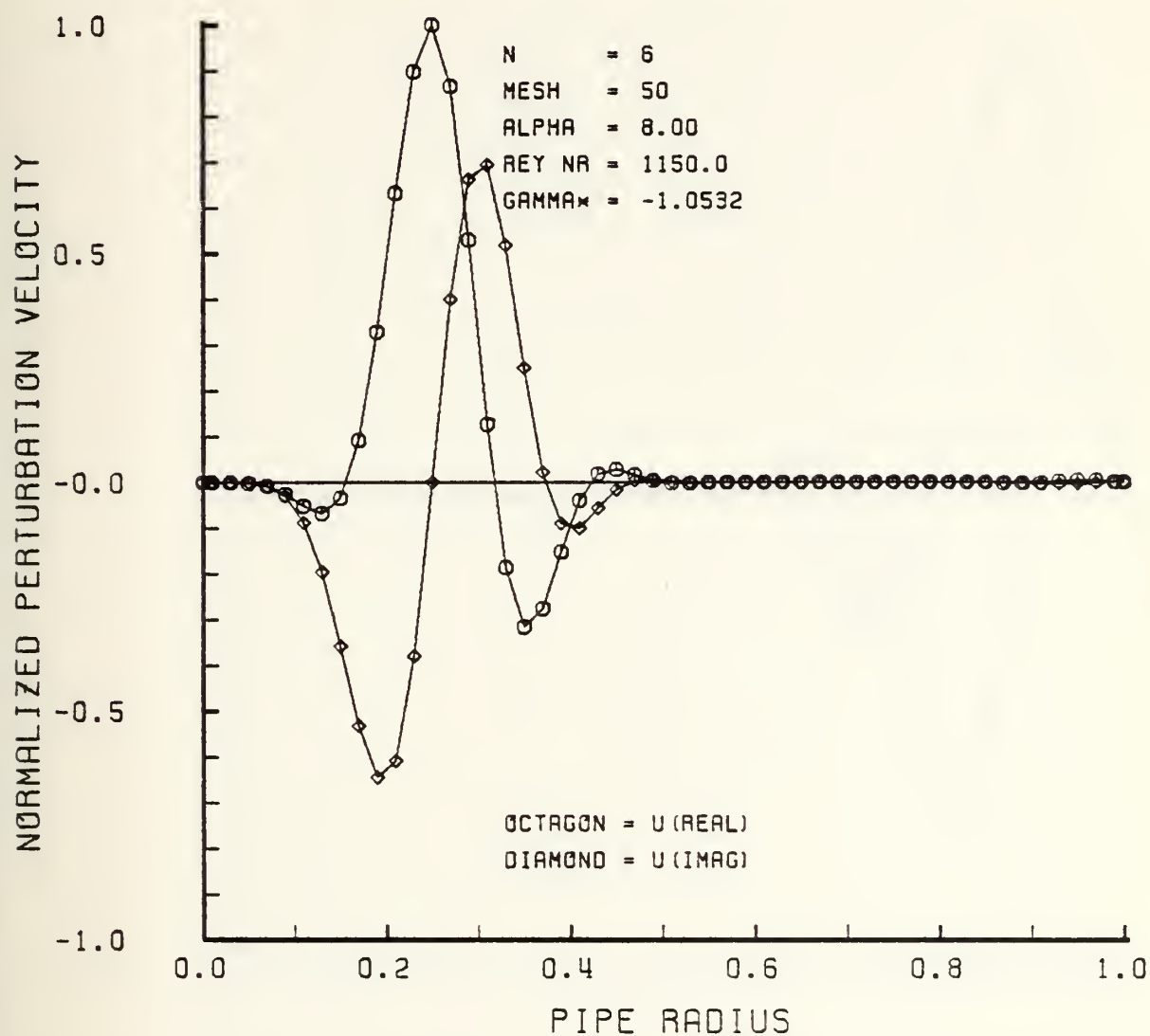


Figure 6-32

NORMALIZED PERTURBATION VELOCITY VS RADIUS

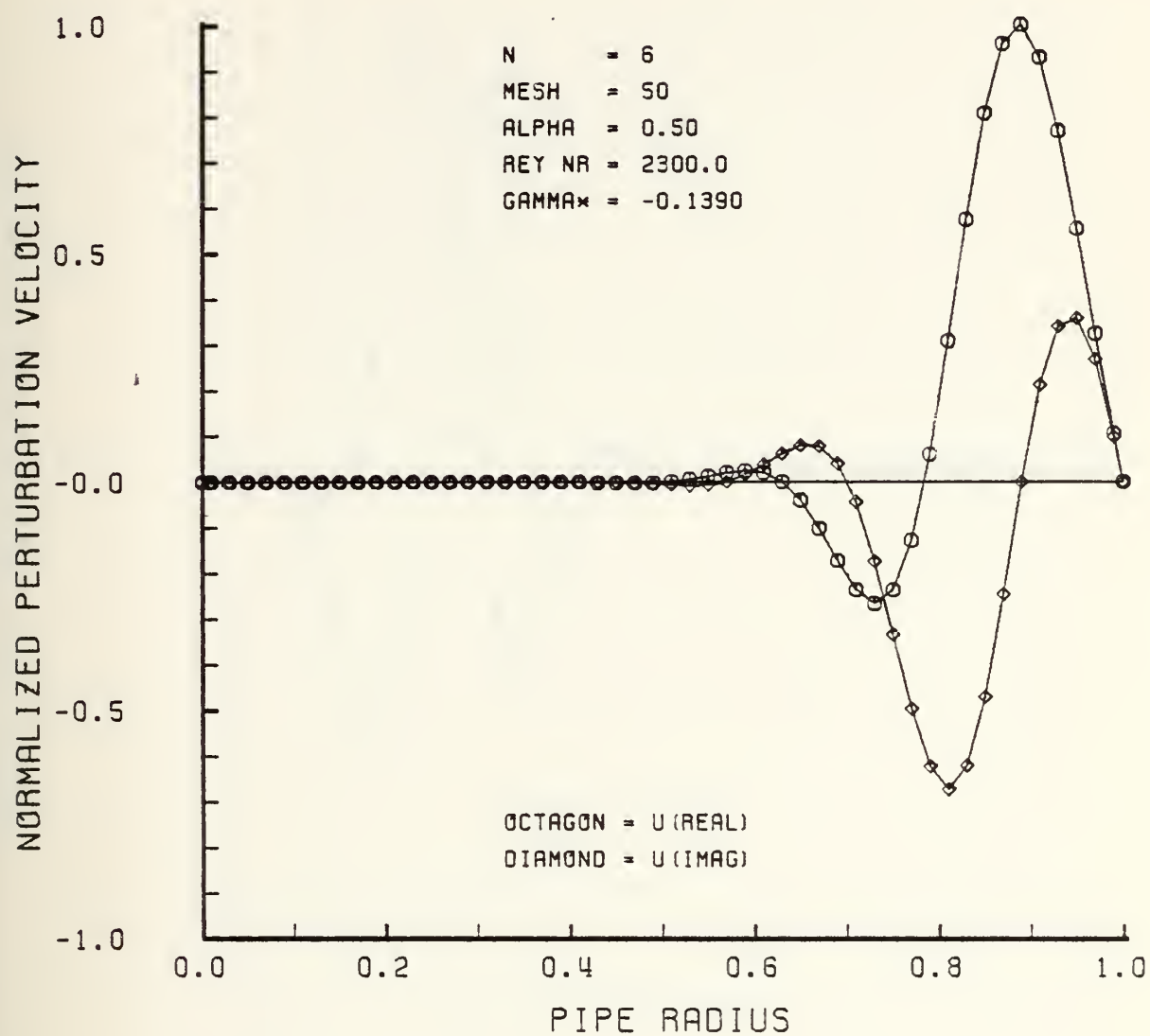


Figure 6-33

NORMALIZED PERTURBATION VELOCITY VS RADIUS

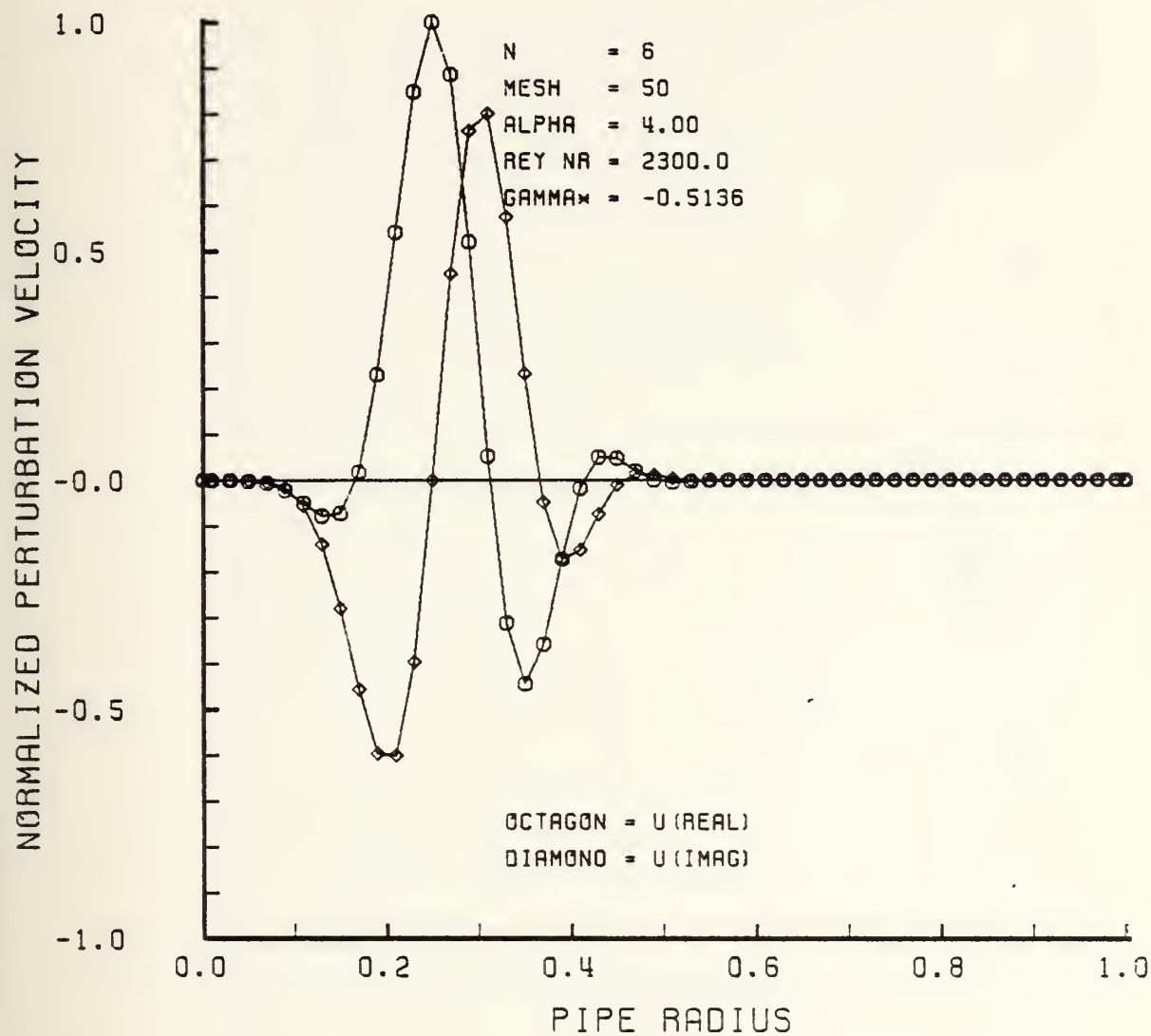


Figure 6-34

NORMALIZED PERTURBATION VELOCITY VS RADIUS

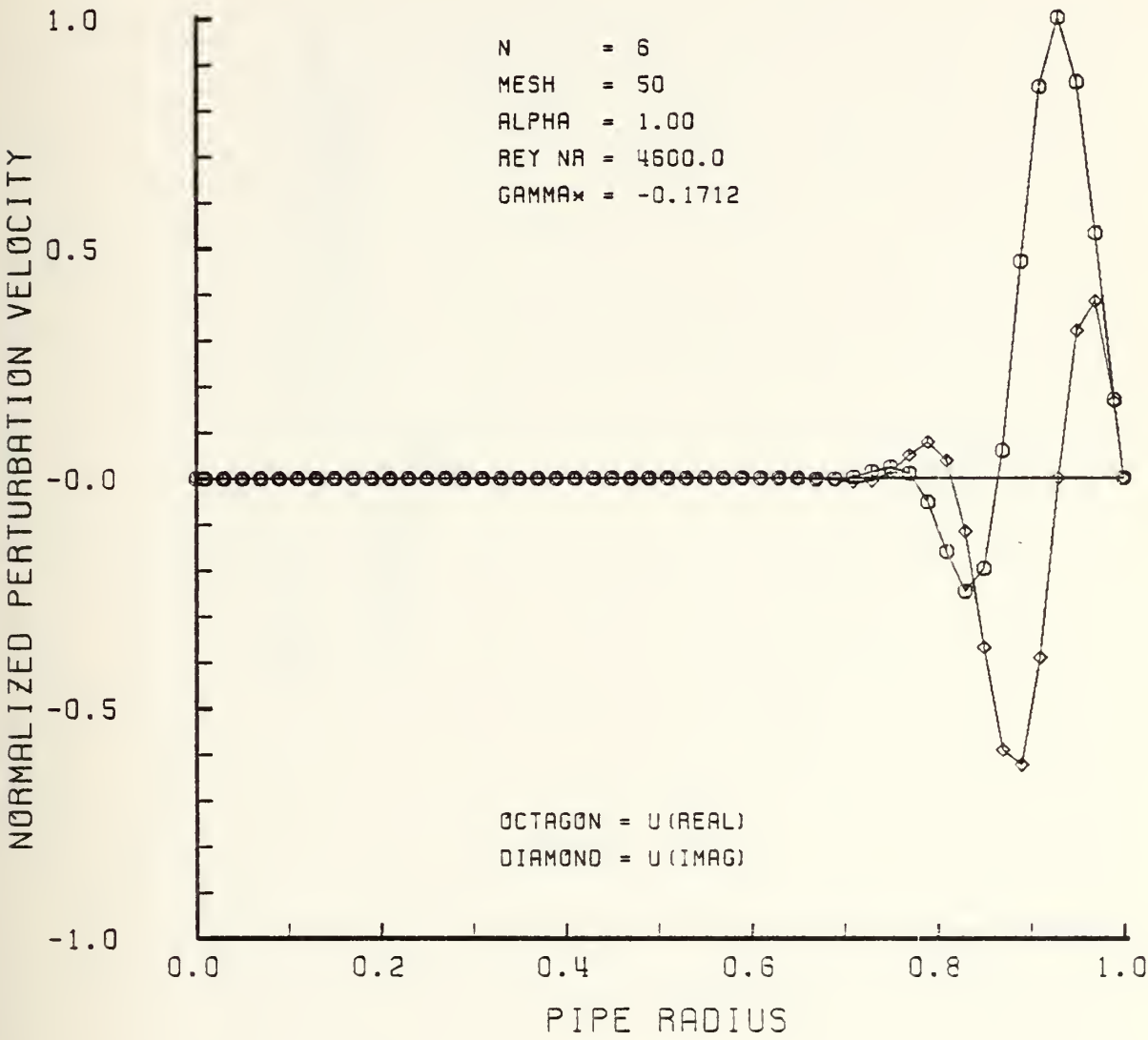


Figure 6-35

NORMALIZED PERTURBATION VELOCITY VS RADIUS

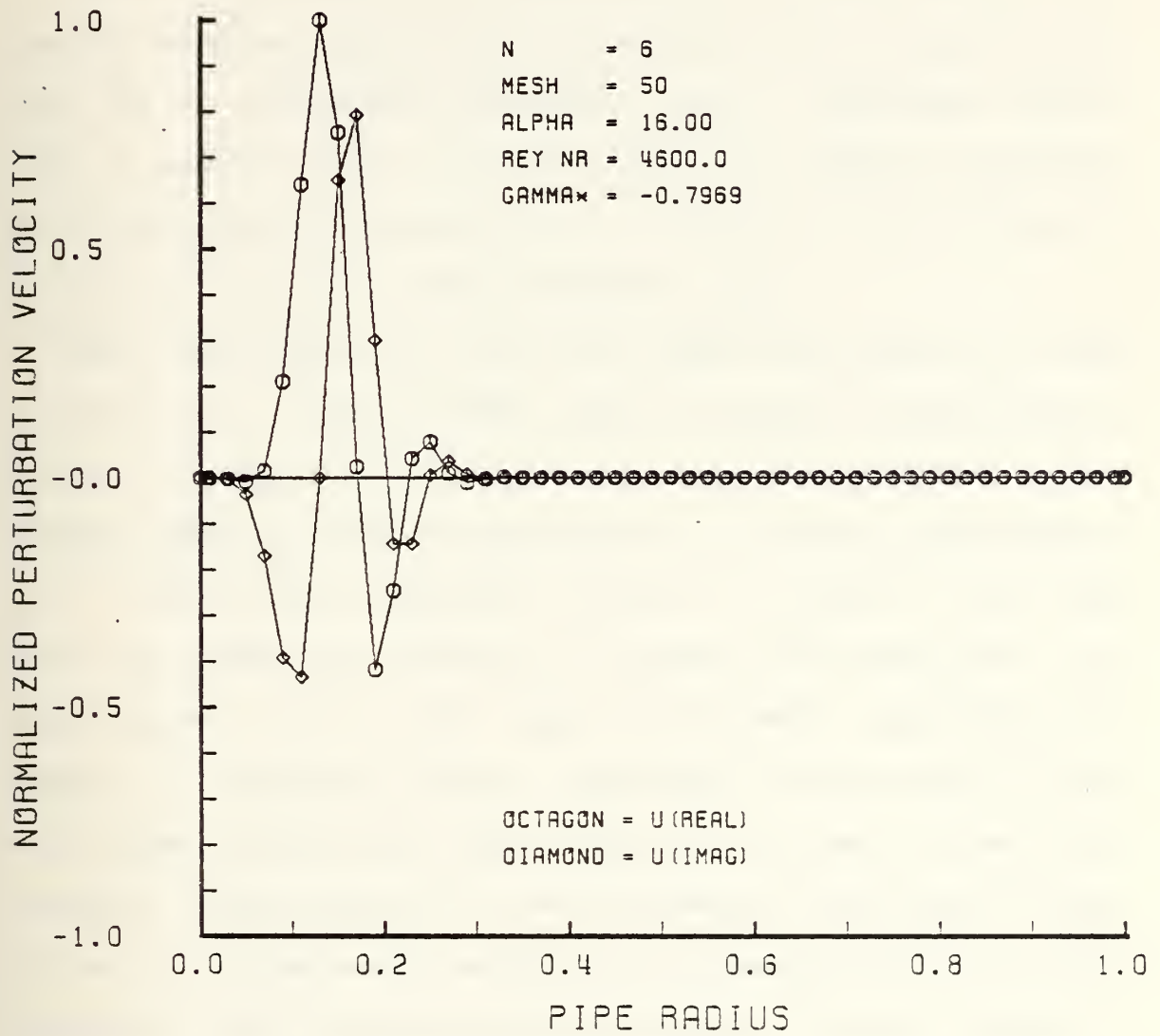


Figure 6-36

D. NUMERICAL ACCURACY

Numerical accuracy of the solutions of the governing vorticity transport equations was verified by substituting the least stable eigenvalue and its corresponding eigenvector into the eigensystem relation given in equation (5-39). The error vector was examined to determine the residual error of the solution. For the most part the error was of the order 10^{-12} to 10^{-9} , a most satisfactory result.

Upon closer examination of the error vector and the stability trends in the plots, it became evident that the accuracy of the numerical solution for the governing equations was not only dependent on the Reynolds number as previously mentioned but on the axial wave number as well. Plots of the perturbation velocity vs. radius for very large axial wave numbers are contained in Figures 6-37 through 6-39. The three figures, one for each angular wave number investigated, are examples of inaccurate solutions. Dependence of the solution on Reynolds number and axial wave number, became more evident as Re and α were increased. Rapid excursions of the perturbation velocity over a small portion of the pipe radius indicate that the computational mesh was not sufficiently fine to approximate the perturbation velocity function in the region of activity. This supposition can also be supported by examining the error vector where the residual error was found to be of the order 10^{-1} or worse, in the region of perturbation activity. Recall for $n = 1$ that some of the activity remained at the wall as α was increased. Refer to Figures 6-20 through 6-23. The residual error was

nominally of the order 10^{-5} in this region. Therefore, the true representation of the perturbation velocity is directly dependent upon an accurate numerical solution of the governing equations. These inaccuracies can be resolved by using a nonuniform mesh in the region of interest as suggested by Arnold. It is suspected, however, that after a thorough analysis of the effects of the problem parameters and mesh size on the solution have been investigated, only small values of the axial wave number below about 10.0 and Reynolds numbers in the vicinity of 1150 will be of primary interest. It is felt by this investigator that a mesh size of $N = 50$ and the wide range of problem parameters used here yielded solutions that satisfied the governing vorticity transport equations to a high degree and were sufficient to show stability trends.

NORMALIZED PERTURBATION VELOCITY VS RADIUS

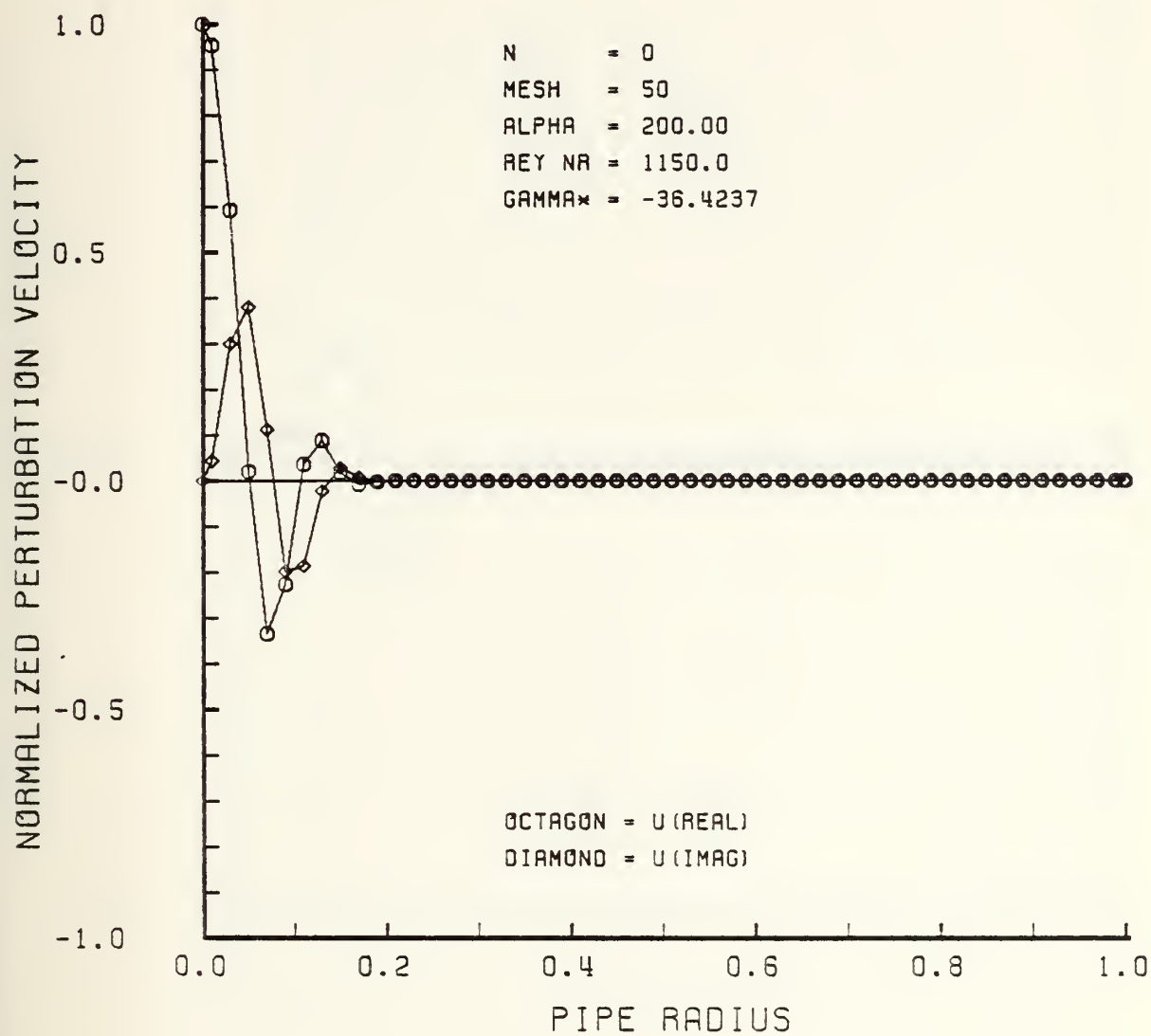


Figure 6-37

NORMALIZED PERTURBATION VELOCITY VS RADIUS

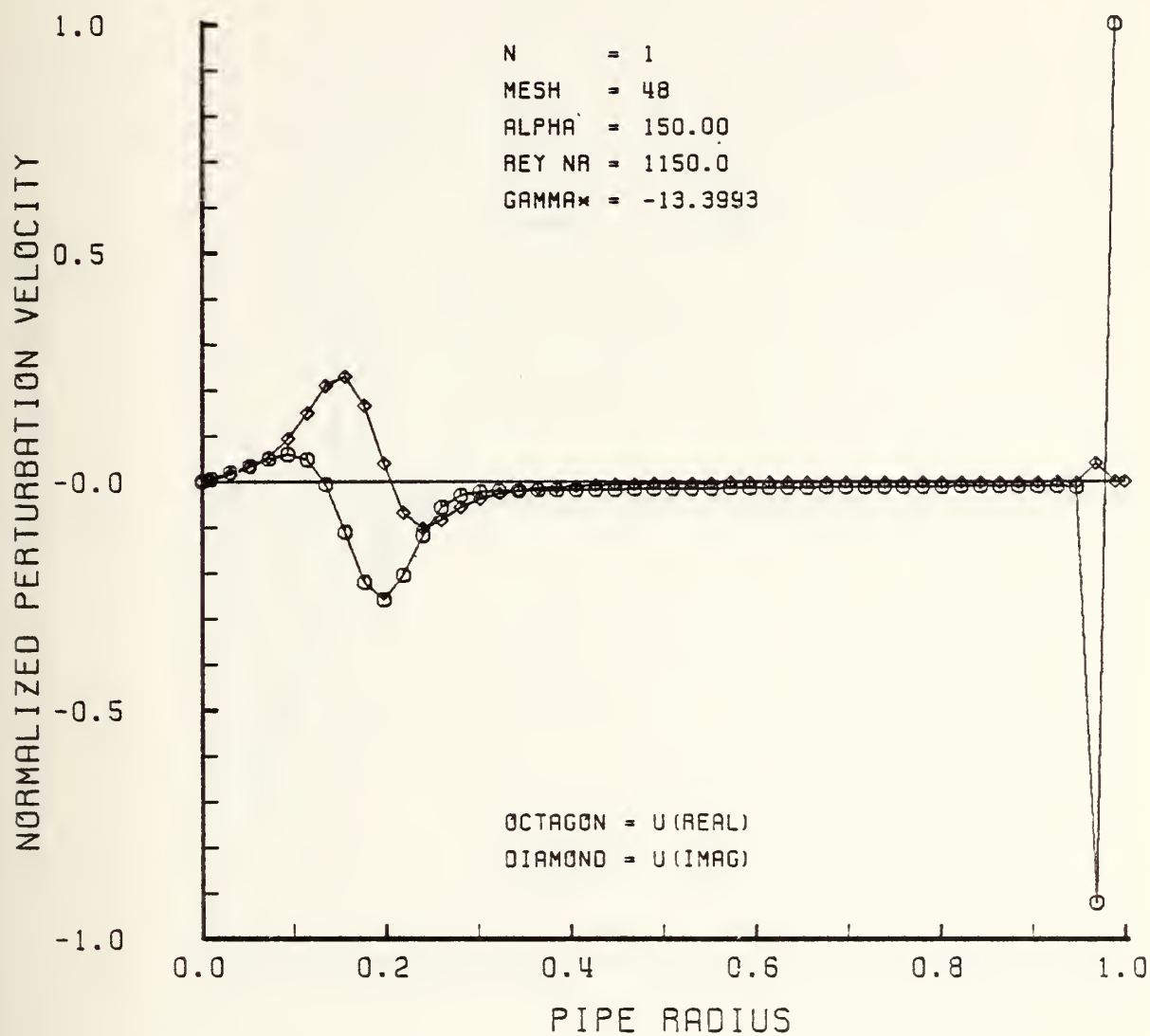


Figure 6-38

NORMALIZED PERTURBATION VELOCITY VS RADIUS

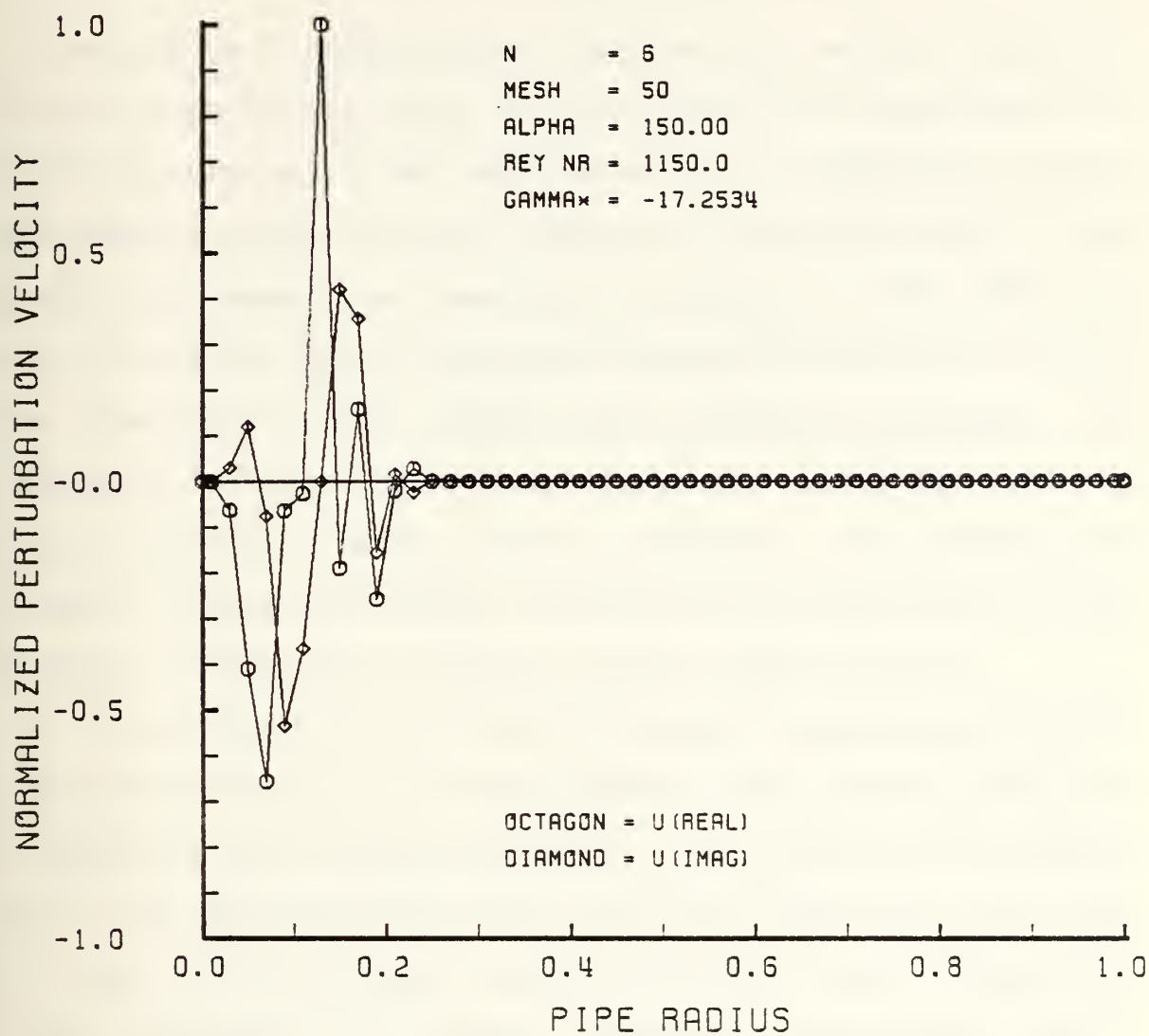


Figure 6-39

VII. RECOMMENDATIONS AND CONCLUSIONS

The problem of predicting the transition from laminar to turbulent flow of incompressible fluids in circular pipes has been pursued for nearly 100 years and has been presented here in a straightforward manner. The governing equations for the dynamics of this problem consist of the Navier-Stokes equation and the continuity equation. After taking the curl of the Navier-Stokes equation and applying the continuity principle, the linearized vorticity transport vector equation is obtained. The velocity vector potential function, which contains functions of r and a complex exponential factor, was then introduced. The resulting two linearly independent equations form the basis for the solution of the problem in the form of the vorticity transport matrix equation.

A valid solution of the governing equations was made possible because of two factors; (1) the advancements in the linearized theory by introducing a purely imaginary exponential form of the axial wave number, and (2) the rigorous method in which the boundary conditions at the pipe axis were derived and those constraints enforced. After an appropriate change of variables was performed, the governing equations were transformed into an equivalent pair of coupled, homogeneous differential equations that were solved in eigenvalue problem format. Accurate solutions of the governing equations were achieved by the refinement and combination of several standard methods of numerical analysis. These methods include; (1) the approximation of the governing equations along

a computational radial mesh developed by the half-station method, (2) the use of central and noncentral finite difference approximations having consistent fourth order truncation error, and (3) the use of complex, double precision number representations.

It was this author's intention from the outset to make this work as complete as possible. This was accomplished by including the development of the theory, the derivation of the boundary conditions, and a detailed explanation of the numerical methods used as well as obtaining solutions to the governing equations. This will enable future investigators to use this thesis as a starting point and as a single source reference for follow-on studies of this subject.

The conclusions of this numerical analysis follow directly from the results of the pipe flow stability problem which were discussed thoroughly in the previous chapter.

The most significant findings are:

- (1) for $n = 0$, the flow is stable at all Re and α .
- (2) for $n = 1$, the flow appears to be unstable at all Re for small values of α . This result is unfortunately in direct conflict with experimental observations.
- (3) for $n = 1$, unstable eigenvalues are associated with perturbation activity at the wall.
- (4) for $n = 6$, the flow is stable at all Re and α .

The following observations are also of interest:

- (5) for $n = 0, 1$, and 6 , increasing Reynolds number has a destabilizing effect on the flow.
- (6) for $n = 0, 1$, and 6 , increasing axial wave number has a stabilizing effect on the flow for fixed Re .
- (7) for $n = 1$ and 6 , increasing axial wave number causes a shift in the perturbation activity from the wall to the axis for fixed Re .

The results for angular wave numbers $n = 1$ and 6 are believed to be new. Conclusions (1), (5), (6), and (7) are in agreement with experimental results or previous theoretical investigations.

It is this author's opinion that the numerical analysis of the vorticity transport equations is now complete for angular wave numbers $n = 0$ and 6. It is felt, however, that the numerical results for angular wave number $n = 1$ warrant further study. The unresolved paradox is quite puzzling in that for $n = 1$ the flow appears to be unstable at all Reynolds numbers. Continued numerical investigations for $n = 1$ and follow-on studies of other angular wave numbers should prove fruitful in establishing a theory which predicts the transition from laminar to turbulent flow of fluids in pipes.

APPENDIX A

COEFFICIENTS OF THE VORTICITY TRANSPORT EQUATIONS

The generalized coefficient matrices which appear in the basic vorticity transport equations (2-40) are defined below.

$$[M_4] = \frac{1}{Re} \begin{bmatrix} 0 & 0 \\ 0 & -1 \end{bmatrix} \quad (A-1)$$

$$[M_3] = \frac{1}{Re} \begin{bmatrix} 0 & \frac{in}{r} \\ 0 & -\frac{2}{r} \end{bmatrix} \quad (A-2)$$

$$[M_2] = \frac{1}{Re} \begin{bmatrix} \left(\frac{n^2}{r^2} + \alpha^2 \right) & \frac{2 in}{r^2} \\ -\frac{4 in}{r^2} & \left(\frac{2n^2 + 3}{r^2} + 2\alpha^2 \right) \end{bmatrix} + \begin{bmatrix} 0 & 0 \\ 0 & 2i\alpha(1-r^2) \end{bmatrix} \quad (A-3)$$

$$[M_1] = \frac{1}{Re} \begin{bmatrix} -\left(\frac{n^2}{r^3} - \frac{\alpha^2}{r} \right) & -in \left(\frac{n^2 + 1}{r^3} + \frac{\alpha^2}{r} \right) \\ \frac{4 in}{r^3} & -\left(\frac{2n^2 + 3}{r^3} - \frac{2\alpha^2}{r} \right) \end{bmatrix} + \begin{bmatrix} 0 & 2n\alpha\left(\frac{1}{r}-r\right) \\ 0 & 2i\alpha\left(\frac{1}{r}-r\right) \end{bmatrix} \quad (A-4)$$

$$[M_0] = \frac{1}{Re} \begin{bmatrix} - \left(\frac{n^2(n^2 - 1)}{r^4} + \frac{(2n^2 + 1) \alpha^2}{r^2} + \alpha^4 \right) & -in \left(\frac{n^2 - 1}{r^4} + \frac{3\alpha^2}{r^2} \right) \\ 4 in \left(\frac{n^2 - 1}{r^4} + \frac{\alpha^2}{r^2} \right) & - \left(\frac{(n^2 + 3)(n^2 - 1)}{r^4} + \frac{2(n^2 + 1) \alpha^2}{r^2} + \alpha^4 \right) \end{bmatrix}$$

$$+ \begin{bmatrix} -2i\alpha \left(\frac{n^2}{r^2} - (n^2 - \alpha^2) - \alpha^2 r^2 \right) & 2n\alpha \left(\frac{1}{r^2} + 1 \right) \\ -4n\alpha \left(\frac{1}{r^2} - 1 \right) & -2i\alpha \left(\frac{n^2 + 1}{r^2} - (n^2 + 1 - \alpha^2) - \alpha^2 r^2 \right) \end{bmatrix}$$

(A-5)

$$[N_2] = \begin{bmatrix} 0 & 0 \\ 0 & -1 \end{bmatrix}$$

(A-6)

$$[N_1] = \begin{bmatrix} 0 & \frac{in}{r} \\ 0 & -\frac{1}{r} \end{bmatrix}$$

(A-7)

$$[N_0] = \begin{bmatrix} \left(\frac{n^2}{r^2} + \alpha^2 \right) & \frac{in}{r^2} \\ -\frac{2 in}{r^2} & \left(\frac{n^2 + 1}{r^2} + \alpha^2 \right) \end{bmatrix}$$

(A-8)

APPENDIX B

COEFFICIENTS OF THE TRANSFORMED VORTICITY TRANSPORT EQUATIONS FOR $n = 0, 1$, and 6

A. COEFFICIENTS FOR $n = 0$

Since the vorticity transport equations uncouple for $n = 0$, only the solution for the eigenfunction $Q(r)$ is sought. Therefore the details of the complete coefficient matrices are not required. The coefficients which appear here represent the matrix element (2,2) and correspond to the primed quantities of equation (2-43).

$$M_4' = - \frac{r}{Re} \quad (B-1)$$

$$M_3' = - \frac{6}{Re} \quad (B-2)$$

$$M_2' = \frac{1}{Re} \left(- \frac{3}{r} + 2\alpha^2 r \right) + 2i\alpha (r - r^3) \quad (B-3)$$

$$M_1' = \frac{1}{Re} \left(\frac{3}{r^2} + 6\alpha^2 \right) + 6i\alpha (1 - r^2) \quad (B-4)$$

$$M_0' = - \frac{\alpha^4 r}{Re} + 2i\alpha^3 (r^3 - r) \quad (B-5)$$

$$N_2' = - r \quad (B-6)$$

$$N_1' = - 3 \quad (B-7)$$

$$N_0' = \alpha^2 r \quad (B-8)$$

These coefficients also appear and are computed in part III of the main investigative computer program for $n = 0$.

B. COEFFICIENTS for $n = 1$

Since the vorticity transport equations do not uncouple for $n = 1$, the eigenfunctions $P(r)$ and $Q(r)$ must be solved for simultaneously. With the introduction of the additional parameter as a result of the change of variables, $H(0)$ appears explicitly as an unknown in the system of equations. This requires the addition of two coefficient matrices to equation (2-40). The 2×1 column matrix $[M_5']$ appears on the left side of equation (2-47) and one 2×1 column matrix $[N_3']$ appears on the right side of equation (2-47). The complete coefficient matrices for $n = 1$ are defined below.

$$[M_4'] = \begin{bmatrix} 0 & 0 \\ 0 & -\frac{r^2}{Re} \end{bmatrix} \quad (B-9)$$

$$[M_3'] = \begin{bmatrix} 0 & \frac{ir}{Re} \\ 0 & -\frac{10r}{Re} \end{bmatrix} \quad (B-10)$$

$$[M_2'] = \begin{bmatrix} \frac{1}{Re} (1 + \alpha^2 r^2) & \frac{8i}{Re} \\ -\frac{4i}{Re} & \frac{1}{Re} (2\alpha^2 r^2 - 19) + 2i\alpha (r^2 - r^4) \end{bmatrix} \quad (B-11)$$

$$\begin{aligned}
[M_1'] = & \begin{bmatrix} \frac{1}{\text{Re}} \left(\frac{3}{r} + 5\alpha^2 r \right) & 2\alpha(r - r^3) \\ 0 & \frac{1}{\text{Re}} \left(\frac{3}{r} + 10\alpha^2 r \right) \end{bmatrix} \\
+ & \begin{bmatrix} 0 & \frac{i}{\text{Re}} \left(\frac{12}{r} - \alpha^2 r \right) \\ -\frac{12i}{\text{Re}r} & 10i\alpha (r - r^3) \end{bmatrix}
\end{aligned} \tag{B-12}$$

$$\begin{aligned}
[M_0'] = & \begin{bmatrix} \frac{\alpha^2}{\text{Re}} (1 - \alpha^2 r^2) & 2\alpha(3 - r^2) \\ -4\alpha(1 - r^2) & \frac{1}{\text{Re}} (4\alpha^2 - \alpha^4 r^2) \end{bmatrix} \\
+ & \begin{bmatrix} -2i\alpha(1 - r^2 + \alpha^2 r^2 - \alpha^2 r^4) & \frac{-5i\alpha^2}{\text{Re}} \\ \frac{4i\alpha^2}{\text{Re}} & 2i\alpha\{2(1 - r^2) - \alpha^2(r^2 - r^4)\} \end{bmatrix}
\end{aligned} \tag{B-13}$$

$$[M_5'] = \begin{bmatrix} 2\alpha(2 - \alpha^2 + \alpha^2 r^2) + \frac{i\alpha^4}{\text{Re}} \\ -\frac{\alpha^4}{\text{Re}} - 2i\alpha^3 (1 - \alpha r^2) \end{bmatrix} \tag{B-14}$$

$$[N_2'] = \begin{bmatrix} 0 & 0 \\ 0 & -r^2 \end{bmatrix} \quad (B-15)$$

$$[N_1'] = \begin{bmatrix} 0 & ir \\ 0 & -5r \end{bmatrix} \quad (B-16)$$

$$[N_0'] = \begin{bmatrix} 1 + \alpha^2 r^2 & 3i \\ -2i & -2 + \alpha^2 r^2 \end{bmatrix} \quad (B-17)$$

$$[N_3'] = \begin{bmatrix} -i\alpha^2 \\ \alpha^2 \end{bmatrix} \quad (B-18)$$

These coefficients also appear and are computed in Part III of the main investigative computer program for $n = 1$.

C. COEFFICIENTS for $n = 6$

The vorticity transport equations for $n = 6$ remain coupled. There are no additional parameters introduced with the change of variables to $P(r)$ and $Q(r)$. The system of equations take the form of equation (2-40) once again. The complete coefficient matrices for $n = 6$ are defined below.

$$[M_4] = \begin{bmatrix} 0 & 0 \\ 0 & -\frac{r^3}{Re} \end{bmatrix} \quad (B-19)$$

$$[M_3] = \begin{bmatrix} 0 & \frac{6ir^2}{Re} \\ 0 & -\frac{14r^2}{Re} \end{bmatrix} \quad (B-20)$$

$$[M_2] = \begin{bmatrix} \frac{r^2}{Re} (36 + \alpha^2 r^2) & 0 \\ 0 & \frac{r}{Re} (21 + 2\alpha^2 r^2) \end{bmatrix} + \begin{bmatrix} 0 & \frac{66ir}{Re} \\ -\frac{24ir^2}{Re} & 2i\alpha(r^3 - r^5) \end{bmatrix} \quad (B-21)$$

$$\begin{aligned}
[M_1'] = & \begin{bmatrix} \frac{1}{\text{Re}} (252r + 9 \alpha^2 r^2) & 12\alpha(r^2 - r^4) \\ 0 & \frac{1}{\text{Re}} (315 + 14\alpha^2 r^2) \end{bmatrix} \\
& + \begin{bmatrix} 0 & -\frac{i}{\text{Re}} (42 + 6\alpha^2 r^2) \\ -\frac{168ir}{\text{Re}} & 14i\alpha(r^2 - r^4) \end{bmatrix} \quad (\text{B-22})
\end{aligned}$$

$$\begin{aligned}
[M_0'] = & \begin{bmatrix} -\frac{1}{\text{Re}} (972 + 57\alpha^2 r^2 + \alpha^4 r^4) & 24\alpha(2r - r^3) \\ -24\alpha(r^2 - r^4) & -\frac{1}{\text{Re}} \left(\frac{1152}{r} + 56\alpha^2 r + \alpha^4 r^3 \right) \end{bmatrix} \\
& + \begin{bmatrix} -2i\alpha r^2 \{36 - 36r^2 + \alpha^2 r^2 (1 - r^2)\} & -\frac{i}{\text{Re}} \left(\frac{768}{r} + 36\alpha^2 r \right) \\ \frac{i}{\text{Re}} (648 + 24\alpha^2 r^2) & -56i\alpha(r - r^3) - 2i\alpha^3(r^3 - r^5) \end{bmatrix} \quad (\text{B-23})
\end{aligned}$$

$$[N_2'] = \begin{bmatrix} 0 & 0 \\ 0 & -r^3 \end{bmatrix} \quad (\text{B-24})$$

$$[N_1'] = \begin{bmatrix} 0 & 6ir^2 \\ 0 & -7r^2 \end{bmatrix} \quad (B-25)$$

$$[N_0'] = \begin{bmatrix} 36r^2 + \alpha^2 r^4 & 24ir \\ -12ir^2 & 28r + \alpha^2 r^3 \end{bmatrix} \quad (B-26)$$

These coefficients also appear and are computed in part III of the main investigative computer program for $n = 6$.

APPENDIX C

COEFFICIENTS OF THE BOUNDARY EQUATIONS AT THE AXIS

The matrices which appear in the boundary equations at the axis, equations (3-4) through (3-8) are defined below.

$$[C_1] = \begin{bmatrix} -n^2 & -in \\ +4in & -(n^2 + 3) \end{bmatrix} \quad (C-1)$$

$$[C_2] = \begin{bmatrix} -n^2 & -2in \\ +4in & -(n^2 + 4) \end{bmatrix} \quad (C-2)$$

$$[C_3] = \begin{bmatrix} -\frac{n^2}{2} & -\frac{3}{2}in \\ +2in & -\frac{1}{2}(n^2 + 3) \end{bmatrix} \quad (C-3)$$

$$[C_4] = \begin{bmatrix} -\left\{2n^2 - (2n^2 + 1)\frac{i\alpha}{Re}\right\} & -in\left(2 - \frac{3i\alpha}{Re}\right) \\ +4in\left(1 - \frac{i\alpha}{Re}\right) & -2(n^2 + 1)\left(1 - \frac{i\alpha}{Re}\right) \end{bmatrix} \quad (C-4)$$

$$[D_4] = \begin{bmatrix} + n^2 & + in \\ - 2 in & + (n^2 + 1) \end{bmatrix} \quad (C-5)$$

$$[C_5] = \begin{bmatrix} - \frac{n}{6} & - \frac{2i}{3} \\ + \frac{2i}{3} & - \frac{n}{6} \end{bmatrix} \quad (C-6)$$

$$[C_6] = \begin{bmatrix} - n & - 2i \\ + 2i & - n \end{bmatrix} \quad (C-7)$$

$$[C_7] = \begin{bmatrix} - \frac{n^2}{24} & - \frac{5 in}{24} \\ + \frac{in}{6} & - \frac{(n^2 - 5)}{24} \end{bmatrix} \quad (C-8)$$

$$[C_8] = \begin{bmatrix} - \left\{ n^2 - \left(n^2 - \frac{3}{2} \right) \frac{i\alpha}{Re} \right\} & - in \left(3 - \frac{5i\alpha}{2Re} \right) \\ + 2 in \left(1 - \frac{i\alpha}{Re} \right) & - (n^2 - 3) \left(1 - \frac{i\alpha}{Re} \right) \end{bmatrix} \quad (C-9)$$

$$[D_8] = \begin{bmatrix} + \frac{n^2}{2} & + \frac{3 in}{2} \\ - in & + \frac{(n^2 - 3)}{2} \end{bmatrix} \quad (C-10)$$

$$[C_9] = \begin{bmatrix} \left(\frac{i\alpha^3}{Re} + 2n^2 - 2\alpha^2 \right) & -2 \text{ in} \\ -4 \text{ in} & \left(\frac{i\alpha^3}{Re} + 2n^2 + 2 - 2\alpha^2 \right) \end{bmatrix} \quad (C-11)$$

$$[D_9] = \begin{bmatrix} 1 & 0 \\ 0 & 1 \end{bmatrix} \quad (C-12)$$

Column matrices used in equation (5-36) for $n = 1$.

$$[C_9^*] = \begin{bmatrix} \left(\frac{\alpha^3}{Re} - 4i + 2i\alpha^2 \right) \\ \left(-2\alpha^2 + \frac{i\alpha^3}{Re} \right) \end{bmatrix} \{H(0)\} \quad (C-13)$$

$$[D_9^*] = \begin{bmatrix} -i \\ 1 \end{bmatrix} \{H(0)\} \quad (C-14)$$

APPENDIX D

SPECIAL CONDITIONS AT THE AXIS

The determinates are formed from the corresponding matrices as defined in Appendix C. For angular wave numbers $n \geq 6$, all of the determinates become non-singular.

$$|C_1| = n^2 (n^2 - 1) \quad (D-1)$$

$$|C_2| = n^2 (n^2 - 4) \quad (D-2)$$

$$|C_3| = \frac{n^2}{4} (n^2 - 9) \quad (D-3)$$

$$\begin{aligned} |i\alpha[C_4] - \gamma[D_4]| = (n^2 - 1) \left\{ -2\alpha^2 \left(1 - \frac{i\alpha}{\text{Re}} \right) \left[2n^2 - (2n^2 - 1) \frac{i\alpha}{\text{Re}} \right] \right. \\ \left. + \gamma i\alpha \left[4n^2 - (4n^2 - 1) \frac{i\alpha}{\text{Re}} \right] + \gamma^2 n^2 \right\} \quad (D-4) \end{aligned}$$

$$|C_5| = \frac{1}{36} (n^2 - 16) \quad (D-5)$$

$$|C_6| = (n^2 - 4) \quad (D-6)$$

$$|C_7| = \frac{n^2}{576} (n^2 - 25) \quad (D-7)$$

$$\begin{aligned}
|i\alpha[C_8] - \gamma[D_8]| &= (n^2 - 9) \left\{ -\alpha^2 \left(1 - \frac{i\alpha}{\text{Re}} \right) \left[- \left(n^2 - \frac{1}{2} \right) \frac{i\alpha}{\text{Re}} + n^2 \right] \right. \\
&\quad \left. + \frac{\gamma i \alpha^3}{2} \left[- \left(n^2 - \frac{1}{2} \right) \frac{i\alpha}{\text{Re}} + 2n^2 \right] + \frac{\gamma^2 \alpha^4 n^2}{4} \right\} \quad (D-8)
\end{aligned}$$

A. MAIN INVESTIGATIVE PROGRAM FOR $n = 0$

```

//WALLACE JOB (2027, 0084), ' THESIS N = 0', CLASS=B
//* MAIN LINES={10}
// EXEC FRTXCLGP, IMSL=DP, REGION.GO=1024K
// FORT.SYSIN DD *
C*****
C THIS PROGRAM WAS DEVELOPED TO PERFORM A NUMERICAL ANALYSIS
C OF THREE DIMENSIONAL PIPE FLOW STABILITY FOR AXIAL WAVE
C NUMBER N = 0. THE PROGRAM IS DIVIDED INTO EIGHT PARTS.
C THE FIRST PART COMPUTES THE CENTRAL FINITE DIFFERENCE
C COEFFICIENTS FOR THE DERIVATIVES OF Q(R) ONLY, AT THE
C INTERIOR MESH POINTS ALONG THE PIPE RADIUS. IN THE SECOND
C PART, PRE-COMPUTED NON-CENTRAL FINITE DIFFERENCE
C COEFFICIENTS FOR THE DERIVATIVES OF Q(R) AT POINTS
C NEAR THE AXIS AND WALL ARE READ IN AS DATA. THE THIRD PART
C COMPUTES THE VORTICITY TRANSPORT EQUATION COEFFICIENTS OF
C Q(R) AND THEIR RESPECTIVE DERIVATIVES AT ALL RADIAL MESH
C POINTS (STATIONS). THE FOURTH PART COMPUTES THE A AND B
C MATRIX ELEMENTS, WHICH MAKE-UP THE EIGENSYSTEM TO BE SOLVED
C IN THE FORMAT, A * X = GAMMA * B * X. IN THE FIFTH PART
C THE A AND B MATRICES COMPRISING THE EIGENSYSTEM ARE SOLVED
C IN THE SUBROUTINE EIGZC. THE RESULTING EIGENVALUES AND
C CORRESPONDING EIGENVECTOR REPRESENT GAMMA AND THE COLUMN
C VECTOR X, RESPECTIVELY, AND ARE SOLUTIONS OF THE GOVERNING
C PARTIAL DIFFERENTIAL EQUATIONS. THE SIXTH PART VERIFIES
C THE SOLUTION OF THE PDE AND THE MAGNITUDE OF THE RESIDUAL
C IS DETERMINED. THE SEVENTH PART COMPUTES THE NORMALIZED
C*****
PIP00010
PIP00020
PIP00030
PIP00040
PIP00050
PIP00060
PIP00070
PIP00080
PIP00090
PIP00100
PIP00110
PIP00120
PIP00130
PIP00140
PIP00150
PIP00160
PIP00170
PIP00180
PIP00190
PIP00200
PIP00210
PIP00220
PIP00230
PIP00240
PIP00250
PIP00260
PIP00270
PIP00280
PIP00290
PIP00300
PIP00310
PIP00320
PIP00330
PIP00340
PIP00350
PIP00360
PIP00370
PIP00380
PIP00390
PIP00400
PIP00410
PIP00420
PIP00430
PIP00440
PIP00450
PIP00460
PIP00470
PIP00480

```



```

DATA A1DER/7*{0.0D0,0.0D0} //,A2DER/7*{0.0D0,0.0D0} //
DATA A3DER/7*{0.0D0,0.0D0} //,A4DER/7*{0.0D0,0.0D0} //
DATA X1(1) 0.0 //,Y1(1) 0.0 //,X1(2) 1.0 //,Y1(2) 0.0 //
DATA MESH/50/

```

PART I

COMPUTE CENTRAL DIFFERENCE COEFFICIENTS FOR THE

DERIVATIVES OF Q(R) AT INTERIOR MESH POINTS.

COMPUTE CENTRAL DIFFERENCE COEFFICIENTS FOR FOURTH ORDER

DERIVATIVE OF Q(R) AT POINTS 4 - 47

```

DMESH = DFLOAT(MESH)
H4TH = DMESH ** 4
ATEMP = (-1.0D0/6.0D0) * H4TH
A4DER(1) = DCMPLX(ATEMP,0.0D0)
A4DER(7) = A4DER(1)
ATEMP = 2.0D0 * H4TH
A4DER(2) = DCMPLX(ATEMP,0.0D0)
A4DER(6) = A4DER(2)
ATEMP = -6.5D0 * H4TH
A4DER(3) = DCMPLX(ATEMP,0.0D0)
A4DER(5) = A4DER(3)
ATEMP = (56.0D0/6.0D0) * H4TH
A4DER(4) = DCMPLX(ATEMP,0.0D0)

```

COMPUTE CENTRAL DIFFERENCE COEFFICIENTS FOR THIRD ORDER

DERIVATIVE AT POINTS 4 - 47

```

H3RD = DMESH ** 3
ATEMP = 0.125D0 * H3RD
A3DER(1) = DCMPLX(ATEMP,0.0D0)
A3DER(7) = -A3DER(1)
A3DER(6) = DCMPLX(H3RD,0.0D0)
A3DER(2) = -A3DER(6)
ATEMP = (13.0D0/8.0D0) * H3RD
A3DER(3) = DCMPLX(ATEMP,0.0D0)
A3DER(5) = -A3DER(3)

```

COMPUTE CENTRAL DIFFERENCE COEFFICIENTS FOR SECOND ORDER

```

PIP00970
PIP00980
PIP00990
PIP01000
PIP01010
PIP01020
PIP01030
PIP01040
PIP01050
PIP01060
PIP01070
PIP01080
PIP01090
PIP01100
PIP01110
PIP01120
PIP01130
PIP01140
PIP01150
PIP01160
PIP01170
PIP01180
PIP01190
PIP01200
PIP01210
PIP01220
PIP01230
PIP01240
PIP01250
PIP01260
PIP01270
PIP01280
PIP01290
PIP01300
PIP01310
PIP01320
PIP01330
PIP01340
PIP01350
PIP01360
PIP01370
PIP01380
PIP01390
PIP01400
PIP01410
PIP01420
PIP01430
PIP01440

```


[illegible]

DERIVATIVE AT POINTS 2 - 43

```
H2ND      * H2ND
ATEMP     * ATEMP
A2DER(1)  = DCMPLEX(ATEMP,0.0D0)
A2DER(2)  = A2DER(2)
A2DER(3)  = DCMPLEX(ATEMP,0.0D0)
A2DER(4)  = A2DER(3)
A2DER(5)  = -2.5D0 * H2ND
A2DER(6)  = DCMPLEX(ATEMP,0.0D0)
```

COMPUTE CENTRAL DIFFERENCE COEFFICIENTS FOR FIRST ORDER

DERIVATIVE AT POINTS 2 - 43

```

H1ST      = DMESH
A1TEMP    = (1,0,DO/12,0D0) * H1ST
A1DER     = DCMPLEX(ATEMP,0.0D0)
A1DER     = -A1DER
A1TEMP    = (-8,0,DO/12,0D0) * H1ST
A1DER     = DCMPLEX(ATEMP,0.0D0)
A1DER     = -A1DER

```

[illegible]

PART II

READ IN PRE-COMPUTED NON-CENTRAL DIFFERENCE COEFFICIENTS FOR

ALL DERIVATIVES OF $Q(R)$ AT POINTS NEAR THE AXIS.

BOUNDARY CONDITIONS AT THE AXIS ARE: $D_3 Q(0) = 0$ AND $DQ(0) = 0$.

FOR SECOND EQUATION IN $Q(R)$ ONLY, FOR $N = 0$.

```

51 READ(5,59) I,J,K
   IF(I.EQ.9) GO TO 54
   HTEMP = DMESH ** I
   DO 52 KKK = 1,K
     READ(5,* ) AATEMP * HTEMP
     AAXIS(I,J,KKK) = DCMPLX(AATEMP,0.0D0)
52 CONTINUE
   GO TO 51
54 CONTINUE

```

READ IN PRE-COMPUTED NON-CENTRAL DIFFERENCE COEFFICIENTS FOR


```

C C C C C C C C C C
      ALL DERIVATIVES OF Q(R) AT POINTS NEAR THE WALL.
      BOUNDARY CONDITIONS AT THE WALL ARE: DQ(1)=0 AND Q(1)=0.
      FOR SECOND EQUATION IN Q(R) ONLY, FOR N = 0.

55 READ(5,59) I,J,K
   IF(I.EQ.9) GO TO 57
   HTEMP = DMESH ** I
   JJ = 4 - J
   SIGN = 1.0 DO
   IF(I.EQ.1) SIGN = -SIGN
   IF(I.EQ.3) SIGN = -SIGN
   DO 56 KKK = 1, K
     KK = 7 - KKK
     READ(5,*) WATEMP
     WATEMP = WATEMP * HTEMP * SIGN
     AWALL(I,JJ,KK) = DCMPLX(WATEMP,0.0D0)
56 CONTINUE
   GO TO 55
57 CONTINUE
59 FORMAT(I1,1X,I1,1X,I1)

      REARRANGING SOME OF THE DATA IN THE AXIS AND WALL
      COEFFICIENT MATRICES

DO 58 I = 1,6
  AAAXIS(2,3,I) = A2DER(I + 1)
  AAAXIS(1,3,I) = A1DER(I + 1)
  AWALL(2,1,I) = A2DER(I)
  AWALL(1,1,I) = A1DER(I)
58 CONTINUE

      READ IN COEFFICIENTS TO DETERMINE Q(0)

DO 10 I = 1,6
  READ(5,*) A6INV(I)
10 CONTINUE

C*****
      READ IN ALPHA AND REYNOLDS NR

      IPILOT = 0
19 CONTINUE
   READ(5,*) ALPHA,RE

```

```

PIP01930
PIP01940
PIP01950
PIP01960
PIP01970
PIP01980
PIP01990
PIP02000
PIP02010
PIP02020
PIP02030
PIP02040
PIP02050
PIP02060
PIP02070
PIP02080
PIP02090
PIP02100
PIP02110
PIP02120
PIP02130
PIP02140
PIP02150
PIP02160
PIP02170
PIP02180
PIP02190
PIP02200
PIP02210
PIP02220
PIP02230
PIP02240
PIP02250
PIP02260
PIP02270
PIP02280
PIP02290
PIP02300
PIP02310
PIP02320
PIP02330
PIP02340
PIP02350
PIP02360
PIP02370
PIP02380
PIP02390
PIP02400

```


IF (ALPHA.LT.0.0D0) G3 TO 180

PART III

COMPUTATION OF THE VORTICITY TRANSPORT EQUATION COEFFICIENTS

FOR Q(R) ONLY AND THE RESPECTIVE DERIVATIVES.

PRE-COMPUTE CONSTANTS INVOLVING ALPHA IN THE COEFFICIENTS

```

DTEMPR = (-6.0D0/RE)
D3TEMP = DCMPLX(DTEMPR,0.0D0)
E1TEMP = DCMPLX(-3.0D0,0.0D0)
ALSO = ALPHA * ALPHA
AL2 = ALPHA + ALPHA
AL22 = ALSO + ALSO
AL62 = 6.0D0 * ALSO
AL6 = 6.0D0 * ALPHA
AL3RD = ALSO * ALPHA
AL4TH = AL3RD * ALPHA
AL23 = AL3RD + AL3RD

```

```

DO 60 I = 1,MESH
R = (DFLOAT(I) - 0.5D0) / DMESH
R2 = R * R
R3 = R2 * R
RAD(I) = DCMPLX(R,0.0D0)
DTEMPR = (-R/RE)
D4(I) = DCMPLX(DTEMPR,0.0D0)
D3(I) = D3TEMP
DTEMPR = ((-3.0D0/R) + (AL22 * R))/RE
DTEMPI = (R - R3)
D2(I) = DCMPLX(DTEMPR,DTEMPI)
DTEMPR = ((3.0D0/(R2)) + AL62)/RE
DTEMPI = AL6 * (1.0D0 - R2)
D1(I) = DCMPLX(DTEMPR,DTEMPI)
DTEMPR = -(AL4TH * R)/RE
DTEMPI = -(AL23 * (R3 - R))
D0(I) = DCMPLX(DTEMPR,DTEMPI)
E2TEMP = -R
E2(I) = DCMPLX(E2TEMP,0.0D0)
E1(I) = E1TEMP
E1TEMP = ALSO * R
E0(I) = DCMPLX(E2TEMP,0.0D0)

```

60 CONTINUE

PIP02410
PIP02410
PIP02430
PIP02430
PIP02440
PIP02440
PIP02450
PIP02450
PIP02460
PIP02460
PIP02470
PIP02470
PIP02480
PIP02480
PIP02490
PIP02490
PIP02500
PIP02500
PIP02510
PIP02510
PIP02520
PIP02520
PIP02530
PIP02530
PIP02540
PIP02540
PIP02550
PIP02550
PIP02560
PIP02560
PIP02570
PIP02570
PIP02580
PIP02580
PIP02590
PIP02590
PIP02600
PIP02600
PIP02610
PIP02610
PIP02620
PIP02620
PIP02630
PIP02630
PIP02640
PIP02640
PIP02650
PIP02650
PIP02660
PIP02660
PIP02670
PIP02670
PIP02680
PIP02680
PIP02690
PIP02690
PIP02700
PIP02700
PIP02710
PIP02710
PIP02720
PIP02720
PIP02730
PIP02730
PIP02740
PIP02740
PIP02750
PIP02750
PIP02760
PIP02760
PIP02770
PIP02770
PIP02780
PIP02780
PIP02790
PIP02790
PIP02800
PIP02800
PIP02810
PIP02810
PIP02820
PIP02820
PIP02830
PIP02830
PIP02840
PIP02840
PIP02850
PIP02850
PIP02860
PIP02860
PIP02870
PIP02870
PIP02880
PIP02880


```

169 NGAM = I
170 CONTINUE
175 WRITE(6,175) NGAM,GAMMAX,MESH,ALPHA,RE
175 FORMAT(1X,/,1X,LEAST STABLE,EIGENVALUE NR, I3,1X,=,D27.18,4X,
1 MESH =,I3,4X,ALPHA =,D10.3,4X,REYNOLDS NR =,D17.10,/)
*****

```

CCCCCCCCCCCC

PART VI

VERIFY THAT THE LEAST STABLE EIGENVALUE AND CORRESPONDING
EIGENVECTOR SATISFY THE GOVERNING PARTIAL DIFFERENTIAL
EQUATIONS. RESIDUAL ERROR IS OUTPUT AS EPSILON.

```

DO 351 I = 1,MESH
SUMA = ZERO
SUMB = ZERO
DO 350 J = 1,MESH
SUMA = SUMA + { A(I,J) * EIGVEC(J,NGAM) }
SUMB = SUMB + { B(I,J) * EIGVEC(J,NGAM) }
350 CONTINUE
ERROR(I) = SUMA - ( SUMB * EIGVAL(NGAM) )
351 CONTINUE
WRITE(6,375)
375 FORMAT(1X,/,15X,EPILON = A * X - GAMMA * B * X,/,)
380 FORMAT(1X,2D30.18)
*****

```

CCCCCCCCCCCC

PART VII

COMPUTATION OF AXIAL PERTURBATION VELOCITY U(R).

OUTPUT THE EIGENVECTOR CORRESPONDING TO THE LEAST STABLE
EIGENVALUE, GAMMA*.

```

398 WRITE(6,398)
398 FORMAT(1X,/,5X,STABLE EIGENVALUE,/,)
DO 400 I = 1,MESH
Q(I) = EIGVEC(I,NGAM)
WRITE(6,399) Q(I)
*****

```



```

399 FORMAT(5X, D30.18, 3X, D30.18)
400 CONTINUE
C
C
C      COMPUTATION OF DQ(R)
DO 410 J = 1, 3
DQ(J) = ZERO
DO 410 K = 1, 6
DQ(J) = DQ(J) + Q(K) * AAXIS(1, J, K)
410 CONTINUE
C
M = MESH - 3
DO 420 J = 4, M
DQ(J) = ZERO
DO 420 K = 1, 7
L = J - 4 + K
DQ(J) = DQ(J) + Q(L) * A1DER(K)
420 CONTINUE
C
MM = M - 3
DO 430 J = 1, 3
L = J + M
DQ(L) = ZERO
DO 430 K = 1, 6
N = MM + K
DQ(L) = DQ(L) + Q(N) * AVAL(1, J, K)
430 CONTINUE
C
DO 440 I = 1, MESH
U(I) = Q(I) * TWO + RAD(I) * D2(I)
440 CONTINUE
C
C      COMPUTE Q(0)
Q06 = ZERO
DO 441 I = 1, 6
A6CPX = DCMPLEX(A6INV(I), 0.0D0)
Q06 = Q06 + (A6CPX * Q(I))
441 CONTINUE
C
C      REARRANGE DATA FOR PLOT ROUTINE
M2 = MESH + 2
DO 450 I = 1, MESH
II = M2 - I
III = II - 1
U(II) = U(III)
RAD(II) = RAD(III)

```



```

PIP05770
PIP05780
PIP05790
PIP05800
PIP05810
PIP05820
PIP05830
PIP05840
PIP05850
PIP05860
PIP05870
PIP05880
PIP05890
PIP05900
PIP05910
PIP05920
PIP05930
PIP05940
PIP05950
PIP05960
PIP05970
PIP05980
PIP05990
PIP06000
PIP06010
PIP06020
PIP06030
PIP06040
PIP06050
PIP06060
PIP06070
PIP06080
PIP06090
PIP06100
PIP06110
PIP06120
PIP06130
PIP06140
PIP06150
PIP06160
PIP06170
PIP06180
PIP06190
PIP06200
PIP06210
PIP06220
PIP06230
PIP06240

```

```

CALL SYMBOL(XO,YO,YHF,'GAMMA*'='0.0,9)
CALL NUMBER(XN,YO,YHF,GAMPLT,0.0,4)
YO = YO - 3.4
CALL SYMBOL(XO,YO,YHF,'OCTAGON' = U(REAL)',0.0,17)
YO = YO - DELY
CALL SYMBOL(XO,YO,YHF,'DIAMOND' = U(IMAG)',0.0,17)
YO = YO - DELY
CALL SYMBOL(XO,YO,YHF,'TRIANGLE' = U AMPL',0.0,17)

WRITE THE AXIS LABELS

XO = XO - 2.55
YO = YO + 0.3
YHT = 0.12
CALL SYMBOL(XO,YO,YHF,'NORMALIZED PERTURBATION VELOCITY',90.,32)
XO = XO + 2.8
YO = YO - 1.0
CALL SYMBOL(XO,YO,YHF,'PIPE RADIUS',0.0,11)
RETURN
END

```

C
C
C
C

/*
//GO;
4 1 6

```

0.149055277542135411D+01
-0.146728551300678589D+01
-0.952808034464035489D+00
0.131474814501754689D+01
-0.443066268162952040D+00
0.578588951948733141D-01
-0.529970874070089781D+01
0.109232811728783830D+02
-0.803543362016894491D+01
0.276664742824026710D+01
-0.380985744383800062D+00
0.261995041349871033D-01
0.182995357263197173D+01
-0.649259024806782037D+01
0.932687952743622972D+01
-0.649679291508053325D+01
0.199910835799184738D+01
-0.166558294911753445D+00
0.307102076124568124D+01
-0.551704152249136515D+01
0.319074394463668409D+01
-0.848010380622840620D+00

```

4 2 6

4 3 6

3 1 5

3	2	5	0. 103287197231834257D+00	PIIP06259
			0. 909602076124564229D+00	PIIP06260
			-0. 444204152249132234D+00	PIIP06270
			-0. 121842560553634427D+01	PIIP06280
			-0. 857698961937716886D+00	PIIP06290
			-0. 104671280276816742D+00	PIIP06300
3	3	5	-0. 290960207612458177D+01	PIIP06310
			0. 644420415224915999D+01	PIIP06320
			-0. 47815743946369992D+01	PIIP06330
			0. 114230103806228555D+01	PIIP06340
			0. 104671280276815715D+00	PIIP06350
2	1	4	-0. 122289932619896935D+01	PIIP06360
			0. 135121878715814558D+01	PIIP06370
			-0. 139565992865636493D+00	PIIP06380
			0. 112465319064606085D-01	PIIP06390
2	2	4	0. 124975227903289943D+01	PIIP06400
			-0. 249955410225921892D+01	PIIP06410
			0. 133308561236623224D+01	PIIP06420
			-0. 832837891399130642D-01	PIIP06430
1	1	3	-0. 666666666666666685D+00	PIIP06440
			0. 750000000000000000D+00	PIIP06450
			-0. 833333333333333148D-01	PIIP06460
1	2	3	-0. 999999999999999778D+00	PIIP06470
			0. 749999999999999773D+00	PIIP06480
			0. 250000000000000139D+00	PIIP06490
9	0	0		PIIP06500
4	1	6	0. 1150000000000000714D+03	PIIP06510
			-0. 384444444444444450255D+02	PIIP06520
			0. 16400000000000003858D+02	PIIP06530
			-0. 522448979591849794D+01	PIIP06540
			0. 112345679012349509D+01	PIIP06550
			-0. 115702479338847558D+00	PIIP06560
4	2	6	-0. 260000000000000029D+02	PIIP06570
			0. 176666666666667016D+02	PIIP06580
			-0. 1120000000000002302D+02	PIIP06590
			0. 395918367346951072D+01	PIIP06600
			-0. 666666666666700491D+00	PIIP06610
			0. 578512396694251807D-01	PIIP06620
4	3	6	0. 1000000000000085265D+01	PIIP06630
				PIIP06640
				PIIP06650
				PIIP06660
				PIIP06670
				PIIP06680
				PIIP06690
				PIIP06700
				PIIP06710
				PIIP06720

0.0D0
 0.5D0
 1.0D0
 2.0D0
 4.0D0
 8.0D0
 16.0D0
 32.0D0
 0.5D0
 1.0D0
 2.0D0
 4.0D0
 8.0D0
 16.0D0
 32.0D0
 1.0D0
 /*
 //

575.0D0
 575.0D0
 575.0D0
 575.0D0
 575.0D0
 575.0D0
 1150.0D0
 1150.0D0
 1150.0D0
 1150.0D0
 1150.0D0
 1150.0D0
 1150.0D0
 1.0D0

P07210
 P07220
 P07230
 P07240
 P07250
 P07260
 P07270
 P07280
 P07290
 P07300
 P07310
 P07320
 P07330
 P07340
 P07350
 P07360
 P07370
 P07380
 P07390

B. MAIN INVESTIGATIVE PROGRAM FOR $n = 1$

PIP000010
PIP000020
PIP000030
PIP000040
PIP000050
PIP000060
PIP000070
PIP000080
PIP000090
PIP000100
PIP000110
PIP000120
PIP000130
PIP000140
PIP000150
PIP000160
PIP000170
PIP000180
PIP000190
PIP000200
PIP000210
PIP000220
PIP000230
PIP000240
PIP000250
PIP000260
PIP000270
PIP000280
PIP000290
PIP000300
PIP000310
PIP000320
PIP000330
PIP000340
PIP000350
PIP000360
PIP000370
PIP000380
PIP000390
PIP000400
PIP000410
PIP000420
PIP000430
PIP000440
PIP000450
PIP000460
PIP000470
PIP000480

```

C*****
C//WALLACE JOB (2027,0084), 'THIS IS N = 1', CLASS=C
C//*MAIN LINES={10}
C// EXEC FRTXCL3P,IMSL=DP,REGION.GO=2048K
C//PORT.SYSIN DD *
C*****
C      THIS PROGRAM WAS DEVELOPED TO PERFORM A NUMERICAL ANALYSIS
C      OF THREE DIMENSIONAL PIPE FLOW STABILITY FOR AXIAL WAVE
C      NUMBER N = 1. THE PROGRAM IS DIVIDED INTO EIGHT PARTS.
C      THE FIRST PART COMPUTES THE CENTRAL FINITE DIFFERENCE
C      COEFFICIENTS FOR THE DERIVATIVES OF P(R) AND Q(R) AT THE
C      INTERIOR MESH POINTS ALONG THE PIPE RADIUS. IN THE SECOND
C      PART, PRE-COMPUTED NON-CENTRAL FINITE DIFFERENCE
C      COEFFICIENTS FOR THE DERIVATIVES OF P(R) AND Q(R) AT POINTS
C      NEAR THE AXIS AND WALL ARE READ IN AS DATA. THE THIRD PART
C      COMPUTES THE VORTICITY TRANSPORT EQUATION COEFFICIENTS OF
C      P(R) AND Q(R) AND THEIR RESPECTIVE DERIVATIVES AT ALL RADIAL
C      MESH POINTS (STATIONS). THE FOURTH PART COMPUTES THE A AND B
C      MATRIX ELEMENTS, WHICH MAKE-UP THE EIGENSYSTEM TO BE SOLVED
C      IN THE FORMAT, A * X = GAMMA * B * X. IN THE FIFTH PART
C      THE A AND B MATRICES COMPRISING THE EIGENSYSTEM ARE SOLVED
C      IN THE SUBROUTINE EIGZC. THE RESULTING EIGENVALUES AND
C      CORRESPONDING EIGENVECTOR REPRESENT GAMMA AND THE COLUMN
C      VECTOR X, RESPECTIVELY, AND ARE SOLUTIONS OF THE GOVERNING
C      PARTIAL DIFFERENTIAL EQUATIONS. THE SIXTH PART VERIFIES
C      THE SOLUTION OF THE PDE AND THE MAGNITUDE OF THE RESIDUAL
C      IS DETERMINED. THE SEVENTH PART COMPUTES THE NORMALIZED

```



```

PIP00490
PIP00500
PIP00510
PIP00520
PIP00530
PIP00540
PIP00550
PIP00560
PIP00570
PIP00580
PIP00590
PIP00600
PIP00610
PIP00620
PIP00630
PIP00640
PIP00650
PIP00660
PIP00670
PIP00680
PIP00690
PIP00700
PIP00710
PIP00720
PIP00730
PIP00740
PIP00750
PIP00760
PIP00770
PIP00780
PIP00790
PIP00800
PIP00810
PIP00820
PIP00830
PIP00840
PIP00850
PIP00860
PIP00870
PIP00880
PIP00890
PIP00900
PIP00910
PIP00920
PIP00930
PIP00940
PIP00950
PIP00960

```

AXIAL PERTURBATION VELOCITY U(R). THE EIGHTH AND LAST
 PART PLOTS THE PERTURBATION VELOCITY VERSUS PIPE RADIUS.
 REQUIRED SUBROUTINES ARE INCLUDED AT THE END OF THE PROGRAM
 LISTING. THIS IS A GENERALIZED PROGRAM FOR VARIABLE SIZED
 MESH UP TO A MAXIMUM MESH SIZE OF 48. BECAUSE OF THE
 LARGE AMOUNT OF MEMORY REQUIRED TO RUN THIS PROGRAM, IT
 CAN ONLY BE RUN IN THE BATCH MODE (MVS). AVERAGE CPU TIME
 REQUIRED FOR ONE SET OF DATA, I.E. ONE AXIAL WAVE NUMBER
 AND ONE REYNOLDS NUMBER, IS 58 SECONDS.

DEFINE PROGRAM VARIABLES AND ARRAYS.

```

COMPLEX*16 A(100,100), B(100,100), AWALLO(4,3,6), A1DERQ(7)
COMPLEX*16 ZERO, ONE, AAXISO(4,3,6), A4DERQ(7), A3DERQ(7), A2DERQ(7)
COMPLEX*16 D3Q1(50), D2Q1(50), D1Q1(50), D0Q1(50), D0Q2(50), E0Q2(50)
COMPLEX*16 D4Q2(50), D3Q2(50), D2Q2(50), D1Q2(50), E1Q2(50), E0Q2(50)
COMPLEX*16 F1Q1(50), E0Q1(50), F2Q2(50), E2Q2(50), F1Q2(50), E1Q2(50)
COMPLEX*16 AAXISP(2,2,5), AWALLP(2,2,5), A1DERP(5), A2DERP(5)
COMPLEX*16 D2P1(50), D1P1(50), D0P1(50), D3P2(50), D2P2(50), D1P2(50)
COMPLEX*16 D0P2(50), E0P1(50), E1P1(50), E2P2(50)
COMPLEX*16 EIGA(100), EIGB(100), EIGVEC(100,100), EIGVAL(100)
COMPLEX*16 AA(100,100), BB(100,100), ONEIMG, TWO, THREE
COMPLEX*16 Q(50), DQ(50), PP(50), JJ(52), RAD(52), UNORM(52)
COMPLEX*16 AI5P(6), AI5D2P(6), AI6D2Q(6), HCA1(52), HCA2(52)
COMPLEX*16 H0B1(52), H0B2(52), HJ, Q0
COMPLEX*16 H0D1PA, H0D2PA, Q0D1QA, Q0D2QA, Q0D3QA, Q0D1QB, BETA
COMPLEX*16 H0D4QA, Q0D2QB, Q0TE1A, Q0TE2A, H0D1QA, H0D2QA, H0D3QA
COMPLEX*16 H0D4QB, H0D1QB, H0D2QB, AAXQ1, AAXQ2, AWAQ1, AWAQ2
COMPLEX*16 D2P01, D2P02, D2Q01, D2Q02, D0P01, D0P02, D0Q01, D0Q02
COMPLEX*16 D0H01, D0H02, E0P01, E0P02, E0Q01, E0Q02, E0H01, E0H02
COMPLEX*16 ERROR(100), WK(1,1), SUMA, SUMB
REAL*8 GAMR(100), GAMM, AX, DMESH
REAL*8 H4TH, H3RD, H2ND, H1ST, HTEMP, ATEMP, AATEMP, WATEMP, R, RE, ALPHA
REAL*8 TEMPR, TEMPI, SIGN, R2, R3, R4
REAL*8 AL2, AL4, AL16, ALSQ, AL4TH, GAMNOR(52), URDP(52), UIDP(52)
REAL*8 UAMP(52), AMPMAX, AMTEMP, ALSQ2, ALSQ4, ALSQ5, ALSQ10, AL3RD2

```



```

PIP000970
PIP000980
PIP000990
PIP001000
PIP001010
PIP001020
PIP001030
PIP001040
PIP001050
PIP001060
PIP001070
PIP001080
PIP001090
PIP001100
PIP001110
PIP001120
PIP001130
PIP001140
PIP001150
PIP001160
PIP001170
PIP001180
PIP001190
PIP001200
PIP001210
PIP001220
PIP001230
PIP001240
PIP001250
PIP001260
PIP001270
PIP001280
PIP001290
PIP001300
PIP001310
PIP001320
PIP001330
PIP001340
PIP001350
PIP001360
PIP001370
PIP001380
PIP001390
PIP001400
PIP001410
PIP001420
PIP001430
PIP001440

```

```

C C C
REAL*4 RADR(52),UR(52),UI(52),AMPNOR(52)
REAL*4 X1(2),Y1(2),ALPLOT,REPLCT,GAMPLT,RMESH
INTEGER MESH,M,MM,M2,IMAX,MP,MFP,MESH2,MH0,MQ0,NGAM

      INITIALIZE THE COEFFICIENT ARRAYS AND SEVERAL CONSTANTS
      DATA ZERO/(0.0D0,0.0D0,0.0D0),ONE/(1.0D0,0.0D0),TWO/(2.0D0,0.0D0)/
      DATA ONEIMG/(0.0D0,1.0D0)/
      DATA THREE/(3.0D0,6.0D0)/
      DATA AAXISQ/72*(0.0D0,0.0D0)/,AWALLQ/72*(0.0D0,0.0D0)/
      DATA A1DERQ/7*(0.0D0,6.0D0)/,A2DERQ/7*(0.0D0,0.0D0)/
      DATA A3DERQ/7*(0.0D0,0.0D0)/,A4DERQ/7*(0.0D0,0.0D0)/
      DATA AAXISP/20*(0.0D0,0.0D0)/,AWALLP/20*(0.0D0,0.0D0)/
      DATA A1DERP/5*(0.0D0,6.0D0)/,A2DERP/5*(0.0D0,0.0D0)/
      DATA X1(1)/0.0/,X1(2)/1.0/,Y1(1)/0.0/,Y1(2)/6.0/
      DATA MESH/48/

*****
PART I
*****
      COMPUTE CENTRAL DIFFERENCE COEFFICIENTS FOR FOURTH ORDER
      DERIVATIVE OF Q(R) AT INTERIOR MESH POINTS.

      DMESH = DFLQAT(MESH)
      H4TH = DMESH**4
      A4DERQ(1) = (-1.0D0/6.0D0)*H4TH
      A4DERQ(7) = A4DERQ(1)
      ATEMP = 2.0D0*H4TH
      A4DERQ(2) = DCMLPX(ATEMP,0.0D0)
      A4DERQ(6) = A4DERQ(2)
      ATEMP = -6.5D0*H4TH
      A4DERQ(3) = DCMLPX(ATEMP,0.0D0)
      A4DERQ(5) = A4DERQ(3)
      ATEMP = (56.0D0/6.0D0)*H4TH
      A4DERQ(4) = DCMLPX(ATEMP,0.0D0)

      COMPUTE CENTRAL DIFFERENCE COEFFICIENTS FOR THIRD ORDER
      DERIVATIVE OF Q(R) AT INTERIOR MESH POINTS.

      H3RD = DMESH**3
      ATEMP = 0.125D0*H3RD
      A3DERQ(1) = DCMLPX(ATEMP,0.0D0)
      A3DERQ(7) = -A3DERQ(1)
      A3DERQ(6) = DCMLPX(H3RD,0.0D0)

*****
C C C C C C C C C C

```



```

A3DERQ(2) = -A3DERQ(5)
ATEMP = (13.0D0/8.0D0) * H3RD
A3DERQ(3) = DCMPLX(ATEMP, 0.0D0)
A3DERQ(5) = -A3DERQ(3)

```

```

      COMPUTE CENTRAL DIFFERENCE COEFFICIENTS FOR SECOND ORDER
      DERIVATIVES OF P(R) AND Q(R) AT INTERIOR MESH POINTS.

```

```

H2ND = DMESH ** 2
ATEMP = (-1.0D0/12.0D0) * H2ND
A2DERQ(2) = DCMPLX(ATEMP, 0.0D0)
A2DERQ(6) = A2DERQ(2)
ATEMP = (16.0D0/12.0D0) * H2ND
A2DERQ(3) = DCMPLX(ATEMP, 0.0D0)
A2DERQ(5) = A2DERQ(3)
ATEMP = -2.5D0 * H2ND
A2DERQ(4) = DCMPLX(ATEMP, 0.0D0)
A2DERP(1) = A2DERQ(2)
A2DERP(2) = A2DERQ(3)
A2DERP(3) = A2DERQ(4)
A2DERP(4) = A2DERQ(5)
A2DERP(5) = A2DERQ(5)

```

```

      COMPUTE CENTRAL DIFFERENCE COEFFICIENTS FOR FIRST ORDER
      DERIVATIVES OF P(R) AND Q(R) AT INTERIOR MESH POINTS.

```

```

H1ST = DMESH
ATEMP = (1.0D0/12.0D0) * H1ST
A1DERQ(2) = DCMPLX(ATEMP, 0.0D0)
A1DERQ(6) = -A1DERQ(2)
ATEMP = (-8.0D0/12.0D0) * H1ST
A1DERQ(3) = DCMPLX(ATEMP, 0.0D0)
A1DERQ(5) = -A1DERQ(3)
A1DERP(1) = A1DERQ(2)
A1DERP(2) = A1DERQ(3)
A1DERP(4) = A1DERQ(5)
A1DERP(5) = A1DERQ(5)

```

PART II

```

      READ IN PRE-COMPUTED NON-CENTRAL DIFFERENCE COEFFICIENTS FOR
      ALL DERIVATIVES OF P(R) AT POINTS NEAR THE AXIS.

```

```

PIP01450
PIP01460
PIP01470
PIP01480
PIP01490
PIP01500
PIP01510
PIP01520
PIP01530
PIP01540
PIP01550
PIP01560
PIP01570
PIP01580
PIP01590
PIP01600
PIP01610
PIP01620
PIP01630
PIP01640
PIP01650
PIP01660
PIP01670
PIP01680
PIP01690
PIP01700
PIP01710
PIP01720
PIP01730
PIP01740
PIP01750
PIP01760
PIP01770
PIP01780
PIP01790
PIP01800
PIP01810
PIP01820
PIP01830
PIP01840
PIP01850
PIP01860
PIP01870
PIP01880
PIP01890
PIP01900
PIP01910
PIP01920

```



```

C C
C      BOUNDARY CONDITIONS AT THE AXIS ARE: DP(0) = 0 AND Q(0) = VAR.
41 READ(5,49) I,J,K
   IF(I.EQ.9) GO TO 44
   HTEMP = DMESH ** I
   DO 42 KKK = 1,K
     READ(5,*) AATEMP * HTEMP
     AATEMP = AATEMP * HTEMP
     AAXISP(I,J,KKK) = DCMPLX(AATEMP,0.0D0)
42 CONTINUE
   GO TO 41
44 CONTINUE

C C C C C
C      READ IN PRE-COMPUTED NON-CENTRAL DIFFERENCE COEFFICIENTS
C      FOR P(0) AND D2P(J).
70 DO 70 I = 1,5
   READ(5,*) AATEMP
   AISP(I) = DCMPLX(AATEMP,0.0D0)
   CONTINUE = ZERO
   DO 71 I = 1,5
     READ(5,*) AATEMP * {DMESH ** 2}
     AATEMP = AATEMP * {DMESH ** 2}
     AISD2P(I) = DCMPLX(AATEMP,0.0D0)
     CONTINUE
     AISD2P(6) = ZERO

C C C C C C C C
C      READ IN PRE-COMPUTED NON-CENTRAL DIFFERENCE COEFFICIENTS FOR
C      ALL DERIVATIVES OF P(R) AT POINTS NEAR THE WALL.
C      BOUNDARY CONDITION AT THE WALL IS: P(1) = I * H(0)
45 READ(5,49) I,J,K
   IF(I.EQ.9) GO TO 47
   HTEMP = DMESH ** I
   JJ = 3 - J
   SIGN = 1.0D0
   IF(I.EQ.1) SIGN = -SIGN
   DO 46 KKK = 1,K
     KK = 6 - KKK
     READ(5,*) WATEMP * HTEMP * SIGN
     WATEMP = WATEMP * HTEMP * SIGN
     AWALLP(I,JJ,KK) = DCMPLX(WATEMP,0.0D0)
     CONTINUE
   GO TO 45
46 CONTINUE

```



```

47 CONTINUE
49 FORMAT(I1, 1X, I1, 1X, I1)
      READ IN PRE-COMPUTED NON-CENTRAL DIFFERENCE COEFFICIENTS FOR
      ALL DERIVATIVES OF Q(R) AT POINTS NEAR THE AXIS.
      BOUNDARY CONDITION AT THE AXIS IS: DQ(J) = 0.

51 READ(5, 49) I, J, K
   IF(I.EQ.9) GO TO 54
   HTEMP = DMESH ** I
   DO 52 KKK = 1, K
     READ(5, *) AATEMP * HTEMP
     AATEMP = AATEMP * HTEMP
     AAXISQ(I, J, KKK) = DCMPLX(AATEMP, 0.0D0)
   GO TO 51
52 CONTINUE
54 CONTINUE

      READ IN PRE-COMPUTED NON-CENTRAL DIFFERENCE COEFFICIENTS
      FOR D2Q(0).

DO 72 I = 1, 6
  READ(5, *) AATEMP
  AATEMP = AATEMP * (DMESH ** 2)
  AIGD2Q(I) = DCMPLX(AATEMP, 0.0D0)
72 CONTINUE

      READ IN PRE-COMPUTED NON-CENTRAL DIFFERENCE COEFFICIENTS FOR
      ALL DERIVATIVES OF Q(R) AT POINTS NEAR THE WALL.
      BOUNDARY CONDITIONS AT THE WALL ARE: DQ(1) = 2 * H(0) AND
      Q(1) = - H(0).

55 READ(5, 49) I, J, K
   IF(I.EQ.9) GO TO 57
   HTEMP = DMESH ** I
   JJJ = 4 - J
   SIGN = 1.0D0
   IF(I.EQ.1) SIGN = -SIGN
   IF(I.EQ.3) SIGN = -SIGN
   DO 56 KKK = 1, K
     KK = 7 - KKK
     READ(5, *) WATEMP

```


PIP02890
 PIP02900
 PIP02910
 PIP02920
 PIP02930
 PIP02940
 PIP02950
 PIP02960
 PIP02970
 PIP02980
 PIP02990
 PIP03000
 PIP03010
 PIP03020
 PIP03030
 PIP03040
 PIP03050
 PIP03060
 PIP03070
 PIP03080
 PIP03090
 PIP03100
 PIP03110
 PIP03120
 PIP03130
 PIP03140
 PIP03150
 PIP03160
 PIP03170
 PIP03180
 PIP03190
 PIP03200
 PIP03210
 PIP03220
 PIP03230
 PIP03240
 PIP03250
 PIP03260
 PIP03270
 PIP03280
 PIP03290
 PIP03300
 PIP03310
 PIP03320
 PIP03330
 PIP03340
 PIP03350
 PIP03360

WATEMP = WATEMP * HTEMP * SIGN
 AVALLO(I,JJ,KK) = DCMPLX(WATEMP,0.0D0)
 56 CONTINUE
 GO TO 55
 57 CONTINUE

CCCCC

REARRANGE SOME OF THE DATA FOR DQ(R) AND D2Q(R) IN THE
 AAXISQ AND AVALLO COEFFICIENT MATRICES.

DO 58 I = 1,6
 AAXISQ(2,3,I) = A2DERQ(I + 1)
 AAXISQ(1,3,I) = A1DERQ(I + 1)
 AVALLO(2,1,I) = A2DERQ(I)
 AVALLO(1,1,I) = A1DERQ(I)
 58 CONTINUE

58

CCCC

READ IN ALPHA AND REYNOLDS NR

IPLOT = 0
 19 CONTINUE
 READ(5,*) ALPHA,RE
 IF(ALPHA.LT.0.0D0) GO TO 180

19

CCCCCCCCCCCC

PART III

COMPUTATION OF THE VORTICITY TRANSPORT EQUATION COEFFICIENTS
 FOR P(R) AND Q(R) AND THEIR RESPECTIVE DERIVATIVES.
 PRE-COMPUTE CONSTANTS INVOLVING ALPHA IN THE EQUATIONS.

AL2 = ALPHA + ALPHA
 AL4 = AL2 + AL2
 AL10 = 10.0D0 * ALPHA
 ALSQ = ALPHA * ALPHA
 AL4TH = ALSQ * ALSQ
 ALSQ2 = ALSQ + ALSQ
 ALSQ4 = ALSQ2 + ALSQ2
 ALSQ5 = ALSQ4 + ALSQ
 ALSQ10 = ALSQ5 + ALSQ5
 AL3RD2 = ALSQ * ALPHA * 2.0D0

CCCC

COMPUTE THE INCREMENTAL PIPE RADIUS AT INTERIOR MESH POINTS.

DO 60 I = 1,MESH

R = (DFLOAT(I) - 0.5D0) / DMESH

R2 = R * R

R3 = R2 * R

R4 = R3 * R

KAD(I) = DCMPLX(R, 0.0D0)

VORTICITY TRANSPORT EQN COEFFICIENTS FOR P(R), DP(R) & D2P(R)

FIRST EQUATION FIRST QUADRANT

TEMPR = (1.0D0 + ALSQ * R2) / RE

D2P1(I) = DCMPLX(TEMPR, 0.0D0)

TEMPR = ((3.0D0/R) + (R*ALSQ5)) / RE

D1P1(I) = DCMPLX(TEMPR, 0.0D0)

TEMPR = ALSQ * (1.0D0 - ALSQ*R2) / RE

TEMP1(I) = -AL2 * (1.0D0 - R2 + (ALSQ*R2) - (ALSQ*R4))

DOP1(I) = DCMPLX(TEMP1, TEMPI)

TEMPR = 1.0D0 + (ALSQ * R2)

EOP1(I) = DCMPLX(TEMPR, 0.0D0)

V T E COEFFICIENTS FOR Q(R), DQ(R), D2Q(R) AND D3Q(R)

FIRST EQUATION SECOND QUADRANT

TEMP1 = R / RE

D3Q1(I) = DCMPLX(0.0D0, TEMPI)

TEMP1 = 8.0D0 / RE

D2Q1(I) = DCMPLX(0.0D0, TEMPI)

TEMPR = AL2 * (R - R3)

TEMP1 = ((12.0D0/R) - (ALSQ*R)) / RE

D1Q1(I) = DCMPLX(TEMPR, TEMPI)

TEMPR = AL2 * (3.0D0 - R2)

TEMP1 = -ALSQ5 / RE

D0Q1(I) = DCMPLX(TEMPR, TEMPI)

E1Q1(I) = DCMPLX(0.0D0, R)

E0Q1(I) = DCMPLX(0.0D0, 3.0D0)

VORTICITY TRANSPORT EQN COEFFICIENTS FOR H(0)

FIRST EQUATION

TEMPR = AL2 * (2.0D0 - ALSQ + (ALSQ*R2))

TEMP1 = AL4TH / RE

H0A1(I) = DCMPLX(TEMPR, TEMPI)

TEMP1 = -ALSQ

H0B1(I) = DCMPLX(0.0D0, TEMPI)

VORTICITY TRANSPORT EQN COEFFICIENTS FOR P(R), DP(R) & D2P(R)

PIP033370
PIP033380
PIP033390
PIP033400
PIP033410
PIP033420
PIP033430
PIP033440
PIP033450
PIP033460
PIP033470
PIP033480
PIP033490
PIP033500
PIP033510
PIP033520
PIP033530
PIP033540
PIP033550
PIP033560
PIP033570
PIP033580
PIP033590
PIP033600
PIP033610
PIP033620
PIP033630
PIP033640
PIP033650
PIP033660
PIP033670
PIP033680
PIP033690
PIP033700
PIP033710
PIP033720
PIP033730
PIP033740
PIP033750
PIP033760
PIP033770
PIP033780
PIP033790
PIP033800
PIP033810
PIP033820
PIP033830
PIP033840

C
C
C
C
C
C

PART IV

COMPUTATION OF THE A AND B MATRIX ELEMENTS.
INITIALIZE THE A AND B MATRICES

```
DO 198 I = 1,100
DO 198 J = 1,100
A(I,J) = ZERO
B(I,J) = ZERO
CONTINUE
198 MHO = 2 * MESH + 1
MQO = 2 * MESH + 2
```

C
C
C
C
C

A AND B MATRIX ELEMENTS IN TERMS OF P(R)

FIRST EQUATION FIRST QUADRANT

```
DO 200 J = 1,2
DO 200 K = 1,5
AORDER = ZERO
IF (K.EQ.J) AORDER = ONE
A(J,K) = AAXISP(2,J,K)*D2P1(J) + AAXISP(1,J,K)*D1P1(J) +
1 AORDER*DOP1(J) + AORDER*EOP1(J)
```

200

```
CONTINUE
MP = MESH - 2
DO 210 J = 3,MP
DO 210 K = 1,5
L = J - 3 + K
AORDER = ZERO
IF (L.EQ.J) AORDER = ONE
A(J,L) = A2DERP(K)*D2P1(J) + A1DERP(K)*D1P1(J) + AORDER*DOP1(J)
B(J,L) = AORDER*EOP1(J)
```

210

```
CONTINUE
MMP = MP - 3
DO 221 J = 1,2
L = J + MP
HOD1PA = ZERO
HOD2PA = ZERO
DO 220 K = 1,5
N = MMP + K
AORDER = ZERO
IF (N.EQ.L) AORDER = ONE
A(L,N) = AAWALLP(2,J,K)*D2P1(L) + AAWALLP(1,J,K)*D1P1(L) +
1 B(L,N) = AORDER*EOP1(L)
HOD2PA = HOD2PA + AAWALLP(2,J,K)
```

PIP04330
PIP04340
PIP04350
PIP04360
PIP04370
PIP04380
PIP04390
PIP04400
PIP04410
PIP04420
PIP04430
PIP04440
PIP04450
PIP04460
PIP04470
PIP04480
PIP04490
PIP04500
PIP04510
PIP04520
PIP04530
PIP04540
PIP04550
PIP04560
PIP04570
PIP04580
PIP04590
PIP04600
PIP04610
PIP04620
PIP04630
PIP04640
PIP04650
PIP04660
PIP04670
PIP04680
PIP04690
PIP04700
PIP04710
PIP04720
PIP04730
PIP04740
PIP04750
PIP04760
PIP04770
PIP04780
PIP04790
PIP04800


```

260 B(J,LL) = A1DERQ(K)*E1Q1(J) + AODER*EQ1(J)
CONTINUE 3
MM = M - 1,3
DO 266 J = 1,3
L = J + M
HOD3QA = ZERO
HOD2QA = ZERO
HOD1QA = ZERO
HOD1QB = ZERO
DO 265 K = 1,6
KK = MM + K - K
NN = MM + K
NN = N + K MESH
AODER = ZERO
IF(N.EQ.L) AODER = ONE
1 A(L,NN) = AVALLO(3,J,K)*D3Q1(L) + AVALLO(2,J,K)*D2Q1(L) +
B(L,NN) = AVALLO(1,J,K)*D1Q1(L) + AODER*D3Q1(L)
HTEMP = (1.0D0 - ((2.0D0 * DFLJAT(KK) - 1.0D0) / DMESH))
BETA = DCMELX(HTMP,0.0D0)
AWAQ1 = AVALLO(1,J,K)
AWAQ2 = AVALLO(2,J,K)
IF(J.EQ.1) AWAQ1 = ZERO
IF(J.EQ.1) AWAQ2 = ZERO
HOD1QA = HOD1QA + (AWAQ1 * BETA)
HOD2QA = HOD2QA + (AWAQ2 * BETA)
HOD3QA = HOD3QA + (AWAQ2(3,J,K) * BETA)
HOD1QB = HOD1QB + (AWAQ1 * BETA)
CONTINUE
265 HOD1QA = HOD1QA + TWJ
IF(J.EQ.1) HOD1QA = ZERO
HOD1QB = HOD1QB + TWJ
IF(J.EQ.1) HOD1QB = ZERO
HOD1QA = HOD1QA * D121(L)
HOD2QA = HOD2QA * D221(L)
HOD3QA = HOD3QA * D321(L)
HOD1QB = HOD1QB * E121(L)
HQA1(L) = HOD1QA + HOD3QA + HQA1(L)
HQB1(L) = HOD1QB + HQB1(L)
266 CONTINUE

```

C C C C C

A AND B MATRIX ELEMENTS IN TERMS OF H(0)

FIRST EQUATION

```

DO 267 I = 1, MESH
A(I,MH0) = HQA1(I)
B(I,MH0) = HQB1(I)

```


267 CONTINUE

A AND B MATRIX ELEMENTS IN TERMS OF P(R)

SECOND EQUATION THIRD QUADRANT

```
DO 270 J = 1, 2
JJ = J + MESH
DO 270 K = 1, 5
AORDER = ZERO
IF (K.EQ.J) AORDER = ONE
A(JJ,K) = AAXISP(2,J,K)*D2P2(J) + AAXISP(1,J,K)*D1P2(J) +
1 AORDER*DOP2(J)
B(JJ,K) = AORDER*EOP2(J)
```

```
270 CONTINUE
DO 275 J = 3, MP
JJ = J + MESH
DO 275 K = 1, 5
L = J - 3 + K
AORDER = ZERO
IF (L.EQ.J) AORDER = ONE
A(JJ,L) = A1DERP(K)*D2P2(J) + A1DERP(K)*D1P2(J) + AORDER*DOP2(J)
B(JJ,L) = AORDER*EOP2(J)
```

```
275 CONTINUE
DO 281 J = 1, 2
L = J + MP
LL = L + MESH
HOD1PA = ZERO
HOD2PA = ZERO
DO 280 K = 1, 5
N = MMP + K
AORDER = ZERO
IF (N.EQ.L) AORDER = ONE
A(LL,N) = AWALLP(2,J,K)*D2P2(L) + AWALLP(1,J,K)*D1P2(L) +
1 AORDER*DOP2(L)
B(LL,N) = AORDER*EOP2(L)
HOD1PA = HOD1PA + AWALLP(1,J,K)
HOD2PA = HOD2PA + AWALLP(2,J,K)
```

```
280 CONTINUE
HOD1PA = HOD1PA * D1P2(L)
HOD2PA = HOD2PA * D2P2(L)
HOD2(L) = HOD2(L) - (ONEIMG * (HOD1PA + HOD2PA))
```

```
281 CONTINUE
```

A AND B MATRIX ELEMENTS IN TERMS OF Q(R)

SECOND EQUATION FOURTH QUADRANT

PIP05770
PIP05780
PIP05790
PIP05800
PIP05810
PIP05820
PIP05830
PIP05840
PIP05850
PIP05860
PIP05870
PIP05880
PIP05890
PIP05900
PIP05910
PIP05920
PIP05930
PIP05940
PIP05950
PIP05960
PIP05970
PIP05980
PIP05990
PIP06000
PIP06010
PIP06020
PIP06030
PIP06040
PIP06050
PIP06060
PIP06070
PIP06080
PIP06090
PIP06100
PIP06110
PIP06120
PIP06130
PIP06140
PIP06150
PIP06160
PIP06170
PIP06180
PIP06190
PIP06200
PIP06210
PIP06220
PIP06230
PIP06240


```

DO 286 J = 1, 3
JJ = J + MESH
QD1QA = ZERO
QD2QA = ZERO
QD3QA = ZERO
QD4QA = ZERO
QD1QB = ZERO
QD2QB = ZERO
DO 285 K = 1, 6
KK = K + MESH
AODER = ZERO
IF (K.EQ.J) AODER = ONE
A(JJ, KK) = AAXISQ(4, J, K) * D4Q2(J) + AAXISQ(3, J, K) * D3Q2(J) +
1 A(JJ, KK) = AAXISQ(2, J, K) * D2Q2(J) + AAXISQ(1, J, K) * D1Q2(J) +
2 AODER * D0Q2(J)
1 B(JJ, KK) = AAXISQ(2, J, K) * E2Q2(J) + AAXISQ(1, J, K) * E1Q2(J) +
AAXQ1 = AAXISQ(1, J, K)
AAXQ2 = AAXISQ(2, J, K)
IF (J.EQ.3) AAXQ1 = ZERO
IF (J.EQ.3) AAXQ2 = ZERO
QD1QA = QD1QA + AAXQ1
QD2QA = QD2QA + AAXQ2
QD3QA = QD3QA + AAXISQ(3, J, K)
QD4QA = QD4QA + AAXISQ(4, J, K)
QD1QB = QD1QB + AAXQ1
QD2QB = QD2QB + AAXQ2
CONTINUE
285 QD1QA = QD1QA * D1Q2(J)
QD2QA = QD2QA * D2Q2(J)
QD3QA = QD3QA * D3Q2(J)
QD4QA = QD4QA * D4Q2(J)
QD1QB = QD1QB * E1Q2(J)
QD2QB = QD2QB * E2Q2(J)
A(JJ, MQ) = - (QD1QA + QD2QA + QD3QA + QD4QA)
B(JJ, MQ) = - (QD1QB + QD2QB)
CONTINUE
286 JJ = J + MESH
DO 290 J = 1, 7
L = J - 4
LL = L + MESH
AODER = ZERO
IF (L.EQ.J) AODER = ONE
A(JJ, LL) = A4DERQ(K) * D4Q2(J) + A3DERQ(K) * D3Q2(J) +
1 A(JJ, LL) = A2DERQ(K) * D2Q2(J) + A1DERQ(K) * D1Q2(J) +
2 A(JJ, LL) = A2DERQ(K) * E2Q2(J) + AODER * D0Q2(J)
CONTINUE
290

```



```

DO 296 J = 1, 3
  L = J + M
  LL = L + MESH
  HOD1QA = ZERO
  HOD2QA = ZERO
  HOD3QA = ZERO
  HOD4QA = ZERO
  HOD1QB = ZERO
  HOD2QB = ZERO
DO 295 K = 1, 6
  KK = 7 - K
  NN = MM + K
  NN = NN + MESH
  AODER = ZERO
  IF (N.EQ.L) AODER = ONE
  A(LL, NN) = AVALLO(4, J, K) * D4Q2(L) + AVALLO(3, J, K) * D3Q2(L) +
1  AVALLO(2, J, K) * D2Q2(L) + AVALLO(1, J, K) * D1Q2(L) +
2  AODER * DQ2(L)
1  B(LL, NN) = AVALLO(2, J, K) * E2Q2(L) + AVALLO(1, J, K) * E1Q2(L) +
  AODER * EQ2(L)
  HTEMP = (1.0D0 - ((2.0D0 * DFLDAR(KK) - 1.0D0) / DMESH))
  BETA = DCMPLX(HTEMP, 0.0D0)
  AWAQ1 = AVALLO(1, J, K)
  AWAQ2 = AVALLO(2, J, K)
  IF (J.EQ.1) AWAQ1 = ZERO
  IF (J.EQ.1) AWAQ2 = ZERO
  HOD1QA = HOD1QA + (AWAQ1 * BETA)
  HOD2QA = HOD2QA + (AWAQ2 * BETA)
  HOD3QA = HOD3QA + (AWALLQ(3, J, K) * BETA)
  HOD4QA = HOD4QA + (AWALLQ(4, J, K) * BETA)
  HOD1QB = HOD1QB + (AWAQ1 * BETA)
  HOD2QB = HOD2QB + (AWAQ2 * BETA)
295 CONTINUE
  HOD1QA = TWO
  HOD1QB = TWO
  IF (J.EQ.1) HOD1QA = ZERO
  IF (J.EQ.1) HOD1QB = ZERO
  HOD1QA = HOD1QA * D1Q2(L)
  HOD2QA = HOD2QA * D2Q2(L)
  HOD3QA = HOD3QA * D3Q2(L)
  HOD4QA = HOD4QA * D4Q2(L)
  HOD1QB = HOD1QB * E1Q2(L)
  HOD2QB = HOD2QB * E2Q2(L)
  H0A2(L) = HOD1QA + HOD2QA + HOD3QA + HOD4QA
  H0B2(L) = HOD1QB + HOD2QB
296 CONTINUE
  A AND B MATRIX ELEMENTS IN TERMS OF H(0)
C
C

```


C
C
C

SECOND EQUATION

```
DO 297 I = 1, MESH
  II = I + MESH
  A(II, MH0) = H0A2(I)
  B(II, MH0) = H0B2(I)
  297 CONTINUE
```

297

C
C
C
C
C
C
C

A AND B MATRIX ELEMENTS FOR THE TWO SPECIAL BOUNDARY

CONDITION EQUATIONS INVOLVING GAMMA.

FIRST EQUATION COEFFICIENTS

```
TEMPR = 4.0D0 / RE
D2P01 = DCMLPX(TEMPR, 0.0D0)
TEMPI = 20.0D0 / RE
D2Q01 = DCMLPX(0.0D0, TEMPI)
TEMPR = ALSQ / RE
TEMPI = -AL2
DOP01 = DCMLPX(TEMPR, TEMPI)
TEMPR = 6.0D0 * ALPHA
TEMPI = -ALSQ5 / RE
DQ001 = DCMLPX(TEMPR, TEMPI)
TEMPI = AL4 - AL3RD2
TEMPR = AL4TH / RE
DOH01 = DCMLPX(TEMPR, TEMPI)
EOP01 = ONE
EOQ01 = DCMLPX(0.0D0, 3.0D0)
TEMPI = -ALSQ
EOH01 = DCMLPX(0.0D0, TEMPI)
```

SECOND EQUATION COEFFICIENTS

```
TEMPI = -16.0D0 / RE
D2P02 = DCMLPX(0.0D0, TEMPI)
D2Q02 = DCMLPX(TEMPR, 0.0D0)
TEMPR = -AL4
TEMPI = ALSQ4 / RE
DOP02 = DCMLPX(TEMPR, TEMPI)
DQ002 = DCMLPX(TEMPR, AL4)
TEMPR = -AL4TH / RE
TEMPI = -AL3RD2
DOH02 = DCMLPX(TEMPR, TEMPI)
EOQ02 = DCMLPX(0.0D0, -2.0D0)
EOP02 = DCMLPX(-2.0D0, 0.0D0)
EOH02 = DCMLPX(ALSQ, 0.0D0)
```

C
C
C

PI P07210
PI P07220
PI P07230
PI P07240
PI P07250
PI P07260
PI P07270
PI P07280
PI P07290
PI P07300
PI P07310
PI P07320
PI P07330
PI P07340
PI P07350
PI P07360
PI P07370
PI P07380
PI P07390
PI P07400
PI P07410
PI P07420
PI P07430
PI P07440
PI P07450
PI P07460
PI P07470
PI P07480
PI P07490
PI P07500
PI P07510
PI P07520
PI P07530
PI P07540
PI P07550
PI P07560
PI P07570
PI P07580
PI P07590
PI P07600
PI P07610
PI P07620
PI P07630
PI P07640
PI P07650
PI P07660
PI P07670
PI P07680

380 FORMAT(1X, 2D30.18)

PART VII

COMPUTATION OF AXIAL PERTURBATION VELOCITY U(R).
 OUTPUT THE EIGENVECTOR CORRESPONDING TO THE LEASE STABLE
 EIGENVALUE, GAMMA*.

```

400 DO 400 I = 1, MESH
    II = I + MESH
    P(I) = EIGVEC(I, NGAM)
    Q(I) = EIGVEC(II, NGAM)
    CONTINUE
    H0 = EIGVEC(MH0, NGAM)
    Q0 = EIGVEC(MQ0, NGAM)
    WRITE(6, 401) EIGVAL(NGAM)
401 FORMAT(1X, //, 5X, 'EIGENVECTOR CORRESPONDING TO', 2D27.18, /)
    DO 402 I = 1, MESH
    II = I + MESH
    WRITE(6, 404) I, P(I), II, Q(I)
404 FORMAT(2X, I2, 2D28.18, 2X, I2, 2D23.18)
402 CONTINUE
    WRITE(6, 403) H0, Q0
403 FORMAT(1X, //, 2X, 'H0', 2D28.18, 2X, 'Q0', 2D28.18, //)

```

COMPUTATION OF DQ(R)

```

410 DO 411 J = 1, 3
    DQ(J) = ZERO
    Q0D1QA = ZERO
    DO 410 K = 1, 6
        AAXQ1 = AAXISO(1, J, K)
        IF(J.EQ.3) AAXQ1 = ZERO
        DQ(J) = DQ(J) + Q(K) * AAXISQ(1, J, K)
        Q0D1QA = Q0D1QA + AAXQ1
    CONTINUE
411 DQ(J) = DQ(J) - (Q0D1QA * Q0)
    CONTINUE
C
420 DO 420 J = 4, M
    DQ(J) = ZERO
420 DO 420 K = 1, 7
    L = J - 4 + K

```

PIPO8650
 PIP08660
 PIP08670
 PIP08680
 PIP08690
 PIP08700
 PIP08710
 PIP08720
 PIP08730
 PIP08740
 PIP08750
 PIP08760
 PIP08770
 PIP08780
 PIP08790
 PIP08800
 PIP08810
 PIP08820
 PIP08830
 PIP08840
 PIP08850
 PIP08860
 PIP08870
 PIP08880
 PIP08890
 PIP08900
 PIP08910
 PIP08920
 PIP08930
 PIP08940
 PIP08950
 PIP08960
 PIP08970
 PIP08980
 PIP08990
 PIP09000
 PIP09010
 PIP09020
 PIP09030
 PIP09040
 PIP09050
 PIP09060
 PIP09070
 PIP09080
 PIP09090
 PIP09100
 PIP09110
 PIP09120


```

C      420 DQ(J) = DQ(J) + (Q(L) * A1DER2(K))
C      CONTINUE
C      DO 431 J = 1,3
C      L = J + M
C      DQ(L) = ZERO
C      HOD1QA = ZERO
C      DO 430 K = 1,6
C      AWAQ1 = AWAQ(1,J,K)
C      IF(J.EQ.1) AWAQ1 = ZERO
C      KK = 7 - K
C      N = MM + K
C      HTEMP = 1.0D0 - ((2.0D0 * DFLCAT(KK) - 1.0D0) / DMESH)
C      BETA = DCMELX(HTEMP,0.0D0)
C      HOD1QA = HOD1QA + (AWAQ1 * BETA)
C      DQ(L) = DQ(L) + (Q(N) * AWAQ(1,J,K))
C      430 CONTINUE
C      HOD1QA = HOD1QA + TWO
C      IF(J.EQ.1) HOD1QA = ZERO
C      DQ(L) = DQ(L) + (HOD1QA * H0)
C      431 CONTINUE
C
C      DO 440 I = 1,MESH
C      U(I) = RAD(I) * ((THREE*Q(I)) + (RAD(I)*DQ(I)) - (ONEIMG*P(I)))
C      440 CONTINUE
C      REARRANGE DATA FOR PLOT ROUTINE
C      M2 = MESH + 2
C      DO 450 I = 1,MESH
C      II = M2 - I
C      III = II - 1
C      U(II) = U(III)
C      RAD(II) = RAD(III)
C      450 CONTINUE
C      RAD(1) = ZERO
C      RAD(M2) = ONE
C      U(1) = ZERO
C      U(M2) = ZERO
C      DO 460 I = 1,M2
C      RADR(I) = DREAL(RAD(I))
C      460 CONTINUE
C      COMPUTE THE NORMALIZED PERTURBATION VELOCITY AND
C      NORMALIZED AMPLITUDE AND OUTPUT THE RESULTS.
C      DO 465 I = 1,M2

```

```

PIP091300
PIP091400
PIP091500
PIP091600
PIP091700
PIP091800
PIP091900
PIP092000
PIP092100
PIP092200
PIP092300
PIP092400
PIP092500
PIP092600
PIP092700
PIP092800
PIP092900
PIP093000
PIP093100
PIP093200
PIP093300
PIP093400
PIP093500
PIP093600
PIP093700
PIP093800
PIP093900
PIP094000
PIP094100
PIP094200
PIP094300
PIP094400
PIP094500
PIP094600
PIP094700
PIP094800
PIP094900
PIP095000
PIP095100
PIP095200
PIP095300
PIP095400
PIP095500
PIP095600
PIP095700
PIP095800
PIP095900
PIP096000

```



```

180 GO TO 19
    CONTINUE
    CALL PLOT(0.0,0.0,999)
    STOP
    END

```

C.....

```

SUBROUTINE TITLE1

```

```

SUBROUTINE TO WRITE TITLE ON PLOTS

```

```

SUBROUTINE TITLE1(XO,YO,RMESH,ALPLOT,REPLCT,GAMPLT)

```

```

RN = 1.0

```

```

YHT = 0.14

```

```

CALL NEWPEN(2)

```

```

CALL SYMBOL(XO,YO,YHT

```

```

1,NORMALIZED PERTURBATION VELOCITY VS RADIUS',0.0,42)

```

```

YHT = 0.08

```

```

DELY = 0.20

```

```

CALL NEWPEN(1)

```

```

YO = YO - 0.8

```

```

XO = XO + 2.5

```

```

XN = XO + .75

```

```

CALL SYMBOL(XO,YO,YHT,'N' = ',0.0,9)

```

```

CALL NUMBER(XN,YO,YHT,RN,0.0,-1)

```

```

YO = YO - DELY

```

```

CALL SYMBOL(XO,YO,YHT,'MESH' = ',0.0,9)

```

```

CALL NUMBER(XN,YO,YHT,RMESH,0.0,-1)

```

```

YO = YO - DELY

```

```

CALL SYMBOL(XO,YO,YHT,'ALPHA' = ',0.0,9)

```

```

CALL NUMBER(XN,YO,YHT,ALPLOT,0.0,2)

```

```

YO = YO - DELY

```

```

CALL SYMBOL(XO,YO,YHT,'REV NR' = ',0.0,9)

```

```

CALL NUMBER(XN,YO,YHT,REPLCT,0.0,1)

```

```

YO = YO - DELY

```

```

CALL SYMBOL(XO,YO,YHT,'GAMMA*' = ',0.0,9)

```

```

CALL NUMBER(XN,YO,YHT,GAMPLT,0.0,4)

```

```

YO = YO - 3.4

```

```

CALL SYMBOL(XO,YO,YHT,'OCTAGON' = U(REAL)',0.0,17)

```

```

YO = YO - DELY

```

```

CALL SYMBOL(XO,YO,YHT,'DIAMOND' = U(IMAG)',0.0,17)

```

```

YO = YO - DELY

```

```

CALL SYMBOL(XO,YO,YHT,'TRIANGLE' = U AMPL ',0.0,17)

```

```

WRITE THE AXIS LABELS

```

```

XO = XO - 2.55

```

C
C
C
C

PIP10090
PIP10100
PIP10110
PIP10120
PIP10130
PIP10140
PIP10150
PIP10160
PIP10170
PIP10180
PIP10190
PIP10200
PIP10210
PIP10220
PIP10230
PIP10240
PIP10250
PIP10260
PIP10270
PIP10280
PIP10290
PIP10300
PIP10310
PIP10320
PIP10330
PIP10340
PIP10350
PIP10360
PIP10370
PIP10380
PIP10390
PIP10400
PIP10410
PIP10420
PIP10430
PIP10440
PIP10450
PIP10460
PIP10470
PIP10480
PIP10490
PIP10500
PIP10510
PIP10520
PIP10530
PIP10540
PIP10550
PIP10560


```

YO = YO + 0.3
YHT = 0.12
CALL SYMBOL(XO, YO, YHT, 'NORMALIZED PERTURBATION VELOCITY', 90., 32)
XO = XO + 2.8
YO = YO - 1.0
CALL SYMBOL(XO, YO, YHT, 'PIPE RADIUS', 0.0, 11)
RETURN
END

/*
//30, SYSIN DD *
2 1 5
-0.75414464179988427D+00
0.37221235445036506D+00
0.61900532859680124D+00
-0.28537596210775519D+00
0.483027432405761783D-01
2 2 5
0.128374777975133259D+01
-0.257055456877836685D+01
0.138809946714031485D+01
-0.104795737122556964D+00
0.350305900927518066D-02
1 1 4
-0.102651515151515138D+01
0.139772727272727271D+01
-0.4431818181818135D+00
0.719696969696969474D-01
1 2 4
-0.602272727272726405D+00
0.34090909090909071733D-01
0.64772727272727373D+00
-0.79545454545454470D-01
9 0 0
0.137690108792184640D+01
-0.611956039076375065D+00
0.330456261101242083D+00
-0.11240008809946189D+00
0.169987788632325644D-01
-0.442650976909413263D+01
-0.780067100848626405D+01
0.484236234458257542D+01
-0.173889875666073834D+01
-0.2706976514770296355D+00
2 1 5
-0.541666666666665809D+01
0.244444444444444176D+01
-0.4999999999999994837D+00
0.952380952380948859D-01

```


2	2	5	-0.9259259259258898790-02
			0.174999999999992450+01
			-0.277777777777775930+01
			0.149999999999991780+01
			-0.1428571428571396850+00
1	1	4	0.9259259259258759140-02
			0.1666666666666658650+00
			0.100000000000000220+01
			-0.299999999999998920+00
			0.4761904761904763380-01
1	2	4	-0.9999999999999973350+00
			0.1666666666666642980+00
			0.6000000000000011990+00
			-0.7142857142857128580-01
9	0	0	
4	1	6	0.1150000000000007140+03
			-0.38444444444444502550+02
			0.1640000000000038580+02
			-0.5224489795918497940+01
			0.1123456790123495090+01
			-0.1157024793388475580+00
4	2	6	-0.26000000000000080290+02
			0.17666666666666701600+02
			-0.1120000000000023020+02
			0.3959183673469510720+01
			-0.66666666666667004910+00
			0.5785123966942518070-01
4	3	6	0.10000000000000852650+01
			-0.6222222222222804080+01
			0.9200000000000457590+01
			-0.6448979591836899030+01
			0.1987654320987697790+01
			-0.1652892561983525520+00
3	1	5	-0.174999999999997510+02
			0.1111111111111076030+00
			0.1200000000000013720+01
			-0.3469387755102073950+00
			0.4320987654321039110-01
3	2	5	-0.1349999999999996800+02
			-0.388888888888882130+01

P	I	P	111050
P	I	P	111060
P	I	P	111070
P	I	P	111080
P	I	P	111090
P	I	P	111100
P	I	P	111110
P	I	P	111120
P	I	P	111130
P	I	P	111140
P	I	P	111150
P	I	P	111160
P	I	P	111170
P	I	P	111180
P	I	P	111190
P	I	P	111200
P	I	P	111210
P	I	P	111220
P	I	P	111230
P	I	P	111240
P	I	P	111250
P	I	P	111260
P	I	P	111270
P	I	P	111280
P	I	P	111290
P	I	P	111300
P	I	P	111310
P	I	P	111320
P	I	P	111330
P	I	P	111340
P	I	P	111350
P	I	P	111360
P	I	P	111370
P	I	P	111380
P	I	P	111390
P	I	P	111400
P	I	P	111410
P	I	P	111420
P	I	P	111430
P	I	P	111440
P	I	P	111450
P	I	P	111460
P	I	P	111470
P	I	P	111480
P	I	P	111490
P	I	P	111500
P	I	P	111510
P	I	P	111520

-0.142108547152020037D-13
 -0.551020408163266584D+00
 -0.679012345679017859D-01
 3 3 5
 -0.155000000000001137D+02
 -0.9888888888889106D+01
 -0.600000000000005329D+01
 -0.144897959183674985D+01
 0.679012345678990935D-01
 2 1 4
 -0.46666666666666585D+01
 -0.211111111111111127D+01
 -0.319999999999999993D+00
 0.340136054421768521D-01
 2 2 4
 0.999999999999999978684D+00
 -0.2444444444444444930D+01
 -0.132000000000000117D+01
 -0.816326530612245110D-01
 1 1 3
 0.249999999999999999889D+01
 -0.2222222222222222293D+00
 -0.1999999999999999978D-01
 1 2 3
 -0.4500000000000000355D+01
 -0.1333333333333333304D+01
 0.1800000000000000007D+00
 9 0 0
 0.2165625000000000711D+02
 -0.4010416666666673358D+01
 -0.1732500000000004345D+01
 -0.631377551020423478D+00
 -0.148533950617288385D+00
 -0.162706611570253212D-01
 4 1 6
 0.1150000000000000714D+03
 -0.3844444444444450255D+02
 -0.1640000000000003858D+02
 -0.522448979591849794D+01
 -0.112345679012349509D+01
 -0.115702479338847558D+00
 4 2 6
 -0.26000000000000008029D+02
 -0.1766666666666670160D+02
 -0.1120000000000002302D+02
 -0.395918367346951072D+01
 -0.6666666666666700491D+00
 -0.578512396694251807D-01

PIP11530
 PIP11540
 PIP11550
 PIP11560
 PIP11570
 PIP11580
 PIP11590
 PIP11600
 PIP11610
 PIP11620
 PIP11630
 PIP11640
 PIP11650
 PIP11660
 PIP11670
 PIP11680
 PIP11690
 PIP11700
 PIP11710
 PIP11720
 PIP11730
 PIP11740
 PIP11750
 PIP11760
 PIP11770
 PIP11780
 PIP11790
 PIP11800
 PIP11810
 PIP11820
 PIP11830
 PIP11840
 PIP11850
 PIP11860
 PIP11870
 PIP11880
 PIP11890
 PIP11900
 PIP11910
 PIP11920
 PIP11930
 PIP11940
 PIP11950
 PIP11960
 PIP11970
 PIP11980
 PIP11990
 PIP12000

4	3	6	0	1000000000000085265D+01	P	12010
			-0	622222222222280408D+01	P	12020
			-0	920000000000045759D+01	P	12030
			-0	644897959183689905D+01	P	12040
			-0	198765432098769779D+01	P	12050
			-0	165289256198352552D+00	P	12060
3	1	5	-0	174999999999999751D+02	P	12070
			0	11111111111107608D+00	P	12080
			0	12000000000001372D+01	P	12090
			-0	346938775510207395D+00	P	12100
			0	432098765432103911D-01	P	12110
3	2	5	0	13499999999999968D+02	P	12120
			-0	3888888888888218D+01	P	12130
			-0	142108547152020037D-13	P	12140
			0	551020408163266584D+00	P	12150
			-0	679012345679017859D-01	P	12160
3	3	5	-0	1550000000000001137D+02	P	12170
			-0	98888888888889106D+01	P	12180
			-0	600000000000005329D+01	P	12190
			0	144897959183674985D+01	P	12200
			0	679012345678990935D-01	P	12210
2	1	4	-0	466666666666666585D+01	P	12220
			-0	21111111111111027D+01	P	12230
			-0	319999999999999993D+00	P	12240
			0	340136054421768521D-01	P	12250
2	2	4	0	99999999999999978684D+00	P	12260
			-0	244444444444444930D+01	P	12270
			-0	132000000000000117D+01	P	12280
			-0	81632653061224511D-01	P	12290
1	1	3	0	249999999999999889D+01	P	12300
			-0	22222222222222293D+00	P	12310
			-0	199999999999999973D-01	P	12320
1	2	3	-0	450000000000000355D+01	P	12330
			0	133333333333333304D+01	P	12340
			0	180000000000000000D+00	P	12350
9	0	0		1150.0D0	P	12360
0	0	0		1150.0D0	P	12370
0	5	0		1150.0D0	P	12380
1	0	0		1150.0D0	P	12390
2	0	0		1150.0D0	P	12400
					P	12410
					P	12420
					P	12430
					P	12440
					P	12450
					P	12460
					P	12470
					P	12480

4-0D0
 8-0D0
 32-0D0
 0-0D0
 0-0D0
 1-0D0
 2-0D0
 4-0D0
 8-0D0
 16-0D0
 32-0D0
 -1-0D0
 /*
 //

1150:0D0
 1150:0D0
 1150:0D0
 2300:0D0
 2300:0D0
 2300:0D0
 2300:0D0
 2300:0D0
 2300:0D0
 0.0D0

PIP12490
 PIP12500
 PIP12510
 PIP12520
 PIP12530
 PIP12540
 PIP12550
 PIP12560
 PIP12570
 PIP12580
 PIP12590
 PIP12600
 PIP12610
 PIP12620
 PIP12630

PIP000011
PIP000020
PIP000030
PIP000040
PIP000050
PIP000060
PIP000070
PIP000080
PIP000090
PIP001000
PIP001100
PIP001200
PIP001300
PIP001400
PIP001500
PIP001600
PIP001700
PIP001800
PIP001900
PIP002000
PIP002100
PIP002200
PIP002300
PIP002400
PIP002500
PIP002600
PIP002700
PIP002800
PIP002900
PIP003000
PIP003100
PIP003200
PIP003300
PIP003400
PIP003500
PIP003600
PIP003700
PIP003800
PIP003900
PIP004000
PIP004100
PIP004200
PIP004300
PIP004400
PIP004500
PIP004600
PIP004700
PIP004800

```

*****
THIS PROGRAM WAS DEVELOPED TO PERFORM A NUMERICAL ANALYSIS
OF THREE DIMENSIONAL PIPE FLOW STABILITY FOR AXIAL WAVE
NUMBER N = 6. THE PROGRAM IS DIVIDED INTO EIGHT PARTS.
THE FIRST PART COMPUTES THE CENTRAL FINITE DIFFERENCE
COEFFICIENTS FOR THE DERIVATIVES OF P(R) AND Q(R) AT THE
INTERIOR MESH POINTS ALONG THE PIPE RADIUS. IN THE SECOND
PART, PRE-COMPUTED NON-CENTRAL FINITE DIFFERENCE
COEFFICIENTS FOR THE DERIVATIVES OF P(R) AND Q(R) AT POINTS
NEAR THE AXIS AND WALL ARE READ IN AS DATA. THE THIRD PART
COMPUTES THE VORTICITY TRANSPORT EQUATION COEFFICIENTS OF
P(R) AND Q(R) AND THEIR RESPECTIVE DERIVATIVES AT ALL RADIAL
MESH POINTS (STATIONS). THE FOURTH PART COMPUTES THE A AND B
MATRIX ELEMENTS, WHICH MAKE-UP THE EIGENSYSTEM TO BE SOLVED
IN THE FORMAT, A * X = GAMMA * B * X. IN THE FIFTH PART
THE A AND B MATRICES COMPRISING THE EIGENSYSTEM ARE SOLVED
IN THE SUBROUTINE EIGZC. THE RESULTING EIGENVALUES AND
CORRESPONDING EIGENVECTOR REPRESENT GAMMA AND THE COLUMN
VECTOR X, RESPECTIVELY, AND ARE SOLUTIONS OF THE GOVERNING
PARTIAL DIFFERENTIAL EQUATIONS. THE SIXTH PART VERIFIES
THE SOLUTION OF THE PDE AND THE MAGNITUDE OF THE RESIDUAL
IS DETERMINED. THE SEVENTH PART COMPUTES THE NORMALIZED
*****

```



```

AATEMP = AATEMP * HTEMP
AAXISP(I, J, KKK) = DCMPLX(AATEMP, 0.0D0)
42 CONTINUE
GO TO 41
44 CONTINUE

```

CCCCC

```

READ IN PRE-COMPUTED NON-CENTRAL DIFFERENCE COEFFICIENTS FOR
ALL DERIVATIVES OF P(R) AT POINTS NEAR THE WALL.
BOUNDARY CONDITION AT THE WALL IS: P(1) = 0

```

```

45 READ(5, 49) I, J, K
IF(I.EQ.9) GO TO 47
HTEMP = DMESH ** I
JJ = 3 - J
SIGN = 1.0D0
IF(I.EQ.1) SIGN = -SIGN
DO 46 KKK = 1, K
KK = 6 - KKK
READ(5, *) WATEMP
WATEMP = WATEMP * HTEMP * SIGN
AAXISP(I, JJ, KKK) = DCMPLX(WATEMP, 0.0D0)
46 CONTINUE
GO TO 45
47 CONTINUE
49 FORMAT(I1, 1X, I1, 1X, I1)

```

CCCCC

```

READ IN PRE-COMPUTED NON-CENTRAL DIFFERENCE COEFFICIENTS FOR
ALL DERIVATIVES OF Q(R) AT POINTS NEAR THE AXIS.
BOUNDARY CONDITIONS AT THE AXIS ARE: DQ(0) = 0 AND Q(0) = 0.

```

```

51 READ(5, 49) I, J, K
IF(I.EQ.9) GO TO 54
HTEMP = DMESH ** I
DO 52 KKK = 1, K
READ(5, *) AATEMP
AATEMP = AATEMP * HTEMP
AAXISO(I, J, KKK) = DCMPLX(AATEMP, 0.0D0)
52 CONTINUE
GO TO 51
54 CONTINUE

```

CCCCC

```

READ IN PRE-COMPUTED NON-CENTRAL DIFFERENCE COEFFICIENTS FOR
ALL DERIVATIVES OF Q(R) AT POINTS NEAR THE WALL.

```

PIP01930
 PIP01940
 PIP01950
 PIP01960
 PIP01970
 PIP01980
 PIP01990
 PIP02000
 PIP02010
 PIP02020
 PIP02030
 PIP02040
 PIP02050
 PIP02060
 PIP02070
 PIP02080
 PIP02090
 PIP02100
 PIP02110
 PIP02120
 PIP02130
 PIP02140
 PIP02150
 PIP02160
 PIP02170
 PIP02180
 PIP02190
 PIP02200
 PIP02210
 PIP02220
 PIP02230
 PIP02240
 PIP02250
 PIP02260
 PIP02270
 PIP02280
 PIP02290
 PIP02300
 PIP02310
 PIP02320
 PIP02330
 PIP02340
 PIP02350
 PIP02360
 PIP02370
 PIP02380
 PIP02390
 PIP02400


```

AL12 = 12.0D0 * ALPHA
AL14 = 14.0D0 * ALPHA
AL24 = 24.0D0 * ALPHA
ALSQ = ALPHA * ALPHA
ALSQ2 = ALSQ * ALSQ
AL4TH = 5.0D0 * ALSQ
ALSQ6 = 5.0D0 * ALSQ
ALSQ9 = 9.0D0 * ALSQ
ALSQ24 = 24.0D0 * ALSQ
ALSQ36 = 36.0D0 * ALSQ
ALSQ57 = 57.0D0 * ALSQ
AL3RD2 = 2.0D0 * ALSQ * ALPHA

```

CCC

COMPUTE THE INCREMENTAL PIPE RADIUS AT INTERIOR MESH POINTS.

```

DO 60 I = 1,MESH
R = (DFLOAT(I) - 0.5D0) / DMESH
R2 = R * R
R3 = R2 * R
R4 = R3 * R
R5 = R4 * R
RAD(I) = DCMLPX(R,0.0D0)

```

CCCCC

VORTICITY TRANSPORT EQN COEFFICIENTS FOR P(R), DP(R) & D2P(R)

FIRST EQUATION FIRST QUADRANT

```

TEMPR = (R2 * (36.0D0 + ALSQ * R2)) / RE
D2P1(I) = DCMLPX(TEMPR,0.0D0)
TEMPR = ((252.0D0 * R) + (ALSQ3 * R2)) / RE
D1P1(I) = DCMLPX(TEMPR,0.0D0)
TEMPR = - (972.0D0 + (ALS257 * R2) + (AL4TH * R4)) / RE
TEMP1(I) = - (AL2 * R2 * (36.0D0 - (36.0D0 * R2) + (ALSQ * (R2 - R4))))
DOP1(I) = DCMLPX(TEMPR,TEMP1)
TEMPR = (36.0D0 * R2) + (ALSQ * R4)
EOP1(I) = DCMLPX(TEMPR,0.0D0)

```

V T E COEFFICIENTS FOR Q(R), DQ(R), D2Q(R) AND D3Q(R)

FIRST EQUATION SECOND QUADRANT

```

TEMP1 = (6.0D0 * R2) / RE
D3Q1(I) = DCMLPX(0.0D0,TEMP1)
TEMP1 = (6.0D0 * R) / RE
D2Q1(I) = DCMLPX(0.0D0,TEMP1)
TEMPR = AL12 * (R2 - R4)
TEMP1 = - (42.0D0 + (ALSQ6 * R2)) / RE
D1Q1(I) = DCMLPX(TEMPR,TEMP1)

```

CCCCC

```

PIP02890
PIP02900
PIP02910
PIP02920
PIP02930
PIP02940
PIP02950
PIP02960
PIP02970
PIP02980
PIP02990
PIP03000
PIP03010
PIP03020
PIP03030
PIP03040
PIP03050
PIP03060
PIP03070
PIP03080
PIP03090
PIP03100
PIP03110
PIP03120
PIP03130
PIP03140
PIP03150
PIP03160
PIP03170
PIP03180
PIP03190
PIP03200
PIP03210
PIP03220
PIP03230
PIP03240
PIP03250
PIP03260
PIP03270
PIP03280
PIP03290
PIP03300
PIP03310
PIP03320
PIP03330
PIP03340
PIP03350
PIP03360

```


206

C

FIRST EQUATION SECOND QUADRANT

```

DO 250 J = 1, 3
DO 250 K = 1, 6
KK = K + MESH
AODER = ZERO
IF (K.EQ.J) AODER = ONE
A (J, KK) = AAXISQ(3, J, K) * D3Q1(J) + AAXISQ(2, J, K) * D2Q1(J) +
1 AAXISQ(1, J, K) * D1Q1(J) + AAXISQ(0, J, K) * D0Q1(J)
B (J, KK) = AAXISQ(1, J, K) * E1Q1(J)
250 CONTINUE
M = MESH - 3
DO 260 J = 4, M
DO 260 K = 1, 7
L = J - 4 + K
LL = L + MESH
AODER = ZERO
IF (L.EQ.J) AODER = ONE
A (J, LL) = A3DERQ(K) * D3Q1(J) + A2DERQ(K) * D2Q1(J) +
1 A1DERQ(K) * D1Q1(J) + A0DERQ(K) * D0Q1(J)
B (J, LL) = A1DERQ(K) * E1Q1(J)
260 CONTINUE
MM = M - 3
DO 265 J = 1, 3
L = J + M
DO 265 K = 1, 6
KK = 7 - K
NN = MM + K
NN = N + MESH
AODER = ZERO
IF (N.EQ.L) AODER = ONE
A (L, NN) = AWALLQ(3, J, K) * D3Q1(L) + AWALLQ(2, J, K) * D2Q1(L) +
1 AWALLQ(1, J, K) * D1Q1(L) + AWALLQ(0, J, K) * D0Q1(L)
B (L, NN) = AWALLQ(1, J, K) * E1Q1(L)
265 CONTINUE
A AND B MATRIX ELEMENTS IN TERMS OF P(R)
SECOND EQUATION THIRD QUADRANT
DO 270 J = 1, 2
JJ = J + MESH
DO 270 K = 1, 5
AODER = ZERO
IF (K.EQ.J) AODER = ONE
A (JJ, K) = AAXISP(2, J, K) * D2P2(J) + AAXISP(1, J, K) * D1P2(J) +
1 AODER * D0P2(J)
B (JJ, K) = AODER * E0P2(J)

```

C
C
C
C
C

```

PIP04330
PIP04340
PIP04350
PIP04360
PIP04370
PIP04380
PIP04390
PIP04400
PIP04410
PIP04420
PIP04430
PIP04440
PIP04450
PIP04460
PIP04470
PIP04480
PIP04490
PIP04500
PIP04510
PIP04520
PIP04530
PIP04540
PIP04550
PIP04560
PIP04570
PIP04580
PIP04590
PIP04600
PIP04610
PIP04620
PIP04630
PIP04640
PIP04650
PIP04660
PIP04670
PIP04680
PIP04690
PIP04700
PIP04710
PIP04720
PIP04730
PIP04740
PIP04750
PIP04760
PIP04770
PIP04780
PIP04790
PIP04800

```



```

270 CONTINUE
DO 275 J = 3, MP
JJ = J + MESH
DO 275 K = 1, 5
L = J - 3 + K
AORDER = ZERO
IF (L.EQ.J) AORDER = ONE
A(JJ,L) = A2DERP(K)*D2P2(J) + A1DERP(K)*D1P2(J) + AORDER*D0P2(J)
B(JJ,L) = AORDER*E0P2(J)
275 CONTINUE
DO 280 J = 1, 2
LL = J + MP
LL = L + MESH
DO 280 K = 1, 5
N = MMP + K
AORDER = ZERO
IF (N.EQ.L) AORDER = ONE
A(LL,N) = AALLP(2,J,K)*D2P2(L) + AALLP(1,J,K)*D1P2(L) +
1 AORDER*D0P2(L)
B(LL,N) = AORDER*E0P2(L)
280 CONTINUE
C
C
C
C
C
A AND B MATRIX ELEMENTS IN TERMS OF Q(R)
SECOND EQUATION FOURTH QUADRANT
DO 285 J = 1, 3
JJ = J + MESH
DO 285 K = 1, 6
KK = K + MESH
AORDER = ZERO
IF (K.EQ.J) AORDER = ONE
A(JJ,KK) = AAXISQ(4,J,K)*D4Q2(J) + AAXISQ(3,J,K)*D3Q2(J) +
1 AAXISQ(2,J,K)*D2Q2(J) + AAXISQ(1,J,K)*D1Q2(J) +
2 AORDER*D0Q2(J)
B(JJ,KK) = AAXISQ(2,J,K)*E2Q2(J) + AAXISQ(1,J,K)*E1Q2(J) +
1 AORDER*E0Q2(J)
285 CONTINUE
DO 290 J = 4, M
JJ = J + MESH
DO 290 K = 1, 7
L = J - 4 + K
LL = L + MESH
AORDER = ZERO
IF (L.EQ.J) AORDER = ONE
A(JJ,LL) = A4DERQ(K)*D4Q2(J) + A3DERQ(K)*D3Q2(J) +
1 A2DERQ(K)*D2Q2(J) + A1DERQ(K)*E1Q2(J) +
2 A2DERQ(K)*E2Q2(J)
B(JJ,LL) = A2DERQ(K)*E2Q2(J) + AORDER*D0Q2(J) +
1 AORDER*E0Q2(J)
PIP04810
PIP04820
PIP04830
PIP04840
PIP04850
PIP04860
PIP04870
PIP04880
PIP04890
PIP04900
PIP04910
PIP04920
PIP04930
PIP04940
PIP04950
PIP04960
PIP04970
PIP04980
PIP04990
PIP05000
PIP05010
PIP05020
PIP05030
PIP05040
PIP05050
PIP05060
PIP05070
PIP05080
PIP05090
PIP05100
PIP05110
PIP05120
PIP05130
PIP05140
PIP05150
PIP05160
PIP05170
PIP05180
PIP05190
PIP05200
PIP05210
PIP05220
PIP05230
PIP05240
PIP05250
PIP05260
PIP05270
PIP05280

```



```

C      OUTPUT THE EIGENVECTOR CORRESPONDING TO THE LEAST STABLE
C      EIGENVALUE, GAMMA*.
C
      DO 400 I = 1, MESH
      II = I + MESH
      P(I) = EIGVEC(I, NGAM)
      Q(I) = EIGVEC(II, NGAM)
      CONTINUE
400  WRITE(6, 401) EIGVAL(NGAM), EIGVECTOR CORRESPONDING TO', 2D27.18, /)
401  FORMAT('X, // 5X, THE LEAST STABLE EIGENVALUE, GAMMA* =', 2D27.18, /)
      DO 402 I = 1, MESH
      II = I + MESH
      WRITE(6, 404) I, P(I), I, Q(I)
404  FORMAT(2X, I2, 2D28.18, 2X, I2, 2D23.18)
402  CONTINUE

C      COMPUTATION OF DQ(R)
C
      DO 410 J = 1, 3
      DQ(J) = ZERO
      DO 410 K = 1, 6
      DQ(J) = DQ(J) + (Q(K) * AAXIS2(1, J, K))
410  CONTINUE

      DO 420 J = 4, M
      DQ(J) = ZERO
      DO 420 K = 1, 7
      L = J - 4 + K
      DQ(J) = DQ(J) + (Q(L) * A1DER2(K))
420  CONTINUE

      DO 430 J = 1, 3
      L = J + M
      DQ(L) = ZERO
      DO 430 K = 1, 6
      KK = 7 - K
      N = MM + K
      DQ(L) = DQ(L) + (Q(N) * AVAL2(1, J, K))
430  CONTINUE

      DO 440 I = 1, MESH
      U(I) = (RAD(I) ** 2) * ((FOUR * Q(I)) + (RAD(I) * DQ(I)) -
      SIXING * P(I) * RAD(I))
440  CONTINUE

      REARRANGE DATA FOR PLOT ROUTINE
C

```

PIP06250
 PIP06260
 PIP06270
 PIP06280
 PIP06290
 PIP06300
 PIP06310
 PIP06320
 PIP06330
 PIP06340
 PIP06350
 PIP06360
 PIP06370
 PIP06380
 PIP06390
 PIP06400
 PIP06410
 PIP06420
 PIP06430
 PIP06440
 PIP06450
 PIP06460
 PIP06470
 PIP06480
 PIP06490
 PIP06500
 PIP06510
 PIP06520
 PIP06530
 PIP06540
 PIP06550
 PIP06560
 PIP06570
 PIP06580
 PIP06590
 PIP06600
 PIP06610
 PIP06620
 PIP06630
 PIP06640
 PIP06650
 PIP06660
 PIP06670
 PIP06680
 PIP06690
 PIP06700
 PIP06710
 PIP06720

C

```

M2 = MESH + 2
DO 450 I = 1, MESH
  II = M2 - I
  III = II - 1
  U(II) = U(III)
  RAD(II) = RAD(III)
CONTINUE
450 RAD(1) = ZERO
  RAD(M2) = ONE
  U(1) = ZERO
  U(M2) = ZERO
DO 460 I = 1, M2
  RADR(I) = DREAL(RAD(I))
CONTINUE
460

```

C
C
C
C
C

COMPUTE THE NORMALIZED PERTURBATION VELOCITY AND
NORMALIZED AMPLITUDE AND OUTPUT THE RESULTS.

```

DO 465 I = 1, M2
  UAMP(I) = CDABS(U(I))
CONTINUE
465 AMPMAX = UAMP(1)
  IMAX = 1
DO 470 J = 2, M2
  AMTEMP = UAMP(J)
  IF (AMTEMP .GT. AMPMAX) GO TO 471
  AMPMAX = UAMP(J)
  IMAX = J
CONTINUE
471 CONTINUE
470

```

```

WRITE(6,472)
472 FORMAT(1X,23X,'NORMALIZED PERTURBATION VELOCITY',
1 24X,'NORMALIZED AMPLITUDE',/)
DO 475 K = 1, M2
  UAMNOR(K) = UAMP(K) / AMPMAX
  AMPNOR(K) = UAMNOR(K)
  UNORM(K) = U(K) / U(IMAX)
  URDP(K) = DREAL(UNORM(K))
  UR(K) = URDP(K)
  UIDP(K) = DIMAG(UNORM(K))
  UI(K) = UIDP(K)
  KK = K - 1
WRITE(6,466) KK, URDP(K), UIDP(K), UAMNOR(K)
466 FORMAT(1X,13,1X,2030.18,5X,D30.18)
475 CONTINUE

```

C

PIP067730
 PIP067740
 PIP067750
 PIP067760
 PIP067770
 PIP067780
 PIP067790
 PIP06800
 PIP06810
 PIP06820
 PIP06830
 PIP06840
 PIP06850
 PIP06860
 PIP06870
 PIP06880
 PIP06890
 PIP06900
 PIP06910
 PIP06920
 PIP06930
 PIP06940
 PIP06950
 PIP06960
 PIP06970
 PIP06980
 PIP06990
 PIP07000
 PIP07010
 PIP07020
 PIP07030
 PIP07040
 PIP07050
 PIP07060
 PIP07070
 PIP07080
 PIP07090
 PIP07100
 PIP07110
 PIP07120
 PIP07130
 PIP07140
 PIP07150
 PIP07160
 PIP07170
 PIP07180
 PIP07190
 PIP07200

C*****

PART VIII

PLOT THE NORMALIZED PERTURBATION VELOCITY VS PIPE RADIUS.

```

IPILOT = IPILOT + 1
RMESH = FLOAT(MESH)
ALPLOT = ALPHA
REFLOT = RE
GAMPLT = GAMMAX
CALL PLOTG(RADR,UR,M2,1,1,1,1,1,1,1,0,0,1,0,-1,0,1,0,5,0,5,0)
CALL PLOTG(RADR,UI,M2,2,1,5,1,1,1,1,0,0,1,0,-1,0,1,0,5,0,5,0)
CALL PLOTG(RADR,AMEN,R,M2,3,1,2,1,1,1,0,0,1,0,-1,0,1,0,5,0,5,0)
CALL PLOTG(X1,Y1,2,3,1,0,1,1,1,6,0,1,6,-1,0,1,0,5,0,5,0)
XO = 0.15
YO = 5.6
IF(IPILOT.EQ.4) IPILOT = 1
IF(IPILOT.EQ.2) YO = 12.1
IF(IPILOT.EQ.3) YO = 18.6
CALL TITLE1(XO,YO,RMESH,ALPLOT,REFLOT,GAMPLT)
GO TO 19

```

180 CONTINUE
CALL PLOT(0.0,0.0,999)
STOP
END

SUBROUTINE TITLE1

SUBROUTINE TO WRITE TITLE ON PLOTS

SUBROUTINE TITLE1(XO,YO,RMESH,ALPLOT,REFLOT,GAMPLT)

```

RN = 6.0
YHT = 0.14
CALL NEWPEN(2)
CALL SYMBOL(XO,YO,YHT
1,NORMALIZED PERTURBATION VELOCITY VS RADIUS',0.0,42)
YHT = 0.08
DELY = 0.20
CALL NEWPEN(1)
YO = YO - 0.8
XO = XO + 2.5
XN = XO + .75
CALL SYMBOL(XO,YO,YHT,N = '0.0,9)
CALL NUMBER(XN,YO,YHT,RN,0.0,-1)
YO = YO - DELY

```


PIP07690
PIP07700
PIP07710
PIP07720
PIP07730
PIP07740
PIP07750
PIP07760
PIP07770
PIP07780
PIP07790
PIP07800
PIP07810
PIP07820
PIP07830
PIP07840
PIP07850
PIP07860
PIP07870
PIP07880
PIP07890
PIP07900
PIP07910
PIP07920
PIP07930
PIP07940
PIP07950
PIP07960
PIP07970
PIP07980
PIP07990
PIP08000
PIP08010
PIP08020
PIP08030
PIP08040
PIP08050
PIP08060
PIP08070
PIP08080
PIP08090
PIP08100
PIP08110
PIP08120
PIP08130
PIP08140
PIP08150
PIP08160

```
CALL SYMBOL(XO, YO, YHT, 'MESH' = '0.0,9)
CALL NUMBER(XN, YO, YHT, RMESH, 0.0, -1)
YO = YO - DELY
CALL SYMBOL(XO, YO, YHT, 'ALPHA' = '0.0,9)
CALL NUMBER(XN, YO, YHT, ALPLOT, 0.0, 2)
YO = YO - DELY
CALL SYMBOL(XO, YO, YHT, 'REY NR' = '0.0,9)
CALL NUMBER(XN, YO, YHT, REPLOT, 0.0, 1)
YO = YO - DELY
CALL SYMBOL(XO, YO, YHT, 'GAMMA*' = '0.0,9)
CALL NUMBER(XN, YO, YHT, GAMPLT, 0.0, 4)
YO = YO - 3.4
CALL SYMBOL(XO, YO, YHT, 'OCTAGON' = U(REAL), 0.0, 17)
YO = YO - DELY
CALL SYMBOL(XO, YO, YHT, 'DIAMOND' = U(IMAG), 0.0, 17)
YO = YO - DELY
CALL SYMBOL(XO, YO, YHT, 'TRIANGLE' = U AMPL, 0.0, 17)
```

WRITE THE AXIS LABLES

```
XO = XO - 2.55
YO = YO + 0.3
YHT = 0.12
CALL SYMBOL(XO, YO, YHT, 'NORMALIZED PERTURBATION VELOCITY', 90., 32)
XO = XO + 2.8
YO = YO - 1.0
CALL SYMBOL(XO, YO, YHT, 'PIPE RADIUS', 0.0, 11)
RETURN
END
```

/*
//GO, SYSIN DD *

2 1 5
-0.541666666666665808D+01
-0.244444444444444175D+01
-0.499999999999994837D+00
-0.952380952380948859D-01
-0.925925925925889879D-02
2 2 5
0.17499999999999245D+01
-0.27777777777777590D+01
0.14999999999999178D+01
-0.142857142857139685D+00
0.925925925925875914D-02
1 1 4
0.166666666666665865D+00
0.10000000000000022D+01
-0.29999999999999892D+00
0.476190476190476338D-01

3	1	5	0-198765432098769779D+01
			-0-165289256198352552D+00
			-0-174999999999999751D+02
			-0-111111111111107608D+00
			-0-12000000000001372D+01
			-0-346938775510207395D+00
			-0-432098765432103911D-01
3	2	5	0-134999999999999680D+02
			-0-38888888888888218D+01
			-0-142108547152020037D-13
			-0-551020408163266584D+00
			-0-679012345679017859D-01
3	3	5	-0-155000000000001137D+02
			-0-988888888888891060D+01
			-0-60000000000005323D+01
			-0-144897955183674985D+01
			-0-679012345678990936D-01
2	1	4	-0-466666666666666585D+01
			-0-211111111111111027D+01
			-0-319999999999999993D+00
			-0-340136054421768521D-01
2	2	4	0-9999999999999978584D+00
			-0-244444444444444930D+01
			-0-132000000000000117D+01
			-0-816326530612245110D-01
1	1	3	0-249999999999999883D+01
			-0-222222222222222293D+00
			-0-199999999999999973D-01
1	2	3	-0-450000000000000355D+01
			-0-133333333333333304D+01
			0-180000000000000007D+00
9	0	6	
4	1	6	0-1150000000000000714D+03
			-0-3844444444444450255D+02
			-0-1640000000000003858D+02
			-0-522448979591849794D+01
			-0-112345679012349509D+01
			-0-115702479338847553D+00
4	2	6	-0-2600000000000008029D+02

PI	P08650
PI	P08660
PI	P08670
PI	P08680
PI	P08690
PI	P08700
PI	P08710
PI	P08720
PI	P08730
PI	P08740
PI	P08750
PI	P08760
PI	P08770
PI	P08780
PI	P08790
PI	P08800
PI	P08810
PI	P08820
PI	P08830
PI	P08840
PI	P08850
PI	P08860
PI	P08870
PI	P08880
PI	P08890
PI	P08900
PI	P08910
PI	P08920
PI	P08930
PI	P08940
PI	P08950
PI	P08960
PI	P08970
PI	P08980
PI	P08990
PI	P09000
PI	P09010
PI	P09020
PI	P09030
PI	P09040
PI	P09050
PI	P09060
PI	P09070
PI	P09080
PI	P09090
PI	P09100
PI	P09110
PI	P09120

[illegible]

D. PROGRAM TO COMPUTE THE NONCENTRAL FINITE DIFFERENCE COEFFICIENTS

```

CCE000010
CCE000020
CCE000030
CCE000040
CCE000050
CCE000060
CCE000070
CCE000080
CCE000090
CCE000100
CCE000110
CCE000120
CCE000130
CCE000140
CCE000150
CCE000160
CCE000170
CCE000180
CCE000190
CCE000200
CCE000210
CCE000220
CCE000230
CCE000240
CCE000250
CCE000260
CCE000270
CCE000280
CCE000290
CCE000300
CCE000310
CCE000320
CCE000330
CCE000340
CCE000350
CCE000360
CCE000370
CCE000380
CCE000390
CCE000400
CCE000410
CCE000420
CCE000430
CCE000440
CCE000450
CCE000460
CCE000470
CCE000480

```

```

*****
THIS IS A PROGRAM USED TO COMPUTE THE NONCENTRAL FINITE
DIFFERENCE COEFFICIENTS FOR THE DERIVATIVES OF THE FUNCTIONS
P(R) AND Q(R) FOR THE THREE CASES INVESTIGATED. THE DATA
IS THEN READ INTO THE MAIN INVESTIGATIVE PROGRAMS FOR N = 0,
1 AND 6. THE DATA IS ANNOUNCED AS TO IT'S APPLICATION
DEPENDING ON THE BOUNDARY CONDITIONS AT THE AXIS OR WALL.
THESE ANNOTATIONS SHOULD BE REMOVED BEFORE THE DATA IS USED.
THE PROGRAM IS RUN IN THE VM MODE AND THE DATA IS OUTPUT
TO A FILE ON THE USER'S DISK WITH A FILENAME = COEFF AND
FILETYPE = DATAOUT2. THIS IS ACCOMPLISHED WITH THE USE OF
SPECIAL EXEC FILE CALLED, RUNDATA. THIS EXEC FILE IS
LISTED AT THE END OF THE COEFFICIENT PROGRAM. THE PROPER
COMMAND TO RUN THE PROGRAM IS, RUNDATA COEFF T.
*****
REAL*8 A6(6,6), FACT, H(6), XJ, XI, A6INV(6,6), WKAREA(60)
REAL*8 A5(5,5), A4(4,4), A5INV(5,5), A4INV(4,4), A3(3,3), A3INV(3,3)
REAL*8 C(3,4,6), C4X62(4,6), C4X63(4,6)
REAL*8 C4X61(4,5), C4X52(4,5), C4X53(4,5)
REAL*8 C4X51(3,5), C3X52(3,5), C3X53(3,5)
REAL*8 C4X41(4,4), C4X42(4,4), C4X43(4,4)
REAL*8 C2X41(2,4), C2X42(2,4), C2X43(2,4)
REAL*8 C3X31(3,3), C3X32(3,3), C3X33(3,3)
REAL*8 C1X31(1,3), C1X32(1,3), C1X33(1,3)
REAL*8 C46A6(4,6), C46A62(4,5), C46A63(4,6)
REAL*8 C45A5(4,5), C45A52(4,5), C45A53(4,5)
REAL*8 C44A4(4,4), C44A42(4,4), C44A43(4,4)
REAL*8 C24A4(2,4), C24A42(2,4), C24A43(2,4)
REAL*8 C33A3(3,3), C33A32(3,3), C33A33(3,3)
REAL*8 C13A3(1,3), C13A32(1,3), C13A33(1,3)
REAL*8 C2X51(2,5), C2X52(2,5), C2X53(2,5)

```


CCE000490
 CCE000500
 CCE000510
 CCE000520
 CCE000530
 CCE000540
 CCE000550
 CCE000560
 CCE000570
 CCE000580
 CCE000590
 CCE000600
 CCE000610
 CCE000620
 CCE000630
 CCE000640
 CCE000650
 CCE000660
 CCE000670
 CCE000680
 CCE000690
 CCE000700
 CCE000710
 CCE000720
 CCE000730
 CCE000740
 CCE000750
 CCE000760
 CCE000770
 CCE000780
 CCE000790
 CCE000800
 CCE000810
 CCE000820
 CCE000830
 CCE000840
 CCE000850
 CCE000860
 CCE000870
 CCE000880
 CCE000890
 CCE000900
 CCE000910
 CCE000920
 CCE000930
 CCE000940
 CCE000950
 CCE000960

REAL*8 C1X41{1,4}, C1X42{1,4}
 REAL*8 C25A51{2,5}, C25A52{2,5}
 REAL*8 C14A41{1,4}, C14A42{1,4}

THE AA MATRICES ARE 6 X 6, 5 X 5, 4 X 4 & 3 X 3 AND ARE
 CALLED A6,A5,A4 & A3, RESPECTIVELY.

```

DO 10 I=1,6
  FACT = 1.0D0
  XI = DFLOAT(I)
  H(I) = (2.0D0*XI-1.0D0)/2.0D0
  DO 10 J=1,6
    XJ = DFLOAT(J)
    FACT = FACT*(XJ+1.0D0)
  A6(I,J) = (H(I)**(J+1))/FACT
10 CONTINUE
20 FORMAT(1X, D29.18)
  
```

A SUBPROGRAM USED TO COMPUTE THE NONCENTRAL DIFFERENCE
 COEFFICIENTS THE AXIS FOR N = 0.

THE APPLICABLE BOUNDARY CONDITIONS ARE:

DQ(0) = 0 AND D3Q(0) = 0 FOR N = 0 AT THE AXIS.

COMPUTE THE AA MATRICES AND THEIR INVERSES.

```

DO 11 I = 1,6
  A6(I,2) = A6(I,1)
  A6(I,1) = 1.0D0
11 CONTINUE
  CALL LINV2F(A6,6,6,A5INV,10,WKAREA,IER)
DO 150 I = 1,5
  DO 150 J = 1,5
    A5(I,J) = A6(I,J)
150 CONTINUE
  CALL LINV2F(A5,5,5,A5INV,10,WKAREA,IER)
DO 170 I = 1,4
  DO 170 J = 1,4
    A4(I,J) = A6(I,J)
170 CONTINUE
  CALL LINV2F(A4,4,4,A4INV,10,WKAREA,IER)
  
```



```

DO 171 I = 1,3
DO 171 J = 1,3
A3(I,J) = A6(I,J)
171 CONTINUE
CALL LINV2F(A3,3,3,A3INV,10,WKAREA,IER)
C
C      COMPUTE THE CC MATRICES FOR APPROPRIATE POINTS.
C
DO 310 K = 1,3
XK = DFLOAT(K)
H(K) = (2.0D0*XK - 1.0D0)/2.0D0
C {K,2,1} = 1.0D0
C {K,3,1} = 0.0D0
C {K,4,1} = 0.0D0
C {K,3,2} = 1.0D0
C {K,4,2} = 0.0D0
C {K,4,3} = 1.0D0
KK = 6
K6 = 6
DO 330 I = 1,4
DO 325 J = 1, K6
JK = J+KK
XJ = DFLOAT(J)
FACT = FACT*XJ
C(K,I,JK) = (H(K)**J)/FACT
325 CONTINUE
KK = KK+1
K6 = K6+1
330 CONTINUE
DO 331 K = 1,3
DO 331 I = 1,4
C {K,I,1} = 0.0D0
331 CONTINUE
C
C      CONVERT THE 3 DIMENSIONAL CC MATRICES TO APPROPRIATE 2
C      DIMENSIONAL MATRICES.
C
DO 200 I = 1,4
DO 200 J = 1,6
C4X61(I,J) = C(1,I,J)
CONTINUE
DO 201 I = 1,4
DO 201 J = 1,6
C4X62(I,J) = C(2,I,J)
200

```

```

CCE00970
CCE00980
CCE00990
CCE01000
CCE01010
CCE01020
CCE01030
CCE01040
CCE01050
CCE01060
CCE01070
CCE01080
CCE01090
CCE01100
CCE01110
CCE01120
CCE01130
CCE01140
CCE01150
CCE01160
CCE01170
CCE01180
CCE01190
CCE01200
CCE01210
CCE01220
CCE01230
CCE01240
CCE01250
CCE01260
CCE01270
CCE01280
CCE01290
CCE01300
CCE01310
CCE01320
CCE01330
CCE01340
CCE01350
CCE01360
CCE01370
CCE01380
CCE01390
CCE01400
CCE01410
CCE01420
CCE01430
CCE01440

```



```

201 CONTINUE = 1,4
DO 202 I = 1,6
DO 202 J = 1,6
C4X63(I,J) = C(3,I,J)
202 CONTINUE = 1,4
DO 203 I = 1,5
DO 203 J = 1,5
C4X51(I,J) = C4X61(I,J)
203 CONTINUE = 1,4
DO 204 I = 1,4
DO 204 J = 1,4
C4X41(I,J) = C4X61(I,J)
204 CONTINUE = 1,3
DO 220 I = 1,3
DO 220 J = 1,3
C3X31(I,J) = C4X61(I,J)
220 CONTINUE = 1,4
DO 205 I = 1,4
DO 205 J = 1,5
C4X52(I,J) = C4X62(I,J)
205 CONTINUE = 1,4
DO 206 I = 1,4
DO 206 J = 1,4
C4X42(I,J) = C4X62(I,J)
206 CONTINUE = 1,3
DO 208 I = 1,3
DO 208 J = 1,3
C3X32(I,J) = C4X62(I,J)
208 CONTINUE = 1,4
DO 207 I = 1,4
DO 207 J = 1,5
C4X53(I,J) = C4X63(I,J)
207 CONTINUE

```

CC PRE-MULTIPLY THE PROPER AA INVERSE MATRIX BY THE PROPER
CC MATRIX FOR POINTS NEAR THE BOUNDARIES AS REQUIRED.

```

CALL VMULFF(C4X61,A5INV,4,6,6,4,6,6,4,6,6,C46A61,4,IER)
CALL VMULFF(C4X62,A5INV,4,6,6,4,6,6,4,6,6,C46A62,4,IER)
CALL VMULFF(C4X63,A5INV,4,6,6,4,6,6,4,6,6,C46A63,4,IER)
CALL VMULFF(C4X51,A5INV,4,5,5,4,5,5,4,5,5,C45A51,4,IER)
CALL VMULFF(C4X52,A5INV,4,5,5,4,5,5,4,5,5,C45A52,4,IER)
CALL VMULFF(C4X53,A5INV,4,5,5,4,5,5,4,5,5,C45A53,4,IER)
CALL VMULFF(C4X41,A4INV,4,4,4,4,4,4,4,4,4,C44A41,4,IER)
CALL VMULFF(C4X42,A4INV,4,4,4,4,4,4,4,4,4,C44A42,4,IER)
CALL VMULFF(C3X31,A3INV,3,3,3,3,3,3,3,3,3,C33A31,3,IER)
CALL VMULFF(C3X32,A3INV,3,3,3,3,3,3,3,3,3,C33A32,3,IER)

```

CC
CC
CC
CC


```

WRITE(2,210)
WRITE(2,209)
209 FORMAT(1X, 'NONCENTRAL FINITE DIFFERENCE COEFFICIENTS THAT ARE REQUIRED FOR N = 0. ', //, 1X,
1 'FIRING NEAR THE AXIS FOR N = 0. ', //, 1X,
2 'THE COEFFICIENTS APPEAR IN THE MAIN PROGRAM, EXCLUDING COMMENTS. ', //, 1X,
3 'FORMAT REQUIRED BY THE MAIN PROGRAM ARE: ', //, 1X,
4 'THE APPLICABLE BOUNDARY CONDITIONS ARE: ', //, 1X,
5 'DQ(0) = 0 AND D3Q(0) = 0 FOR N = 0 AT THE AXIS. ')
WRITE(2,210)
210 FORMAT(1X, //)
ND = 4
NP = 1
NPTS = 6
WRITE(2,221) ND, NP, NPTS
FORMAT(11, 1X, I1, 1X, I1)
WRITE(2,226) (C46A61(4, J), J=1, NPTS)
NP = NP + 1
WRITE(2,221) ND, NP, NPTS
WRITE(2,220) (C46A62(4, J), J=1, NPTS)
NP = NP + 1
WRITE(2,221) ND, NP, NPTS
WRITE(2,220) (C46A63(4, J), J=1, NPTS)
ND = 3
NP = 1
NPTS = 1
WRITE(2,221) ND, NP, NPTS
WRITE(2,220) (C45A51(3, J), J=1, NPTS)
NP = NP + 1
WRITE(2,221) ND, NP, NPTS
WRITE(2,220) (C45A52(3, J), J=1, NPTS)
NP = NP + 1
WRITE(2,221) ND, NP, NPTS
WRITE(2,220) (C45A53(3, J), J=1, NPTS)
ND = 1
NPTS = 1
WRITE(2,221) ND, NP, NPTS
WRITE(2,220) (C44A41(2, J), J=1, NPTS)
NP = NP + 1
WRITE(2,221) ND, NP, NPTS
WRITE(2,220) (C44A42(2, J), J=1, NPTS)
ND = 1
NP = 1
NPTS = 1
WRITE(2,221) ND, NP, NPTS
WRITE(2,220) (C33A31(1, J), J=1, NPTS)
NP = NP + 1
WRITE(2,221) ND, NP, NPTS

```



```

CCE02410
CCE02420
CCE02430
CCE02440
CCE02450
CCE02460
CCE02470
CCE02480
CCE02490
CCE02500
CCE02510
CCE02520
CCE02530
CCE02540
CCE02550
CCE02560
CCE02570
CCE02580
CCE02590
CCE02600
CCE02610
CCE02620
CCE02630
CCE02640
CCE02650
CCE02660
CCE02670
CCE02680
CCE02690
CCE02700
CCE02710
CCE02720
CCE02730
CCE02740
CCE02750
CCE02760
CCE02770
CCE02780
CCE02790
CCE02800
CCE02810
CCE02820
CCE02830
CCE02840
CCE02850
CCE02860
CCE02870
CCE02880

WRITE(2,20) (C33A32(1,J),J=1,NPTS)
ND = 0
NP = 0
NPTS = 0
WRITE(2,221) ND,NP,NPTS
WRITE(2,225){COEFFICIENTS TO APPROXIMATE Q(0) FOR N = 0. TAKEN',
225 1, FROM THE TOP ROW OF THE A6INV MATRIX.'}
WRITE(2,20) (A6INV(1,J),J=1,5)
*****
C A MODIFIED SUBPROGRAM TO COMPUTE AA MATRIX ELEMENTS FOR
C THE BOUNDARY CONDITIONS NEAR THE AXIS AND THE WALL FOR
C N = 0, 1 AND 6. THE APPLICABLE BOUNDARY CONDITIONS ARE:
C Q(1) = 0 AND DQ(1) = 0 FOR N = 0 AT THE WALL.
C Q(0) = VARIABLE AND DQ(0) = 0 FOR N = 1 AT THE AXIS.
C Q(1) = -H(0) AND DQ(0) = 2H(0) FOR N = 1 AT THE WALL.
C Q(0) = 0 AND DQ(0) = 0 FOR N = 6 AT THE AXIS.
C Q(1) = 0 AND DQ(1) = 0 FOR N = 6 AT THE WALL.
*****
C COMPUTE THE AA MATRICES AND THEIR INVERSES.
DO 400 I=1,6
FACT = 1.0D0
XI = DFLOAT(I)
H(I) = (2.0D0*XI-1.0D0)/2.0D0
DO 400 J=1,6
XJ = DFLOAT(J)
FACT = FACT*(XJ+1.0D0)
A6(I,J) = (H(I)**(J+1))/FACT
400 CONTINUE
CALL LINV2F(A6,6,6,A5INV,10,WKAREA,IER)
DO 401 I = 1,5
DO 401 J = 1,5
A5(I,J) = A6(I,J)
401 CONTINUE
CALL LINV2F(A5,5,5,A5INV,10,WKAREA,IER)
DO 402 I = 1,4

```


CE02890
 CE02900
 CE02910
 CE02920
 CE02930
 CE02940
 CE02950
 CE02960
 CE02970
 CE02980
 CE02990
 CE03000
 CE03010
 CE03020
 CE03030
 CE03040
 CE03050
 CE03060
 CE03070
 CE03080
 CE03090
 CE03100
 CE03110
 CE03120
 CE03130
 CE03140
 CE03150
 CE03160
 CE03170
 CE03180
 CE03190
 CE03200
 CE03210
 CE03220
 CE03230
 CE03240
 CE03250
 CE03260
 CE03270
 CE03280
 CE03290
 CE03300
 CE03310
 CE03320
 CE03330
 CE03340
 CE03350
 CE03360

```

DO 402 J = 1,4
A4(I,J) = A6(I,J)
CONTINUE
CALL LINV2F(A4,4,4,A+INV,10,WKAREA,IER)
DO 403 I = 1,3
DO 403 J = 1,3
A3(I,J) = A6(I,J)
CONTINUE
CALL LINV2F(A3,3,3,A3INV,10,WKAREA,IER)

C
C      COMPUTE THE CC COEFFICIENT MATRICES FOR APPROPRIATE POINTS.
C
DO 405 K = 1,3
XK = DFLOAT(K)
H(K) = (2.0D0*XK - 1.0D0)/2.0D0
C{K,2,1} = 1.0D0
C{K,3,1} = 0.0D0
C{K,4,1} = 0.0D0
C{K,3,2} = 1.0D0
C{K,4,2} = 0.0D0
C{K,4,3} = 1.0D0
KK = 0
KK6 = 6
DO 406 I = 1,4
FACT = 1.0D0
DO 407 J = 1,K6
J = J+KK
XJ = DFLOAT(J)
FACT = FACT*XJ
C(K,I,JK) = (H(K)**J)/FACT
CONTINUE
KK = KK+1
K6 = K6-1
CONTINUE
CONTINUE

C
C      CONVERT THE 3 DIMENSIONAL CC MATRICES TO APPROPRIATE 2
C      DIMENSIONAL MATRICES.
C
DO 408 I = 1,4
DO 408 J = 1,6
C4X61(I,J) = C(1,I,J)
CONTINUE
DO 409 I = 1,4
DO 409 J = 1,6
C4X62(I,J) = C(2,I,J)
CONTINUE
  
```



```

03370
0E03380
0E03390
0E03400
0E03410
0E03420
0E03430
0E03440
0E03450
0E03460
0E03470
0E03480
0E03490
0E03500
0E03510
0E03520
0E03530
0E03540
0E03550
0E03560
0E03570
0E03580
0E03590
0E03600
0E03610
0E03620
0E03630
0E03640
0E03650
0E03660
0E03670
0E03680
0E03690
0E03700
0E03710
0E03720
0E03730
0E03740
0E03750
0E03760
0E03770
0E03780
0E03790
0E03800
0E03810
0E03820
0E03830
0E03840

```

```

4 10 DO 410 I = 1, 4
      DO 410 J = 1, 6
      C4X63(I, J) = C(3, I, J)
      CONTINUE
4 11 DO 411 I = 1, 3
      DO 411 J = 1, 5
      C3X51(I, J) = C4X61(I, J)
      CONTINUE
4 12 DO 412 I = 1, 2
      DO 412 J = 1, 4
      C2X41(I, J) = C4X61(I, J)
      CONTINUE
4 13 DO 413 I = 1, 3
      DO 413 J = 1, 3
      C1X31(I, J) = C4X61(I, J)
      CONTINUE
4 14 DO 414 I = 1, 3
      DO 414 J = 1, 5
      C3X52(I, J) = C4X62(I, J)
      CONTINUE
4 15 DO 415 I = 1, 2
      DO 415 J = 1, 4
      C2X42(I, J) = C4X62(I, J)
      CONTINUE
4 16 DO 416 I = 1, 3
      DO 416 J = 1, 3
      C1X32(I, J) = C4X62(I, J)
      CONTINUE
4 17 DO 417 I = 1, 3
      DO 417 J = 1, 5
      C3X53(I, J) = C4X63(I, J)
      CONTINUE

```

CC CC CC CC PRE-MULTIPLY THE PROPER AA INVERSE MATRIX BY THE PROPER

CC MATRIX FOR POINTS NEAR THE BOUNDARIES AS REQUIRED.

```

      CALL VMULFF(C4X61, A5INV, 4, 6, 6, 4, 6, 4, 6, C46A61, 4, IER)
      CALL VMULFF(C4X62, A6INV, 4, 6, 6, 4, 6, 4, 6, C46A62, 4, IER)
      CALL VMULFF(C4X63, A5INV, 4, 6, 6, 4, 6, 4, 6, C46A63, 4, IER)
      CALL VMULFF(C3X51, A5INV, 3, 5, 5, 3, 5, 3, 5, C35A51, 3, IER)
      CALL VMULFF(C3X52, A5INV, 3, 5, 5, 3, 5, 3, 5, C35A52, 3, IER)
      CALL VMULFF(C3X53, A5INV, 3, 5, 5, 3, 5, 3, 5, C35A53, 3, IER)
      CALL VMULFF(C2X41, A4INV, 2, 4, 4, 2, 4, 4, 2, C24A41, 2, IER)
      CALL VMULFF(C2X42, A4INV, 2, 4, 4, 2, 4, 4, 2, C24A42, 2, IER)
      CALL VMULFF(C1X31, A3INV, 1, 3, 3, 1, 3, 3, 1, 3, C13A31, 1, IER)
      CALL VMULFF(C1X32, A3INV, 1, 3, 3, 1, 3, 3, 1, 3, C13A32, 1, IER)
      WRITE(2, 419)
      FORMAT(2, 418)
4 19 WRITE(2, 418)

```



```

418 FORMAT(1X,'NONCENTRAL FINITE DIFFERENCE COEFFICIENTS THAT ARE REQUIRED',
1 FIED NEAR THE BOUNDARIES FOR N = 0, 1 AND 5.',///,1X,
2 THE COEFFICIENTS APPEAR IN THE ',
3 FORMAT REQUIRED BY THE MAIN PROGRAM, EXCLUDING COMMENTS.',///,1X,
4 THE APPLICABLE BOUNDARY CONDITIONS ARE: ',///,1X,
5 Q(1) = 0 AND DQ(1) = 0 FOR N = 0 AT THE WALL.',///,1X,
6 Q(0) = 0 AND DQ(0) = 0 FOR N = 1 AT THE AXIS.',///,1X,
7 Q(1) = 0 AND DQ(1) = 0 FOR N = 1 AT THE WALL.',///,1X,
8 Q(0) = 0 AND DQ(0) = 0 FOR N = 6 AT THE AXIS.',///,1X,
9 Q(1) = 0 AND DQ(1) = 0 FOR N = 6 AT THE WALL.',///,
ND = 1
NP = 1
NPTS = 6
WRITE(2,20)
(C46A61(4,J), J=1, NPTS)
NP = NP + 1
WRITE(2,20)
(C46A62(4,J), J=1, NPTS)
NP = NP + 1
WRITE(2,20)
(C46A63(4,J), J=1, NPTS)
ND = 1
NP = 1
NPTS = 1
WRITE(2,20)
(C35A51(3,J), J=1, NPTS)
NP = NP + 1
WRITE(2,20)
(C35A52(3,J), J=1, NPTS)
NP = NP + 1
WRITE(2,20)
(C35A53(3,J), J=1, NPTS)
ND = 1
NP = 1
NPTS = 1
WRITE(2,20)
(C24A41(2,J), J=1, NPTS)
NP = NP + 1
WRITE(2,20)
(C24A42(2,J), J=1, NPTS)
ND = 1
NP = 1
NPTS = 1
WRITE(2,20)
(C13A31(1,J), J=1, NPTS)
NP = NP + 1
WRITE(2,20)
(C13A32(1,J), J=1, NPTS)

```



```

ND = 9
NP = 0
NPTS = 0
WRITE(2,221) ND,NP,NPTS
WRITE(2,220)
420 1 FORMAT(1X,COEFFICIENTS TO APPROXIMATE D22(0) FOR N = 1.,
1 TAKEN FROM THE FIRST ROW OF THE A6INV MATRIX.)
WRITE(2,20) (A6INV(1,J),J=1,6)
*****
      A SUBPROGRAM USED TO COMPUTE THE NONCENTRAL FINITE
      DIFFERENCE COEFFICIENTS FOR THE DERIVATIVES OF P(R) AT
      POINTS NEAR THE BOUNDARIES.  COMPUTE THE AA MATRIX ELEMENTS
      FOR THE BOUNDARY CONDITIONS NEAR THE AXIS AND WALL.
      THE APPLICABLE BOUNDARY CONDITIONS FOR N = 1 AND 6 ARE:
      P(1) = I H(0), A VARIABLE, FOR N = 1 AT THE WALL.
      P(0) = 0 FOR N = 6 AT THE AXIS.
      P(1) = 0 FOR N = 6 AT THE WALL.
*****
      COMPUTE THE AA MATRICES AND THEIR INVERSES.
      DO 500 I=1,5
      FACT = 1.0DO
      XI = DFLOAT(I)
      H(I) = (2.0DO*XI-1.0DO)/2.0DO
      DO 500 J=1,5
      XJ = DFLOAT(J)
      FACT = FACT*XJ
      A5(I,J) = (H(I)**J)/FACT
500 CONTINUE
      CALL LINV2F(A5,5,5,A5INV,10,WKAREA,IER)
      DO 501 I = 1,4
      DO 501 J = 1,4
      A4(I,J) = A5(I,J)
501 CONTINUE
      CALL LINV2F(A4,4,4,A4INV,10,WKAREA,IER)
      COMPUTE THE CC COEFFICIENT MATRICES FOR APPROPRIATE POINTS.

```


C

```

C2X51(1,1) = 1.0D0
C2X51(2,1) = 0.0D0
FACT = 1.0D0
DO 502 J = 2,5
  XJ = DFLOAT(J)
  FACT = FACT*(XJ-1.0D0)
C2X51(1,J) = (H(1)**(J-1))/FACT
CONTINUE
DO 503 J = 2,5
  JJ = J-1
  C2X51(2,J) = C2X51(1,JJ)
CONTINUE
DO 504 J = 1,4
  C1X41(1,J) = C2X51(1,J)
CONTINUE
C2X52(1,1) = 1.0D0
C2X52(2,1) = 0.0D0
FACT = 1.0D0
DO 505 J = 2,5
  XJ = DFLOAT(J)
  FACT = FACT*(XJ-1.0D0)
C2X52(1,J) = (H(2)**(J-1))/FACT
CONTINUE
DO 506 J = 2,5
  JJ = J-1
  C2X52(2,J) = C2X52(1,JJ)
CONTINUE
DO 507 J = 1,4
  C1X42(1,J) = C2X52(1,J)
CONTINUE

```

PRE-MULTIPLY THE PROPER AA INVERSE MATRIX BY THE PROPER

CC MATRIX FOR POINTS NEAR THE BOUNDARIES AS REQUIRED.

```

CALL VMULFF(C2X51,A5INV,2,5,5,2,5,C25A51,2,IER)
CALL VMULFF(C2X52,A5INV,2,5,5,2,5,C25A52,2,IER)
CALL VMULFF(C1X41,A4INV,1,4,4,1,4,C14A41,1,IER)
CALL VMULFF(C1X42,A4INV,1,4,4,1,4,C14A42,1,IER)
WRITE(2,508)
FORMAT(1X,/)
WRITE(2,509)

```

```

508 FORMAT(1X,/)
509 FORMAT(1X,/)
1. NONCENTRAL FINITE DIFFERENCE COEFFICIENTS THAT ARE REQUIRED
2. THE BOUNDARIES FOR N = 1 AND 6. , , , 1X,
3. THE COEFFICIENTS APPEAR IN THE PROGRAM, EXCLUDING COMMENTS. , , , 1X,
4. THE APPLICABLE BOUNDARY CONDITIONS FOR N = 1 AND 6 ARE: , , , 1X,

```

```

CCE0481D
CCE0482D
CCE0483D
CCE0484D
CCE0485D
CCE0486D
CCE0487D
CCE0488D
CCE0489D
CCE0490D
CCE0491D
CCE0492D
CCE0493D
CCE0494D
CCE0495D
CCE0496D
CCE0497D
CCE0498D
CCE0499D
CCE0500D
CCE0501D
CCE0502D
CCE0503D
CCE0504D
CCE0505D
CCE0506D
CCE0507D
CCE0508D
CCE0509D
CCE0510D
CCE0511D
CCE0512D
CCE0513D
CCE0514D
CCE0515D
CCE0516D
CCE0517D
CCE0518D
CCE0519D
CCE0520D
CCE0521D
CCE0522D
CCE0523D
CCE0524D
CCE0525D
CCE0526D
CCE0527D
CCE0528D

```



```

CCE05290
CCE05300
CCE05310
CCE05320
CCE05330
CCE05340
CCE05350
CCE05360
CCE05370
CCE05380
CCE05390
CCE05400
CCE05410
CCE05420
CCE05430
CCE05440
CCE05450
CCE05460
CCE05470
CCE05480
CCE05490
CCE05500
CCE05510
CCE05520
CCE05530
CCE05540
CCE05550
CCE05560
CCE05570
CCE05580
CCE05590
CCE05600
CCE05610
CCE05620
CCE05630
CCE05640
CCE05650
CCE05660
CCE05670
CCE05680
CCE05690
CCE05700
CCE05710
CCE05720
CCE05730
CCE05740
CCE05750
CCE05760

```

```

5.P{1} = I H(0) A VARIABLE FOR N = 1 AT THE WALL.,//,1X,
6.P{0} = 0 FOR N = 5 AT THE AXIS.,//,1X,
7.P{1} = 0 FOR N = 5 AT THE WALL.,//,

```

```

ND = 2
NP = 1
NPTS = 5
WRITE(2,221) ND,NP,NPTS
WRITE(2,20) (C25A51(2,J),J=1,NPTS)
NP = NP + 1
WRITE(2,221) ND,NP,NPTS
WRITE(2,20) (C25A52(2,J),J=1,NPTS)
ND = 1
NPTS = 1
WRITE(2,221) ND,NP,NPTS
WRITE(2,20) (C14A41(1,J),J=1,NPTS)
NP = NP + 1
WRITE(2,221) ND,NP,NPTS
WRITE(2,20) (C14A42(1,J),J=1,NPTS)
ND = 0
NPTS = 0
WRITE(2,221) ND,NP,NPTS

```

```

C*****
C A SUBPROGRAM USED TO COMPUTE THE AA MATRIX ELEMENTS FOR
C THE BOUNDARY CONDITIONS NEAR THE AXIS FOR N = 1.
C THE APPLICABLE BOUNDARY CONDITION IS:
C DP(0) = 0 FOR N = 1 AT THE AXIS.
C*****

```

```

C*****
C DO 600 I = 1,5
C A5(I,1) = 1.0D0
C CONTINUE
C 600
C DO 601 I = 1,4
C A4(I,1) = 1.0D0
C CONTINUE
C C2X51(1,1) = 0.0D0
C C2X52(1,1) = 0.0D0
C C1X41(1,1) = 0.0D0
C C1X42(1,1) = 0.0D0
C CALL LINV2F(A5,5,5,A5 INV,10,WKAREA,IER)
C CALL LINV2F(A4,4,4,A4 INV,10,WKAREA,IER)
C*****

```



```

C      PRE-MULTIPLY THE PROPER AA INVERSE MATRIX BY THE PROPER
C      CC MATRIX FOR POINTS NEAR THE BOUNDARIES AS REQUIRED.
C
      CALL VMULFF(C2X51,A5INV,2,5,5,2,5,C25A51,2,IER)
      CALL VMULFF(C2X52,A5INV,2,5,5,2,5,C25A52,2,IER)
      CALL VMULFF(C1X41,A4INV,1,4,4,1,4,C14A41,1,IER)
      CALL VMULFF(C1X42,A4INV,1,4,4,1,4,C14A42,1,IER)
      WRITE(2,605)
      FORMAT(1X,/)
505  WRITE(2,606)
      FORMAT(1X, NONCENTRAL FINITE DIFFERENCE COEFFICIENTS THAT ARE REQUIRED
      1 1. THE AXIS FOR N = 1, //, 1X,
      2 2. THE COEFFICIENTS APPEAR IN THE
      3 3. FORMAT REQUIRED BY THE MAIN PROGRAM, EXCLUDING COMMENTS., //, 1X,
      4 4. THE APPLICABLE BOUNDARY CONDITION IS: //, 1X,
      5 5. DP(0) = 0 FOR N = 1 AT THE AXIS., //)
      ND = 1
      NP = 1
      NPTS = 5
      WRITE(2,221) ND,NP,NPTS
      WRITE(2,20) (C25A51(2,J),J=1,NPTS)
      NP = NP + 1
      WRITE(2,221) ND,NP,NPTS
      WRITE(2,20) (C25A52(2,J),J=1,NPTS)
      ND = 1
      NP = 1
      NPTS = NPTS - 1
      WRITE(2,221) ND,NP,NPTS
      WRITE(2,20) (C14A41(1,J),J=1,NPTS)
      NP = NP + 1
      WRITE(2,221) ND,NP,NPTS
      WRITE(2,20) (C14A42(1,J),J=1,NPTS)
      ND = 0
      NP = 0
      NPTS = 0
      WRITE(2,221) ND,NP,NPTS
      WRITE(2,615)
      FORMAT(1X, COEFFICIENTS TO APPROXIMATE P(J) FOR N = 1.,
      1 1. TAKEN FROM THE FIRST ROW OF THE A5INV MATRIX.,)
      WRITE(2,20) (A5INV(1,J),J=1,5)
      WRITE(2,616)
      FORMAT(1X, COEFFICIENTS TO APPROXIMATE D2P(0) FOR N = 1.,
      1 1. TAKEN FROM THE SECOND ROW OF THE A5INV MATRIX.,)
      WRITE(2,20) (A5INV(2,J),J=1,5)
      STOP
      END

```

```

CCE05770
CCE05780
CCE05790
CCE05800
CCE05810
CCE05820
CCE05830
CCE05840
CCE05850
CCE05860
CCE05870
CCE05880
CCE05890
CCE05900
CCE05910
CCE05920
CCE05930
CCE05940
CCE05950
CCE05960
CCE05970
CCE05980
CCE05990
CCE06000
CCE06010
CCE06020
CCE06030
CCE06040
CCE06050
CCE06060
CCE06070
CCE06080
CCE06090
CCE06100
CCE06110
CCE06120
CCE06130
CCE06140
CCE06150
CCE06160
CCE06170
CCE06180
CCE06190
CCE06200
CCE06210
CCE06220
CCE06230
CCE06240

```


LIST OF REFERENCES

1. Reynolds, O., "An Experimental Investigation of the Circumstances Which Determine Whether the Motion of Water Shall be Direct or Sinuous, and the Law of Resistance in Parallel Channels", Phil. Trans. Royal Society, 174, pp. 935-982, 1883.
2. Salwen, H., and Grosch, C. E., "The Stability of Poiseuille Flow in a Pipe of Circular Cross-section", Journal of Fluid Mechanics, v. 54, part 1, p. 93, 6 March 1972.
3. Garg, V. K., and Rouleau, W. T., "Linear Spatial Stability of Pipe Poiseuille Flow", Journal of Fluid Mechanics, v. 54, part 1, p. 113, 25 November 1973.
4. Gill, A. E., "The Least Damped Disturbances to Poiseuille Flow in a Circular Pipe", Journal of Fluid Mechanics, v. 61, part 1, p. 97, 27 March 1973.
5. Davey, A., and Drazin, P. G., "The Stability of Poiseuille Flow in a Pipe", Journal of Fluid Mechanics, v. 36, part 2, p. 209, 22 August 1968.
6. McIntire, L. V., and Lin, C. H., "Finite Amplitude Instabilities of Second Order Fluids in Plane Poiseuille Flow", Journal of Fluid Mechanics, v. 52, part 2, p. 273, 31 March 1971.
7. Huang, L. M., and Chen, T. S., "Stability of Developing Flow Subject to Non-axisymmetric Disturbances", Journal of Fluid Mechanics, v. 63, part 1, p. 183, 16 April 1973.
8. Leite, R. J., An Experimental Investigation of the Stability of Axially Symmetric Poiseuille Flow, Report No. OSR-TR-56-2, U.S. Air Force Contract AF 18(600)-350, November 1956.
9. Garg, V. K., "Stability of Developing Flow in a Pipe: Non-axisymmetric Disturbances", Journal of Fluid Mechanics, v. 110, p. 209, 15 April 1980.
10. Harrison, W. F., On the Stability of Poiseuille Flow, Ae.E. Thesis, Naval Postgraduate School, Monterey, California, December 1975.
11. Arnold, M. J., Investigation of Pipe Flow Instability and Results for Wave Number Zero, M. S. Thesis, Naval Postgraduate School, Monterey, California, December 1978.

12. Naval Postgraduate School Report NPS67-78-006, A Basic Reformulation of the Pipe Flow Stability Problem and Some Preliminary Numerical Results, by T. H. Gawain, 1 September 1977.
13. Naval Postgraduate School Report NPS67-79-003, A General Linearized Theory of the Stability of Fully Developed Pipe Flow with Particular Reference to the Boundary Conditions at the Axis, by T. H. Gawain, February 1979.
14. Ketter, R. L., and Prawel, S. P. Jr., Modern Methods of Engineering Computation, p. 227, McGraw-Hill, 1969.
15. Gawain, T. H., and Ball, R. E., "Improved Finite Difference Formulas for Boundary Value Problems", International Journal for Numerical Methods in Engineering, v. 12, p. 1151, June 1977.
16. Schlichting, H., Boundary Layer Theory, p. 516, McGraw-Hill, 1968.

INITIAL DISTRIBUTION LIST

	No.	Copies
1. Defense Technical Information Center Cameron Station Alexandria, Virginia 22314	2	
2. Library, Code 0142 Naval Postgraduate School Monterey, California 93940	2	
3. Department Chairman, Code 67 Department of Aeronautics Naval Postgraduate School Monterey, California 93940	1	
4. Professor T. H. Gawain, Code 67Gn Department of Aeronautics Naval Postgraduate School Monterey, California 93940	4	
5. LT David B. Wallace, USN VQ - 1 DET ATSUGI, JAPAN Box 43 FPO Seattle, Washington 98767	1	

200139

Thesis
W222325 Wallace
c.1

A numerical analysis of pipe flow stability.

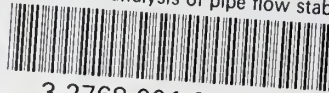
200139

Thesis
W222325 Wallace
c.1

A numerical analysis of pipe flow stability.

thesW222325

A numerical analysis of pipe flow stabil



3 2768 001 92884 9

DUDLEY KNOX LIBRARY